UNIVERSITA' DEGLI STUDI DI MILANO

Department of Agricultural and Environmental Science

PhD School in agriculture, environment and bioenergy

e-NEWtrients: *bioelectrochemical systems at the service of agricultural sciences*

Andrea Goglio
Matr. n. R11908

Tutor: Prof. Stefano Bocchi

Co-tutor: Dr. Andrea Schievano

2019-2020

To all the deluded, to those who speak to the wind.

To the madmen for love, to the visionaries,

to those who will give their lives to make a dream come true.

To the outcasts, to the rejected, to the excluded. To real or presumed madmen.

To men of heart,

to those who persist to believe in true love.

To all those who are still moved.

A tribute to the great impulses, ideas and dreams.

To those who never give up, to those who are derided and judged.

To the daily poets.

To the "winners" therefore, and also

to the losers who are ready to rise and fight again.

To the forgotten heroes and the wanderers.

To those who after fighting and losing for their ideals,

still feels invincible.

To those who are not afraid to say what they think.

To those who have travelled around the world and to those who one day will.

To those who do not want to distinguish between reality and fiction.

To all wandering knights.

Somehow, maybe it's right and it's okay...

to all the actors.

Don Quixote, Miguel de Cervantes

Table of Contents

Abstract 7

Chapter 1 - Microbial recycling cells (MRCs): a new platform of microbial electrochemical technologies based on biocompatible materials, aimed at cycling carbon and nutrients in agro-food systems 9

Chapter 2 - Microbial recycling cells, first steps into a new type of microbial electrochemical technologies, aimed at recovering nutrients from wastewater 46

Chapter 3 - Plant nutrients recovery from organic-rich wastewater using microbial electrochemical technologies based on terracotta 74

Chapter 4 - Electroactive biochar for large-scale environmental applications of microbial electrochemistry 99

Chapter 5 - Air-breathing bio-cathodes based on electro-active biochar from pyrolysis of giant cane stalks 131

Chapter 6 - Capturing carbon and nutrients from organic-rich wastewater by bioelectrochemically-enhanced deposition on electro-active biochar 160

Chapter 7 - Improving microbial oxidation and nutrients recovery from agro-industrial wastewater in constructed wetlands based on electro-active biochar.....185

Chapter 8 - Biochar-terracotta conductive composites: new design for bioelectrochemical systems 203

Chapter 9 - Nutrients-enriched electroactive biochar as soil amendment under anoxic conditions: a circular economy approach 228

Appendix 244

Abstract

It is estimated that demand for food will continue to increase, as a result of population growth, but at the same time, food production will increasingly face huge constraints, such as water scarcity, soil desertification and the increase of fertilizers prices. Wastewater derived from food production chains should be treated in a sustainable way, to minimize environmental contamination, while maximizing the recovery of valuable fractions, such as plant nutrients. Bioelectrochemical systems (BES) have been proposed as solutions to treat different kinds of wastewaters and recover nutrients through bio-electrochemical reactions. In my project, new types of BES are studied, fabricated with biocompatible and biogenic materials starting from vegetable scraps, which could be applied as mean of organic matter and nutrients recovery from organic-rich wastewater streams coming from important agro-food chains, such as farming and agro-industrial productions. This novel type of BES was named 'microbial recycling cells' (MRCs). Biochar produced from controlled pyrolysis of plant materials is electro-conductive and can be used as base to fabricate MRCs, which can be used for this scope. Other materials like earthenware were also used in MRCs architectures, as electrolytic conductors and structural frames. After being enriched of nutrients from wastewaters, biochar-based MRCs can be fully recycled to produce soil improvers and renewable fertilizers. In soil applications, the electrochemical properties of biochar influence soil biogeochemical reactions, with important implications in plant nutrition and the environmental implications of soil-plant systems (e.g. carbon sequestration, CH_4 emissions, etc.). The PhD project was hold in 3 different work packages: WP1) Selection of MRC architectures and optimization of e-biochar properties, WP2) Study of the microbial electrochemical processes driving nutrients deposition, WP3) Study of the properties of nutrients-enriched biochar derived from MRC after their life-cycle, as soil improvers of agricultural soil fertility, with both amending and fertilizing properties.

Chapter 1 - Microbial recycling cells (MRCs): a new platform of microbial electrochemical technologies based on biocompatible materials, aimed at cycling carbon and nutrients in agro-food systems

Andrea Goglio[a], Matteo Tucci[a], Bruno Rizzi[a], Alessandra Colombo[a], Pierangela Cristiani[b], Andrea Schievano[a]*

a - e-BioCenter, Department of Environmental Science and Policy (ESP), Università degli Studi di Milano, Via Celoria 2, 20133 Milan, Italy

b - Ricerca del Sistema Energetico, Via Rubattino 54, 20134 Milano

* Corresponding author; email: andrea.schievano@unimi.it

Published in:

Goglio A., Tucci M., Rizzi B., Colombo A., Cristiani P., Schievano A., 2019. Microbial recycling cells (MRCs): A new platform of microbial electrochemical technologies based on biocompatible materials, aimed at cycling carbon and nutrients in agro-food systems. Science of the Total Environment. doi:10.1016/j.scitotenv.2018.08.324

Abstract

This article reviews the mechanisms that drive nutrients and carbon sequestration from wastewaters by microbial electrochemical technologies (METs). In this framework, a new generation of METs is also presented (to be called microbial recycling cells, MRCs), based on 100%-recyclable materials (biomass-derived char coal, clay, terracotta, paper, ligno-cellulosic plant materials, etc.), which can act as bio-electrodes, separators and structural frames. In traditional METs architectures (based on technological materials such as carbon cloths, plastic panels, membranes, binders), inorganic salts precipitation and adsorption, as well as biofouling due to organic-matter deposition, are considered as main drawbacks that clog and hinder the systems over relatively short periods. In MRCs, these mechanisms should be maximized, instead of being avoided. In this perspective, both inorganic and organic forms of the main nutrients are sequestered from wastewater and deposited on METs modules. Once the systems become saturated, they can entirely be recycled as agricultural soil conditioners or as base for organic-mineral fertilizers.

Keywords

Microbial electrochemical technologies, microbial recycling cell, biochar, wastewater, microalgae, renewable fertilizers

1. Introduction

It is estimated that the demand for food will continue to increase, as a result of population growth, while food production will increasingly face huge constraints, such as water scarcity, soil desertification and the increase of fertilizers prices (Gustavsson et al., 2011). The availability and abundance of soil organic matter and nutrients will be one of the major constraints to achieve a sustainable agricultural production and yield sufficient food supply. While the prices of the main macronutrients (N, P, K, and Mg) are continuously rising, their primary production is decreasingly sustainable. N-fertilizers rely on atmospheric N_2 fixation by the fossil-fuel based Haber-Bosh process, while raw minerals rich in P, K and Mg are extracted from rock mines, with high environmental footprints (Kratz et al., 2016). In parallel, massive fertilization with mineral macronutrients (N, P, K, Ca, Mg), in intensive agriculture practises, strongly contributes to micronutrients (Co, Mn, Fe, Zn, etc.) stripping and soil organic pool oxidation (El-Fouly et al., 2015). Under such conditions, the conservation of soil fertility over long-terms have been severely threatened; pre-desertification, erosion and salinization are

often the undesired consequences, and major threats for food security, as well as for ecosystems preservation (Plaza et al., 2013).

In the meantime, huge amounts of nutrients are released to environmental compartments from agro-food intensive production areas. On one side, crop systems are over-fertilized by mean of mineral fertilizers and, on the other side, wastewater resulting from farms and food transformation factories are often spread untreated to the environment, with deleterious effects on ecosystems. Worldwide, yearly around 337 km^3 of wastewaters are generated, with an high concentrations of organic/inorganic carbon and nutrients (Table 1) (Sato et al., 2013).

Table 1 - Organic matter, inorganic carbon and mineral (as total elements) contents in some of the waste liquid streams of the main agro-food industries

	COD	**BOD_5**	**TSS**	**pH**	**EC**	**N**	**P**	**K**	**Mg**
	g L^{-1}	**g L^{-1}**	**g L^{-1}**		**mS cm^{-1}**	**g L^{-1}**	**g L^{-1}**	**g L^{-1}**	**g L^{-1}**
Swine slurry liquid fraction	4.6-5.6	2-2.1	4.8-4.9	6.9-7.3	3.5-19.1	0.75-0.77	0.01-0.17	n.a.	n.a.
Cow slurry liquid fraction	10.35-15.51	n.a.	12-19	6.3-7.7	n.a.	2.08-2.30	0.63-0.77	1.72-1.89	0.34-0.38
Olive mill (three-phase process)	4–16	2–7	0.8–6	3.5–6	1.5-2.5	1 - 2	1.2 - 0.1	1-5	0.1-0.2
Winery	0.3-49.1	0.2-22.4	0.07-8.6	2.5-12.9	1.1-5.6	0.01-0.4	0.01-0.03	0.01-0.12	0.01-0.02
Brewery	1-10	1-7	0.1-1	7-11	2-4	0.01-0.1	0.01-0.02	0.1	0.1
Cheese factories	1.9-2.7	1.2-1.8	0.5-0.7	7.2-8.8	0.4-2	0.3-0.7	0.4-0.7	n.a.	n.a.
Vegetable and fruit industry	4.4-5.9	0.4-1.7	n.a.	n.a.	n.a.	0.7-0.9	0.1-0.2	n.a.	n.a.

In view of a more sustainable framework based on circular economy, nutrients and organic matter should be removed from wastewater derived from food production chains and recovered as renewed fertilizers/soil conditioners, to preserve the environment, optimize the resources in agricultural systems and increase carbon storage.

METs have been recently introduced as promising solutions to treat different kinds of wastewater and recover minerals through bio-electrochemical reactions (Pandey et al., 2016). Different cell architectures and materials have been studied to fabricate electrodes, current collectors and chambers separators, as well as to provide structural functions to the systems (e.g. rigid frames). In most cases, METs are based on technological and high-grade materials, such as carbon-fibers, graphite, stainless steel, titanium (for electrodes and current collectors), selective membranes, polymeric binders, gas diffusion layers (for separators) and plastic panels (for structural frames). However, one major constraint has been hindering real-world applications of these kind of METs over relatively long-term operations (more than 60 days). In wastewater treatment and bioremediation conditions, cell performances are strongly invalidated by clogging due to deposition of organic matter mixed to inorganic salts on electrodes surfaces (fouling). Therefore, the use of such technological and expensive materials at large scales might become unviable. Instead, researchers should focus on environmentally-friendly and biocompatible materials, because 'building devices for sustainability purposes from materials that may themselves contribute to the accumulation of waste build-up, would be a paradox' (Winfield et al., 2016).

Here, a review of the possible mechanisms, METs architectures and materials that allow to recycle carbon and nutrients is proposed. In this context, a new generation of METs, called microbial recycling cells (MRCs), is rising, based on biogenic, biocompatible materials, that can be completely recycled together with the recovered nutrients and organic carbon, to produce fertilizers and soil-conditioners.

2. Principles and mechanisms for nutrients recovery by METs

This section reports an overview of the main electrochemical, chemical and biological mechanisms that stand at the base for nutrients recovery by METs. Figure 1 resumes the electrochemical cell configurations and the main involved phenomena.

Electricity generated cations transport

The transport of electrons towards the cathode has to be balanced by an equal amount of positive charge through the cathode chamber in order to sustain the electrochemical process maintaining the electro-neutrality in the solutions (Rozendal et al., 2006). METs usually operate with complex electrolytes at a pH close to neutral, so the concentration of cations (such as Na+, K+, NH4+, Ca_2+, and Mg_2+) is about 105 times higher than that of hydrogen ions. Therefore, salt cations are more likely than hydrogen ions to balance charge in the cathodic compartment. This condition is fundamental in Microbial Desalination Cells (MDC), where the presence of a middle chamber between the cathodic and anodic chambers, separated by membranes, is used for specific recovery applications on electrodes. In three-chambers configuration, the middle compartment is limited on one side by a proton exchange membrane (PEM) and by an anion exchange membrane (AEM) (Kim and Logan, 2013). The same design is applicable to induce other ions to migrate in consequence of an electric field. For example, a stacked microbial nutrient recovery cell was used to recover N and P from raw urine (Chen et al., 2017).

pH increase at cathode: salts precipitation and ammonia stripping

The presence of selective membranes or porous separators reduces current densities, increasing internal resistance that led to inefficient supply of cations for cathodic reaction. The unbalance between the hydrogen ions transported across the membrane and the cations consumed to form water at the cathode by the cathodic reaction [1] determines a pH increase in the cathodic solution (Rozendal et al., 2006). Especially in performing air-exposed cathodes, oxygen reduction reaction (ORR) [1] proceed with an exchange of 4 electrons and results in a local increase of the pH (Guerrini et al., 2013; Santoro et al., 2017; Yuan et al., 2013b).

$$O_2 + 4e^- + 2H_2O \rightarrow 4OH^- \qquad [1]$$

The acidic pathway of ORR (below pH 10.5) implicating H+ implies drives the intermediate production of H_2O_2 (involving 2e-) before the final product of H_2O involving 2 more electrons. The alkaline pathway (over pH 10.5) (Equation [1]), on the other hand, has the intermediate production of HO_2 – and OH- and a final production of OH- involving 4 electrons (Erable et al., 2012; Malko et al., 2016; Rojas-Carbonell et al., 2018).

This mechanism enables the recovery of valuable elements from the wastewater (Gajda et al., 2014) through salts precipitation at high pH, such as phosphates/carbonates at pH greater than 8.5 (Carlsson et al., 1997). The cathodic production of OH- may lead to the precipitation of

hydroxides (Lu et al., 2015). In air-cathodes, high cathodic pH coupled to local water evaporation (with consequent local increase of concentrations) cause salts deposition directly onto the cathodic surface (An et al., 2017). Such salts were found to be mainly Ca or Na carbonates and phosphates (Santini et al., 2017). This normally leads to the deactivation of the cathode after around 50-70 days, by diminishing ions mass transport and hindering the contact between the catalytic sites and the solution (Santini et al., 2015). A similar behavior was observed with struvite deposition (Equation [2]), Mg_2+ + NH_4+ PO_{4-3} + $6H_2O \rightarrow NH_4MgPO_4 \bullet 6H_2O$), recovered as N-Mg-P-rich fertilizer (Kelly and He, 2014) .

$$Mg_2+ + NH_4+ PO_{4-3} + 6H_2O \rightarrow NH_4MgPO_4 \bullet 6H_2O \quad [2]$$

Also in this case, struvite precipitation is favored by the increase of pH near the cathode, because the higher is power generation the higher is pH near to the cathode. Therefore, phosphorous removal and power generation are strongly correlated (Santoro et al., 2014). N and P in struvite salts was also recovered from urine using a MFC configuration (Santoro et al., 2013). Zhang et al. (L. Zhang et al., 2012) recovered 94.6% of phosphate with similar systems. In presence of non-optimal ratios between N, P and Mg (1:1:1), as well as of competition with other elements (Le Corre et al., 2009), other P compounds may precipitate (e.g. calcium phosphate), which may have similar interest as fertilizers.

Cathodic pH increase result in the conversion of ammonium into ammonia (NH_3), allowing its recovery as gas, thanks to its volatility (Wu and Modin, 2013; Zamora et al., 2017). Ammonia gaseous streams are generally recovered through an acid trap (H2SO4) and further utilized in agriculture as ammonium sulfate. Alternatively, ammonium is converted to nitrite and nitrate in presence of oxygen (air-exposed surfaces) or by anodic oxidation. Denitrification may occur either in presence of organic molecules or by autrophic denitrifying bacteria, accepting electrons from the cathode. Different setups were developed based on these mechanisms (Virdis et al., 2010; Xie et al., 2011; Zhang and He, 2012), which however don't allow to recover ammonia for further utilization as fertilizer.

Cathodic reductive precipitation

The oxidation of organic matter at the anode can provide electrons for cathodic reductions and recovery of metal ions (Nancharaiah et al., 2015). Moreover, Ssome contaminants can also function as electron mediators at the anode or cathode (Ucar et al., 2017). Depending on their speciation and the properties of the catholyte, the reduced metals can either be deposited on the cathode or precipitate to the bottom of the chamber (Figure 1).

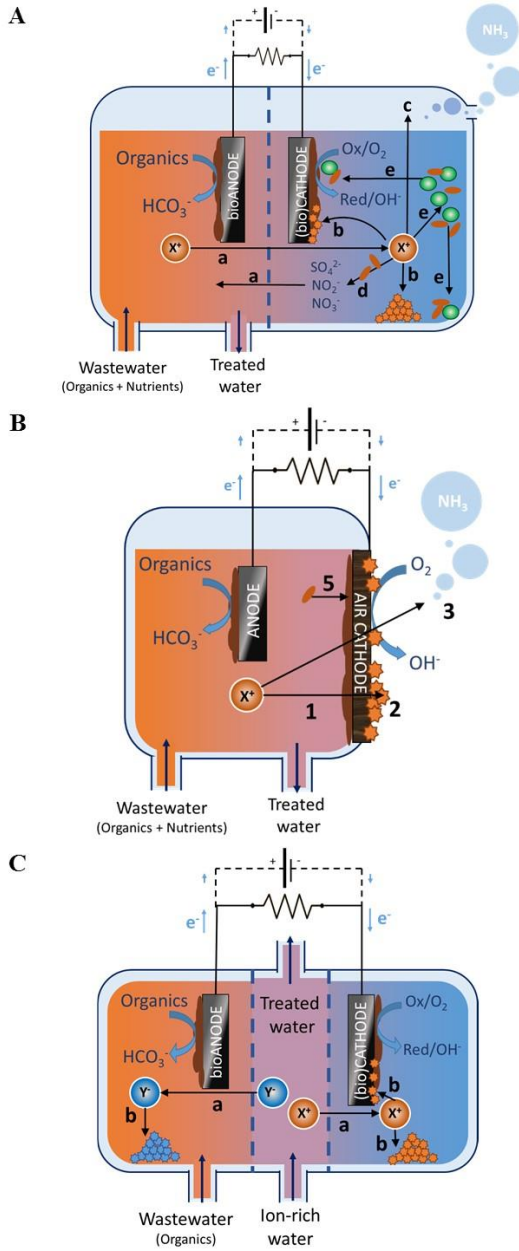

Figure 1 - Mechanisms of nutrient recovery in dual chamber (A), single chamber air-cathode (B) and three camber (C). a) ion migration (X+), b) inorganic salts/hydroxides precipitation (high pH) and cathodic reductive precipitation, c) ammonia stripping, d) microbial oxidations (e.g. nitrification), e) bioaccumulation by microorganisms (including by photosynthesis) and biomass deposition.

In air-cathode METs, it is possible to recover metal ions as Ag(I), Au(III), Cr(VI), Co(III), Cu(II), Hg(II), Se(IV), and V(V). When the electron flow is thermodynamically not favorable (e.g. for reduced metal forms as Ni(II), Pb(II), Cd(II) and Zn(II)) an external power supply would be required (Figure 1). The subsequent reduction of Co(II) to Co(0) for instance, can be achieved in a MEC configuration by providing an external power supply in order to be able to recover cobalt from aqueous solution (Huang et al., 2013).

Zhang et al. obtained simultaneous reduction of Cr(VI) and V(V) to Cr(III) and V(IV) respectively on the cathode of dual chamber MFC using acetate as the electron donor(B. Zhang et al., 2012). Their selective recovery was possible since Cr(III) was deposited mainly on the cathode, while V(IV) remained in the catholyte and was further precipitated by pH adjustment. In a MFC fed with acetate, Huang et al. obtained cobalt leaching from $LiCoO_2$ particles: the oxidation of acetate at the anode generated the electrons necessary for the reduction of solid Co(III) to Co(II) at the cathode.

Tao et al. studied Cu recovery from a copper sulfate ($CuSO_4$) solution in a dual-chamber MFC fed with glucose (Tao et al., 2011). In fact, the potential of the oxidation of glucose can drive the spontaneous reductive precipitation of Cu on the cathode. Starting from a 196 mg L^{-1} Cu(II) solution, removal of Cu(II) ions higher than 99% was obtained, with deposition of both metallic Cu(0) and Cu_2O on the cathodic surface.

In order to recover iron, Fe_3+ can be reduced to Fe_2+ at the cathode of MFCs, with subsequent Fe_2+ re-oxidation and precipitation. This mechanism was applied for instance by Lefebvre et al. (Lefebvre et al., 2012), who performed the treatment of acid mine drainage (AMD) dominated with iron with an acetate-fed MFC. The obtained removal of Fe_3+ was about 99%. Selenite removal was also investigated in a single-chamber air-cathode MFC using acetate or glucose as electron donors (Catal et al., 2009). The anode respiring bacteria performed the reduction of Se(IV) to Se(0) achieving the complete reduction of 200 mg L^{-1} of selenite in 72 h.

Cathodic reductive precipitation was also applied for the sulfate reduction. Wang et al. described a MEC coupled with sulfate-reducing bacteria (SRB), that was used to degrade sulfate-rich wastewater, where salt crystals formed on the electrode, thereby potentially retarding the continuity of sulfate removal during the whole operation (Wang et al., 2017). Luo et al investigated the effect of initial acidity of wastewater on performance of sulfate-reducing biocathodes. MECs with biocathodes were operated with initial pH values of catholyte ranged from 3.0 to 7.0. The optimum initial pH value was 6.0 with a maximum sulfate reductive

rate and biomass of 57 mg L^{-1} d^{-1} and 2.1 ± 0.4 mg g^{-1} (H. Luo et al., 2017). Also Hu et al. investigate the effect of magnetite nanoparticles on the performance of autotrophic sulfate-reducing biocathode in MEC where the sulfate reductive rate reached 152 ± 7.0 g m^{-3} d^{-1}, which was improved by 122% than the MEC without magnetite (Hu et al., 2018).

Bioaccumulation by photosynthetic microorganism

Photosynthetic microorganisms (such as microalgae and cyanobacteria) are able to assimilate considerable amounts of nutrients, for the synthesis of proteins (which may account for 45−60% of their dry weight), nucleic acids, phospholipids, and other cellular constituents (Muñoz and Guieysse, 2006). Phototrophic microorganisms cultivation and METs were successfully combined in order to obtain a more energy positive process for nutrient recovery from wastewater. Combining METs and microalgae cultivation results in a synergistic interaction, where electrochemically active bacteria release electrons, hydrogen ions, and carbon dioxide, at the anode, due to oxidation of organic matter in the wastewater. At cathode, microalgae uptake nitrogen, phosphorus, and carbon dioxide and, supported by solar illumination, make photosynthesis in the anode; in addition, oxygen produced by microalgae metabolism is used as electron acceptor in the cathode (Zhang et al., 2011).

In the anode compartment, the oxidation of organic compounds allows inorganic nutrients to migrate to the cathodic compartment, to be accumulated by photosynthetic metabolism (Figure 1). In oxygen-driven cathodes, photosynthesis contributes to increase O^2 concentration in the cathodic liquid enhancing cathodic oxygen reduction reaction (Colombo et al., 2017). The obtained biomass may undergo downstream extractions to obtain several different metabolites and secondary products, including animal feed additives, plant-roots stimulants and fertilizers. Xiao and colleagues (Xiao et al., 2012) developed an integrated photo-bioelectrochemical system in which the algal bioreactor was used as cathodic compartment in order to provide dissolved oxygen and to strip off nutrients. The system achieved around 98% of ammonium removal and 63% of total nitrogen removal, while also decreasing the chemical oxygen demand of 92%, and phosphate of 82% and producing electrical energy at the same time. In a sediment-type MFC, Zhang et al. obtained about 70% of P removal, with simultaneous COD and N removal in a photo-microbial fuel cell that featured a culture of Chlorella vulgaris in the cathodic compartment and the anode buried in the sediment (Zhang et al., 2011). A removal of 87,6% of nitrogen was obtained, in which 75% was due to Chlorella vulgaris uptake and 22% due to nitrification and denitrification processes occurring in that system. Bioaccumulation of minerals also include the growth of heterotrophic microorganisms, that

tend to produce thicken biofilm structures (biofouling on solid surfaces), as well as deposit at the bottom of the reactor (Figure 1). A recent review more exhaustively summarizes this topic (S. Luo et al., 2017).

3. Architectures and materials of METs applied to nutrients recovery

METs architecture has become recently considerably flexible in order to meet a large number of possible applications (Logan et al., 2006). Different reactor geometries (flat plate, tubular, spherical, etc.), electrodes separator (membrane, salt bridge, or mechanical structure), and cathode types (water cathode or air-cathode, abiotic cathode, or biocathode) introduce terms of differentiation in METs architectures.

Recently, different kinds of set-up have been studied to recover soluble nutrients by means of a variety of architectures and sizes of METs (Kelly and He, 2014). The main available architectural solutions are displayed in Figure 2A-D.

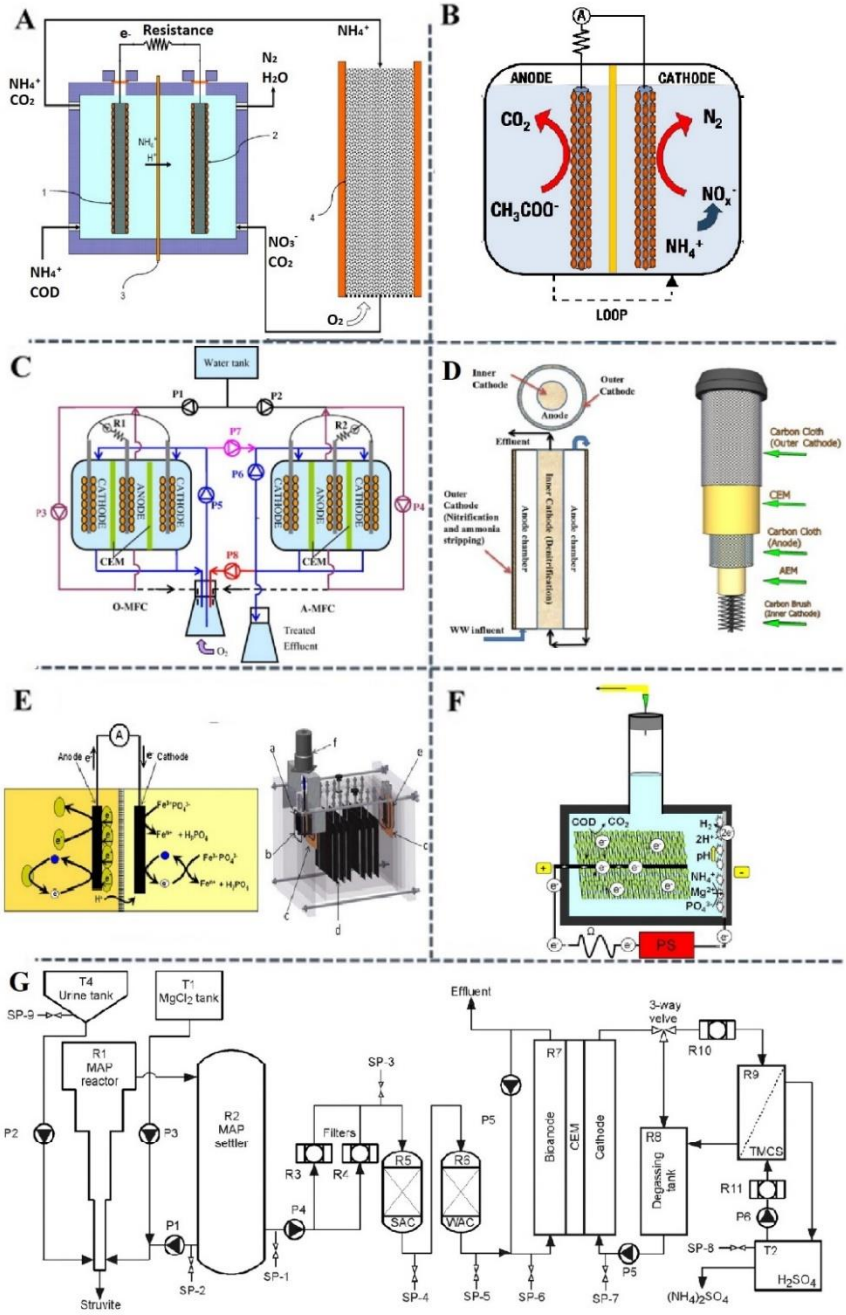

Figure 2 - Different kinds of METs architecture for: A-D) nitrogen recovery, E-F) phosphorous recovery, G) pilot scale reactor for N and P recovery. Reprinted (adapted) with permission from (Cusick and Logan, 2012; Fischer et al., 2011; Virdis et al., 2010, 2008; Xie et al., 2011; Zamora et al., 2017; Zhang and He, 2012). Copyright © 2017, Elsevier.

In Figure 2A , the wastewater flow in the anode compartment of the MFC for organic removal then pass into an aerobic bioreactor in which ammonia was biologically oxidized to nitrate; finally, nitrate was reduced to nitrogen gas in the cathode when the stream returned to the MFC cathode (Virdis et al., 2008). Figure 2B is the subsequent design integrated the aerobic process into the cathode in which simultaneous nitrification and denitrification was accomplished with simplify the reactor structure and reduce the cost associated with ion exchange membranes (Virdis et al., 2010). In Figure 2C, a coupled MFC system consisted of two MFCs, one with dual aerobic biocathodes and the other containing dual anoxic biocathodes: the wastewater was flow into the anodes of the two MFCs individually and the effluents were collectively sent to the aerobic biocathodes, whose effluents were then transferred into the anoxic biocathodes (Xie et al., 2011). In Figure 2D, the batch operated dual-cathode MFC was further developed to a continuously operated system in tubular configuration and it was found that nitrate removal involved both bioelectrochemical denitrification in the anoxic cathode and heterotrophic denitrification in the anode (Zhang and He, 2012). Other applied different kinds of innovative architectures, as a single-chamber or two-chamber system specifically for P recovery (Figure 2E-F). Phosphorus recovery in struvite was first investigated in Figure 2A in a double chamber MFC to reduce $FePO_3$ in digested sludge for converting insoluble phosphate to soluble form and then the mobilized phosphate was precipitated in struvite by adding magnesium and ammonia (Fischer et al., 2011). Struvite formation was accomplished within a MET by using a single chamber microbial electrolysis cell (MEC), increasing the localized pH adjacent the cathode electrode, which was important to struvite formation by precipitation. (Fig. 2B) (Cusick and Logan, 2012).

According to the literature, many studies were also focused on pilot-scale METs architectures for the nutrients recovery. A two-step treatment system for nutrient and energy recovery from urine was successfully operated for six months by Zamora et al. (Zamora et al., 2017) and is displayed in Figure 2G. In a first step, in a MEC, P was recovered as struvite, and the effluent of this reactor was used for nitrogen recovery (as ammonia) and hydrogen production. The MEC was coupled to a trans-membrane-chemisorption module, in which the ammonia nitrogen was recovered as an ammonium sulphate solution.

In photosynthetic-cathodes METs, system configurations have to be suitable for the growth of photosynthetic microorganisms and for optimization of system performance; the role of such organisms can be to provide organic matter or oxygen through photosynthesis.

Different system architectures have been proposed, that can be classified in two main categories: the photobioreactor for microalgae cultivation externally linked to the MET components, defined as a coupled system and the photobioreactor incorporated inside the MET components, defined as an IPB (S. Luo et al., 2017).

With the separate coupling of the elements, a photobioreactor (PBR) continuously provides biomass for the supply of MET; PBR can be placed both upstream and downstream MET (Gajda et al., 2015a; Walter et al., 2015).

In a IPB, photosynthetic microorganisms can grow in contact with both electrodes (single chamber configuration), or can grow within anode or cathode, which are separated by ion exchange membrane (double chamber configuration) (S. Luo et al., 2017).

In air-cathode MFCs, there is the need of a solid porous material to create the interface between the liquid phase of the anodic chamber and the gaseous phase in contact with the cathode. Gas diffusion electrodes have been typically applied to both air-breathing cathodes (in MFC). Microbial biofilms grow on both the anode and the inner side of the cathode. The cathodic biofilm helps in preserving anaerobic conditions in the anodic chamber. Air diffuses only in a relatively thin layer and forms a decreasing gradient towards the anodic compartment (Cristiani et al., 2013). Up to date, in typical air-driven METs configurations, microporous layers (MPL) are used to separate the liquid in the anodic chamber from the air-exposed cathodic surface, while increasing cathodic surface area (Ghadge et al., 2015; Papaharalabos et al., 2013) and guaranteeing low ionic resistance (Cindrella et al., 2009; Cristiani et al., 2013). Usually, MPL are based on blends of hydrophobic polymeric binders (PTFE, Nafion® etc.) and conductive powders used as catalysts (carbon black, metals etc.), spread on carbon fibres or other conductive materials (Santoro et al., 2015).

4. MRCs: low-tech architectures based on fully recyclable biocompatible materials

In most environmental applications of METs (such as water treatment, bioremediation, etc.), a series of phenomena tend to invalidate the electrochemical performances of the systems, over long-term operations (typically over 40-60 days) (Noori et al., 2016; Santini et al., 2017, 2015). Especially for gas-liquid interfaces (e.g. air-exposed cathodes), Figure 3 summarizes the most relevant mechanisms concurring to system failures (Marzorati et al., 2018; Santini et al., 2017). When the system works properly, pH tends to increase in close proximity of the cathode (pH > 9), leading to inorganic salts deposition, carbonates precipitation and accumulation as a layer between the cathode and the biofilm, thus preventing charge transfer processes (Santini

et al., 2015). In addition, water evaporation from MPLs or separators at air-water interface contributes to salts precipitation (Santini et al., 2017). Combined biofouling and salts depositions tend to clog MPLs, electrodes and separators, increasing the internal resistance and deactivating the system. These mechanisms have been considered as strong constraints for the development of applicable METs technologies (Cheng et al., 2006; Jiang et al., 2011; Yu et al., 2017). When METs are based on high-tech and non-biocompatible materials, continuous maintenance would be needed to guarantee stable electrochemical performances (Clauwaert et al., 2008). This may result in harming the economic and environmental feasibility of the application of such systems at large scales.

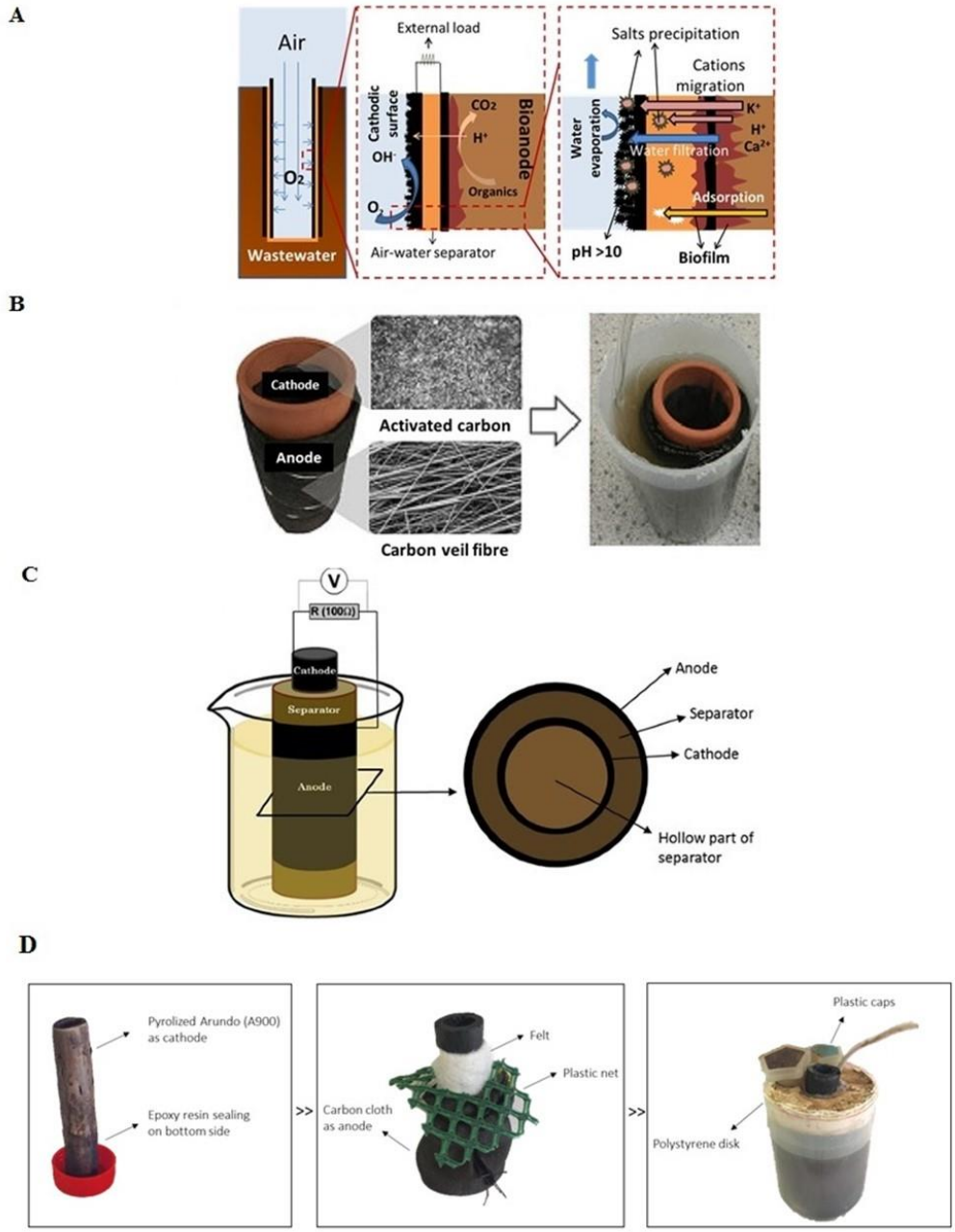

Figure 3 - A) overview of the phenomena involved in hindering long-term operation of air-exposed cathodes; (B) a schematic representation of terracotta-based cylinders used to build air-cathode MFCs (Gajda et al., 2015); (C) cylindrical ligno-cellulosic materials (Marzorati et al., 2018); (D) pyrolysed ligno-cellulosic materials as cathode (Marzorati et al., 2017). Reprinted (adapted) with permission from (Gajda et al., 2015; Marzorati et al., 2018). Copyright © 2017, Elsevier.

The exclusive use of low-tech, biocompatible and fully recyclable materials in the fabrication of electrodes, separators and structural frames may represent a more effective strategy to widen their applicability. The possibility of scaling-up METs in several environmental applications relies on the replacement of expensive components. Recently, researchers have been focusing on the use of several biodegradable secondary materials, in a circular-economy approach. Good examples of such materials, already studied or at present under investigation, are terracotta (Colombo et al., 2017; Pasternak et al., 2015; Winfield et al., 2013) and ligno-cellulosic biomass, as porous separators (Marzorati et al., 2018), and char-coal derived from pyrolysis of ligno-cellulosic biomass (biochar), as conductive and electro-active material for electrodes. Other examples are waste paper/cardboard, natural rubber, agricultural residues (maize stalks, straw, etc.), starch-based bio-plastic, egg shell membranes, etc. These kinds of METs architectures could substitute expensive carbon cloth electrodes, which still represents the state-of-the-art, with other cheap carbon-based matrix deriving from agriculture by-products. Here, we revise a series of possible materials proposed in the literature as base for either electrodes, current collectors, separators, porous layers or architectural/structural elements.

Bio-charcoal to fabricate electrodes

Many experiments used different types of biomass to fabricate electrodes. This includes, for example, chestnut shells (Chen et al., 2018), crop plants (Chen et al., 2012), pinewood chips (Huggins et al., 2014) or corrugated cardboard (Chen et al., 2012). As most relevant experiences, anodes were fabricated from cardboard (inexpensive abundant material used in packaging) by carbonization. Examples of cathodes made of bio-charcoal were fabricated first by Yuan et al. (Yuan et al., 2013a). They were able to avoid the complex synthetic steps or specific machinery in production of nitrogen-doped carbon materials. They converted sewage sludge into electro-conductive biochar and tested it as cathode in MFCs. Very high catalytic activity for the ORR were achieved, due to high surface area and N and Fe enrichment. In another work, bananas were employed as sources of biochar (Yuan et al., 2014) to fabricate MFCs cathodes. Activation steps with KOH followed and were found successful in an ORR catalysis enhancement. Finally, biochar found another application in the MFCs as a manganese oxide electro-catalytic support in a study by Huggins et al. (Huggins et al., 2014). The cost of the electrode's material was decreased down to 0.02 USD, almost 5000 times lower than a similar electrode, prepared from a commercially available activated carbon, supporting the manganese oxide catalyst.

Ceramics as separators and structural materials

Crucial factors in scaling-up METs are the performance and costs of separators as well as of structural frames (Li et al., 2011). In air-exposed cathodes, porous materials with intrinsic structural rigidity are needed to act as air-water interface separators, that resist to water pressure, under given depths. The addition of rigid separators between electrodes has the advantage of adding a self-structured element that conveys rigidity to the whole system. Here, we will discuss low cost and environmentally sustainable membranes/separators that have been used in METs and could be utilized as MRCs. An overview of the involved phenomena is displayed in Figure 3A.

Ceramic materials are attracting increasing attraction as low-cost and environmentally sustainable separators in MET. This kind of materials show a wide versatility in terms of structure, composition and fabrication techniques, affecting their performances as separator for METs. In fact, ceramics can be optimized for specific applications by changing clay type, porosity, wall thickness and density (Winfield et al., 2016). The first attempt to use ceramic material as separator was performed by Park and Zeikus (2003) (Park and Zeikus, 2003) who used a 1 mm thickness porcelain septum in a single chamber MFC, obtaining a performance comparable to a dual chamber MFC equipped with a Proton Exchange Membrane. Since then, many authors reported various study on this materials, obtaining promising results.

The cost of this material is extremely low as it does not require rare components, complex technology or huge amount of energy to be fabricated. Earthenware is generally made of natural clay (variable amount of Al_2O_3, CaO, Fe_2O_3, K_2O, MgO, Na_2O, P_2O_5, SiO_2, SO_3, TiO_2), dried and baked at a temperature between 600 and 1200°C. Pasternak et al. (2015) (Pasternak et al., 2015) reported a cost for earthenware of 5.82 USD m^{-3}, while Behera et al. (2010) built a MFC with an off-the-shelf earthen pot (volume = 400 mL); which cos its cost was 0.1 USD in the Indian Market (Behera et al., 2010). The low cost and availability of this material allows the application of MFC as power source for off-grid lighting in poor regions of the world (Ajayi and Weigele, 2012).

The porosity of a ceramic membrane is a key factor for the effectiveness of its application, as it can influence the chemical composition and pH of the contained electrolyte (Winfield et al., 2013b) as well as the ion exchange rate. Winfield et al. (Winfield et al., 2013b) compared two different ceramic types and the one with higher water absorption (16.6%) produced a higher output than the other (9.1% water absorption), because of the enhanced ionic migration.

Moreover, different ceramic materials were compared in another study, and the best power performance was obtained with the highest porosity (14%) (Kadier et al., 2016).

The rate of cations transport is also strongly related to the presence of exchangeable cations in the clay (Ghadge and Ghangrekar, 2015). Among the constituent minerals of the clay, some possesses high availability of exchangeable cationic sites and, therefore, high cation exchange capacity. Examples of these minerals are such as Montmorillonite, Kaolinite, Smectite, Vermiculite etc., (Carroll, 1959). Ghadge et al. (Rao and Venkatarangaiah, 2014) compared two different clay ware, one derived from a red soil rich in aluminium and silica and another from a black soil containing higher percentages of iron, calcium and magnesium. As a result, the best performance as separator in terms of power density was obtained with the separator made of red soil.

Due to its rigidity, ceramic can be used as separator and structural element at the same time, as displayed in Figure 3B. In this case it is possible to avoid plastic-based rigid materials, which can also contribute to the environmental impact of the construction of the METs (Winfield et al., 2016). This configuration has been used with many different purposes, ranging from an electrocoagulation system for the recovery of heavy metals (Gajda et al., 2017), to water treatment systems (Ieropoulos et al., 2017) and low-cost power suppliers (Ajayi and Weigele, 2012; Behera and Ghangrekar, 2011; Gajda et al., 2015b). Finally, terracotta was studied for nutrients recovery coupled to the Spirulina platensis cultivation in the cathodic compartment of a photo-microbial fuel cells. In this case the photosynthetic oxygen generation rates were sufficient to sustain cathodic oxygen reduction (Colombo et al., 2017).

Paper-based separators

Paper separators represent an interesting alternative to the common membrane used in METs, because paper is an ubiquitous and cheap material, and its wastes still represent an issue (Winfield et al., 2015). An experiment showed that when compared to a plastic grid and to j-cloth, baking paper achieved the worst power performance as separator of air cathode MFC (Oliot et al., 2017). However, the system increased its stability over time, due to the more efficient protection of the bio-anode against the oxygen diffusion.

Winifield et al. (2015) (Winfield et al., 2015) built tubular single-chamber air-cathode MFCs using different kinds of paper: photocopier, cigarette, tissue, newspaper, brown bag and filter. The photocopier paper MFC resulted in generating the highest power, despite its lower porosity. This is probably due to some short circuit phenomena occurring with the more porous paper.

Furthermore, two tetrahedron photocopier paper MFCs were successfully used to transmit radio signals through the implementation of a power management system. This is the proof that this small and low power systems can be employed for useful practical applications.

Due to its mechanical properties, paper can be used also as a structural material, which can be easily shaped in origami style to crate small portable MET architectures (Winfield et al., 2015; Yu et al., 2016).

Rubber-based membranes

Natural rubber has also been taken into account as a candidate for sustainable low-cost membranes. Winfield et al. (Winfield et al., 2013c) used a natural rubber derived from condoms as separator for MFCs. The material was initially impermeable to cations, and after that a slow start-up phase, an increasing working voltage was generated, due to its partial biodegradation.

In another experiment, the performance of MSC MRC with laboratory gloves rubber has been found comparable to the performance of an MFC equipped with cation exchange membrane in terms of power production and COD removal, proving he presence of proton transfer pathways in the material (Winfield et al., 2014). After that, it was possible to completely degrade this material in 285 days under composting condition.

Ligno-cellulosic separators

Recently, as alternative to terracotta and other rigid separators, Marzorati et al. made use of the natural cylindrical shape of Giant Canes (Arundo Donax L.) and Maize stalks to build tubular MFCs (Figure 3C), which showed electrochemical performances in line with other systems in the literature (Marzorati et al., 2018). Maize stalks and Giant Canes are biogenic and biodegradable, available as agricultural by-products or side cultures, and they possess cylindrical shape and a porous texture. For these reasons were considered ideal candidates in building MFCs architectures. The aim in this case was nutrients recovery, rather than energy harvesting (due to low power densities, around 40 mW m^{-2}). This kind of separators were meant as sponges over time of macro and micro nutrients, recovered from the wastewater. At the end of their operational period acting as MFCs separators between anode and cathode, they were supposed to be reused as fertilizers to agricultural production. It was verified that ions migration, during MFCs operation, and the high pH conditions in the proximity of the cathode caused deposition of nutrients (N, K, Mg, Ca) inside the ligno-cellulosic separators. Ca and Mg were also remarkably recovered on the cathode. Phosphorous in particular, remarkably

decreased in the separators, while increasing in the anolyte. This was attributed to partial biodegradation of the lingo-cellulosic matrix. This drawback was not negligible and some other solutions (pre-digestion of the matrix, pyrolysis as to directly fabricate the cathode) were considered as to prevent/avoid or at least limit the biodegradation (Figure 3D).

Starch-based bio-plastics as membranes

An experiment proved the feasibility of using starch-based bio-plastic derived from compostable bags as MFC membranes (Winfield et al., 2013a). Although this material showed a limited lifetime (8 months) and lower power densities compared to the commercially available cation exchange membranes, it proved to be an efficient separator for a stable microbial environment, until natural degradation caused the failure of the system.

Egg shells as membranes

Egg shell membrane has been successfully implemented as separator in small MFC-based water quality sensor (Chouler et al., 2017). Despite its lower power output, the best sensitivity to COD was obtained with this membrane, in comparison to Nafion®, a synthetic polymer and a membrane less configuration.

5. MRCs: downstream production of fertilizers and soil conditioners

In MRCs, air-cathodes are used as 'sponges' for recalcitrant organic matter, inorganic carbon and inorganic salts, through a series of phenomena (see Figure 3). After their working life, nutrients-saturated MRCs modules could be substituted with new ones and fully recycled as organic-mineral conditioners/fertilizers for agricultural soil application. This idea would work only if alternative air-water separators and electrodes were fabricated using low-cost, biogenic and biocompatible materials, as reviewed in the previous section.

According to the literature, most of these materials can be used as base to produce soil conditioners. Firstly, biochar has deeply been studied as mean of carbon storage, soil fertility/quality improver and it is able to modify soil microbial habitats and directly influence the microbial metabolisms. In natural forests, biochar derived from natural organic biomass burning forms a considerable proportion of the soil's organic carbon. Soils within the Amazon-basin contain numerous sites where the 'dark earth of the Indians' (Terra preta de Indio) exist and are composed of variable quantities of highly stable organic black carbon. The apparent high agronomic fertility of these sites, as compared to tropical soils in general, has always attracted interest (Atkinson et al., 2010). Biochar's high porosity increases water retention of

the soil and in the same time increase the nutrients availability for the plants; also, it improves the soil structure and its mechanical properties (Table 2).

Table 2 – Effect of biochar application on soil structure, properties and nutrients availability

Soil structure an properties			**Nutrients availability**	
	Soil 1 + Biochar	**Soil 2 + Biochar**	**Soil + Biochar**	
pH	Increasing 1 point pH	Increasing 6 points pH		
SOC (%)	27.4 %	144 %	**Al (cmol kg^{-1})**	n.a.
CEC (cmol kg^{-1})	7.41 %	263 %	**Ca (cmol kg^{-1})**	+ 434 %
BS (%)	- 42 %	n.a.	**K (cmol kg^{-1})**	+ 27 %
MBC (mg kg^{-1})	51 %	n.a.	**Mg (cmol kg^{-1})**	+ 26 %
Porosity (%)	41 %	n.a.	**Na (cmol kg^{-1})**	+ 4 %
Ksat (cm h^{-1})	26 %	n.a.	**N (cmol kg^{-1})**	+ 6 %
MWD (cm)	11 %	n.a.	**C (cmol kg^{-1})**	+ 25 %
SER (g m^{-2} h^{-1})	-63 %	n.a.	**Reference**	(van Zwieten et al., 2010)
Reference	(Jien and Wang, 2013)	(Forján et al., 2017)		

SOC: soil organic carbon, CEC: cation exchange capacity, BS: base saturation percentage, MBC: microbial biomass carbon, Ksat: saturated hydraulic conductivity, MWD: mean weight diameter of soil aggregates, SER: soil erosion rate

Over the last decades, the use of biochar to improve soil fertility was largely studied (Ralebitso-Senior and Orr, 2016). It has been shown that biochar may induce changes in soil structure and stability, nutrients and energy cycling, carbon-storage capacity, aeration, water use efficiency and disease resistance (Brussaard et al., 2007; Lehmann et al., 2011). Besides chemical and structural changes, soil amendment with biochar influences the microbial abundance and composition (Grossman et al., 2010; O'Neill et al., 2009). These microbiological shifts influence several important soil processes, such as denitrification and ammonification (Yanai et al., 2007), methane oxidation (Reddy et al., 2014), biological nitrogen fixation (Rondon et al., 2007) and carbon fixation and degradation (Lehmann and Joseph, 2015; Ralebitso-Senior and Orr, 2016). Biochar was also held responsible of important influences on intercellular signaling,

by sorption of key-molecules (Lehmann et al., 2011; Masiello et al., 2013). However, it has been difficult to fully justify such important influences of biochar on soil microbial ecology.

Besides, being biochar redox-active and electrically conductive (Kloss et al., 2012) it may act as soil-fertility promoter, not only indirectly by changing the soil structure and chemistry, but also by directly mediating electron transfer processes, i.e., by functioning as an electron shuttle for soil microbial communities (Kappler et al., 2014). Meanwhile, a reasonable number of studies found certain types of biochar in soil acting as promoter of direct interspecies electron transfer for different syntrophic associations of microorganisms, thanks to its electrical conductivity and stimulating the capacity of EET by pili or other direct membrane mediators. Chen et al. demonstrated that biochar acts as promoter of direct interspecies electron transfer for different syntrophic associations of microorganisms, thanks to its electrical conductivity and stimulating capacity of extracellular electron transfer by pili or other direct membrane mediators (Chen et al., 2014). Swarnalakshmi at al. recently prepared a cyanobacterial-biofilmed (Anabaena) bio-fertilizer based on charcoal and soil, containing Azotobacter, Mesorhizobium, Serratia and Pseudomonas strains (Swarnalakshmi et al., 2013). Enhancements of up to 50% of nitrogenase activity were observed, as compared to control experiments.

Finally, the recalcitrant structure of biochar makes it an ideal candidate in long-term carbon storage in agricultural soil, as strategy to mitigate climate change (Qian et al., 2015).

Terracotta and residual ceramic materials are used as soil amendments, to alleviate soil compaction, to increase water retention, hydraulic conductivity, cation-exchange capacity and to improve other soil physical properties (Wu et al., 2017). Other materials, such as ligno-cellulosic, rubber, bio-plastics and paper used as separators or structural frames might undergo a composting process, before being re-utilized in soil.

Microalgal biomass production at cathodes could be used as soil conditioner with the added value of potential biofertilizers and biostimulants (Brown and Saa, 2015). The use of microalgal biomass, both in direct-to-field application, both in seed's growing medium, have shown to determine an enhancement of nutrient uptake, biomass accumulation, and of crop yields (Faheed and Fattah, 2008; Shaaban, 2001). This effect is due to microalgae richness in macronutrients, in particular nitrogen (N) and phosphorus (P), and to presence of substances such as phytohormones, vitamins, carotenoids, amino acids, and antifungal substances, all of which are recognized to be plant growth-promoting. Nutrients recovered from wastewater,

concentrated in micro algal biomass, can be so recycled as biofertilizers, lowering environmental impact of the whole integrated process (Arashiro et al., 2018). Microalgal biomass has also been evaluated for use in bioremediation processes; i.e. Arthrospira spp. has shown biosorption activity of copper, cobalt, zinc, and manganese from aqueous solutions (Dmytryk et al., 2014). Biomass of Arthrospira Platensis have been successfully tested for enhancement of bioremediation of oil-contaminated soils, stimulating oil-degrading bacterial communities, and improving degradation due to surfactant activity of phycocyanin (Decesaro et al., 2017).

All MRCs materials could be directly (or after secondary processes) applied as soil conditioners, improving the cation/anion exchange capacity, increasing the adsorption of ions in soils, as possible to observe in Figure 4. Ion exchange is one of the most important mechanism in soil to guarantee availability of the most important micro- and macronutrients for plants.

Figure 4 – MRCs structural elements (electrodes, separators, frames), after being saturated by nutrients, might be shredded and recycled as soil conditioners/fertilizers.

The enrichment of such materials with organic and inorganic forms of nutrients, recovered from wastewaters should be thought as a mean of decreasing the need of chemical fertilizers. Particular attention should be paid to this aspect, by quantitative and qualitative

determination of such nutrients and their availability to plants, after the applications to soil of saturated-MRCs.

On the opposite point of view, however, any wastewater might contain relevant concentrations of both organic (antibiotics, herbicides, pesticides, etc.) and inorganic contaminants (e.g. heavy metals), as well as pathogenic microbial strains. This is true for any industrial stream including wastewater produced at farm level or in food-transformation industries. It is really important to control the wastewater, and in case include secondary processes to avoid the presence of contaminants in the solid material, before eventual reuse in agricultural soils. Organic contaminants (such as pharmaceuticals and other emerging pollutants) could undergo biodegradation and bioanodic oxidation, according to their recalcitrance (Domínguez-Garay et al., 2016). Specific assays should assess the fate of specific contaminants in MRCs systems, to avoid possible accumulation on the solid material, by adsorption. Regarding inorganic contaminants, their possible occurrence at significant concentrations in wastewater might hinder the possibility to directly re-use the materials after MRCs' life cycle, as soil conditioners. In such cases, MRC separators/electrodes could be thought as 'sponges' for soluble heavy metals and post-treated, for their extraction. In any of such cases, specific characterization (according to local regulations on soil improvers, composts, growing media, etc.) should be performed on MRCs-derived materials, to assess the presence of contaminants and pathogens, before their use as soil conditioners.

6. Conclusions

METs built with low-cost, biogenic and biocompatible materials, can recover carbon and nutrients from organic-rich wastewater streams coming from farming and agro-industrial productions. At the end of the operational period of MRCs, becoming saturated by micro and macronutrients, electrodes would be reused as organic-mineral fertilizers, in a circular economy concept. In soil applications, the possibility of interactions of electro-active METs components (as e-biochar) with soil microbiome, rhizosphere and plants roots, opens a new research frontier that might be called electro-fertilization. The concept of MRCs could strongly increase the possibility of the scaling-up of this technology; starting from organic scraps obtaining resource and preserving the soil in a view of circular economy.

Acknowledgment

This work was financed by the SIR 2014 Grant (PROJECT RBSI14JKU3, BiofuelcellAPP), Italian Ministry of University and Research (MIUR) and by the Research Fund for the Italian Electrical System in compliance with the Decree of March 19th, 2009.

References

Ajayi, F.F., Weigele, P.R., 2012. A terracotta bio-battery. Bioresour. Technol. 116, 86–91. doi:10.1016/j.biortech.2012.04.019

An, J., Li, N., Wan, L., Zhou, L., Du, Q., Li, T., Wang, X., 2017. Electric field induced salt precipitation into activated carbon air-cathode causes power decay in microbial fuel cells. Water Res. 123, 369–377. doi:10.1016/j.watres.2017.06.087

Arashiro, L.T., Montero, N., Ferrer, I., Acién, F.G., Gómez, C., Garfí, M., 2018. Life cycle assessment of high rate algal ponds for wastewater treatment and resource recovery. Sci. Total Environ. 622–623, 1118–1130. doi:10.1016/J.SCITOTENV.2017.12.051

Behera, M., Ghangrekar, M.M., 2011. Electricity generation in low cost microbial fuel cell made up of earthenware of different thickness. Water Sci. Technol. 64, 2468–2473. doi:10.2166/wst.2011.822

Behera, M., Jana, P.S., Ghangrekar, M.M., 2010. Performance evaluation of low cost microbial fuel cell fabricated using earthen pot with biotic and abiotic cathode. Bioresour. Technol. 101, 1183–1189. doi:10.1016/j.biortech.2009.07.089

Brown, P., Saa, S., 2015. Biostimulants in agriculture. Front. Plant Sci. 6, 671. doi:10.3389/fpls.2015.00671

Brussaard, L., de Ruiter, P.C., Brown, G.G., 2007. Soil biodiversity for agricultural sustainability. Agric. Ecosyst. Environ. 121, 233–244. doi:10.1016/j.agee.2006.12.013

Carlsson, H., Aspegren, H., Lee, N., Hilmer, A., 1997. Calcium phosphate precipitation in biological phosphorus removal systems. Water Res. 31, 1047–1055. doi:10.1016/S0043-1354(96)00282-5

Carroll, D., 1959. Ion Excahnge in Clays and Other Minerals. Bull. Geol. Soc. Am. 70, 749–780. doi:10.1130/0016-7606(1959)70

Catal, T., Bermek, H., Liu, H., 2009. Removal of selenite from wastewater using microbial fuel cells. Biotechnol. Lett. 31, 1211–1216. doi:10.1007/s10529-009-9990-8

Chen, Q., Pu, W., Hou, H., Hu, J., Liu, B., Li, J., Cheng, K., Huang, L., Yuan, X., Yang, C., Yang, J., 2018. Activated microporous-mesoporous carbon derived from chestnut shell as a sustainable anode material for high performance microbial fuel cells. Bioresour. Technol. 249, 567–573. doi:10.1016/j.biortech.2017.09.086

Chen, S., He, G., Hu, X., Xie, M., Wang, S., Zeng, D., Hou, H., Schröder, U., 2012. A Three-Dimensionally Ordered Macroporous Carbon Derived From a Natural Resource as Anode for Microbial Bioelectrochemical Systems. ChemSusChem 5, 1059–1063. doi:10.1002/cssc.201100783

Chen, S., Rotaru, A.-E., Shrestha, P.M., Malvankar, N.S., Liu, F., Fan, W., Nevin, K.P., Lovley, D.R., 2014. Promoting interspecies electron transfer with biochar. Sci. Rep. 4, 5019. doi:10.1038/srep05019

Chen, X., Gao, Y., Hou, D., Ma, H., Lu, L., Sun, D., Zhang, X., Liang, P., Huang, X., Ren, Z.J., 2017. The Microbial Electrochemical Current Accelerates Urea Hydrolysis for Recovery of Nutrients from Source-Separated Urine. Environ. Sci. Technol. Lett. 4, 305–310. doi:10.1021/acs.estlett.7b00168

Cheng, S., Liu, H., Logan, B.E., 2006. Increased power generation in a continuous flow MFC with advective flow through the porous anode and reduced electrode spacing. Environ. Sci. Technol. 40, 2426–2432. doi:10.1021/es051652w

Chouler, J., Bentley, I., Vaz, F., O'Fee, A., Cameron, P.J., Di Lorenzo, M., 2017. Exploring the use of cost-effective membrane materials for Microbial Fuel Cell based sensors. Electrochim. Acta 231, 319–326. doi:10.1016/j.electacta.2017.01.195

Cindrella, L., Kannan, A.M., Lin, J.F., Saminathan, K., Ho, Y., Lin, C.W., Wertz, J., 2009. Gas diffusion layer for proton exchange membrane fuel cells-A review. J. Power Sources. doi:10.1016/j.jpowsour.2009.04.005

Clauwaert, P., Aelterman, P., Pham, T.H., De Schamphelaire, L., Carballa, M., Rabaey, K., Verstraete, W., 2008. Minimizing losses in bio-electrochemical systems: the road to applications. Appl. Microbiol. Biotechnol. 79, 901–913. doi:10.1007/s00253-008-1522-2

Colombo, A., Marzorati, S., Lucchini, G., Cristiani, P., Pant, D., Schievano, A., 2017. Assisting cultivation of photosynthetic microorganisms by microbial fuel cells to enhance nutrients recovery from wastewater. Bioresour. Technol. 237, 240–248. doi:10.1016/j.biortech.2017.03.038

Cristiani, P., Carvalho, M.L., Guerrini, E., Daghio, M., Santoro, C., Li, B., 2013. Cathodic and anodic biofilms in Single Chamber Microbial Fuel Cells. Bioelectrochemistry 92, 6–13. doi:10.1016/j.bioelechem.2013.01.005

Cusick, R.D., Logan, B.E., 2012. Phosphate recovery as struvite within a single chamber microbial electrolysis cell. Bioresour. Technol. 107, 110–115. doi:10.1016/j.biortech.2011.12.038

Decesaro, A., Rampel, A., Machado, T.S., Thomé, A., Reddy, K., Margarites, A.C., Colla, L.M., 2017. Bioremediation of Soil Contaminated with Diesel and Biodiesel Fuel Using Biostimulation with Microalgae Biomass. J. Environ. Eng. 143, 04016091. doi:10.1061/(ASCE)EE.1943-7870.0001165

Dmytryk, A., Saeid, A., Chojnacka, K., 2014. Biosorption of microelements by Spirulina: towards technology of mineral feed supplements. ScientificWorldJournal. 2014, 356328. doi:10.1155/2014/356328

Domínguez-Garay, A., Boltes, K., Esteve-Núñez, A., 2016. Cleaning-up atrazine-polluted soil by using Microbial Electroremediating Cells. Chemosphere 161, 365–371. doi:10.1016/J.CHEMOSPHERE.2016.07.023

El-Fouly, M.M., Fawzi, A.F.A., Abou El-Nour, E.A.A., Zeidan, M.S., Firgany, A.H., 2015. African Journal of Agricultural Research Impact of long-term intensive cropping under continuous tillage and unbalanced use of fertilizers on soil nutrient contents in a small holding village 10, 4850–4857. doi:10.5897/AJAR2015.10499

Erable, B., Féron, D., Bergel, A., 2012. Microbial catalysis of the oxygen reduction reaction for microbial fuel cells: A review. ChemSusChem 5, 975–987. doi:10.1002/cssc.201100836

Faheed, F.A. (Sohag U. (Egypt). B.D.., Fattah, Z.A. (Sohag U. (Egypt). B.D.., 2008. Journal of agriculture and social sciences., Journal of Agriculture and Social Sciences (Pakistan). Friends Science Publishers.

Fischer, F., Bastian, C., Happe, M., Mabillard, E., Schmidt, N., 2011. Microbial fuel cell enables phosphate recovery from digested sewage sludge as struvite. doi:10.1016/j.biortech.2011.02.089

Gajda, I., Greenman, J., Melhuish, C., Ieropoulos, I., 2015a. Self-sustainable electricity production from algae grown in a microbial fuel cell system. Biomass and Bioenergy 82, 87–93. doi:10.1016/J.BIOMBIOE.2015.05.017

Gajda, I., Greenman, J., Melhuish, C., Santoro, C., Li, B., Cristiani, P., Ieropoulos, I., 2014. Water formation at the cathode and sodium recovery using Microbial Fuel Cells (MFCs). Sustain. Energy Technol. Assessments 7, 187–194. doi:10.1016/j.seta.2014.05.001

Gajda, I., Stinchcombe, A., Greenman, J., Melhuish, C., Ieropoulos, I., 2017. Microbial fuel cell ??? A novel self-powered wastewater electrolyser for electrocoagulation of heavy metals. Int. J. Hydrogen Energy 42, 1813–1819. doi:10.1016/j.ijhydene.2016.06.161

Gajda, I., Stinchcombe, A., Greenman, J., Melhuish, C., Ieropoulos, I., 2015b. Ceramic MFCs with internal cathode producing sufficient power for practical applications. Int. J. Hydrogen Energy 40, 14627–14631. doi:10.1016/j.ijhydene.2015.06.039

Ghadge, A.N., Ghangrekar, M.M., 2015. Development of low cost ceramic separator using mineral cation exchanger to enhance performance of microbial fuel cells. Electrochim. Acta 166, 320–328. doi:10.1016/j.electacta.2015.03.105

Ghadge, A.N., Jadhav, D.A., Pradhan, H., Ghangrekar, M.M., 2015. Enhancing waste activated sludge digestion and power production using hypochlorite as catholyte in clayware microbial fuel cell. Bioresour. Technol. 182, 225–231. doi:10.1016/j.biortech.2015.02.004

Grossman, J.M., O'Neill, B.E., Tsai, S.M., Liang, B., Neves, E., Lehmann, J., Thies, J.E., 2010. Amazonian Anthrosols Support Similar Microbial Communities that Differ Distinctly from Those Extant in Adjacent, Unmodified Soils of the Same Mineralogy. Microb. Ecol. 60, 192–205. doi:10.1007/s00248-010-9689-3

Guerrini, E., Cristiani, P., Trasatti, S.P.M., 2013. Relation of anodic and cathodic performance to pH variations in membraneless microbial fuel cells. Int. J. Hydrogen Energy 38, 345–353. doi:10.1016/j.ijhydene.2012.10.001

Gustavsson, J., Food and Agriculture Organization of the United Nations., ASME/Pacific Rim Technical Conference and Exhibition on Integration and Packaging of MEMS, N., 2011. Global

food losses and food waste : extent, causes and prevention : study conducted for the International Congress "Save Food!" at Interpack 2011 Du ̈sseldorf, Germany. Food and Agriculture Organization of the United Nations.

Hu, J., Zeng, C., Liu, G., Luo, H., Qu, L., Zhang, R., 2018. Magnetite nanoparticles accelerate the autotrophic sulfate reduction in biocathode microbial electrolysis cells. Biochem. Eng. J. 133, 96–105. doi:10.1016/J.BEJ.2018.01.036

Huang, L., Guo, R., Jiang, L., Quan, X., Sun, Y., Chen, G., 2013. Cobalt leaching from lithium cobalt oxide in microbial electrolysis cells. Chem. Eng. J. 220, 72–80. doi:10.1016/j.cej.2012.12.092

Huggins, T., Wang, H., Kearns, J., Jenkins, P., Ren, Z.J., 2014. Biochar as a sustainable electrode material for electricity production in microbial fuel cells. Bioresour. Technol. 157, 114–119. doi:10.1016/j.biortech.2014.01.058

Ieropoulos, I., Pasternak, G., Greenman, J., 2017. Urine disinfection and in situ pathogen killing using a Microbial Fuel Cell cascade system. PLoS One 12, 1–12. doi:10.1371/journal.pone.0176475

Jiang, D., Curtis, M., Troop, E., Scheible, K., McGrath, J., Hu, B., Suib, S., Raymond, D., Li, B., 2011. A pilot-scale study on utilizing multi-anode/cathode microbial fuel cells (MAC MFCs) to enhance the power production in wastewater treatment. Int. J. Hydrogen Energy 36, 876–884. doi:10.1016/j.ijhydene.2010.08.074

Kadier, A., Simayi, Y., Abdeshahian, P., Azman, N.F., Chandrasekhar, K., Kalil, M.S., 2016. A comprehensive review of microbial electrolysis cells (MEC) reactor designs and configurations for sustainable hydrogen gas production. Alexandria Eng. J. doi:10.1016/j.aej.2015.10.008

Kappler, A., Wuestner, M.L., Ruecker, A., Harter, J., Halama, M., Behrens, S., 2014. Biochar as an Electron Shuttle between Bacteria and Fe(III) Minerals. Environ. Sci. Technol. Lett. 1, 339–344. doi:10.1021/ez5002209

Kelly, P.T., He, Z., 2014. Nutrients removal and recovery in bioelectrochemical systems: A review. Bioresour. Technol. 153, 351–360. doi:10.1016/j.biortech.2013.12.046

Kim, Y., Logan, B.E., 2013. Microbial desalination cells for energy production and desalination. Desalination, New Directions in Desalination 308, 122–130. doi:10.1016/j.desal.2012.07.022

Kloss, S., Zehetner, F., Dellantonio, A., Hamid, R., Ottner, F., Liedtke, V., Schwanninger, M., Gerzabek, M.H., Soja, G., 2012. Characterization of Slow Pyrolysis Biochars: Effects of Feedstocks and Pyrolysis Temperature on Biochar Properties. J. Environ. Qual. 41, 990. doi:10.2134/jeq2011.0070

Kratz, S., Schick, J., Schnug, E., 2016. Trace elements in rock phosphates and P containing mineral and organo-mineral fertilizers sold in Germany. doi:10.1016/j.scitotenv.2015.08.046

Le Corre, K.S., Valsami-Jones, E., Hobbs, P., Parsons, S.A., 2009. Phosphorus Recovery from Wastewater by Struvite Crystallization: A Review. Crit. Rev. Environ. Sci. Technol. 39, 433–477. doi:10.1080/10643380701640573

Lefebvre, O., Neculita, C.M., Yue, X., Ng, H.Y., 2012. Bioelectrochemical treatment of acid mine drainage dominated with iron. J. Hazard. Mater. 241–242, 411–417. doi:10.1016/j.jhazmat.2012.09.062

Lehmann, J., Joseph, S., 2015. Biochar for Environmental Management: Science, Technology and Implementation. Taylor & Francis.

Lehmann, J., Rillig, M.C., Thies, J., Masiello, C.A., Hockaday, W.C., Crowley, D., 2011. Biochar effects on soil biota – A review. Soil Biol. Biochem. 43, 1812–1836. doi:10.1016/j.soilbio.2011.04.022

Li, W.-W., Sheng, G.-P., Liu, X.-W., Yu, H.-Q., 2011. Recent advances in the separators for microbial fuel cells. Bioresour. Technol. 102, 244–252. doi:10.1016/j.biortech.2010.03.090

Logan, B.E., Hamelers, B., Rozendal, R., Schröder, U., Keller, J., Freguia, S., Aelterman, P., Verstraete, W., Rabaey, K., 2006. Microbial fuel cells: Methodology and technology. Environ. Sci. Technol. doi:10.1021/es0605016

Lu, Z., Chang, D., Ma, J., Huang, G., Cai, L., Zhang, L., 2015. Behavior of metal ions in bioelectrochemical systems: A review. J. Power Sources 275, 243–260. doi:10.1016/j.jpowsour.2014.10.168

Luo, H., Teng, W., Liu, G., Zhang, R., Lu, Y., 2017. Sulfate reduction and microbial community of autotrophic biocathode in response to acidity. Process Biochem. 54, 120–127. doi:10.1016/J.PROCBIO.2016.12.025

Luo, S., Berges, J.A., He, Z., Young, E.B., 2017. Algal-microbial community collaboration for energy recovery and nutrient remediation from wastewater in integrated photobioelectrochemical systems. Algal Res. 24, 527–539. doi:10.1016/J.ALGAL.2016.10.006

Malko, D., Kucernak, A., Lopes, T., 2016. In situ electrochemical quantification of active sites in Fe–N/C non-precious metal catalysts. Nat. Commun. 7, 13285. doi:10.1038/ncomms13285

Marzorati, S., Goglio, A., Trasatti, S., n.d. Giant Cane as Low-cost Material for Microbial Fuel Cells Architectures 114.

Marzorati, S., Schievano, A., Colombo, A., Lucchini, G., Cristiani, P., 2018. Ligno-cellulosic materials as air-water separators in low-tech microbial fuel cells for nutrients recovery. doi:10.1016/j.jclepro.2017.09.142

Masiello, C.A., Chen, Y., Gao, X., Liu, S., Cheng, H.Y., Bennett, M.R., Rudgers, J.A., Wagner, D.S., Zygourakis, K., Silberg, J.J., 2013. Biochar and microbial signaling: Production conditions determine effects on microbial communication. Environ. Sci. Technol. 47, 11496–11503. doi:10.1021/es401458s

Muñoz, R., Guieysse, B., 2006. Algal-bacterial processes for the treatment of hazardous contaminants: A review. Water Res. 40, 2799–2815. doi:10.1016/j.watres.2006.06.011

Nancharaiah, Y. V., Venkata Mohan, S., Lens, P.N.L., 2015. Metals removal and recovery in bioelectrochemical systems: A review. Bioresour. Technol. 195, 102–114. doi:10.1016/j.biortech.2015.06.058

Noori, M.T., Jain, S.C., Ghangrekar, M.M., Mukherjee, C.K., 2016. Biofouling inhibition and enhancing performance of microbial fuel cell using silver nano-particles as fungicide and cathode catalyst. doi:10.1016/j.biortech.2016.08.061

O'Neill, B., Grossman, J., Tsai, M.T., Gomes, J.E., Lehmann, J., Peterson, J., Neves, E., Thies, J.E., 2009. Bacterial community composition in Brazilian Anthrosols and adjacent soils characterized using culturing and molecular identification. Microb. Ecol. 58, 23–35. doi:10.1007/s00248-009-9515-y

Oliot, M., Etcheverry, L., Mosdale, A., Basseguy, R., Délia, M.L., Bergel, A., 2017. Separator electrode assembly (SEA) with 3-dimensional bioanode and removable air-cathode boosts microbial fuel cell performance. J. Power Sources 356, 389–399. doi:10.1016/j.jpowsour.2017.03.016

Pandey, P., Shinde, V.N., Deopurkar, R.L., Kale, S.P., Patil, S.A., Pant, D., 2016. Recent advances in the use of different substrates in microbial fuel cells toward wastewater treatment and simultaneous energy recovery. Appl. Energy 168, 706–723. doi:10.1016/j.apenergy.2016.01.056

Papaharalabos, G., Greenman, J., Melhuish, C., Santoro, C., Cristiani, P., Li, B., Ieropoulos, I., 2013. Increased power output from micro porous layer (MPL) cathode microbial fuel cells (MFC), in: International Journal of Hydrogen Energy. Pergamon, pp. 11552–11558. doi:10.1016/j.ijhydene.2013.05.138

Park, D.H., Zeikus, J.G., 2003. Improved fuel cell and electrode designs for producing electricity from microbial degradation. Biotechnol. Bioeng. 81, 348–355. doi:10.1002/bit.10501

Pasternak, G., Greenman, J., Ieropoulos, I., 2015. Comprehensive Study on Ceramic Membranes for Low-Cost Microbial Fuel Cells. ChemSusChem 88–96. doi:10.1002/cssc.201501320

Plaza, C., Courtier-Murias, D., Fernández, J.M., Polo, A., Simpson, A.J., 2013. Physical, chemical, and biochemical mechanisms of soil organic matter stabilization under conservation tillage systems: A central role for microbes and microbial by-products in C sequestration. Soil Biol. Biochem. 57, 124–134. doi:10.1016/j.soilbio.2012.07.026

Qian, K., Kumar, A., Zhang, H., Bellmer, D., Huhnke, R., 2015. Recent advances in utilization of biochar. Renew. Sustain. Energy Rev. doi:10.1016/j.rser.2014.10.074

Ralebitso-Senior, T.K., Orr, C.H., 2016. Biochar Application: Essential Soil Microbial Ecology. Elsevier Science.

Rao, A.N.S., Venkatarangaiah, V.T., 2014. rt ic le in Pr es s rt ic le in Pr es. J. Electrochem. Sci. Eng. 4, 315–326. doi:10.5599/jese.2014.

Reddy, K.R., Yargicoglu, E.N., Yue, D., Yaghoubi, P., 2014. Enhanced Microbial Methane Oxidation in Landfill Cover Soil Amended with Biochar. J. Geotech. Geoenvironmental Eng. 140, 04014047. doi:10.1061/(ASCE)GT.1943-5606.0001148

Rojas-Carbonell, S., Artyushkova, K., Serov, A., Santoro, C., Matanovic, I., Atanassov, P., 2018. Effect of pH on the Activity of Platinum Group Metal-Free Catalysts in Oxygen Reduction Reaction. doi:10.1021/acscatal.7b03991

Rondon, M.A., Lehmann, J., Ramírez, J., Hurtado, M., 2007. Biological nitrogen fixation by common beans (Phaseolus vulgaris L.) increases with bio-char additions. Biol. Fertil. Soils 43, 699–708. doi:10.1007/s00374-006-0152-z

Rozendal, R.A., Hamelers, H.V.M., Buisman, C.J.N., 2006. Effects of membrane cation transport on pH and microbial fuel cell performance. Environ. Sci. Technol. 40, 5206–5211. doi:10.1021/es060387r

Santini, M., Guilizzoni, M., Lorenzi, M., Atanassov, P., Marsili, E., Fest-, S., Cristiani, P., Santoro, C., Fest-Santini, S., Cristiani, P., Santoro, C., 2015. Three-dimensional X-ray microcomputed tomography of carbonates and biofilm on operated cathode in single chamber microbial fuel cell. Biointerphases 031009, 1–10. doi:10.1116/1.4930239

Santini, M., Marzorati, S., Fest-Santini, S., Trasatti, S., Cristiani, P., 2017. Carbonate scale deactivating the biocathode in a microbial fuel cell. J. Power Sources 356, 400–407. doi:10.1016/j.jpowsour.2017.02.088

Santoro, C., Arbizzani, C., Erable, B., Ieropoulos, I., 2017. Microbial fuel cells: From fundamentals to applications. A review. J. Power Sources. doi:10.1016/j.jpowsour.2017.03.109

Santoro, C., Artyushkova, K., Gajda, I., Babanova, S., Serov, A., Atanassov, P., Greenman, J., Colombo, A., Trasatti, S., Ieropoulos, I., Cristiani, P., 2015. Cathode materials for ceramic based microbial fuel cells (MFCs). Int. J. Hydrogen Energy 40, 14706–14715. doi:10.1016/j.ijhydene.2015.07.054

Santoro, C., Babanova, S., Artyushkova, K., Atanassov, P., Greenman, J., Cristiani, P., Trasatti, S., Schuler, A.J., Li, B., Ieropoulos, I., 2014. The effects of wastewater types on power generation and phosphorus removal of microbial fuel cells (MFCs) with activated carbon (AC) cathodes. Int. J. Hydrogen Energy 39, 21796–21802. doi:10.1016/J.IJHYDENE.2014.09.167

Santoro, C., Ieropoulos, I., Greenman, J., Cristiani, P., Vadas, T., Mackay, A., Li, B., 2013. Power generation and contaminant removal in single chamber microbial fuel cells (SCMFCs) treating human urine. Int. J. Hydrogen Energy 38, 11543–11551. doi:10.1016/j.ijhydene.2013.02.070

Sato, T., Qadir, M., Yamamoto, S., Endo, T., Zahoor, A., 2013. Agricultural Water Management Global, regional, and country level need for data on wastewater generation, treatment, and use. Agric. Water Manag. 130, 1–13. doi:10.1016/j.agwat.2013.08.007

Shaaban, M.M., 2001. Nutritional Status and Growth of Maize Plants as Affected by Green Microalgae as Soil Additives. Online J. Biol. Sci. 1, 475–479.

Swarnalakshmi, K., Prasanna, R., Kumar, A., Pattnaik, S., Chakravarty, K., Shivay, Y.S., Singh, R., Saxena, A.K., 2013. Evaluating the influence of novel cyanobacterial biofilmed biofertilizers on soil fertility and plant nutrition in wheat. Eur. J. Soil Biol. 55, 107–116. doi:10.1016/j.ejsobi.2012.12.008

Tao, H.C., Liang, M., Li, W., Zhang, L.J., Ni, J.R., Wu, W.M., 2011. Removal of copper from aqueous solution by electrodeposition in cathode chamber of microbial fuel cell. J. Hazard. Mater. 189, 186–192. doi:10.1016/j.jhazmat.2011.02.018

Ucar, D., Zhang, Y., Angelidaki, I., 2017. An Overview of Electron Acceptors in Microbial Fuel Cells. Front. Microbiol. 8, 643. doi:10.3389/fmicb.2017.00643

Virdis, B., Rabaey, K., Rozendal, R.A., Yuan, Z., Rg Keller, J., 2010. Simultaneous nitrification, denitrification and carbon removal in microbial fuel cells. doi:10.1016/j.watres.2010.02.022

Virdis, B., Rabaey, K., Yuan, Z., Rg Keller, J., 2008. Microbial fuel cells for simultaneous carbon and nitrogen removal. doi:10.1016/j.watres.2008.03.017

Walter, X.A., Greenman, J., Taylor, B., Ieropoulos, I.A., 2015. Microbial fuel cells continuously fuelled by untreated fresh algal biomass. Algal Res. 11, 103–107. doi:10.1016/J.ALGAL.2015.06.003

Wang, K., Sheng, Y., Cao, H., Yan, K., Zhang, Y., 2017. A novel microbial electrolysis cell (MEC) reactor for biological sulfate-rich wastewater treatment using intermittent supply of electric field. Biochem. Eng. J. 125, 10–17. doi:10.1016/J.BEJ.2017.05.009

Winfield, J., Chambers, L.D., Rossiter, J., Greenman, J., Ieropoulos, I., 2015. Urine-activated origami microbial fuel cells to signal proof of life. J. Mater. Chem. A 3, 7058–7065. doi:10.1039/C5TA00687B

Winfield, J., Chambers, L.D., Rossiter, J., Greenman, J., Ieropoulos, I., 2014. Towards disposable microbial fuel cells: Natural rubber glove membranes. Int. J. Hydrogen Energy 39, 21803–21810. doi:10.1016/j.ijhydene.2014.09.071

Winfield, J., Chambers, L.D., Rossiter, J., Ieropoulos, I., 2013a. Comparing the short and long term stability of biodegradable, ceramic and cation exchange membranes in microbial fuel cells. Bioresour. Technol. 148, 480–6. doi:10.1016/j.biortech.2013.08.163

Winfield, J., Gajda, I., Greenman, J., Ieropoulos, I., 2016. A review into the use of ceramics in microbial fuel cells. Bioresour. Technol. 215, 296–303. doi:10.1016/j.biortech.2016.03.135

Winfield, J., Greenman, J., Huson, D., Ieropoulos, I., 2013b. Comparing terracotta and earthenware for multiple functionalities in microbial fuel cells. Bioprocess Biosyst. Eng. 36, 1913–1921. doi:10.1007/s00449-013-0967-6

Winfield, J., Ieropoulos, I., Rossiter, J., Greenman, J., Patton, D., 2013c. Biodegradation and proton exchange using natural rubber in microbial fuel cells. Biodegradation 24, 733–739. doi:10.1007/s10532-013-9621-x

Wu, H., Lai, C., Zeng, G., Liang, J., Chen, J., Xu, J., Dai, J., Li, X., Liu, J., Chen, M., Lu, L., Hu, L., Wan, J., 2017. The interactions of composting and biochar and their implications for soil amendment and pollution remediation: a review. Crit. Rev. Biotechnol. 37, 754–764. doi:10.1080/07388551.2016.1232696

Wu, X., Modin, O., 2013. Ammonium recovery from reject water combined with hydrogen production in a bioelectrochemical reactor. Bioresour. Technol. 146, 530–536. doi:10.1016/j.biortech.2013.07.130

Xiao, L., Young, E.B., Berges, J.A., He, Z., 2012. Integrated photo-bioelectrochemical system for contaminants removal and bioenergy production. Environ. Sci. Technol. 46, 11459–11466. doi:10.1021/es303144n

Xie, S., Liang, P., Chen, Y., Xia, X., Huang, X., 2011. Simultaneous carbon and nitrogen removal using an oxic/anoxic-biocathode microbial fuel cells coupled system. Bioresour. Technol. 102, 348–354. doi:10.1016/j.biortech.2010.07.046

Yanai, Y., Toyota, K., Okazaki, M., 2007. Effects of charcoal addition on N2O emissions from soil resulting from rewetting air-dried soil in short-term laboratory experiments: Original article. Soil Sci. Plant Nutr. 53, 181–188. doi:10.1111/j.1747-0765.2007.00123.x

Yu, W., Zhang, D., Graham, N.J.D., 2017. Membrane fouling by extracellular polymeric substances after ozone pre-treatment: Variation of nano-particles size. Water Res. 120, 146–155. doi:10.1016/j.watres.2017.04.080

Yu, Y., Han, Y., Lou, B., Zhang, L., Han, L., Dong, S., 2016. A miniature origami biofuel cell based on a consumed cathode. Chem. Commun. 52, 13499–13502. doi:10.1039/C6CC07466A

Yuan, H., Deng, L., Qi, Y., Kobayashi, N., Tang, J., 2014. Nonactivated and Activated Biochar Derived from Bananas as Alternative Cathode Catalyst in Microbial Fuel Cells. Sci. World J. 2014, 832850. doi:10.1155/2014/832850

Yuan, Y., Yuan, T., Wang, D., Tang, J., Zhou, S., 2013a. Sewage sludge biochar as an efficient catalyst for oxygen reduction reaction in an microbial fuel cell. Bioresour. Technol. 144, 115–120. doi:10.1016/j.biortech.2013.06.075

Yuan, Y., Zhou, S., Tang, J., 2013b. In situ investigation of cathode and local biofilm microenvironments reveals important roles of OH- and oxygen transport in microbial fuel cells. Environ. Sci. Technol. 47, 4911–4917. doi:10.1021/es400045s

Zamora, P., Georgieva, T., Ter Heijne, A., Sleutels, T.H.J.A., Jeremiasse, A.W., Saakes, M., Buisman, C.J.N., Kuntke, P., 2017. Ammonia recovery from urine in a scaled-up Microbial Electrolysis Cell. J. Power Sources 356, 491–499. doi:10.1016/j.jpowsour.2017.02.089

Zhang, B., Feng, C., Ni, J., Zhang, J., Huang, W., 2012. Simultaneous reduction of vanadium (V) and chromium (VI) with enhanced energy recovery based on microbial fuel cell technology. J. Power Sources 204, 34–39. doi:10.1016/j.jpowsour.2012.01.013

Zhang, F., He, Z., 2012. Integrated organic and nitrogen removal with electricity generation in a tubular dual-cathode microbial fuel cell. Process Biochem. 47, 2146–2151. doi:10.1016/j.procbio.2012.08.002

Zhang, L., Ma, J., Liu, Y., Li, D., Shi, H., Cai, L., 2012. Improvement of biological total phosphorus release and uptake by low electrical current application in lab-scale bio-electrochemical reactors. Bioelectrochemistry 88, 92–96. doi:10.1016/j.bioelechem.2012.06.005

Zhang, Y., Noori, J.S., Angelidaki, I., 2011. Simultaneous organic carbon, nutrients removal and energy production in a photomicrobial fuel cell (PFC). Energy Environ. Sci. 4, 4340. doi:10.1039/c1ee02089g.

Chapter 2 - Microbial recycling cells, first steps into a new type of microbial electrochemical technologies, aimed at recovering nutrients from wastewater

Andrea Goglio[a], Stefania Marzorati[a], Laura Rago[a], Deepak Pant[b], Pierangela Cristiani[c], Andrea Schievano[a]*

a e-Bio Center, University of Milan, Via Celoria 2, 20133 Milan, Italy

b Separation & Conversion Technology, Flemish Institute for Technological Research (VITO), Boeretang 200, 2400 Mol, Belgium

c Ricerca del Sistema Energetico, Via Rubattino 54, 20134 Milano

* Corresponding author: andrea.schievano@unimi.it

Published in:

Goglio A., Marzorati S., Rago L., Pant D., Cristiani P., Schievano A., 2019. Microbial recycling cells: first steps into a new type of microbial electrochemical technologies, aimed at recovering nutrients from wastewater. Bioresource Technology. doi:10.1016/j.biortech.2019.01.039

Abstract

The aim of this work were to study terracotta-based porous air-water separators (4 mm thickness) in microbial recycling cells (MRCs) fed with cow manure (CM), swine manure (SM) and dairy wastewater (DW). Over 125 days, besides the removal of 60-90% of soluble-COD, considerable fractions of the main macronutrients (C, N, P, K, Fe, Mn, Ca, Mg) were removed from the wastewater and deposited on the terracotta separators as both inorganic salts and biomass deposits. Water evaporation at air-water interface as well as the high cathodic pH (10-12), induced by oxygen reduction to OH-, were the predominant factors leading to precipitation. The separators were saturated of up to 10 g per kg of terracotta of the main macronutrients, with negligible concentrations of the main inorganic contaminants. These materials could be directly reused as nutrients-enriched solid conditioners for agricultural soils.

Keywords

Nutrients recovery; wastewater treatment; microbial electrochemical technologies; microbial recycling cells; terracotta.

1. Introduction

It is estimated that demand for food will continue to increase, as a result of population growth, but at the same time, food production will increasingly face huge constraints, such as water scarcity, soil desertification and the increase of fertilizers prices (Gustavsson et al., 2011). The recovery of organic/inorganic carbon and mineral nutrients from wastewater derived from food production chains is widely recognized as a priority to minimize environmental contamination, while treating water (Verstraete et al., 2009). Nutrients removal from water solution and recovery as renewed fertilizers is of particular interest, because of the potential threat of natural water bodies over-fertilization, the limited mining resource and high cost associated with nutrient production (Rittmann et al., 2011).

Research in the field of microbial electrochemical technologies (METs) has been tremendously expanding over the last decades. In microbial fuel cells (MFCs), microporous layers (MPL) electrodes have been used to separate the liquid in the anodic chamber from the air-exposed cathodic surface, while increasing cathodic surface area (Ghadge et al., 2015) and guaranteeing low ionic resistance (Cristiani et al., 2013). Usually, MPL are based on blends of hydrophobic polymeric binders (PTFE, Nafion® etc. and conductive powders used as catalysts (carbon black, metals etc.), spread on carbon fibres or other conductive materials (Santoro et al., 2015).

Several mechanisms have been limiting the development of applicable MFC technologies. Over relatively short-term operations (50-100 days), clogging and biofouling due to organic materials as well as inorganic salts deposition on electrodes surfaces, strongly invalidate cell performances (Santini et al., 2017). When the system works properly, pH tends to increase in close proximity of the cathode (pH > 9), leading to inorganic salts (carbonates, phosphates, hydroxides, etc.) precipitation and accumulation as a layer on cathode's surface, thus impeding charge transfer processes (Santini et al., 2015). In addition, water evaporation from MPLs or separators at air-water interface contributes to salts precipitation (Santini et al., 2017). Combined biofouling and salts depositions tend to clog the MPL, increasing the internal resistance and deactivating the system (Mathuriya and Pant, 2018).

In a recent review, we proposed a new type of METs, called Microbial Recycling Cells (MRCs), dedicated to recover carbon and nutrients from wastewater, to fabricate bio-based renewable fertilizers (Goglio et al., 2019). In MRCs, biofouling and salts deposition are viewed as a key-advantages: air-exposed cathodes and MPLs could be used as 'sponges' for recalcitrant organic matter, inorganic carbon and nutrients. Once saturated (typically after 40-80 days) (Santini et al., 2017), MRC modules could be substituted with new ones and fully recycled as organic-mineral fertilizers for agricultural soil application. This concept works only if alternative air-water separators and electrodes were fabricated using low-cost, largely available, biogenic/biocompatible and fully-recyclable materials (e.g. clay, biomass, etc.). The whole material of MRCs (enriched by mineral/organic forms of nutrients) can return to soil, and thereby return to the original status, i.e. be 'recycled'.

Air-water interface porous separators based on polymeric binders (used in MPLs) and membranes would not be applicable for these purposes, because of their high cost and their incompatibility with the environment. Alternatively, terracotta (earthenware) was introduced in recent studies as low-cost and biocompatible air-water separator (Pasternak et al., 2015). Terracotta cylinders were used to build air-cathode MFCs and to separate anode and cathode (Winfield et al., 2016). Current generation in cylindrical terracotta-MFCs contributed to produce an electro-osmotic drag of water molecules, cations migration and catholyte formation in proportion to MFC power performance (Gajda et al., 2014). Also, increased pH and water evaporation from the air-water interface contributed to salts precipitation and heavy metals recovery (Gajda et al., 2015). Moreover, the possibility of recovering macronutrients (e.g. N, P, K, Ca, Mg, etc.) was shown. Ammonium ions are dragged by electro-osmotic forces to the cathodic surface, where pH is typically higher than pH=9; under such conditions ammonia

stripping (Santoro et al., 2013) and struvite precipitation (Merino-Jimenez et al., 2017) can be favoured to recover nutrients as insoluble salts. Ammonium was also reported to undergo anaerobic or microaerophilic oxidations to nitrites and nitrates, respectively at the anode and at the air-water interface. Successive denitrification was also reported, in presence of bioavailable organic carbon (Virdis et al., 2010). Finally, suspended organic matter can be recovered by biofouling. Organic matter in the form of microbial cells, extracellular polymeric substances, complex and recalcitrant organic molecules usually contribute to create layers on the electrode or separator surfaces (Noori et al., 2016).

In this work, the behaviour of terracotta air-water separators was studied in lab-scale MRCs, proposing them as mean of organic matter and nutrients recovery from organic-rich wastewater streams coming from agro-food chains, such as farming and cheese production.

2. Materials and Methods

In this experiment, terracotta separators were studied as air-water interface in air-cathode MRCs, to recover organic matter, inorganic carbon and nutrients, from 3 different types of wastewater: cow manure (CM), swine manure (SM) and dairy-industry wastewater (DW) (sampled from a cheese factory). Six MRCs (built with glassy lab-scale reactors) were studied over a relatively long period (125 days): 2 trials for each wastewater were run using terracotta as air-water separator. Hereafter, each couple of reactors were called, according to the wastewater fed, CM, SM and DW.

The electrochemical performances of the MRCs and the water losses by evaporation from the air-water interface were measured over time. The fate of soluble fractions of organic matter and nutrients was monitored in the liquid phase along the observed period. Particular attention was focused on nitrogen and its main forms. Microbial analyses were performed to describe the system. At the end of the experiment, terracotta separators and cathodes were characterized, to evaluate the enrichment in organic matter and nutrients achieved along the test.

2.1 MRCs configuration

Figure S1 shows the MRC reactors configurations with the terracotta separator. The MFCs were built with simple Pyrex® bottles of 120 mL volume.

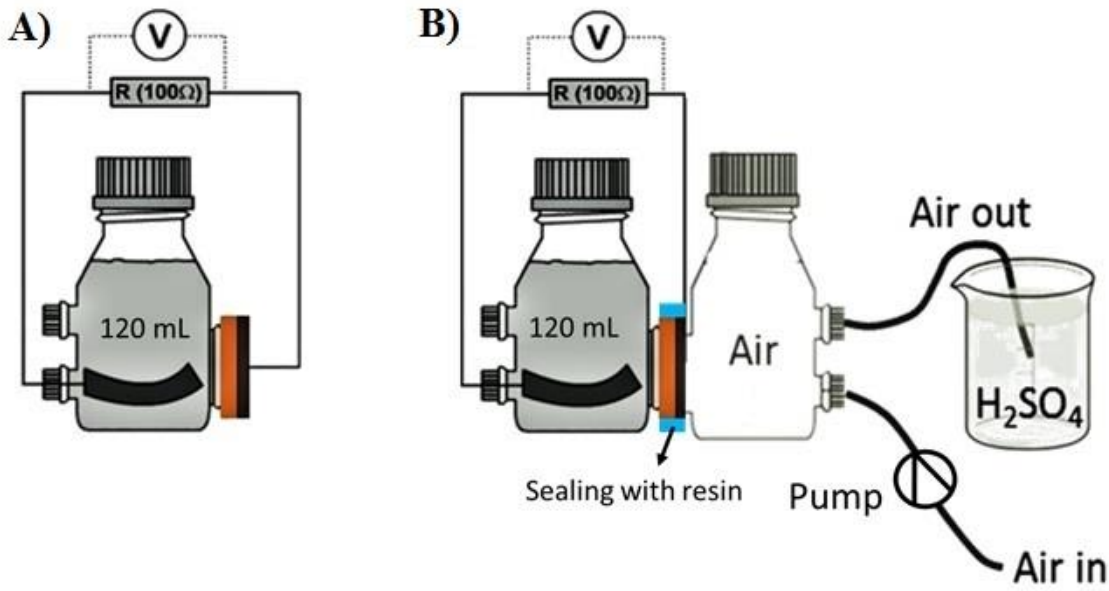

Figure S1 – A) Configuration of the lab-scale reactors used as MRCs in this experiment. B) Configuration of the control experiment for the evaluation of ammonia volatilization: a counter-chamber is placed on the air-side and a forced (peristaltic pump) air flow (1-3 mL min^{-1}) is bubbled in a H_2SO_4 (1 N) solution. NH_4+ is determined in the solution every 10 days of operation.

The anode was fabricated using 30 cm^2 of plain carbon cloth (SAATI C1, Appiano Gentile, Italy) and it was rolled on itself to increase the chance of bacterial growth and placed at the bottom of the cell. Cathodes (25 cm^2 of geometric area, 1 g of dry weight) were made of carbon cloth, modified by a MPL made of activated carbon/PTFE mixture (10:7 on dry weight basis) (Santoro et al., 2015). Cathodes were positioned at the air-exposed side of the terracotta separator. Anode and cathode were electrically connected through an external load of 100 Ω and positioned at a distance of 2 cm. Connections were insulated with non-conductive epoxy resin. The terracotta separator was characterised by 4 mm of thickness, pore size in the range 60-500 nm, 10 g of dry weight and 25 cm^2 of geometric area, between the anolyte and the cathode.

2.2 BET analysis

The Brunauer-Emmett-Teller (BET) specific surface area was obtained from N_2 adsorption/desorption isotherms at 77 K using a Micromeritics Tristar II apparatus (Tristar II 3020). Specific surface area was determined by the instrumental software. Porosity distribution

was evaluated for each sample by using BJH method. Before measurements, sample powders were heat-treated at 150 °C for 4 h under a N_2 flow to remove adsorbed foreign species.

2.3 Inoculation and experimental set-up

All MRCs were inoculated with raw wastewaters and then always fed in parallel with identical timing. The chemical characteristics of the raw wastewaters and their content of organic matter and nutrients are reported in Table 1.

Table 1 – Characterization of the wastewater streams. All values for elements refer to soluble fractions (after filtration with 0.45 μm mesh). Values in brackets report the ratios TOC/element.

Parameter	Unit	CM	SM	DW
pH		7.46	8.35	8.16
El. Conductivity	mS cm^{-2}	9.88	8.54	1.48
COD	g L^{-1}	12.5	5.66	0.84
TOC	mg L^{-1}	4.22	1.87	0.28
Macronutrients				
TKN	g L^{-1} (TOC/N)	1.55 (2.7)	1.92 (1)	0.1 (2.8)
P	mg L^{-1} (TOC/P)	262 (16.1)	114 (16.4)	12 (23.3)
K	g L^{-1} (TOC/K)	2.92 (1.4)	1.72 (1.1)	0.51 (0.5)
Ca	mg L^{-1} (TOC/Ca)	853 (4.9)	151 (12.4)	91 (3.1)
Mg	mg L^{-1} (TOC/Mg)	265 (15.9)	39 (47.9)	16 (17.5)
Fe	mg L^{-1} (TOC/Fe)	44 (95.9)	5 (347)	1 (280)
Mn	mg L^{-1} (TOC/Mn)	8 (527.5)	2 (935)	<1 (-)
Micronutrients / heavy metals				
Ni	mg L^{-1}	0.02	0.008	<0.001

Cu	mg L^{-1}	0.2	0.11	0.011
Zn	mg L^{-1}	2.4	1.6	0.018
As	mg L^{-1}	0.003	0.003	<0.001
Cd	mg L^{-1}	0.004	<0.001	<0.001
Pb	mg L^{-1}	<0.001	<0.001	<0.001

The first batch cycle was considered as an acclimation. When the current dropped over time, the reactors were emptied and fed again with fresh wastewater. After this, the reactors were periodically refilled with additional wastewater, to compensate the volume decrease due to water evaporation through air-water separators. At day 56, sodium acetate (3 g L^{-1}) was added as standard substrate, to compare MRCs parameters for clarity, the experimental operations are resumed in Table 2.

Table 2 – Experimental set-up and wastewater feeding conditions (refilled volumes after water evaporation)

Operation days	**Feeding**			
		CM	**SM**	**DW**
Day 0	Raw sewage (mL)	120	120	120
Day 34	Raw sewage (mL)	120	120	120
Day 56	Sodium acetate (g_{COD} L^{-1})	2.34	2.34	2.34
Day 72	Raw sewage (mL)	15	24	68
Day 85	Raw sewage (mL)	13	34	57
Day 100	Raw sewage (mL)	10	24	59
Day 117	Raw sewage (mL)	1	6	33

2.4 Electrochemical analyses

Throughout the duration of the experiment, several electrochemical measurements were carried out: current density trends, open circuit potential (OCP) and power curves. For each MRC, the potential difference across an external load of 100 Ω was recorded every 20 minutes using a multichannel Data Logger (Graphtech midi Logger GL820). The anodic OCP were periodically measured versus an Ag/AgCl reference electrode after 30 min equilibration time.

Power curves were periodically recorded with a two-electrode configuration. Before each electrochemical measurement, 1 h of equilibration time was found necessary to allow the system, disconnected from the data logger, to reach OCP. The anode was set as working electrode and the cathode as reference electrode. A linear sweep polarization (scan rate v=0.010 V min-1) was recorded from the cell OCP to 10 mV. The power was calculated by P = I • V, normalized by the cathodic area and plotted vs current density.

2.5 Physico-chemical characterization of the process

Water evaporation from the air-water interfaces were monitored over time by weight measurements of the reactors. pH profiles near the air-water interface were measured, using a potentiometric microelectrodes and the measurements were performed under open circuit conditions and the positions of microelectrode were determined by a computer controlled micromechanical movement system (NSC-A1 Stepper Motor Controller, Newmark Systems Inc.) (Guerrini et al., 2013).

The chemical composition of the wastewaters along the cycles was monitored by several parameters: Chemical oxygen demand (COD), Total Kjeldahl Nitrogen (TKN) and total content of the main macronutrients (P, Ca, K, Mg, Fe, Mn) analysed by inductively coupled plasma mass spectrometry (ICP-MS). In addition, the enrichment in these elements on the terracotta separators was determined at the end of the experiment.

2.6 Evaluation of nitrogen removal mechanisms

A control experiment was run in double with SM, to evaluate the different mechanisms that play a role in Nitrogen removal. NH_3 evaporation from the air-water interface was evaluated as shown in Figure S1). A counter-chamber was used on the cathode side, to capture and quantify NH3 emissions due to stripping at the cathode. A trap of H_2SO_4 was used to entrap ammonia and quantify it at the end of the experiment. $N\text{-}NH_4^+$, $N\text{-}NO_2^-$ and $N\text{-}NO_3^-$ were monitored in the liquid phase along a batch cycle (days 34-56). Sodium acetate (3 g L^{-1}) was

spiked in the solution, to evaluate denitrification mechanisms in presence of a readily-available carbon source as electron donor.

2.7 Details of analytical procedures

The soluble fractions of COD (sCOD) in the anolyte were determined using spectrophotometric method after specific reactions using test kits (Hach Company, Loveland, CO, USA). The samples were filtered (0.2 μm Nylon filters) before COD analysis. TKN was determined by titration of ammonium ions, after digestion in concentrated H_2SO_4, as indicated by standard methods (APHA). ICP-MS was used to measure total and soluble contents of single elements in the anolyte, membrane and electrodes. For total content, weighted amounts of materials were digested by a microwave digestion system (Anton Paar MULTIWAVE-ECO) in Teflon tubes filled with 10 mL of 65% HNO_3 by applying a one-step temperature ramp (210 °C reached in 10 min and maintained for further 10 min). After 20 min of cooling time, the mineralized samples were transferred in polypropylene test tubes. Both solutions of mineralized samples and extracted soluble fractions were diluted 1:100 with 0.3 M HNO_3 in MILLI-Q water and the concentration of elements was measured by ICP-MS (BRUKER Aurora-M90 ICP-MS).

2.8 DNA extraction

DNA samples were obtained from the air-cathode MRCs at the end of the experiment. Small pieces of anodic carbon cloth were cut and combined for DNA extraction. The terracotta biofilm sample obtained scraping the cathodic biofilm from the internal side of the terracotta with a sterile spatula. Total DNA was extracted from approximately 0.25 g of samples using a PowerBiofilm DNA Isolation Kit (MoBio Laboratories, Inc., Carlsbad, CA) according to the manufacturer's instructions. Quantity and quality of the DNA were measured by spectrophotometer (BioPhotometer, Eppendorf,). DNA was visualized under UV light in a 1% gel electrophoresis with TBE 0.5× (Tris-Borate 50 mM; EDTA 0.1 mM; pH 7.5–8).

2.9 Illumina MiSeq sequencing

Genomic DNA was PCR amplified using a two-stage “targeted amplicon sequencing (TAS)” protocol (Bybee et al., 2011; Green et al., 2015). The sequencing was performed as described previously (Rago et al., 2018). The primers contained 5’ common sequence tags (known as common sequence 1 and 2, CS1 and CS2) as described previously (Moonsamy et al., 2013). Two primer sets were used for this study, including CS1_341F/CS2_806R (Bacteria), CS1_ARC344F/CS2_ARC806R (Archaea) (Rago et al., 2017).

Library preparation and pooling was performed at the DNA Services (DNAS) facility, Research Resources Center (RRC), University of Illinois at Chicago (UIC). Sequencing was performed at the W.M. Keck Center for Comparative and Functional Genomics at the University of Illinois at Urbana-Champaign (UIUC).

Forward and reverse reads were merged using PEAR (Zhang et al., 2014). Ambiguous nucleotides and primer sequences were trimmed (quality threshold p = 0.01). After trimming, reads containing internal ambiguous nucleotides, lacking either primer and/or shorter than 300 bp were discarded. Chimeric sequences were identified with the USEARCH algorithm (Edgar, 2010) and removed. Further analyses were performed with the QIIME tools (J Gregory Caporaso et al., 2010). Sequences with a similarity higher than 97% were grouped in Operational Taxonomic Units (OTUs) and representative sequences for each OTU were aligned to the SILVA SSU Ref dataset (Quast et al., 2013) using the PyNAST method (J. G. Caporaso et al., 2010). In Figure 5 are represented the taxonomic affiliations at phylum and genus level and the respective relative abundance, included in the OTU tables.

3. Results and Discussion

3.1 Current generation trends

The current density trends during the operational period of 125 days are plotted in Figures 1 - A, B, and C.

CM reactors produced peak current densities of around 500 mA m-2 (referred to cathodic geometric area), along 125 operation days. After 8 days of lag phase during acclimation, the system started producing current. After acclimation, the current density slightly increased and remained almost constant for 15 days. During the cycle fed with sodium acetate, the current production of CMs reached around 300 mA m-2, lasting less than previous cycles. SM systems produced an oscillating current signal along 125 days, with peak current density of around 800 mA m-2, the highest among the tested wastewater types. This is likely due to the fact that SM was richer in readily bioavailable sCOD, as compared to CM. DWs showed trends current densities around 150 mA m-2. A significant current production began at day 4, yielding the maximum current density. Then, for this system, throughout its operational period, current density was lower, consistent with the lower concentrations of sCOD (844 mgCOD L-1, Table 1).

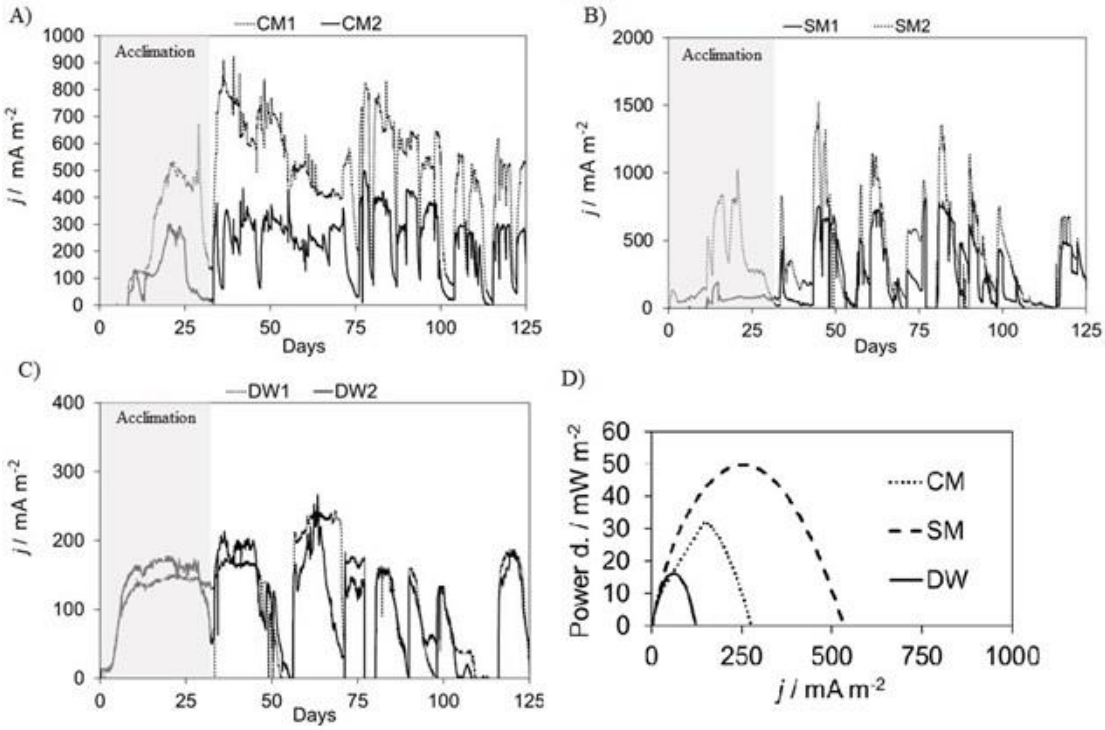

Figure 1 – Current density trends during 125 days observation of the MRCs fed with cow-manure (A), swine manure (B), dairy wastewater (C). Power curves (D) representing average electrochemical performances of the tested MRCs systems, along the observed period.

After day 75, all MRCs in parallel showed decreasing trends of current density. This might be attributable to deposition phenomena of inorganic salts as well as of organic matter. Santini et al. (Santini et al., 2017) recently observed a biocathode inactivation over time due to carbonate scale deposition in air-cathode MFCs, already after around 40-50 days. Previous works by the same group (Santini et al., 2015) documented the presence of a thick layer of carbonate formed as a consequence of the alkalinity induced by the ORR on cathodes operated for long time in single chamber MFCs. In particular, this phenomenon was found to significantly hinder MFC performances after around 60 days of operation.

3.2 Electrochemical characterizations

Figure 1-D shows the power density curves measured on all reactors, during average current production (avoiding peaks of electrochemical performances). The power density curves evidenced a consistent difference among the different wastewaters confirming the data

obtained during the monitoring of the current density trend. In Table 3 some electrochemical parameters are summarized, to characterize the MRCs.

Table 3 – Electrochemical characteristics, average water evaporation rates and pH within the terracotta and cathodic materials, along the observation period

Reactors		CM	SM	DW
Coulombic Efficiency	% on initial sCOD	16	16	28
Average power density	mW m^{-2}	33	67	17
Anodic OCP	mV *vs* Ag/AgCl	-492	-498	-523
pH at the terracotta separator		9.66±0.11	9.69±0.04	9.75±0.01
pH at the cathode		9.37±0.04	9.64±0.20	10.02±0.02

The terracotta separator was likely impeding proper electrolytic contact of the cathode with the solution, resulting in relatively low power densities. In this experiment, the plain terracotta surface was particularly exposed to air contact, and consistent water evaporation (Figure 2, Section 3.3) probably contributed to high electrolytic resistance. However, the goal of MRCs systems is not to produce high amount of electricity and energy harvesting, while to recover nutrients and treat wastewater. The observed power densities might be sufficient to induce cations migration and other mechanisms to drive salts sequestration from the anolyte. In addition, other configurations of terracotta MRCs (e.g. cylindrical, with the cathode placed in the internal surface) were reported with much lower internal resistance (Santoro et al., 2015). Therefore, there is quite sufficient space for optimizing these systems and maximizing the electrochemical performances.

The configuration also affected the CE, that achieved relatively low percentages on the bioavailable sCOD (Table 3). The consistent water evaporation occurred and the high electrolytic resistance likely affected the CE. Also, the direct contact of wastewater with air through the porosity of terracotta, probably favoured carbon removal through aerobic respiration, both at the terracotta-air interface and at the liquid surface. Other carbon-consuming processes, such as denitrification at the terracotta interface might have counted in lowering CE (Rago et al., 2018). An optimized configuration would in this case improve the

contribution of bioelectrochemical paths towards COD removal. However, it is important to keep in mind that in MRCs, unlike in MFCs, achieving high CE is not the goal and might not correspond to high nutrients recovery. The electrochemical process is one of the mechanisms that can drive to organics mineralization and nutrients removal from the liquid phase. These aspects are further discussed in Section 3.3 and 3.4.

3.3 - Effects of the MRCs on the wastewater liquid phase

Cumulative water evaporation trends are reported in Figure 2-A for all MRCs along the observed period.

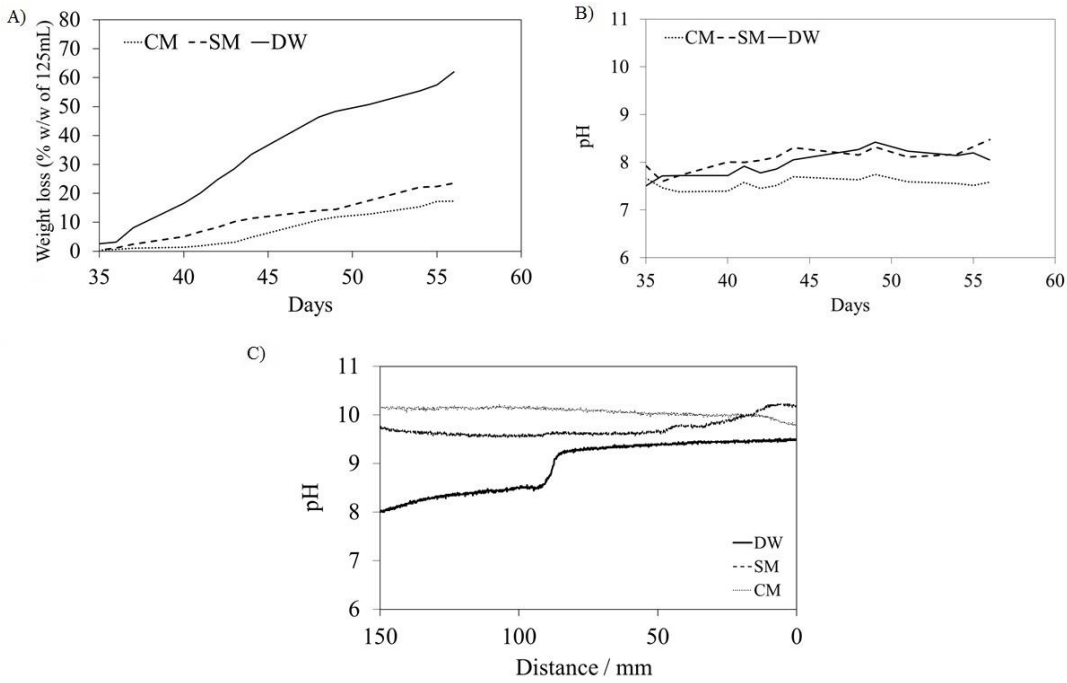

Figure 2 - Weight loss due to water evaporation (A), pH trends in the bulk liquid of anodic chambers (B), along a representative period (days 35 – 55) and pH profiles in the vicinity (15 mm, measured by microelectrodes) of the anodic side of the terracotta separator of MRCs fed by cow manure, swine manure and dairy wastewater (C).

Water evaporation resulted in all cases considerable and it was favored with more diluted wastewaters (such as DW), while higher organic matter concentrations (CM and SM) likely limited water evaporation throught the porous separator. Indeed, water evaporation rates were comparable for CM and SM, while being relatively higher in DW (Table 3).

Evaporation was mainly favored by the relatively big pores of the terracotta layer. Figure 3 reports the distribution of pores volume and surface area on pores diameters.

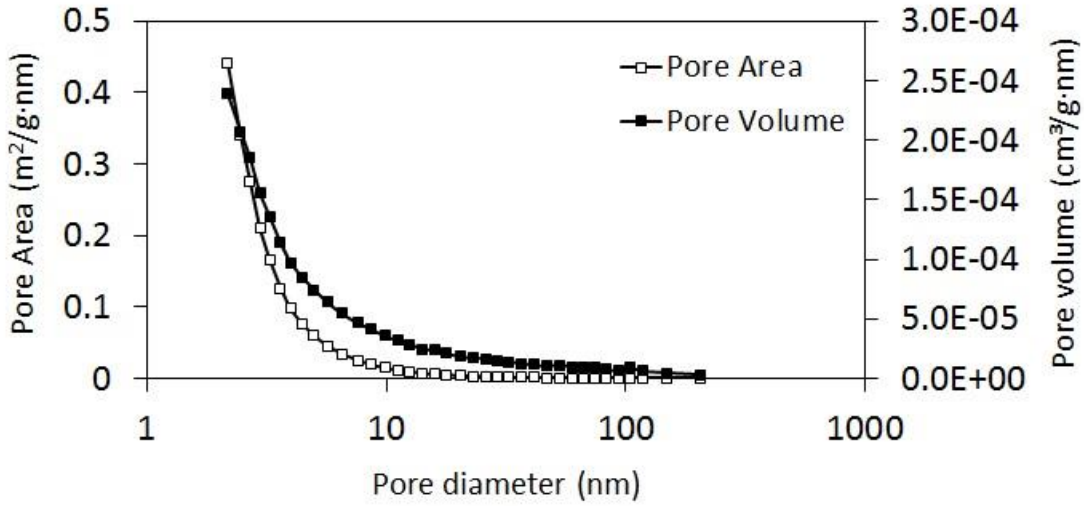

Figure 3 – BET analysis of the terracotta separator: pore area and volume distribution over pore diameters.

The total specific surface area was around 0.868 m^2 g^{-1} with pore size in the range. Thus, the total surface area available to air-water exposure in each MRC reactor (each terracotta separator weighted around 10 g) was around 8.7 m^2. Water capillary diffusion, as well as electro-osmotic forces induced by the electric field, as previously found in other experiments (Gajda et al., 2015), contributed to water evaporation in contact with this relatively abundant surface area.

Figure 2-B shows that the pH in the anodic compartment remained almost constant in CMs and slightly higher for both in SMs and DWs. Depending on the buffer capacity of the liquid medium, slight increases in pH is typical in anaerobic environments, as result of volatile fatty acids consumption (De Bere, 2000). Regardless to the type of wastewater, the pH never exceeded pH 8.5 in the bulk liquid phase.

Contrarily, in the vicinity of the air-water interface, the pH profile measured by microelectrodes was found always over pH 9 (Figure 2-C). In the vicinity of the terracotta separators on the anodic side, pH was nearly 10 in all MRC systems. Although the presence of terracotta separators induced a considerable internal resistance to the electrochemical cells (Table 3), the current densities obtained by all MRCs were sufficient to induce consistent pH

increases (around pH 10) at the air-water interface. The pH profile within the pores of the terracotta separators and at the cathode were indirectly measured at the end of the experiment, after shredding the material. In all cases, the pH in the separator as well as at the cathode was in the range 9.5 – 10 (Table 3). This phenomenon was already observed in previous experiments and linked to the surplus of hydroxyl free radicals liberated by incomplete the cathodic oxygen reduction reaction (Winfield et al., 2016). Measurements on the catholyte formed by electroosmotic water transport through terracorra separators was found up to pH 13 (Gajda et al., 2015). This is indeed a key point to favor inorganic salt depositions (e.g. struvite, Ca-carbonates, Mg-Carbonates, organophosphates, oxydes and other salts etc.) within the internal porosity of the terracotta separators (Santini et al., 2015;). This finding encourages the use of MRCs, made of low-cost air-water porous separators, to improve nutrients recovery as precipitated salts within the terracotta separators and at the cathode.

Figure 4 shows that in all MRCs a considerable amount of the soluble fractions (after filtration at 2 µm) of organic carbon (measured as COD), N, P, Ca, K, Mg, Fe and Mn and were removed from all the wastewaters.

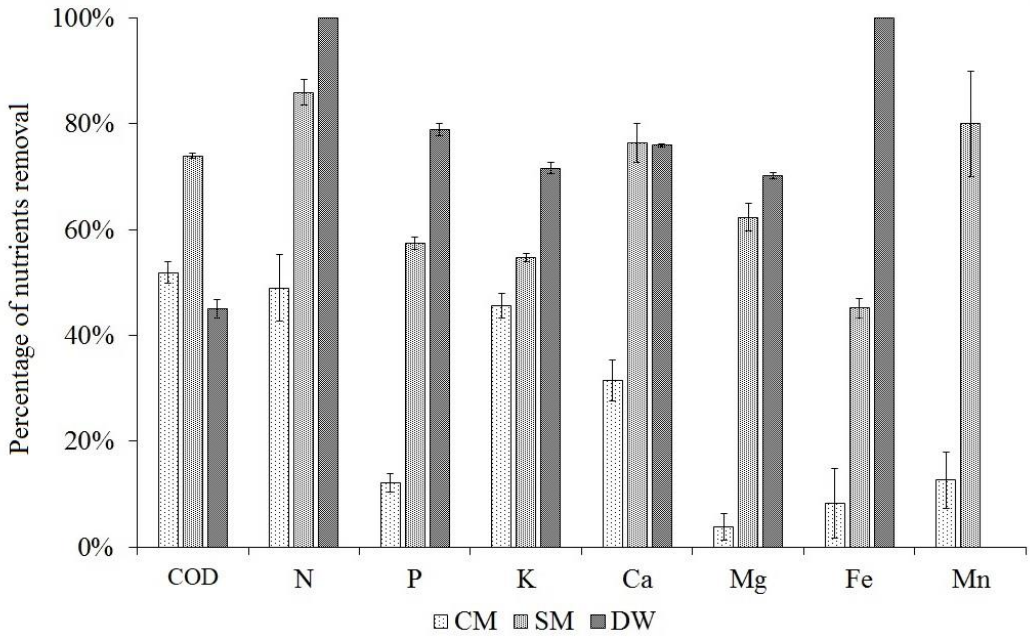

Figure 4 – Removal efficiency of the soluble fraction of the main nutrients from the bulk liquid phase after 125 days, reported as percentage of the initial concentration in the wastewater. MRCs were fed with cow manure (A), swine manure (B) and dairy wastewater (C). Error bars stand for standard deviations of duplicate experiments, under identical conditions.

Although the configuration and architecture of this lab-scale system was not optimized, organic carbon (as soluble-COD) was removed with relatively high efficiency.

Soluble nitrogen forms were removed from the liquid phase with particular efficiency. In the case of DW, N was undetectable at the end of the experiment, while SM showed over 80% removal and CM around 50% (Figure 4). A discussion on the possible fate of N forms is reported more in detail in the following Section 3.4. The soluble forms of the other elements (P, Ca, K, Mg, Fe, Mn) could be removed from the bulk liquid in principle by: a) precipitation of inorganic salts on the air-water interface separators, thanks to high pH and locally increased concentrations due to water evaporation; b) deposition of organic fractions on the terracotta inner surface; c) fouling, precipitation or settling in the anodic chamber. Moreover, are also investigated the amount of the heavy metals in the Table 5 to confirm the possibility to use these kinds of wastewater as a substrate for a treatment to recovery nutrients.

3.4 – Nitrogen removal and analysis of microbial communities

Total nitrogen was efficiently removed from the liquid phase (Figure 4). To give more details to this aspect, ammonium ion removal was measured along one batch cycle (days 34-54) of the SM-systems.

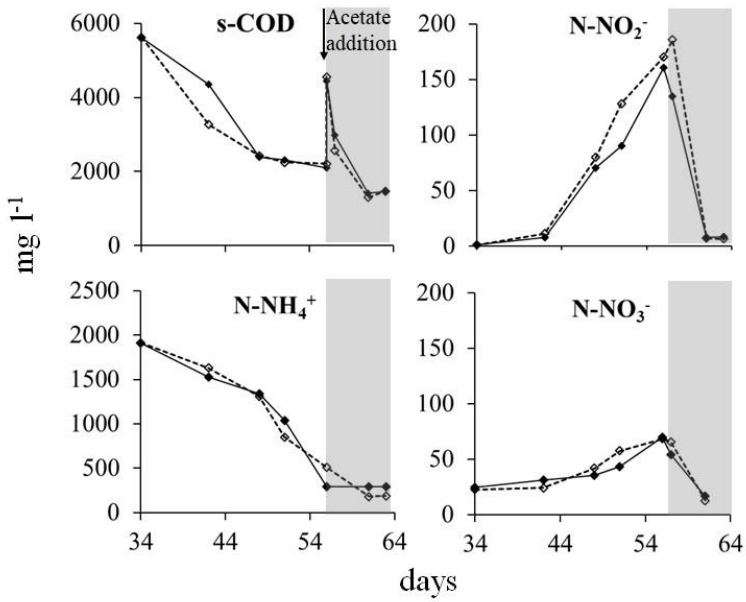

Figure 5 – Removal trends for sCOD, N-NH4+, N-NO2- and N-NO3- from the liquid phase of MRCs fed with swine manure, in duplicate experiments under identical conditions. One representative batch cycle (days 34 – 56) followed by a spike of sodium acetate (3 g L-1) are shown.

Figure 5 reports the trends of replicate experiments, together with the trends of sCOD, $N\text{-}NH_4^+$, $N\text{-}NO_2^-$ and $N\text{-}NO_3^-$ concentrations. Ammonium removal followed a parallel trend to sCOD.

The ammonium removal rate observed in Figure 5 could be ascribable to a range of different phenomena: a) anaerobic ammonium oxidation (Anammox) (Qiao et al., 2018); b) exoelectrogenic NH_4^+ oxidation at the anode (Yang et al., 2017); c) nitrification at the air-water interface, thanks to the possible presence of microaerophilic conditions in the biofilm at the water-side surface of the terracotta separator; d) gaseous ammonia (NH^3) stripping at the terracotta/cathode, due to high pH and water evaporation (Figure 2) and e) nitrogen deposition as part of precipitated salts (e.g. struvite) either on the terracotta or within the anodic chamber.

After around 20 days (from day 34 to day 56), $N\text{-}NH_4^+$ reached the minimum value (around 300 mg L^{-1}) while nitrites and nitrates concentrations increased to their maximum values (up to 180 mg L^{-1} and 65 mg L^{-1} respectively). After the acetate addiction of 3 g L^{-1}, the accumulation of nitrites and nitrates showed a fast inversion of tendency, and they decreased till the lowest values after five days (day 61) in both cases. In this period, it was present also a fast consumption of sCOD (from around 4.6 to 1.3 g L^{-1}). These results indicate that the nitrifying metabolism was associated to the presence of sCOD and so probably it was carried out by heterotrophic microorganisms. The amount of $N\text{-}NH_3$ captured by the H_2SO_4 trap was modest. It corresponded to around 4% of the initial amount of $N\text{-}NH_4^+$ in the wastewater. Instead, nitrification and denitrification processes showed that the highest contribution to N removal is given by nitrification/denitrification processes in the reactor. The ability of air-exposed MFC systems (with a range of different architectures) to remove mineral nitrogen was often reported (Sotres et al., 2016; Virdis et al., 2010; Yan et al., 2012; Zhao et al., 2016).

Here, anodic and terracotta biofilms were analysed to investigate the microbial community. The cathodic microbiology was not analysed because the pore dimension of terracotta substantially impeded microorganism to reach the external surface of the separator and the cathode, as already explained in a previous study (Rago et al., 2018). In fact, pores diameters were below 100 nm by 99.9% of their total volume. Around 50% of pores volume was associated to pores diameters <2 nm (micropores), while the other half was in the range 2 – 50 nm (mesopores) (Figure 3).

Both anodic and terracotta biofilm communities showed a similar composition, as shown by the phylum representation (Figure 6A).

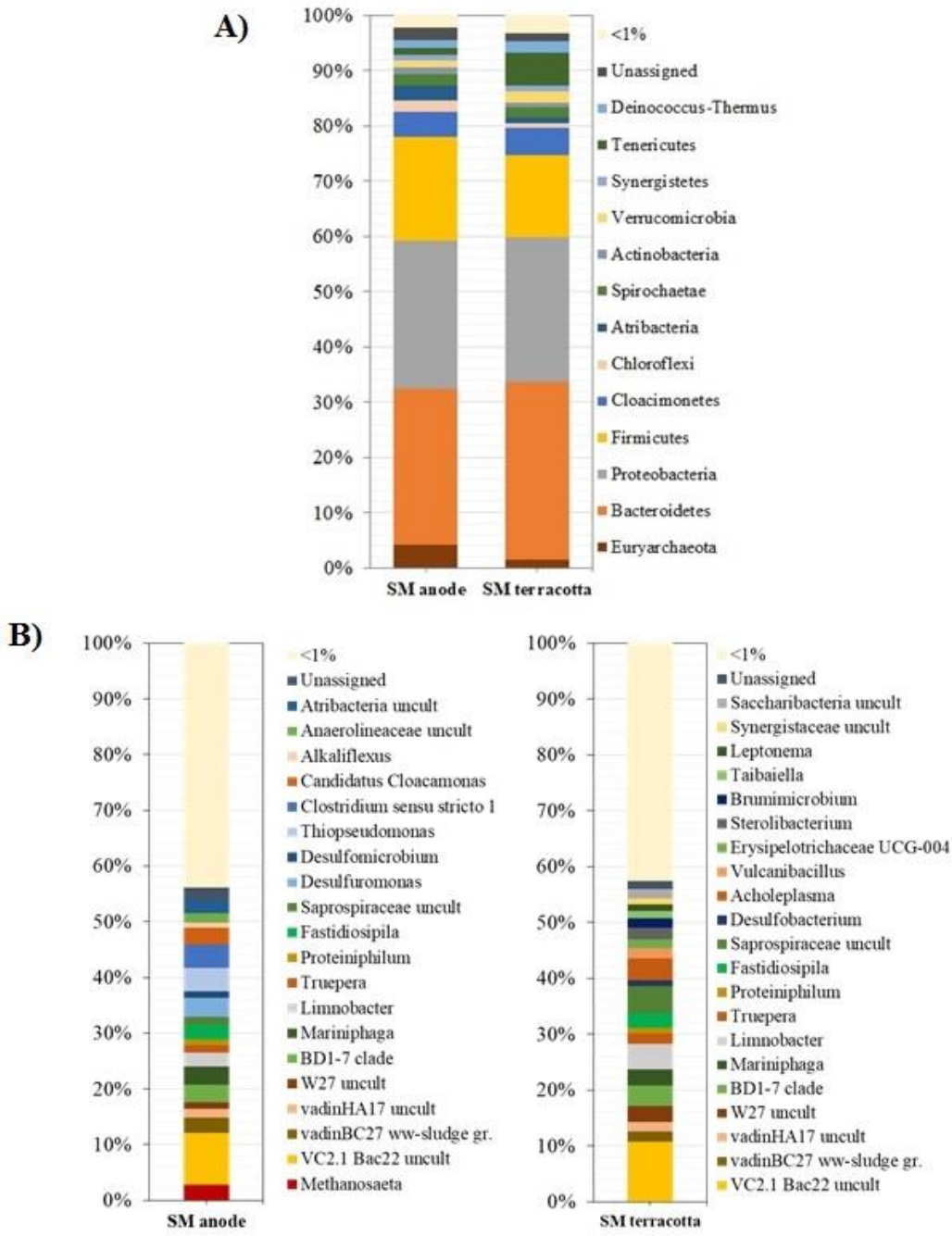

Figure 6 - Phylum (A) and genus (B) representation of Illumina 16S rRNA gene amplicon sequencing, resulted from biofilms sampled on the anode and on the terracotta-water interface, in MRCs fed with swine manure.

Bacteriodetes phylum was the main present (28-31% in anodic and terracotta biofilms) and it is often reported in the MFC biofilms (Montpart et al., 2018). Proteobacteria (around 25% in both samples) and Firmicutes (18-14% in anodic and terracotta biofilms) phyla are commonly found in bioelectrochemical systems playing important roles in bioelectroactive biofilms (Logan, 2009; Parameswaran et al., 2010; Patil et al., 2009; Rago et al., 2016). Euryachaeota phylum was more present in anodic (4%) than in terracotta community (1%) indicating that the anodic condition was more anoxic (Rago et al., 2017).

The genus representation (Figure 6B) showed that fermentative bacteria mainly colonized both communities. The anodic exoelectrogenic community was more present on the anode (conductive material) than on terracotta (inert material), as already observed in a previous study (Rago et al., 2018). The main difference in composition between the two communities was the high presence of well-known electroactive genera only in the anodic community and the presence of microaerophilic and facultative microorganisms in terracotta biofilm. This exoelectrogenic community was mainly represented by Clostridium sensu stricto I (4.3%), Desulfuromonas (3.5%) Desulfomicrobium (1.1%) genera (Rago et al., 2017, 2018). On the other side, several members of Leptonema sp., Taibaiella sp., Brumimicrobium sp., Acholeplasma sp., that were present only in terracotta biofilm, were previously described as microaerophilic, or strictly or facultative aerobic Bacteria (Bowman, 2015; Brown et al., 2015; Huntemann et al., 2013; Zhang et al., 2013). These microbes might have played an important role at the air-water interface, to justify the observed efficient nitrification (Figure 5). Some facultative anaerobes or anaerobic genera retrieved in both anodic and terracotta communities (Sterolibacterium sp., Vulcanobacillus sp. and Thiopseudomonas sp.) were associated to nitrate reduction (or denitrification) process (Cai et al., 2015; Chiang et al., 2007; Tan et al., 2015), in presence of available organic carbon. This was evident after the addition of sodium acetate at day 56 (Figure 5).

Instead, the 16S rRNA gene sequencing in both the anodic and terracotta communities (with a presence higher than the 1% of the total OTUs) did not show the presence of well-known anammox or electroactive-nitrifying microorganisms (Figure 6). However, we cannot exclude that such processes might have contributed to ammonium removal. Some of the observed genera, that were not previously associated to these metabolisms, likely contributed to the observed nitrification process. For a deeper insight into these mechanisms, future experiments should aim at looking at metabolic pathways.

3.5 – Deposition of nutrients on air-water separators

In all cases, MRCs were efficient in removing most nutrients from the wastewater and one of the reasons was the deposition of salts and organic molecules on the terracotta separator. A complete balance of nutrients was not possible to be addressed in this experiment. The systems were not tight enough and, possible precipitation/settling in the anodic chamber was not taken into account. Also, the systems were not optimized to maximize nutrients deposition on the separator.

Table 4 – Total amounts of nutrients (measured as total element) recovered per kg of terracotta separators along 125 days of operation for MRCs and TOC/element ratios.

	CM	**SM**	**DW**
Mg (*g kg^{-1}*)	1.86	2.33	0.23
K (*g kg^{-1}*)	0.62	2.35	-
Ca (*g kg^{-1}*)	3.75	5.45	-
Mn (*mg kg^{-1}*)	51	164	-
Fe (*g kg^{-1}*)	2.89	9.14	2.41
P (*g kg^{-1}*)	0.20	1.05	0.38
TKN (*g kg^{-1}*)[a]	0.32	0.30	0.10
TOC *(g kg^{-1})*[b]	1.32	1.93	0.74
TOC/Mg	0.71	0.83	3.27
TOC/K	2.12	0.82	-
TOC/Ca	0.35	0.35	-
TOC/Mn	0.03	0.01	-
TOC/Fe	0.46	0.21	0.31
TOC/P	6.60	1.84	1.93
TOC/TKN	4.13	6.43	7.40

However, it is interesting to consider the amount of nutrients stored on the terracotta separators along the observed period (Table 4).

These amounts were calculated as difference of total elements measured at the end of the experiment and on the raw terracotta, before the experiment. Overall, all nutrients were recovered in comparable amounts in all the MRC systems. The terracotta separators increased their content in elements by over 10-fold, as compared to their initial amount. Ammonium and metals cations were likely to be dragged by electro-osmotic forces to the cathode, through the terracotta pores, where different mechanisms favoured their immobilization. Typically, terracotta has intrinsically high cation exchange capacity and the flux of cations to the cathode could be 'intercepted' by sorption on the terracotta. Also, the high pH in the vicinity of the cathode likely induced insoluble salts precipitation (e.g. carbonates, hydroxides) within the porous structure of terracotta.

The amount of TOC found on the terracotta was relatively low, as compared to the other elements. Especially for P, Ca, Fe, Mg and Mn, the TOC/element ratios measured on the terracotta at the end of the experiment (Table 4) were particularly low, as compared to the raw wastewater (Table 1). Thus, inorganic salts and hydroxides deposition/precipitation were probably prevalent phenomena, over organic matter fouling/deposition on the terracotta. These data evidence the selective deposition of inorganic forms of most nutrients, over organic molecules.

P is typically present in manures and wastewaters either in organic forms and/or as inorganic anions (Ekpo et al., 2016). Organic P forms could deposit on the terracotta separator or the cathode only by fouling mechanisms. Most of organic P was expected to be retained and/or settled in the anodic chamber. Inorganic forms of P, as they are found mainly as anions, were expected to be attracted to the anode, by electroosmotic forces. Possible precipitation of P as struvite at the cathode, reported in several articles to be related to high pH (Almatouq and Babatunde, 2016), probably worked only for a small fractions of total P. Phosphorous was already found to precipitate in microbial electrochemical systems (Kim et al., 2018). Struvite minerals are typically insoluble at pH>9 (Tansel et al., 2018).

Deposition of Ca and Mg is likely to happen as insoluble carbonates at pH over 9. This was already observed in several cases, at cathodic air-water interfaces in METs (Marzorati et al., 2018; Santini et al., 2017).

3.6 – Perspectives

After a terracotta separator gets saturated with organic and inorganic forms of various nutrients, it could be ready to be re-utilized as soil conditioner. Soil conditioners and amendments have the characteristic of improving physical and chemical characteristics of soil, such as its structure, making slight fertilization, facilitate water retention, cation exchange capacity and plant roots growth (Wu et al., 2016). Terracotta has the composition of clay, which is known to have high cation exchange capacity and be a good soil conditioner (Rossini-Oliva et al., 2017). Soil amendments with terracotta and other residual ceramic materials have been suggested to alleviate the soil compaction, to increase water retention, the hydraulic conductivity, the cation-exchange capacity and to improve other soil physical properties (Wu et al., 2017).

The enrichment in nutrients after the experiment in MRCs likely happens due to particularly high pH conditions and ionic concentrations during the process. The reuse of the terracotta separators, enriched of nutrients (Table 4), might bring the additional advantage of releasing macro- and micro- nutrients, once applied to agricultural soils. Once distributed as soil amendment, these nutrients would return in soluble forms, available for plant roots uptake, having a partial fertilization effect. More detailed chemical characterization and study could help in elucidate the forms and the availability of the nutrients, measured here as total content. Future study should also aim at applying these materials to soil and study their effects on plant growth.

Another important point should be assessed, as part of the MRCs concept. Any wastewater, even when produced at farm level or in food-transformation industries, might contain relevant concentrations of both organic (antibiotics, herbicides, pesticides, etc.) and inorganic contaminants (e.g. heavy metals). Organic contaminants could undergo biodegradation and bioanodic oxidation, according to their recalcitrance (Domínguez-Garay et al., 2016). Specific assays should assess the fate of specific contaminants in MRCs systems, to avoid possible accumulation on the solid material, by adsorption.

Regarding inorganic contaminants, their possible occurrence at significant concentrations in wastewater might hinder the possibility to directly re-use the materials after MRCs' life cycle, as soil conditioners. Here, the main heavy-metals (Ni, Cu, Zn, As, Cd and Pb) were measured in the wastewaters at the end of the experiment and their possible accumulation verified on the terracotta separators (Table 5). According to their provenience (farming and food-

transformation industry), substantially low concentrations of heavy metals initially were present in the tested wastewaters (Table 1).

Table 5 – Concentrations of potential inorganic contaminants recovered on the terracotta separators after their working period (125 days).

	Ni	Cu	Zn	As	Cd	Pb
Concentration on terracotta separator (mg kg^{-1})						
CM	<0.2	36.1	51.4	<0.2	<0.2	<0.2
SM	30.6	6.1	33.8	<0.2	<0.2	<0.2
DW	24.4	<0.2	7.7	1.6	<0.2	<0.2
Standards/limits for soil conditioners						
European union[1]	25	70	300	10	1	100
USA[2]	420	1500	2800	41	39	300

[1] Voluntary standard EU ECO Label for Soil improvers and growing media

[2] EPA CFR40/503 Sludge Rule

In the case of CM, most heavy-metals were likely bounded to the organic suspended fractions and tended to accumulate in the liquid phase (negative removal efficiency). Contrarily, MRCs treating SM and DW were relatively efficient in removing the large part of heavy metals. In all cases, a net increase in content was measured on the terracotta separator (Table 5). When compared to a relatively restrictive voluntary standard-limit (EU ECO Label) for Soil improvers and growing media (Table 5), the retrieved concentrations of all heavy-metals on the ceramic materials confirmed their possible direct reuse as soil conditioners. However, depending on the type of wastewater treated, these values might change and accurate characterization should be done. Eventually, post treatments to recover heavy metals from the ceramic materials might be proposed, before agricultural re-use.

4. Conclusions

The electrochemical forces generated by anodic oxidations, the local increase of cathodic pH driven by incomplete oxygen reduction reaction and local water evaporation were the main

drivers towards cation migration to the cathode and to inorganic salts or organic matter deposition on the separator. After an operational period of around 125 days, terracotta-based porous air-water separators were saturated with relatively high amounts of the main macronutrients. Terracotta is a relatively low-cost and biocompatible material, which could be directly recycled as base for organic-mineral fertilizers and soil conditioners, in agricultural applications. Further studies should elucidate in more detail a mass balance of nutrients and carbon, to better understand their organic/inorganic forms and improve deposition mechanisms.

Acknowledgements

This work was financed by the SIR 2014 Grant (PROJECT RBSI14JKU3), Italian Ministry of University and Research (MIUR) by the Research Fund for the Italian Electrical System in compliance with the Decree of March, 19th 2009. Authors thank Dr. Mariangela Longhi for BET measurements.

References

Almatouq, A., Babatunde, A.O., 2016. Concurrent phosphorus recovery and energy generation in mediator-less dual chamber microbial fuel cells: Mechanisms and influencing factors. Int. J. Environ. Res. Public Health 13. doi:10.3390/ijerph13040375

Bowman, J.P., 2015. Brumimicrobium, in: Bergey's Manual of Systematics of Archaea and Bacteria. John Wiley & Sons, Ltd, Chichester, UK, pp. 1–5. doi:10.1002/9781118960608.gbm00287

Brown, D.R., Bradbury, J.M., Johansson, K.-E., 2015. Acholeplasma, in: Bergey's Manual of Systematics of Archaea and Bacteria. John Wiley & Sons, Ltd, Chichester, UK, pp. 1–13. doi:10.1002/9781118960608.gbm01256

Cai, J., Zheng, P., Xing, Y., Qaisar, M., 2015. Effect of electricity on microbial community of microbial fuel cell simultaneously treating sulfide and nitrate. J. Power Sources 281, 27–33. doi:10.1016/j.jpowsour.2015.01.165

Chiang, Y.R., Ismail, W., Müller, M., Fuchs, G., 2007. Initial steps in the anoxic metabolism of cholesterol by the denitrifying Sterolibacterium denitrificans. J. Biol. Chem. 282, 13240–13249. doi:10.1074/jbc.M610963200

Cristiani, P., Carvalho, M.L., Guerrini, E., Daghio, M., Santoro, C., Li, B., 2013. Cathodic and anodic biofilms in Single Chamber Microbial Fuel Cells. Bioelectrochemistry 92, 6–13. doi:10.1016/j.bioelechem.2013.01.005

De Bere, L., 2000. Anaerobic digestion of solid waste: state-of-the-art. Water Sci. Technol. 41.

Domínguez-Garay, A., Boltes, K., Esteve-Núñez, A., 2016. Cleaning-up atrazine-polluted soil by using Microbial Electroremediating Cells. Chemosphere 161, 365–371. doi:10.1016/J.CHEMOSPHERE.2016.07.023

Ekpo, U., Ross, A.B., Camargo-Valero, M.A., Fletcher, L.A., 2016. Influence of pH on hydrothermal treatment of swine manure: Impact on extraction of nitrogen and phosphorus in process water. Bioresour. Technol. 214, 637–644. doi:10.1016/j.biortech.2016.05.012

Gajda, I., Greenman, J., Melhuish, C., Santoro, C., Li, B., Cristiani, P., Ieropoulos, I., 2015. Electro-osmotic-based catholyte production by Microbial Fuel Cells for carbon capture. Water Res. doi:10.1016/j.watres.2015.08.014

Gajda, I., Greenman, J., Melhuish, C., Santoro, C., Li, B., Cristiani, P., Ieropoulos, I., 2014. Water formation at the cathode and sodium recovery using Microbial Fuel Cells (MFCs). Sustain. Energy Technol. Assessments 7, 187–194. doi:10.1016/j.seta.2014.05.001

Ghadge, A.N., Jadhav, D.A., Pradhan, H., Ghangrekar, M.M., 2015. Enhancing waste activated sludge digestion and power production using hypochlorite as catholyte in clayware microbial fuel cell. Bioresour. Technol. 182, 225–231. doi:10.1016/j.biortech.2015.02.004

Goglio, A., Tucci, M., Rizzi, B., Colombo, A., Cristiani, P., Schievano, A., 2019. Microbial recycling cells (MRCs): A new platform of microbial electrochemical technologies based on biocompatible materials, aimed at cycling carbon and nutrients in agro-food systems. Sci. Total Environ. 649. doi:10.1016/j.scitotenv.2018.08.324

Guerrini, E., Cristiani, P., Trasatti, S.P.M., 2013. Relation of anodic and cathodic performance to pH variations in membraneless microbial fuel cells. Int. J. Hydrogen Energy 38, 345–353. doi:10.1016/j.ijhydene.2012.10.001

Gustavsson, J., Food and Agriculture Organization of the United Nations., ASME/Pacific Rim Technical Conference and Exhibition on Integration and Packaging of MEMS, N., 2011. Global food losses and food waste : extent, causes and prevention : study conducted for the

International Congress "Save Food!" at Interpack 2011 Düsseldorf, Germany. Food and Agriculture Organization of the United Nations.

Huntemann, M., Stackebrandt, E., Held, B., Nolan, M., Lucas, S., Hammon, N., Deshpande, S., Cheng, J.-F., Tapia, R., Goodwin, L.A., Pitluck, S., Liolios, K., Pagani, I., Ivanova, N., Mavromatis, K., Mikhailova, N., Pati, A., Chen, A., Palaniappan, K., Land, M., Rohde, M., Gronow, S., Göker, M., Detter, J.C., Bristow, J., Eisen, J.A., Markowitz, V., Woyke, T., Hugenholtz, P., Kyrpides, N.C., Klenk, H.-P., Lapidus, A., 2013. Genome sequence of the phylogenetically isolated spirochete Leptonema illini type strain (3055T). Stand. Genomic Sci. 8, 177–187. doi:10.4056/sigs.3637201

Kim, J.H., An, B. min, Lim, D.H., Park, J.Y., 2018. Electricity production and phosphorous recovery as struvite from synthetic wastewater using magnesium-air fuel cell electrocoagulation. Water Res. 132, 200–210. doi:10.1016/J.WATRES.2018.01.003

Logan, B.E., 2009. Exoelectrogenic bacteria that power microbial fuel cells. Nat. Rev. Microbiol. 7, 375–381. doi:10.1038/nrmicro2113

Marzorati, S., Lorenzi, M., Fest-Santini, S., Santini, M., Trasatti, S.P.M., Schievano, A., Cristiani, P., 2016. Quantitative study of carbonates deposition in biocathodes by 3-D X-ray microcomputed tomography, in: Aulenta, F., Majone, M. (Eds.), ISMET-EU. Rome, p. 41.

Marzorati, S., Schievano, A., Colombo, A., Lucchini, G., Cristiani, P., 2018. Ligno-cellulosic materials as air-water separators in low-tech microbial fuel cells for nutrients recovery. doi:10.1016/j.jclepro.2017.09.142

Mathuriya, A.S., Pant, D., 2018. Assessment of expanded polystyrene as a separator in microbial fuel cell. Environ. Technol. 1–10. doi:10.1080/09593330.2018.1435740

Merino-Jimenez, I., Celorrio, V., Fermin, D.J., Greenman, J., Ieropoulos, I., 2017. Enhanced MFC power production and struvite recovery by the addition of sea salts to urine. Water Res. 109, 46–53. doi:10.1016/j.watres.2016.11.017

Montpart, N., Rago, L., Baeza, J.A., Guisasola, A., 2018. Oxygen barrier and catalytic effect of the cathodic biofilm in single chamber microbial fuel cells. J. Chem. Technol. Biotechnol. doi:10.1002/jctb.5561

Noori, M.T., Jain, S.C., Ghangrekar, M.M., Mukherjee, C.K., 2016. Biofouling inhibition and enhancing performance of microbial fuel cell using silver nano-particles as fungicide and cathode catalyst. doi:10.1016/j.biortech.2016.08.061

Parameswaran, P., Zhang, H., Torres, C.I., Rittmann, B.E., Krajmalnik-Brown, R., 2010. Microbial community structure in a biofilm anode fed with a fermentable substrate: The significance of hydrogen scavengers. Biotechnol. Bioeng. 105, 69–78. doi:10.1002/bit.22508

Pasternak, G., Greenman, J., Ieropoulos, I., 2015. Comprehensive Study on Ceramic Membranes for Low-Cost Microbial Fuel Cells. ChemSusChem 88–96. doi:10.1002/cssc.201501320

Patil, S.A., Surakasi, V.P., Koul, S., Ijmulwar, S., Vivek, A., Shouche, Y.S., Kapadnis, B.P., 2009. Electricity generation using chocolate industry wastewater and its treatment in activated sludge based microbial fuel cell and analysis of developed microbial community in the anode chamber. Bioresour. Technol. 100, 5132–5139. doi:10.1016/j.biortech.2009.05.041

Qiao, S., Yin, X., Zhou, J., Wei, L., Zhong, J., 2018. Integrating anammox with the autotrophic denitrification process via electrochemistry technology. Chemosphere 195, 817–824. doi:10.1016/j.chemosphere.2017.12.058

Rago, L., Baeza, J.A., Guisasola, A., 2016. Increased performance of hydrogen production in microbial electrolysis cells under alkaline conditions. Bioelectrochemistry 109, 57–62. doi:10.1016/j.bioelechem.2016.01.003

Rago, L., Cristiani, P., Villa, F., Zecchin, S., Colombo, A., Cavalca, L., Schievano, A., 2017. Influences of dissolved oxygen concentration on biocathodic microbial communities in microbial fuel cells. Bioelectrochemistry 116, 39–51. doi:10.1016/j.bioelechem.2017.04.001

Rago, L., Zecchin, S., Marzorati, S., Goglio, A., Cavalca, L., Cristiani, P., Schievano, A., 2018. A study of microbial communities on terracotta separator and on biocathode of air breathing microbial fuel cells. Bioelectrochemistry 120, 18–26. doi:10.1016/j.bioelechem.2017.11.005

Rittmann, B.E., Mayer, B., Westerhoff, P., Edwards, M., 2011. Capturing the lost phosphorus. Chemosphere 84, 846–853. doi:10.1016/j.chemosphere.2011.02.001

Rossini-Oliva, S., Mingorance, M.D., Peña, A., 2017. Effect of two different composts on soil quality and on the growth of various plant species in a polymetallic acidic mine soil. Chemosphere 168, 183–190. doi:10.1016/j.chemosphere.2016.10.040

Santini, M., Guilizzoni, M., Lorenzi, M., Atanassov, P., Marsili, E., Fest-, S., Cristiani, P., Santoro, C., Fest-santini, S., 2015. Three-dimensional X-ray microcomputed tomography of carbonates and biofilm on operated cathode in single chamber microbial fuel cell Three-dimensional X-ray microcomputed tomography of carbonates and biofilm on operated cathode in single chamber microbial 031009, 1–10. doi:10.1116/1.4930239

Santini, M., Marzorati, S., Fest-Santini, S., Trasatti, S., Cristiani, P., 2017. Carbonate scale deactivating the biocathode in a microbial fuel cell. J. Power Sources 356, 400–407. doi:10.1016/j.jpowsour.2017.02.088

Santoro, C., Artyushkova, K., Gajda, I., Babanova, S., Serov, A., Atanassov, P., Greenman, J., Colombo, A., Trasatti, S., Ieropoulos, I., Cristiani, P., 2015. Cathode materials for ceramic based microbial fuel cells (MFCs). Int. J. Hydrogen Energy 40, 14706–14715. doi:10.1016/j.ijhydene.2015.07.054

Santoro, C., Ieropoulos, I., Greenman, J., Cristiani, P., Vadas, T., Mackay, A., Li, B., 2013. Power generation and contaminant removal in single chamber microbial fuel cells (SCMFCs) treating human urine, in: International Journal of Hydrogen Energy. Pergamon, pp. 11543–11551. doi:10.1016/j.ijhydene.2013.02.070

Sotres, A., Cerrillo, M., Viñas, M., Bonmatí, A., 2016. Nitrogen removal in a two-chambered microbial fuel cell: Establishment of a nitrifying-denitrifying microbial community on an intermittent aerated cathode. Chem. Eng. J. 284, 905–916. doi:10.1016/j.cej.2015.08.100

Tan, W.-B., Jiang, Z., Chen, C., Yuan, Y., Gao, L.-F., Wang, H.-F., Cheng, J., Li, W.-J., Wang, A.-J., 2015. Thiopseudomonas denitrificans gen. nov., sp. nov., isolated from anaerobic activated sludge. Int. J. Syst. Evol. Microbiol. 65, 225–229. doi:10.1099/ijs.0.064634-0

Tansel, B., Lunn, G., Monje, O., 2018. Struvite formation and decomposition characteristics for ammonia and phosphorus recovery: A review of magnesium-ammonia-phosphate interactions. Chemosphere 194, 504–514. doi:10.1016/j.chemosphere.2017.12.004

Verstraete, W., Van de Caveye, P., Diamantis, V., 2009. Maximum use of resources present in domestic “used water.” Bioresour. Technol. 100, 5537–5545. doi:10.1016/j.biortech.2009.05.047

Virdis, B., Rabaey, K., Rozendal, R.A., Yuan, Z., Rg Keller, J., 2010. Simultaneous nitrification, denitrification and carbon removal in microbial fuel cells. doi:10.1016/j.watres.2010.02.022

Winfield, J., Gajda, I., Greenman, J., Ieropoulos, I., 2016. A review into the use of ceramics in microbial fuel cells. Bioresour. Technol. 215, 296–303. doi:10.1016/j.biortech.2016.03.135

Wu, H., Lai, C., Zeng, G., Liang, J., Chen, J., Xu, J., Dai, J., Li, X., Liu, J., Chen, M., Lu, L., Hu, L., Wan, J., 2017. The interactions of composting and biochar and their implications for soil amendment and pollution remediation: a review. Crit. Rev. Biotechnol. 37, 754–764. doi:10.1080/07388551.2016.1232696

Wu, H., Zeng, G., Liang, J., Chen, J., Xu, J., Dai, J., Li, X., Chen, M., Xu, P., Zhou, Y., Li, F., Hu, L., Wan, J., 2016. Responses of bacterial community and functional marker genes of nitrogen cycling to biochar , compost and combined. Appl. Microbiol. Biotechnol. 100, 8583–8591. doi:10.1007/s00253-016-7614-5

Yan, H., Saito, T., Regan, J.M., 2012. Nitrogen removal in a single-chamber microbial fuel cell with nitrifying biofilm enriched at the air cathode. Water Res. 46, 2215–2224. doi:10.1016/j.watres.2012.01.050

Yang, Y., Li, X., Yang, X., He, Z., 2017. Enhanced nitrogen removal by membrane-aerated nitritation-anammox in a bioelectrochemical system. Bioresour. Technol. 238, 22–29. doi:10.1016/j.biortech.2017.04.022

Zhang, L., Wang, Y., Wei, L., Wang, Y., Shen, X., Li, S., 2013. Taibaiella smilacinae gen. nov., sp. nov., an endophytic member of the family Chitinophagaceae isolated from the stem of Smilacina japonica, and emended description of Flavihumibacter petaseus. Int. J. Syst. Evol. Microbiol. 63, 3769–3776. doi:10.1099/ijs.0.051607-0

Zhao, H., Zhao, J., Li, F., Li, X., 2016. Performance of denitrifying microbial fuel cell with biocathode over nitrite. Front. Microbiol. 7, 1–7. doi:10.3389/fmicb.2016.00344

Chapter 3 - Plant nutrients recovery from organic-rich wastewater using microbial electrochemical technologies based on terracotta

Andrea Goglio[a], Stefania Marzorati[a], Sarah Zecchin[b], Simone Quarto[c], Ermelinda Falletta[c], Lucia Cavalca[b], Andrea Schievano[a*]

a e-BioCenter, Department of Environmental Science and Policy, University of Milan, Via Celoria 2, 20133 Milan, Italy

b e-BioCenter, Department of Food Environmental and Nutritional Science, University of Milan, Via Mangiagalli 25, 20133 Milan, Italy

c Department of Chemistry, University of Milan, Via Golgi 19, 20133 Milan, Italy

* Corresponding author: andrea.schievano@unimi.it

Abstract

Terracotta has been proposed as a biocompatible and low-cost material to fabricate porous air-water separators for microbial recycling cells (MRCs), a category of microbial electrochemical technologies aimed at extracting plant nutrients from agro-food wastewater and recycling them as fertilizers. Here, we tested the performance of cylindrical-shaped MRCs, where terracotta is used as porous air-water separator, to improve access to oxygen for cathodic reactions and facilitate plant-nutrients deposition on the material. Anodes and cathodes were both composed of carbon cloth (projected area of 1500 cm^2 and 360 cm^2, respectively), connected across 150 Ω external load. Tests were performed using swine manure and using an SS-free artificial wastewater (equal sCOD = 6 g L^{-1}), as a control to assess biofouling phenomena. Over 250 operation days, consistent amounts of the main nutrients (C, N, P, K, Mg, Mn, Fe) were removed from wastewaters with an efficiency from 97% to 48% based on the elements and deposited on the terracotta separators. Cation electro-migration mechanisms generated by the MRCs and high cathodic pH values (over 10) were the predominant factors leading to inorganic salts precipitation on the terracotta separators. This study aims at introducing cylindrical MRCs in view of recovering nutrients and organic matter from wastewaters and doing a comparison between biofouling and salts deposition phenomenas.

Keywords

Microbial electrochemical technologies, microbial recycling cells, nutrients recovery, terracotta, wastewater, circular economy

1. Introduction

The recovery of organic/inorganic forms of carbon and nutrients from wastewater derived from food production chains is widely recognized as a priority to minimize environmental contamination, while recirculating valuable streams of plant nutrients (Verstraete et al., 2009). Researchers should focus on environmentally friendly processes and biocompatible materials, because 'building devices for sustainability purposes from materials that may themselves contribute to the accumulation of waste build-up, would be a paradox (Winfield et al., 2016).

Particular types of microbial electrochemical technologies (MET) that allow recycling carbon and nutrients from food-chain were recently proposed (called microbial recycling cells, MRCs), based on biogenic/biocompatible materials, which can be completely recycled together with the recovered nutrients and organic carbon, to produce fertilizers and soil-conditioners (Goglio

et al., 2019b). Such an approach should be in advantage, as compared to different kinds of architectures of MET, previously studied to recover soluble nutrients (Kelly and He, 2014). Indee, typical air-driven MET configurations (e.g. microbial fuel cells) include microporous layers (MPL) or gas-diffusion layers (GDL), used to separate the liquid in the anodic chamber from the air-exposed cathodic surface, while increasing cathodic surface area (Ghadge et al., 2015; Papaharalabos et al., 2013) and guaranteeing low ionic resistance (Cindrella et al., 2009; Cristiani et al., 2013). Air diffuses only in a relatively thin layer and forms a decreasing gradient towards the anodic compartment (Cristiani et al., 2013). Usually, MPL and GDL are based on blends of hydrophobic polymeric binders (PTFE, Nafion® etc.) and conductive powders used as catalysts (carbon black, metals etc.), spread on carbon fibers or other conductive materials (Santoro et al., 2015).

In the concept of MRCs, a series of generally unwanted phenomena that tend to invalidate the electrochemical performances of MET over long-term operations (typically over 60–90 days) (Noori et al., 2016; Santini et al., 2017, 2015b), are instead the goal. When the bioelectrochemical cell works properly, pH tends to increase in close proximity of the cathode (pH 9-11), leading to inorganic salts precipitation (e.g. carbonates) and accumulation in layers within the cathodic biofilm (Santini et al., 2015b). In addition, water evaporation from MPL/GDL or separators at the air-water interface contributes to salts precipitation (Santini et al., 2017). Also, suspended organic matter can be recovered by biofouling. Organic matter in the form of microbial cells, extracellular polymeric substances, complex and recalcitrant organic molecules usually contribute to create layers on the electrode or separator surfaces (Noori et al., 2016; Rago et al., 2018). Combined biofouling and salts precipitation concur to accumulate nutrients in either organic or inorganic forms on the materials surface. As these mechanisms tend to clog MPLs, electrodes and separators, increasing the internal resistance and deactivating the electrochemical system, they have been considered as strong constraints for the development of applicable air-driven MET (e.g. microbial fuel cells) (Cheng et al., 2006; Jiang et al., 2011; Yu et al., 2017). In MRCs, on the contrary, such mechanisms should be pursued.

However, if MRCs were based on high-tech and non-biocompatible materials, periodical maintenance would be needed to extract the nutrients and guarantee stable electrochemical performances to the system over long term. The possibility of applying MRCs relies instead on the replacement of such expensive components with low-tech, biocompatible and fully recyclable materials in the fabrication of electrodes, separators and structural frames.

Recently, lab-scale MRCs were proposed using terracotta (earthenware) as a biocompatible, low cost and fully-recyclable material for porous air-water separators (Goglio et al., 2019a). Such ceramic materials are gaining increasing attraction as low-cost and environmentally sustainable separators in MET (Pasternak et al., 2015; Winfield et al., 2013). This kind of materials are versatile in terms of structure, composition and fabrication techniques and may be optimized for specific applications by changing clay type, porosity, wall thickness and density (Winfield et al., 2016). The porosity of a ceramic membrane is a key factor for the effectiveness of its application, as it can influence the chemical composition and pH of the contained electrolyte as well as the ion exchange rate (Winfield et al., 2013). The rate of cations transport is also strongly related to the presence of exchangeable cations in the clay (Ghadge and Ghangrekar, 2015). Among the constituent minerals of the clay, some possesses high availability of exchangeable cationic sites and, therefore, high cation exchange capacity. In recent applications, terracotta separators were used with cylindrical architecture, as air-water separators in microbial fuel cells (Winfield et al., 2016). Current generation in cylindrical terracotta-MFCs contributed to produce cations migration and catholyte formation in proportion to MFC power performance (Gajda et al., 2014). Also, increased pH and water evaporation from the air-water interface contributed to salts precipitation (Gajda et al., 2015a).

In this work, we tested cylindrical-shaped terracotta separators in MRCs, to look at the performances and the mechanisms that drive nutrients sequestration from agro-food wastewater.

2. Materials and methods

In this experiment, cylindrical terracotta separators were studied as air-water interface in air-cathode MRCs, to recover organic matter, inorganic carbon macro- and micro-nutrients. The objective was to compare the performance of nutrients recovery, in presence or absence of suspended solids in the wastewater. Two different types of wastewater were used: swine manure (SM) and artificial suspended solid-free wastewater (AW). Also, the effect of the electrochemical system was tested by running controls under open circuit potential conditions (OCP). The artificial wastewater was chosen using a receipt for a mixed microbial culture medium, according to previous literature (Parameswaran et al., 2009; Pasternak et al., 2015). Briefly, it was a 100 mM phosphate buffer solution (PBS; 70 g Na_2HPO_4 and 12 g KH_2PO_4 per litre) with the following components in 1 L of deionized water: NH_4Cl (0.41 g); 1 mL of 4 g L^{-1} $FeCl_2$ solution; 10 mL of mineral medium. The mineral media had the composition described by

Parameswaran et al. (Parameswaran et al., 2009): EDTA (0.5 g L^{-1}), $CoCl_2 \cdot 6H_2O$ (0.082 g L^{-1}), $CaCl_2 \cdot 2H_2O$ (0.114 g L^{-1}), H_3BO_3 (0.01 g L^{-1}), $Na_2MoO_4 \cdot 2H_2O$ (0.02 g L^{-1}), Na_2SeO_3 (0.001 g L^{-1}), $Na_2WO_4 \cdot 2H_2O$ (0.01 g L^{-1}), $NiCl_2 \cdot 6H_2O$ (0.02 g L^{-1}), $MgCl_2$ (1.16 g L^{-1}), $MnCl_2 \cdot 4H_2O$ (0.59 g L^{-1}), $ZnCl_2$ (0.05 g L^{-1}), $CuSO_4 \cdot 5H_2O$ (0.01 g L^{-1}), $AlK(SO_4)_2$ (0.01 g L^{-1}).

The 8 MRCs were studied over 250 days: 2 trials for each wastewater were run using terracotta as air-water separator (MRC) with 2 controls (OCP) to assess the role of the electrochemical circuit in driving nutrients deposition on the separator and cathode. The electrochemical performances of the MRCs were measured over time. The fate of soluble fractions of organic matter and nutrients was monitored in the liquid phase along the observed period and at the end of the test were characterized the enrichment in organic matter and macro- and micro-nutrients of the cylindrical terracotta separators. Moreover, it was studied in the deep the real reuse of the nutrients that enriched the terracotta at the end of the experiment with 3 different extractions to simulate the real solubility of the elements.

2.1 Cylindrical MRCs configuration and experimental set-up

Cylindrical MRC reactors (volume 2 L) were designed with a cylindrical terracotta air-water separator (20 cm height, 5 cm internal diameter, 4 mm thickness and a pore size in the range 60-500 nm). Anodes and cathodes were both composed of carbon cloth (projected area of 1500 cm^2 and 360 cm^2, respectively) (SAATI C1, Appiano Gentile, Italy) and they were rolled different times around the internal or external face of the separator and also on itself to increase the chance of bacterial growth. The cathodes were also modified by a MPL made of activated carbon/PTFE mixture (10:7 on dry weight basis) (Santoro et al., 2015). Cathodes were positioned at the air-exposed side of the terracotta separator. Anode and cathode were electrically connected through an external load of 150 Ω. Connections were insulated with non-conductive epoxy resin. For the OCP reactors we utilised the same design, materials, treatments and size of electrodes without though that anode and cathode were not electrically connected.

All MRCs were inoculated with swine manure to have the same microbial community in all trials and then always fed in parallel with identical timing. After this, the reactors were periodically refilled with additional milliQ water to take stable the volume of the reactors. In all the 7 cycles, the reactors were emptied and filled with raw swine manure or with artificial wastewater and sodium acetate (6 g L^{-1}).

2.2 Electrochemical analyses

Throughout the duration of the experiment, several electrochemical measurements were carried out: current density trends, voltage trends of the open circuit potential, power curves, anodic and cathodic polarization. For each MRC anode and cathode were connected across an external load of 150 Ω and their potential was recorded every 20 minutes using a multichannel Data Logger (Graphtech midi Logger GL820). The same multichannel Data Logger recorded every 20 minutes the voltage trends of the OCPs.

Power curves were measured at the start, middle and at the end of the experiment with a two-electrode configuration. Before each electrochemical measurement, 1 h of equilibration time was found necessary to allow the system, disconnected from the data logger, to reach OCP. The anode was set as working electrode and the cathode as reference electrode. A linear sweep polarization (scan rate v=0.010 V min^{-1}) was recorded from the cell OCP to 10 mV. The power was calculated by P = I • V, normalized by the cathodic area and plotted vs current density.

Moreover, there were performed also anodic and cathodic polarization at the start, middle and at the end of the experiment with a three-electrode configuration. The anode was set as working electrode in the anodic polarization and as counter in the cathodic one, while the cathode was set up in the opposite configuration and the third electrode was the reference in both situation. Both anodic and cathodic polarization were performed with a scan rate of 0.010 V min^{-1} and they were recorded in a range from the anodic OCP to 0.4 V and from the cathodic OCP to - 0.6 V respectively.

2.3 Physico-chemical characterization

The chemical composition of the wastewaters along the cycles was monitored by several parameters: chemical oxygen demand (COD), total nitrogen (TN) and total content of the main macro- and micro-nutrients (K, P, Mg, Fe, Mn) analysed by inductively coupled plasma mass spectrometry (ICP-MS). In addition, the enrichment in these elements on the terracotta separators was determined at the end of the experiment, adding also nitrate (NO_3-), ammonia (NH_4+), inorganic carbon (IC) analyses.

The soluble fractions of COD and TN in the anolyte were determined using spectrophotometric method after specific reactions using test kits (Hach Company, Loveland, CO, USA). The samples were filtered (0.45 µm Nylon filters) before the analysis. ICP-MS (BRUKER Aurora-M90 ICP-MS) was used to measure single elements in the soluble fractions and in the extracts of the

terracotta separators. The extracts of the terracotta separators were made in milliQ water, 2% v v^{-1} $C_6H_8O_7$ and 1% v v^{-1} HCl to simulate the solubility of the nutrients in short, medium and long time. The mixture of terracotta and solutions (ratio 1:10) was mixed for 30 minutes and after that it was filtrated with 0.45 µm nylon filters ("Metodi di Analisi dei Fertilizzanti," 2001.).

The inorganic carbon was analysed using a SIEVERS 820 Portable Total Organic Carbon Analyzer (GE Analytical Instruments, UK). This tool provides an extremely sensitive measurement of the TOC, IC and TC concentration in solutions. Moreover, TN, NO_3- and NH_4+ were measured in the extracts of the terracotta separators using spectrophotometric method after specific reactions using test kits (Hach Company, Loveland, CO, USA).

2.4 Morphological characterization

Scanning Electron Microscopy (SEM) was performed using a Zeiss SEM EVO 50 microscope to analyse the morphology of the terracotta separators at 2 different distances (100 µm and 10 µm) with the raw terracotta and after 250 operation days. The microscopy analysis was joined with a XRD analysis to characterise the composition of the crystals present in the SEM images.

2.5 Characterization of the microbial communities by 16S rRNA Illumina sequencing

DNA isolation was performed from anodes at 100 and 250 days and from terracotta at 250 days, sampled from each of the analysed BES. The samples area was around 18 cm^3 traded with a washout of milliQ water. DNA was isolated from approximately 250 mg of material using DNeasy® PowerSoil® (QIAGEN, Germany) according to manufacturer's instructions. Sequencing of bacterial and archaeal 16S rRNA genes was performed in triplicate from each sample using primer pairs 341F/806R (respectively, 5'-CCTACGGGAGGCAGCAG-3' and 5'-GGACTACHVGGGTWTCTAAT-3') and 344F/806R (respectively, 5'- ACGGGGTGCAGGCGCGA-3' and 5'- GGACTACHVGGGTWTCTAAT-3'). Library preparation, pooling and sequencing was performed at the Center for Genomic Research – DNA Service Facility, University of Illinois at Chicago according to Green et al. (2015) and Bybee et al. (2011).

Forward and reverse reads were merged using PEAR (Zhang et al., 2014). Ambiguous nucleotides and primer sequences were trimmed from the ends and reads with internal ambiguous nucleotides or lacking primer sequence were discarded. Further trimming was performed at quality threshold of 0.01 and resulting reads shorter than 325 bp were discarded. Chimeric sequences were identified using the UCHIME algorithm as compared with the SILVA

SSU Ref dataset (Edgar, 2010; Quast et al., 2013). Further analyses were performed using QIIME (Caporaso et al., 2010). Unique sequences were dereplicated and sequences with similarity of 97% or higher were clustered and taxonomically classified using USEARCH and the SILVA SSU Ref dataset (Edgar, 2010). The microbial communities were compared performing non-metric multidimensional scaling (NMDS, Faith et al., 1987) on Bray-Curtis dissimilarities between the samples, using the R package vegan version 2.5-5 (Oksanen et al., 2018).

3. Results and Discussion

3.1 Current generation trends

Figures 1 - a, b presents the current density trends during the operational period of 250 days both for SM-MRC and AW-MRC. In Figures 1 - c, d, the voltage trends of the SM-OCP and AW-OCP are plotted. The system started to produce current (MRCs) or a showed a difference of potential (OCPs) between anode and cathode.

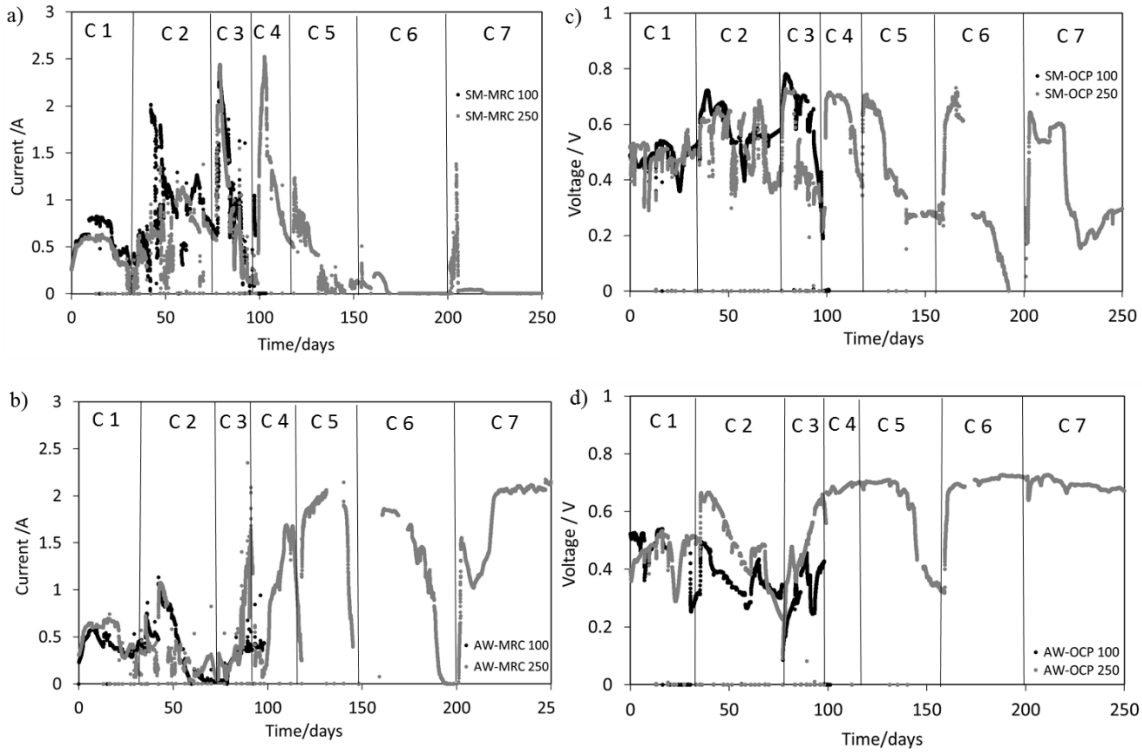

Figure 1 – Current density trends during 250 days of observation: (a) SM-MRCs, (b) AW-MRCs, (c) SM-OCPs and (d) AW-OCPs. The graphs report the span time of each cycle of wastewater feeding in batch mode (C1-7).

In SM-MRCs, after around 120 days of operation, current densities decreased quickly, while in AW-MRCs the current density trend increased cycle by cycle along the whole observation period (250 days). Analysing in deep both trends, it is possible to observe that the SM-MRC in the first cycle produced around 2 A m^{-2} (referred to cathodic geometric area) as the AW-MRC and after that starting with the cycle 2 produce stable peaks at 7 A m^{-2} for other three cycles and decrease cycle by cycle 50% of its current trend arriving at the end with a production close to 0 A m^{-2}. Figure 1b shows the opposite trend of the AW-MRC, where from the second cycle the system started to produce 3 A m^{-2} that with the third one arrived at 6.50 A m^{-2} and it stayed stable for all the operation time except for a slight decrease in the last cycle.

Instead, OCPs with both wastewaters showed similar trends. These differences between the SM-MRC and AW-MRC might be attributable at the two main phenomena, which contribute to the block of the BES after few months of operation: the deposition of inorganic salts and organic matter. Santini et al. (Santini et al., 2017) recently observed a bio-cathode inactivation over time due to carbonate scale deposition in air-cathode MFCs, already after around 60-90 days. Previous works by the same group (Santini et al., 2015b) documented the presence of a thick layer of carbonate formed as a consequence of the alkalinity induced by the ORR on cathodes operated for long time in single chamber MFCs. In particular, this phenomenon was found to significantly hinder MFC performances after around 60 days of operation. As observed by Santini et al. about the increasing of the BES internal resistance due to carbonate scale deposition, Noori et al. analysed that biofouling in MFC can cause severe problems such as hindering proton transfer and increasing the ohmic and charge transfer resistance of cathodes, which results in a rapid decline in MFC performance (Noori et al., 2019).

3.2 Electrochemical characterization

The power curves plotted in the Figures 2 - a, b show and describe perfectly the MRC performances during the operational period of 250 days. In figure 2a is possible to observe how the system lose the possibility of producing current due to the increase of the internal resistance by biofouling phenomena and in figure 2b how the salt deposition is less strong than the biofouling phenomena. Precisely, in SM-MRC the internal resistance increased from 97 Ω during the first cycle to third circle at 298 Ω to the end of the operation time at 311Ω, while the AW-MRC started with a low resistance (33 Ω), than after 100 days was 107 Ω and at the end increase at 163 Ω. These two different kinetics of the increasing of the internal resistance are the explanation of the density current trends of each systems and the electrochemical

explanation how the salt deposition phenomena and the biofouling can affect the performances of the BES.

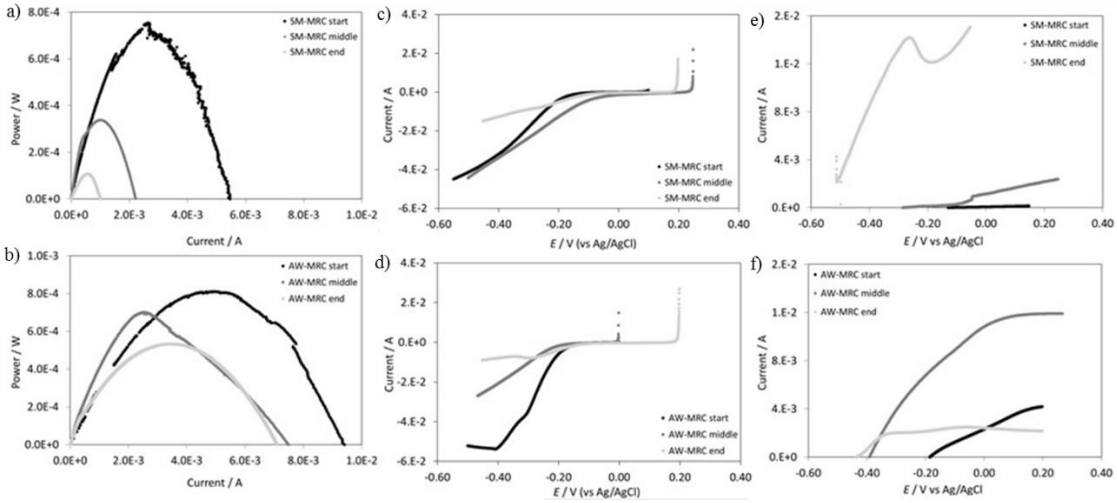

Figure 2 – Electrochemical analysis at the start of the experiment, middle and after 250 days: (a) power curves of SM-MRC, (b) power curves of AW-MRC, (c) cathodic polarizations of SM-MRC, (d) cathodic polarizations of AW-MRC, (e) anodic polarizations of SM-MRC and (f) anodic polarizations of AW-MRC.

Moreover, Figures 2 - c, d show cathodic polarizations of both systems they are performed at the start, at the peak of the third cycle and at the end of the experiment and is showed as cathodes cycle by cycle lose their performance affecting all the system always due at the problems of salts deposition and biofouling.

The situation Figures 2 - e, f, according with the anodic polarisations, it is very different and the two MRCs are totally unlike by the wastewaters and the involved phenomenas. It is possible to observe that the anode in the SM-MRC was not affected by the decreasing performance of the cathode that is limited by the biofouling and it is increasing the anaerobically of the anode improving its performance. In the other hand, the trend in Figure 1 f is drastically different with an inhibition of the anodic compound.

3.3 - Effects of the MRCs on the wastewater treatment and nutrients recovery

Table 1 shows the removal of macro- and micro-nutrients during 250 days of operation time. In this table is interesting the comparison between the MRCs and the OCPs for both the wastewater treatments.

Table 1 - Mean (±standard deviation, n=10) of macro- and micro-nutrients removal yields (as % of the initial content) from liquid phase along batch cycles. Removal yields were calculated from a complete mass balance (input-output) along 250 days of operation time.

	COD	TN	K	P	Mg	Mn	Fe
	(%)	*(%)*	*(%)*	*(%)*	*(%)*	*(%)*	*(%)*
SM-MRC	97±2	88±8	5±7	74±5	48±6	93±3	78±8
SM-OC	98±1	84±9	-24±10	50±0	-21±2	97±1	34±8
AW-MRC	98±2	92±2	-2±5	5±9	2±1	69±10	100±1
AW-OC	97±2	90±3	-32±11	-11±2	-52±9	93±2	-93±7

According with the table is possible to observe that the electrochemical forces involved in the systems play an important role in the treatment processes. Both for SM and AW systems the COD removal is similar in MRC and in the control (OCP) caused by the same mixed microbial population that in anaerobically condition could oxidize the COD. This COD is used in different ways in the MRC and OCP reactors, the electroactive bacteria in the MRCs made the oxidation of the organic matter (COD) in the anode to produce electrons and starting the cations migration and the increasing of the cathodic pH, while in the OCPs the COD was oxidized and GHGs were produced. Moreover, continuing to analyse the Table 1 is possible to observe that for the others elements form there was a huge removal in the MRCs respect the OCPs. Beside, looking at K, P, Mg and Fe is possible to observe even a concentration of elements in the control system. Table 2 shows the pH average in the bulk liquid (wastewater) of anodic chambers and pH at the cathodic air-water interfaces. The pH in all the reactors is quite similar slight increases in pH is typical in anaerobic environments, as result of volatile fatty acids consumption (De Bere, 2000). Interesting is to observe when the MRC works well the pH is at least 1-1.5 point of pH higher of the control or of the BES when does not work properly.

Table 2 - Mean (±standard deviation, n=2) pH values, measured in the bulk liquid of anodic chambers and pH at the cathodic air-water interfaces (measured at the end of the experiment).

	Anodic pH	Cathodic pH
SM-MRC 100	7.93±0.33	10.31
SM-MRC 250	7.63±0.21	8.83
AW-MRC 100	7.76±0.24	9.60
AW-MRC 250	7.75±0.26	10.72
SM-OCP 100	8.03±0.31	9.06
SM-OCP 250	7.60±0.20	9.52
AW-OCP 100	7.74±0.29	9.97
AW-OCP 250	7.81±0.28	9.28

This phenomenon was already observed in previous experiments and linked to the surplus of hydroxyl free radicals liberated by incomplete the cathodic oxygen reduction reaction (Winfield et al., 2016). Measurements on the catholyte formed by electroosmotic water transport through terracorra separators was found up to pH 13 (Gajda et al., 2015b). This is indeed a key point to favor inorganic salt depositions (e.g. struvite, Ca-carbonates, Mg-Carbonates, organophosphates, oxydes and other salts etc.) within the internal porosity of the terracotta separators (Winfield et al., 2016). This finding encourages the use of MRCs, made of low-cost air-water porous separators, to improve nutrients recovery as precipitated salts within the terracotta separators and at the cathode.

In this scenario, it is also interesting focusing on the elements that are recovered on the terracotta cylinder separators, due to demonstrate how the electrochemical systems can affect not only the wastewater treatment but also the nutrients recovery. In Figures 3 and 4 are plotted the amounts of macro- and micro-nutrients recovered from SM and AW on terracotta separators along 100 and 250 days measured under different extractions: milli-q water, $C_6H_8O_7$ 2% v v^{-1} and HCl 1% v v^{-1}. These extractions according with the Italian legislation for the characterization and solubility of fertilisers ("Metodi di Analisi dei Fertilizzanti," 2001)

simulate the solubility of the macro- and micro-nutrients in short, medium and long time in the soil and the following up-taking possibility for the plants.

Figure 3 proves the important role of the electrochemical system in the recovery of nutrient on the terracotta separators from the swine manure. In all the columns is possible to see that the amount recovered in the MRCs was decidedly greater compere to OCPs. Moreover, it is also interesting observe that there is not a huge differences between the MRC 100 d and the MRC 250 d because as describe previously the SM-MRCs at the end of the third cycle were already affected by a decreasing of the performances due to the biofouling phenomena.

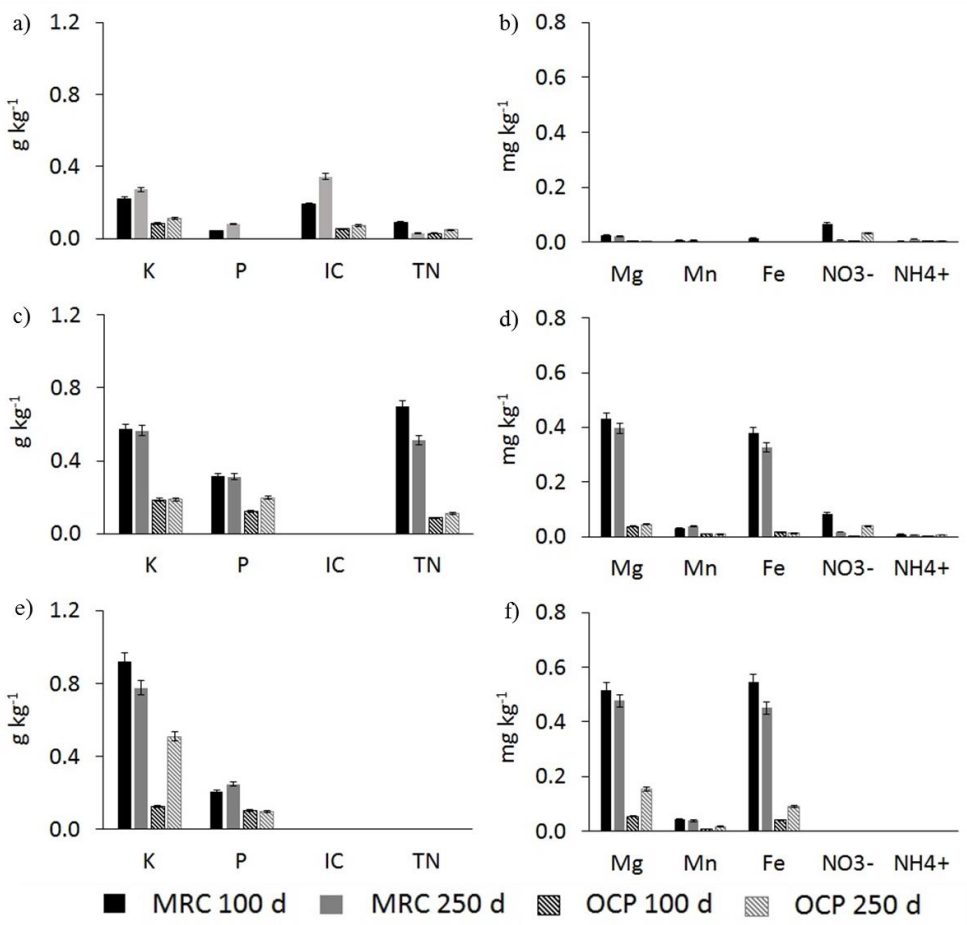

Figure 3 – Amounts of macro- and micro-nutrients recovered from swine manure on terracotta separators along 100 and 250 days measured under different extractions: (a-b) milli-q water, (c-d) $C_6H_8O_7$ 2% v v_{-1} and (e-f) HCl 1% v v_{-1}. Error bars stand for standard deviations of duplicate experiments, under identical conditions.

In other way, Figure 4 shows always the significant differences between MRCs and OCPs also with the artificial wastewater and demonstrated also a continuous increasing of the recovery at the end of the 250 days of operation time. Figures 3 and 4 show the 2 main views of the paper: the electrochemical system affect both the wastewater treatment and the nutrients recovery (Pepè Sciarria et al., 2019; Ye et al., 2019) and also that the salt deposition and the biofouling affect the BES in two different way (Noori et al., 2019; Santini et al., 2017).

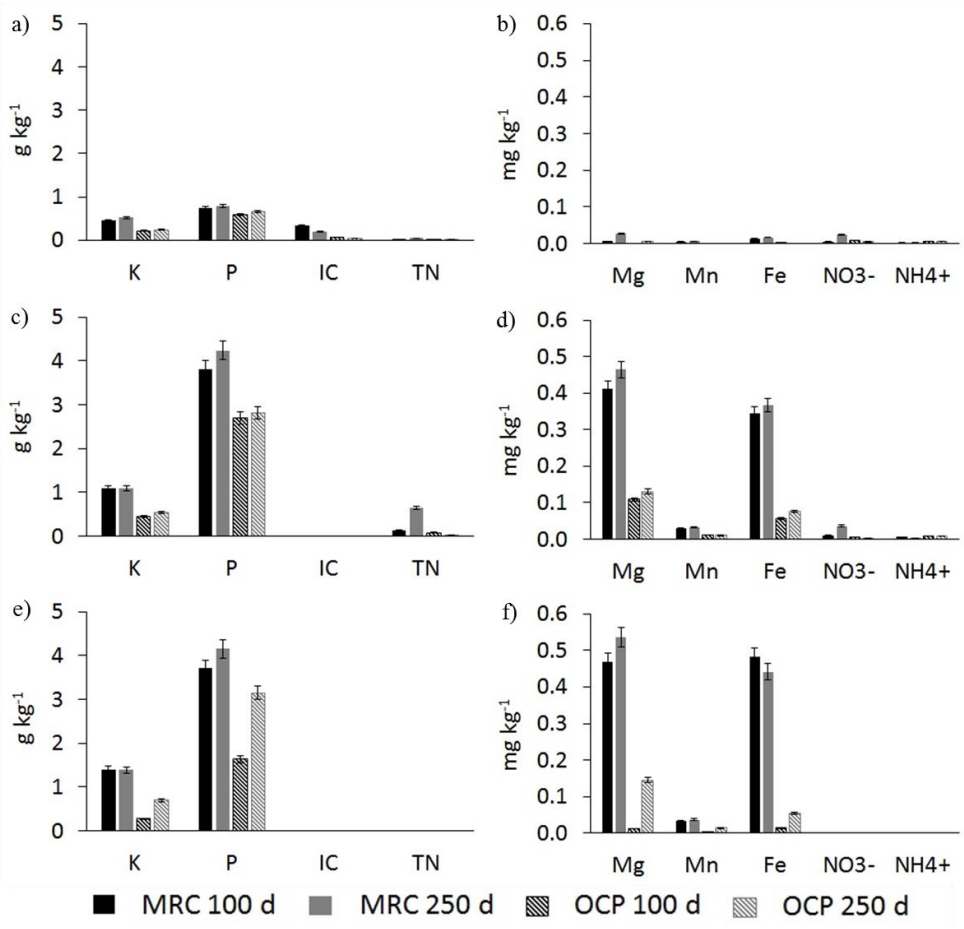

Figure 4 - Amounts of macro- and micro-nutrients recovered from artificial wastewater on terracotta separators along 100 and 250 days measured under different extractions: (a-b) milli-q water, (c-d) $C_6H_8O_7$ 2% v v_{-1} and (e-f) HCl 1% v v_{-1}. Error bars stand for standard deviations of duplicate experiments, under identical conditions.

3.4 – An important awareness: biofouling vs salts deposition

Figure 5 is a combination of SEM images at different scale (10 µm and 100 µm) of the raw terracotta (a, b) and at the end of experiment for SM-MRC (c, d) and AW-MRC (e, f).

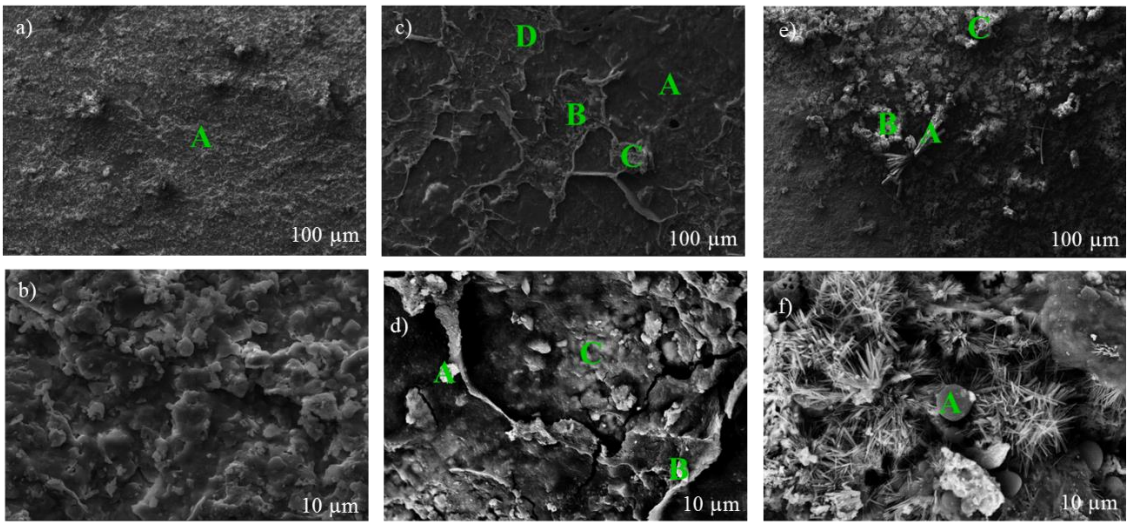

Figure 5 – SEM images taken from representative fragments of the terracotta separators at the beginning of the experiment (a-b) and after 250 days of MRC experiment using SM (c-d) and AW (e-f). Letters A,B,C and D indicate the points where elemental characterization using XRD was performed (data reported in Table 3).

The SEM images show in the detail how the biofouling and the salts deposition can affect and block the systems in two different ways. In sectors c and d it is possible to observe the SM-MRC, where the biofouling is predominant on the salts deposition by the use of swine manure, a typical example of organic-rich wastewater with also a huge amount of suspended solids and a organic compounds at long chain. In these images is possible to see how the biofouling phenomena create a strong mush around the entire terracotta cylinder clogging the system after 100-120 days by hindering proton transfer and increasing the ohmic and charge transfer resistance. In the other way, in the sectors e and f it is possible to observe the formation of the salt crystals by the salts deposition phenomena that according with the performances of these reactors is less powerful than the biofouling.

While, the Table 3 is a XRD analysis of the mush and the crystals presented on the terracotta separator. In addition, these data confirm the different between the two wastewaters and the two phenomenas. Table 3 shows a similar composition of the mush and in the same time explain

a huge inequality by the crystals. The differences in composition for the crystals could be explained in different timing production, confirming that the salts deposition phenomena needs for time to block the system compare to the biofouling. This difference in timing of the two phenomena need more investigation and proof but is a first step to increase the performance, design the treatment and maximising the nutrients recovery based on the wastewaters.

Table 3 - XRD analysis reporting the elemental composition of particular points on the surface of terracotta separators before and after the experiment. Capital letters refer to shown in SEM images reported in Figure 5

		P (% ww^{-1})	K (% ww^{-1})	Ca (% ww^{-1})	Fe (% ww^{-1})	Na (% ww^{-1})	Mg (% ww^{-1})
Before experiment	**a-A**	0.00	3.31	8.39	8.11	0.94	2.01
End of experiment with SM	**c-A**	0.00	4.21	15.58	7.44	5.86	2.51
	c-B	0.00	3.39	3.15	4.06	1.01	1.20
	c-C	0.00	3.81	11.69	9.31	1.48	1.77
	c-D	0.00	2.24	10.40	7.32	0.99	2.29
	d-A	3.11	1.01	41.89	1.01	3.86	1.04
	d-B	11.84	8.69	5.39	1.71	9.14	13.37
	d-C	0.00	3.37	5.58	7.33	1.54	2.70
End of experiment with AW	**e-A**	23.99	14.21	0.00	0.00	8.20	17.47
	e-B	8.68	0.00	0.91	0.00	43.43	0.00
	e-C	24.26	0.94	4.97	0.00	27.58	0.00
	f-A	13.92	7.57	1.95	0.00	21.36	0.00

3.5 – Microbial populations in the different systems

A total of 1160 bacterial and archaeal species were found in the analysed BES. Although most species were shared between the samples (67% on average), a higher number of species was retrieved in the anodes and in the OCP systems, with respect to the terracotta matrices and the MRC systems, respectively (Figure 6a).

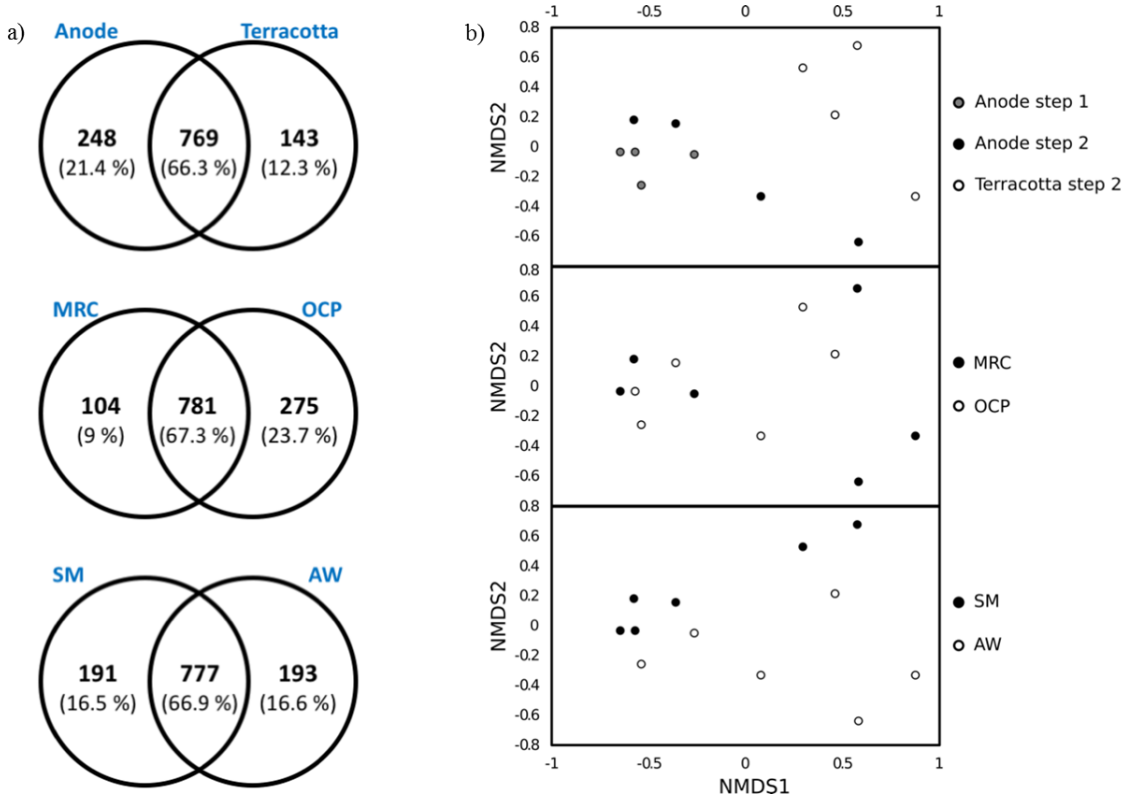

Figure 6 – Diversity if the microbial communities retrieved in the different compartment of the analysed systems in terms of number of species, with specific focus on the shared microbiome (a) and beta diversity, with non-metric multidimensional scaling (NMDS) performed on Bray-Curtis dissimilarities (b).

The use of SM or AW for BES conduction did not select for a different number of species. In terms of microbial community composition, the two major drivers were the different compartments (anode and terracotta) and the use of SM and AW (Figure 6b). At the beginning of the incubation (step 1), in all anodes of all systems Firmicutes was the dominant phylum, accounting for 50% of the total community (Figure 7). Over time, Firmicutes decreased to 40%

on average in all anodes, with a concomitant increase of other phyla according to the BES set-up.

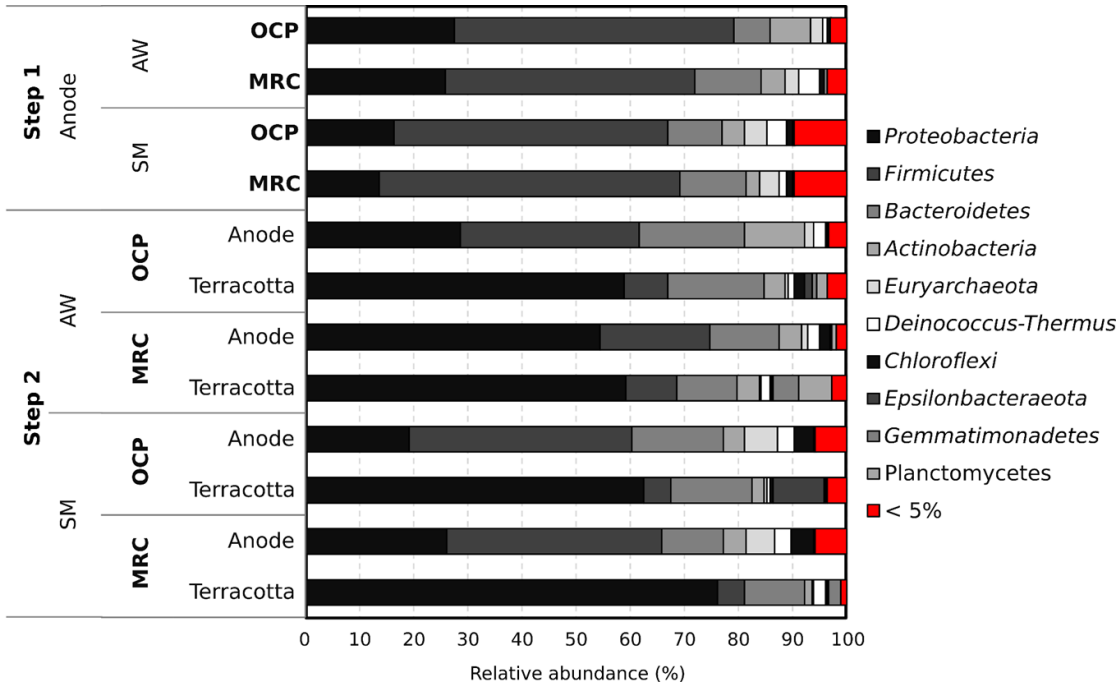

Figure 7 - Relative abundance of the dominant phyla (> 5%) (a) and of Alpha-, Beta- and Gammaproteobacteria (b) in the different compartments.

Specifically, in AW-MRC and SM-MRC Proteobacteria increased of 28.57% and 12.51%, respectively. In AW-OCP, Bacteroidetes and Actinobacteria increased of 12.89% and 3.74%, respectively. In SM-OCP, Bacteroidetes and Euryarchaeota increased of 6.8% and 1.89%, respectively (Table 4). In the terracotta compartments, Proteobacteria were the dominant phylum, ranging from 58.87% to 76.10%, being more abundant in the SM-systems with respect to AW (Figure 7a). The phyla Firmicutes, Proteobacteria and Bacteroidetes have been reported among the dominant taxa enriched in the anodes by several studies (Almatouq et al., 2020; Rago et al., 2018). Whereas in terracotta samples from different BES Gammaproteobacteria were always dominant, in MRC anodes Alphaproteobacteria and Deltaproteobacteria increased in the AW and SM treatment, respectively (Figure 7b). Several studies report the high propensity of Deltaproteobacteria for extracellular electron transfer to anodes (Koch et al., 2019; Wang et al., 2016; Jung and Regan, 2007). In fact, Deltaproteobacteria enriched at the anode are usually related to higher current densities (Logan et al., 2019). At step 2, different species were enriched in the different compartments of the different analysed systems. In SM-

inoculated systems, a number of genera including Clostridium, Methanosaeta, and Fastidiosipila were significantly more abundant in the anodes with respect to terracotta, regardless the electrical circuit applied (Figure 8).

Table 4 – Change in the relative abundance of the 5 major phyla retrieved in the anodes of the analysed systems at step 1 and step 2.

Phylum	Wastewater	System	Step 1 (%)	Step 2 (%)	Difference (%)
Proteobacteria	AW	OCP	27.41	28.68	1.27
		MRC	25.88	54.45	28.57
	SM	OCP	16.21	19.20	2.99
		MRC	13.70	26.21	12.51
Firmicutes	AW	OCP	51.84	32.84	-19
		MRC	46.03	20.14	-25.89
	SM	OCP	50.76	41.04	-9.72
		MRC	55.41	39.73	-15.68
Bacteroidetes	AW	OCP	6.60	19.49	12.89
		MRC	12.14	12.99	0.85
	SM	OCP	10.08	16.88	6.8
		MRC	12.32	11.17	-1.15
Actinobacteria	AW	OCP	7.60	11.34	3.74
		MRC	4.45	4.14	-0.31
	SM	OCP	3.97	3.95	-0.02
		MRC	2.59	4.25	1.66
Euryarchaeota	AW	OCP	2.10	1.40	-0.7
		MRC	2.51	0.96	-1.55

SM	OCP	4.16	6.29	2.13
	MRC	3.35	5.24	1.89

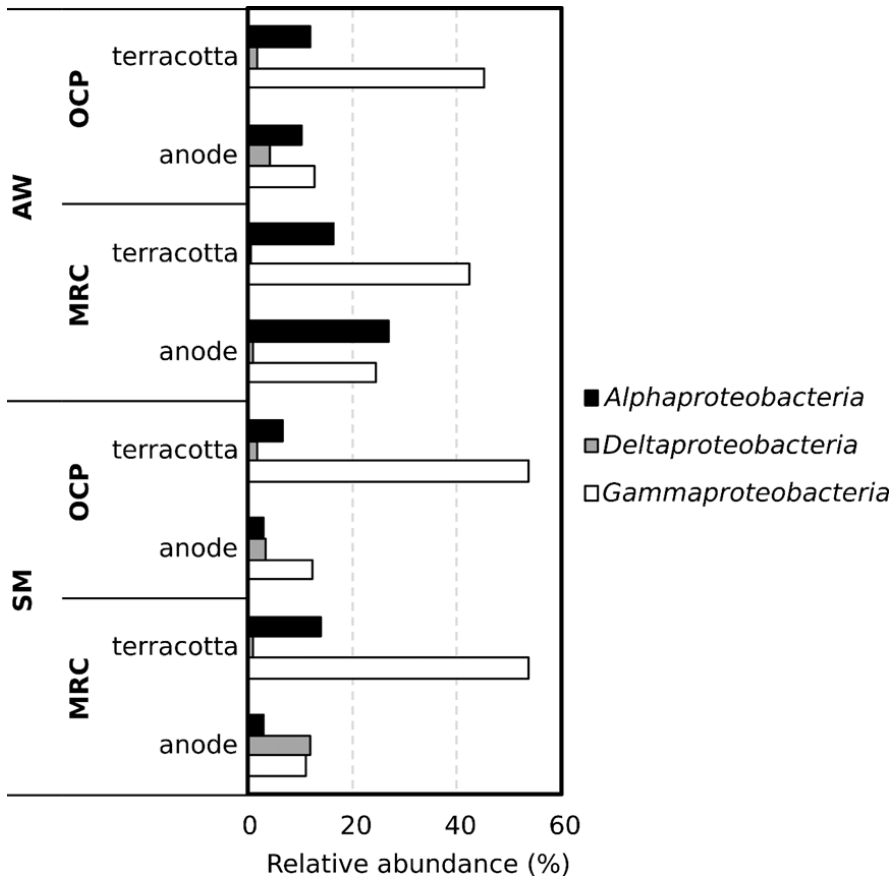

Figure 8 - Relative abundance of the dominant genera retrieved in anodes and terracotta samples from SM-MRC, SM-OCP, AW-MRC and AW-OCP at step 2.

Both Clostridium and Methanosaeta are notoriously electroactive genera (Lovley et al., 2017; Lü et al., 2016), whereas Fastidiosipila has been previously characterized as microaerophilic protein-degrading bacteria, often enriched in anaerobic digesters (Han et al., 2019; Park et al., 2001). In AW-MRC, 3 most abundant genera were identified in the anode of MRC. Among these, only an unassigned genus within the family Rhodobacteraceae (Alphaproteobacteria) was significantly enriched in the anode of AW-MRC, decreasing in the order anodes of AW-MRC > terracotta of AW-MRC > anode of AW-OCP > terracotta of AW-OCP. The genus Clostridium was

enriched in general in the anodes, as observed for the SM-systems, regardless the application of an electrical current. This might indicate a role of Clostridium in the degradation/fermentation of organic matter rather than an active external electron transfer to the anode. It has been shown that in the presence of complex organic substrates, fermentative bacteria may be abundant and support the activity of anodic exoelectrogens (Kiely et al., 2011). In our study, we found the presence of notorious exoelectrogens such as Geobacter sp. and Proteiniphilum sp. (Oliot et al., 2017) at the anodes of MRC with both types of wastewaters, but with very low abundances (data not shown), indicating that other species, including some of the dominants, might play a crucial role both in transferring electrons to the anode and to support the activity of true electroactive microorganisms. Members of the genus Halomonas were highly abundant in the AW-systems, particularly in the terracotta samples and in MRC. Similarly, in the terracotta sampled from SM-MRC; members of Alishewanella were significantly enriched. Both Halomonas and Alishewanella genera include halophilic species (Mata et al., 2001; Vogel et al., 2000; Roh et al., 2009), and were likely promoted by salt deposition and high pH values achieved on terracotta separators. The presence of members of the genus Escherichia in terracotta samples and in OCP systems (data not shown) might be a good indicator of the actual absence of the selective pressure given by an electrical current, since these microorganisms are typically non-exoelectrogenic (Cao et al., 2009).

4. Conclusions

Using terracotta as low-cost porous separator for the air-water interface in MRC, it is possible to see the problem of inorganic salts and organic matter deposition as an add value. The electrochemical forces generated by anodic oxidations are sufficient to increase pH and create a different potential between the electrodes that favor the cations migration and the inorganic salts deposition. Moreover, using a rich-organic wastewater is also possible to maximize the organic matter deposition/recovery (biofouling). After over 100-120 days of operation, these materials can be directly recycled as base for organic-mineral fertilizers and soil conditioners, in agricultural applications in a low-cost and low-tech view of circular economy. Instead, using an artificial wastewater the situation is very different because the system has the first impairment of the electrochemical forces just after 250 days due to the less intensity of the salt deposition compared to the biofouling.

Acknowledgements

This work was financed by the SIR 2014 Grant (PROJECT RBSI14JKU3), Italian Ministry of University and Research (MIUR) by the Research Fund for the Italian Electrical System in compliance with the Decree of March, 19th 2009.

References

Almatouq, A., Babatunde, A.O., Khajah, M., Webster, G., Alfodari, M., 2020. Microbial community structure of anode electrodes in microbial fuel cells and microbial electrolysis cells. J. Water Process Eng. 34:101140. doi:10.1016/j.jwpe.2020.101140

Bybee, S.M., Bracken-Grissom, H., Haynes, B.D., Hermansen, R.A., Byers, R.L., Clement, M.J., Udall, J.A., Wilcox, E.R., Crandall, K.A., 2011. Targeted Amplicon Sequencing (TAS): A scalable Next-Gen Approach to multilocus, multitaxa phylogenetics. Genome Biol. Evol. 3:1312–1323. doi:10.1093/gbe/evr106

Cao, X., Huang, X., Zhang, X., Liang, P., Fan, M., 2009. A mini- microbial fuel cell for voltage testing of exoelectrogenic bacteria. Front. Environ. Sci. Eng. 3:307–312. doi:10.1007/s11783-009-0028-1

Caporaso, J.G., Kuczynski, J., Stombaugh, J., Bittinger, K., Bushman, F.D., Costello, E.K., Fierer, N., Peña, A.G., Goodrich, J.K., Gordon, J.I., Huttley, G.A., Kelley, S.T., Knights, D., Koenig, J.E., Ley, R.E., Lozupone, C.A., McDonald, D., Muegge, B.D., Pirrung, M., Reeder, J., Sevinsky, J.R., Turnbaugh, P.J., Walters, W.A., Widmann, J., Yatsunenko, T., Zaneveld, J., Knight, R., 2010. QIIME allows analysis of high-throughput community sequencing data, Nat. Methods. 7:335–336. doi:10.1038/nmeth.f.303

Cheng, S., Liu, H., Logan, B.E., 2006. Increased power generation in a continuous flow MFC with advective flow through the porous anode and reduced electrode spacing. Environ. Sci. Technol. 40, 2426–2432. https://doi.org/10.1021/es051652w

Cindrella, L., Kannan, A.M., Lin, J.F., Saminathan, K., Ho, Y., Lin, C.W., Wertz, J., 2009. Gas diffusion layer for proton exchange membrane fuel cells—A review. J. Power Sources 194, 146–160. https://doi.org/10.1016/j.jpowsour.2009.04.005

Cristiani, P., Carvalho, M.L., Guerrini, E., Daghio, M., Santoro, C., Li, B., 2013. Cathodic and anodic biofilms in Single Chamber Microbial Fuel Cells. Bioelectrochemistry 92, 6–13. https://doi.org/10.1016/j.bioelechem.2013.01.005

De Bere, L., 2000. Anaerobic digestion of solid waste: state-of-the-art. Water Sci. Technol. 41.

Gajda, I., Greenman, J., Melhuish, C., Ieropoulos, I., 2015a. Simultaneous electricity generation and microbially-assisted electrosynthesis in ceramic MFCs. Bioelectrochemistry 104, 58–64. https://doi.org/10.1016/j.bioelechem.2015.03.001

Gajda, I., Greenman, J., Melhuish, C., Santoro, C., Li, B., Cristiani, P., Ieropoulos, I., 2015b. Electro-osmotic-based catholyte production by Microbial Fuel Cells for carbon capture. Water Res. https://doi.org/10.1016/j.watres.2015.08.014

Gajda, I., Greenman, J., Melhuish, C., Santoro, C., Li, B., Cristiani, P., Ieropoulos, I., 2014. Water formation at the cathode and sodium recovery using Microbial Fuel Cells (MFCs). Sustain. Energy Technol. Assessments 7, 187–194. https://doi.org/10.1016/j.seta.2014.05.001

Ghadge, A.N., Ghangrekar, M.M., 2015. Development of low cost ceramic separator using mineral cation exchanger to enhance performance of microbial fuel cells. Electrochim. Acta 166, 320–328. https://doi.org/10.1016/j.electacta.2015.03.105

Ghadge, A.N., Jadhav, D.A., Pradhan, H., Ghangrekar, M.M., 2015. Enhancing waste activated sludge digestion and power production using hypochlorite as catholyte in clayware microbial fuel cell. Bioresour. Technol. 182, 225–231. https://doi.org/10.1016/j.biortech.2015.02.004

Goglio, A., Marzorati, S., Rago, L., Pant, D., Cristiani, P., Schievano, A., 2019a. Microbial recycling cells: First steps into a new type of microbial electrochemical technologies, aimed at recovering nutrients from wastewater. Bioresour. Technol. 277, 117–127. https://doi.org/10.1016/J.BIORTECH.2019.01.039

Goglio, A., Tucci, M., Rizzi, B., Colombo, A., Cristiani, P., Schievano, A., 2019b. Microbial recycling cells (MRCs): A new platform of microbial electrochemical technologies based on biocompatible materials, aimed at cycling carbon and nutrients in agro-food systems. Sci. Total Environ. 649, 1349–1361. https://doi.org/10.1016/J.SCITOTENV.2018.08.324

Jiang, D., Curtis, M., Troop, E., Scheible, K., McGrath, J., Hu, B., Suib, S., Raymond, D., Li, B., 2011. A pilot-scale study on utilizing multi-anode/cathode microbial fuel cells (MAC MFCs) to enhance the power production in wastewater treatment. Int. J. Hydrogen Energy 36, 876–884. https://doi.org/10.1016/j.ijhydene.2010.08.074

Kelly, P.T., He, Z., 2014. Nutrients removal and recovery in bioelectrochemical systems: A review. Bioresour. Technol. 153, 351–360. https://doi.org/10.1016/j.biortech.2013.12.046

Metodi di Analisi dei Fertilizzanti, n.d. , in: Gazzetta Ufficiale Del 26/01/01 n.21, DM 21/12/00, Suppl. n.8.

Noori, M.T., Ghangrekar, M.M., Mukherjee, C.K., Min, B., 2019. Biofouling effects on the performance of microbial fuel cells and recent advances in biotechnological and chemical strategies for mitigation. Biotechnol. Adv. 107420. https://doi.org/10.1016/J.BIOTECHADV.2019.107420

Noori, M.T., Jain, S.C., Ghangrekar, M.M., Mukherjee, C.K., 2016. Biofouling inhibition and enhancing performance of microbial fuel cell using silver nano-particles as fungicide and cathode catalyst. https://doi.org/10.1016/j.biortech.2016.08.061

Papaharalabos, G., Greenman, J., Melhuish, C., Santoro, C., Cristiani, P., Li, B., Ieropoulos, I., 2013. Increased power output from micro porous layer (MPL) cathode microbial fuel cells (MFC), in: International Journal of Hydrogen Energy. Pergamon, pp. 11552–11558. https://doi.org/10.1016/j.ijhydene.2013.05.138

Parameswaran, P., Torres, C.I., Lee, H.S., Krajmalnik-Brown, R., Rittmann, B.E., 2009. Syntrophic interactions among anode respiring bacteria (ARB) and non-ARB in a biofilm anode: Electron balances. Biotechnol. Bioeng. 103, 513–523. https://doi.org/10.1002/bit.22267

Pasternak, G., Greenman, J., Ieropoulos, I., 2015. Comprehensive Study on Ceramic Membranes for Low-Cost Microbial Fuel Cells. ChemSusChem 88–96. https://doi.org/10.1002/cssc.201501320

Pepè Sciarria, T., Vacca, G., Tambone, F., Trombino, L., Adani, F., 2019. Nutrient recovery and energy production from digestate using microbial electrochemical technologies (METs). J. Clean. Prod. 208, 1022–1029. https://doi.org/10.1016/J.JCLEPRO.2018.10.152

Rago, L., Zecchin, S., Marzorati, S., Goglio, A., Cavalca, L., Cristiani, P., Schievano, A., 2018. A study of microbial communities on terracotta separator and on biocathode of air breathing microbial fuel cells. Bioelectrochemistry 120. https://doi.org/10.1016/j.bioelechem.2017.11.005

Santini, M., Guilizzoni, M., Lorenzi, M., Atanassov, P., Marsili, E., Fest-, S., Cristiani, P., Santoro, C., Fest-santini, S., 2015a. Three-dimensional X-ray microcomputed tomography of carbonates and biofilm on operated cathode in single chamber microbial fuel cell Three-

dimensional X-ray microcomputed tomography of carbonates and biofilm on operated cathode in single chamber microbial 031009, 1–10. https://doi.org/10.1116/1.4930239

Santini, M., Marzorati, S., Fest-Santini, S., Trasatti, S., Cristiani, P., 2017. Carbonate scale deactivating the biocathode in a microbial fuel cell. J. Power Sources 356, 400–407.

Santoro, C., Artyushkova, K., Gajda, I., Babanova, S., Serov, A., Atanassov, P., Greenman, J., Colombo, A., Trasatti, S., Ieropoulos, I., Cristiani, P., 2015. Cathode materials for ceramic based microbial fuel cells (MFCs). Int. J. Hydrogen Energy 40, 14706–14715. https://doi.org/10.1016/j.ijhydene.2015.07.054

Verstraete, W., Van de Caveye, P., Diamantis, V., 2009. Maximum use of resources present in domestic "used water." Bioresour. Technol. 100, 5537–5545. https://doi.org/10.1016/j.biortech.2009.05.047

Winfield, J., Gajda, I., Greenman, J., Ieropoulos, I., 2016. A review into the use of ceramics in microbial fuel cells. Bioresour. Technol. 215, 296–303. https://doi.org/10.1016/j.biortech.2016.03.135

Winfield, J., Greenman, J., Huson, D., Ieropoulos, I., 2013. Comparing terracotta and earthenware for multiple functionalities in microbial fuel cells. Bioprocess Biosyst. Eng. 36, 1913–1921. https://doi.org/10.1007/s00449-013-0967-6

Ye, Y., Ngo, H.H., Guo, W., Chang, S.W., Nguyen, D.D., Liu, Y., Nghiem, L.D., Zhang, X., Wang, J., 2019. Effect of organic loading rate on the recovery of nutrients and energy in a dual-chamber microbial fuel cell. Bioresour. Technol. 281, 367–373. https://doi.org/10.1016/J.BIORTECH.2019.02.108

Yu, W., Zhang, D., Graham, N.J.D., 2017. Membrane fouling by extracellular polymeric substances after ozone pre-treatment: Variation of nano-particles size. Water Res. 120, 146–155. https://doi.org/10.1016/j.watres.2017.04.080

Chapter 4 - Electroactive biochar for large-scale environmental applications of microbial electrochemistry

Andrea Schievano*[1], Raul Berenguer[2,3], Andrea Goglio[1], Stefano Bocchi[1], Stefania Marzorati[1], Laura Rago[1], Ricardo O. Louro[4], Catarina M. Paquete[4], Abraham Esteve-Núñez[3,5]

1 e-BioCenter - Department of Environmental Science and Policy (ESP), Università degli Studi di Milano, Via Celoria 2, 20133 Milan, Italy

2 Instituto Universitario de Materiales, Departamento de Química Física, Universidad de Alicante UA, Apartado 99, 03080-Alicante, Spain

3 IMDEA Water Institute, Av. Punto Com, 2, 28805 Alcalá de Henares, Madrid, Spain

4 Instituto de Tecnologia Química e Biológica António Xavier da Universidade Nova de Lisboa, Av da República (EAN), 2780-157 Oeiras, Portugal

5 University of Alcalá, Department of Chemical Engineering, Ctra. Madrid-Barcelona, km. 33,6, 28871, Alcalá de Henares, Madrid, Spain

*Corresponding author; email: andrea.schievano@unimi.it

Published in:

Schievano A., Berenguer R., Goglio A., Bocchi S., Marzorati S., Rago L., Louro R.O., Paquete C.M., Esteve-Núñez A., 2019. Electroactive biochar for large-scale environmental applications of microbial electrochemistry. ACS Sustainable Chemistry & Engineering. doi:10.1021/acssuschemeng.9b04229

Abstract

Large-scale environmental applications of microbial electrochemical technologies (MET), such as wastewater treatment, bioremediation or soil improvement, would be more feasible if bioelectrodes could be fabricated with simpler materials. Biochar with potentially improved electroactive properties (e-biochar) can be an ideal candidate for this scope, being at the same time widely available, biocompatible and fully recyclable at end-of-life as soil amendment. Here we review the application of biochar to MET, to set benchmarks aimed at tuning the electroactive properties of such materials from the point of view of MET. The precursor biomass, thermochemical process conditions, and pre-, in-situ- and/or post-treatments should tailor optimized combinations of electrical conductivity, capacitance, superficial redox-active and electroactive functional groups, porosity distribution and capacity to host electroactive microbial communities. We also discuss methods to rigorously characterize e-biochar properties and the most relevant multidisciplinary research challenges towards its application in large-scale MET.

Keywords

e-biochar, microbial electrochemical technology, soil microbiology, bioremediation, electron transfer, bioelectrode, wastewater

1. Introduction: a new generation of bioelectrodes?

Microbial electrochemical technologies (MET, see Nomenclature) are based on the capacity of certain microbes to use electrically conductive materials as electron acceptors or donors for their metabolism. Several different mechanisms involved in extracellular electron transfer (ET) to solid conductors have been demonstrated in a number of electroactive microorganisms (see Nomenclature) [1]. The interest in research on MET has grown exponentially and a variety of applications has been proposed. In over 15 years of laboratory- and pilot-scale studies, bioelectrodes (see Nomenclature) have been typically fabricated using 'technological' materials (e.g. carbon fibers, graphite, graphene, carbon nanotubes, precious metals such as titanium, platinum, etc.) [2]. At present, carbon materials represent the most widely used electrodic support, due to their excellent electrochemical properties and stability to corrosion. The most competitive include graphite-based rods, fiber brushes and granules, carbon-fiber cloths, carbon paper sheets, carbon felt and reticulated vitreous carbon [3]. Besides, often METs' architectures and materials have traced the technological features of typical engineered electrochemical cells, such as (abiotic) fuel cells or electrolysis cells. Such designs include

plastic- or metal-based frames as support for electrodes or current collectors [4-8]. Some examples of such electrodes were recently presented at the m^2-scale [9]. However, when MET are envisioned for large-scale environmental applications (e.g. wastewater treatment, soil/water bioremediation, biomass processing, CO_2 fixation, etc.), the use of such materials and architectures might be a substantial challenge, because of their high economic, environmental fabrication costs and low sustainability at end-of-life [10].

In this article, we aim at pointing a spotlight on an emerging class of carbon materials for potential large-scale MET applications. The target materials should simultaneously be electroactive (see Nomenclature), to facilitate MET applications; available in large amounts, at relatively low costs and environmental impacts; and easily recyclable at end-of-life. Carbon materials with several electroactive properties can be also found in large quantities at potentially low costs (e.g. charcoal, black carbon, cokes and graphites). In MET, such materials have been extensively applied as coating layers on bioelectrodes to improve (bio-) electrochemical properties [11]. However, most of them are extracted from fossil reservoirs. More sustainable carbon materials, with similar and more versatile properties, can be produced by thermochemical conversions (see Nomenclature) of biomass and are generally referred to as biochar.

Biochar (see Nomenclature) has been extensively studied in the agricultural sciences framework as soil fertility improver and a way of sequestering chemically-stable carbon over long term [12]. Very rarely, electrochemical properties such as electrical conductivity and superficial electroactivity were considered in this framework. Commercial biochar has typically widely variable and relatively poor structural/mechanical properties (as compared to other carbons), as well as low electrical conductivity [13]. This have generally restricted its technological applications as compared to more performing carbon-based materials.

In the MET field, electrical conductivity has been largely perceived as a key factor on performance of electrode materials. This might be probably due to the strong influence of the electrochemical science branch in this multidisciplinary field: several applications have been based on the possibility to harvest electrons through external circuits, just like in abiotic electrochemical cells (e.g. in microbial fuel cells, MFCs). In such applications, the role of biochar has remained marginal. However, METs embrace a much larger range of possible applications in the field of environmental biotechnology. For instance, one of the most fascinating recent findings was the possibility to enhance interspecies ET in soil microbial communities, by the presence of biochar [14]. In another study, biochar outperformed highly

conductive carbon materials (graphite, coke) in stimulating extracellular ET and enhanced pollutants removal from wastewater in electroactive biofilters [15]. This happened because the superficial electroactivity played a major role, while electrical conductivity was sufficient to allow overall ET towards terminal electron acceptors [15].

Here, we introduce the new concept of electroactive biochar (e-biochar), which constitutes a particular category of biochars, with a range of improved and tailored properties aimed at maximizing electrochemical interactions with microbes. Such materials would be ideal as bulk material for the fabrication of large-scale sustainable METs. So far, only a few studies have systematically focused on potential technological applications of such properties to fabricate large-scale bioelectrodes. In this paper, we set some benchmarks for future efforts in this promising research field.

2. Biochar vs e-biochar

Agriculture-derived biomass by-products and green waste can undergo thermochemical conversions, to yield bioenergy and biochar. Biochar has been largely studied as agricultural soil amendment, capable of favoring soils properties, acting as carbon sink over long term, stimulating soil microbial communities in several important soil processes [16,17]. Among agricultural scientists, biochar was considered as a relatively 'conductive' material, as compared to organic redox-active molecules (e.g. humic acids) 18. Despite this, the potential impacts of biochar's electrochemical properties on microbial communities were rarely considered in this framework. More recently, some authors reported that the presence of biochar promotes interspecies ET in soils [19-24]. In a review, Yuan and colleagues [25] defined biochar as environmentally-sustainable electron donor/acceptor for biogeochemical redox reactions. Biochar acts as rechargeable reservoirs of bioavailable electrons, i.e. the so-called "geobatteries" [22,26]. Functional groups can participate in reversible surface (interfacial) redox reactions with other ambient species, including electroactive microbial communities [25]. Besides, the carbon matrix, organized with variable graphitization degrees, can store, transport and exchange electrons, i.e. the 'geoconductor' mechanism 26. While superficial electroactive functional groups play a key role in local ET [27], extended conductive graphitic structures may enable long-range ET, facilitating external access to electron acceptors/donors. The combination of conductivity and ET capacity is generally referred to as 'electroactivity' [26].

On the other side, material scientists and electrochemists have been considering biochar as an amorphous/low-crystalline material with interesting superficial ET properties, but poor

electrical conductivity (~10^{-2} - 10^{-4} S cm^{-1}, i.e. much lower than technological electrode materials), substantially unsuitable for fast-response abiotic electrochemical applications [28].

Under the perspective of MET, however, the term 'electroactive' should be seen under a new light. Bioelectrodes are typically characterized by much slower ET rates and current densities than abiotic electrodes [29]. Therefore, high surface areas available for microbial EET, features stimulating extracellular ET, and sufficient conductivity may be needed for effective applications in METs, rather than materials with outperforming abiotic electrochemical properties. In this sense, biomass or conventional biochar can undergo thermochemical, chemical and structural treatments, for 'tuning' a wider spectrum of properties, that concur to harmonize the complex mechanisms involved in microbial EET, depending on the final MET application.

The obtained bulk material, 'e-biochar', is proposed as a new class of biochars with tailored conductivity and ET properties for specific METs application. Because widely available, biocompatible and fully recyclable at end-of-life as soil amendment, e-biochar is an ideal candidate to fabricate bioelectrodes for large scale METs applications, as compared to traditional 'technological' carbon conductors.

3. e-biochar: fabrication of biochar with improved electrochemical properties

To obtain ideal e-biochars, fabrication techniques should look at optimizing the main properties that influence electron transfer (ET), conduction and storage [28]. Under abiotic conditions, similarly to other carbon materials, biochar has been described to accept or donate electrons (irreversible superficial redox activity), reversibly transfer electrons (superficial electroactivity) or transport them within the material (electroconductivity) [28]. The porous texture and the available surface area at different pores dimensions have an important influence on these properties [28]. Finally, the capability to host and promote electroactive microbial communities over such surface is the key factor for e-biochar. Pores dimensions are also likely to determine the accessibility of surface area to direct contact with microbes or to biomolecules that promote EET [30–32].

The ideal e-biochar, depending on the application, could be rendered by an equilibrium of all these properties. This tuning is achieved by playing with the structural, textural and chemical nature of the precursor biomass, the conditions used during carbonization, additional chemical/physical treatments and the enrichment of microbial electroactive communities (Figure 1).

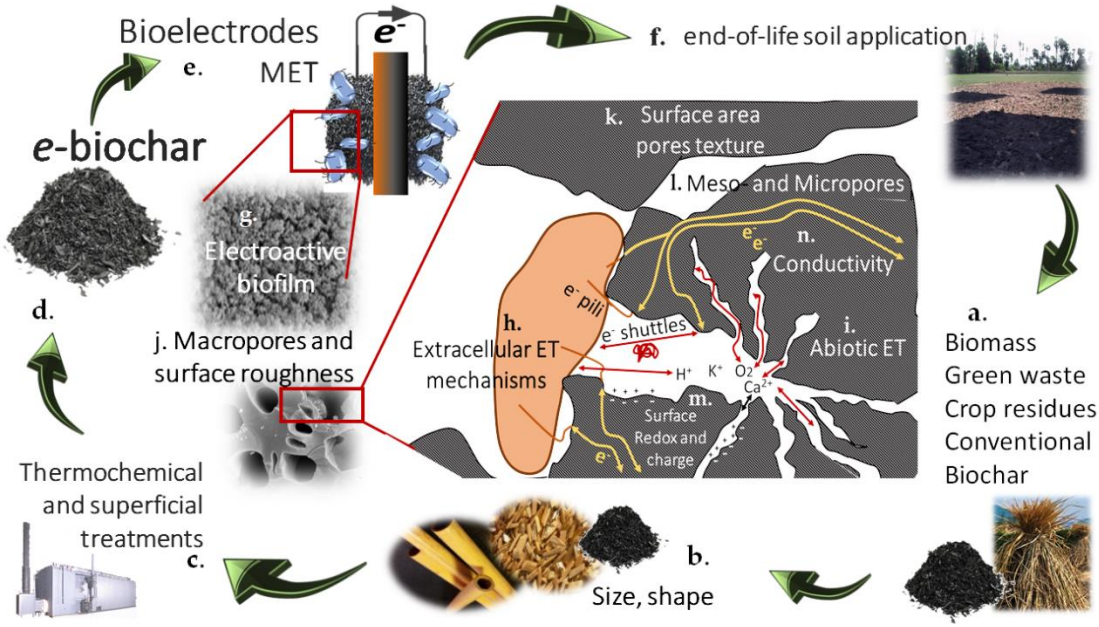

Figure 1 - Low-cost and widely available materials are needed for large-scale environmental applications of microbial electrochemical technologies (MET), when most high-tech materials are substantially excluded. Electroactive biochar (e-biochar) might open a new perspective. Residual biomass derived from agro-forestry and conventional biochars (a) undergo: mechanical pretreatments to set precise conformations (b), optimized thermochemical conversions and specific superficial treatments (c), to sustainably produce electroactive-biochar (e-biochar) (d), as base for the fabrication of bioelectrodes in possible large-scale MET (e). At end-of-life, such electrodes can be used in soil conditioning and e-biochar might contribute to soil fertility (f). The word 'electroactive', under the point of view of MET, includes a series of chemical/textural/structural properties that tend to simultaneously optimize: electroactive biofilm growth (g), microbial extracellular electron transfer (ET) mechanisms (h) and abiotic reversible redox reactions towards ET (i), surface area and pores texture (j), porosity distribution (k,l), surface redox and charge properties (capacitance), due to chemical composition (m) and sufficient electrical conductivity over given distances (n).

Redox-activity, electroactivity and conductivity are related with chemical and structural properties, which are modulated essentially by the temperature and pressures of preparation [33]. Biochar's conductivity is directly related to its structural (graphitic) order (Figure 1-n). Its structure may lie between amorphous (non-graphitic) natural organic molecules (humic/fulvic acids, biopolymers, etc.) and graphitized carbons (with variable 2D/3D crystalline order of polyaromatic layers) [34]. The longer the range of crystalline order, the more delocalized the π-electrons and, thus, the higher electrical conductivity. Higher aromatic content in the biomass may also lead to more conductive e-biochars [35]. Higher carbonization temperatures (> 600°C), slower heating rates and longer treatments (hours) promote structural order [35,36] and, consequently, conductivity [26]. Some electron-donating O-, N- and metals functional groups may increase the conductivity too. By contrast, the presence of electron-demanding functional groups and increased porosity (rendering a larger concentration of textural defects) may decrease the conductivity of e-biochars. If normal biochar's conductivity falls typically in the range 10^{-2} - 10^{-4} S cm^{-1} (far from that of graphites ~10-30 S cm^{-1}), e-biochar might find optimal values in between (10^{-2} - 10 S cm^{-1}) (Table 1). However, deeper investigation is needed to define optimal conductivity ranges, depending on the target application, electrode configuration and dimensions.

Both quantity of available surface area and its quality (presence of electroactive functional groups and the capability of reversible binding/adsorption of ionic positive charges) strongly influence ET and the related phenomena (Figure 1-m), such as pseudocapacitance and double-layer capacitance [28]. Depending on the redox potential of superficial reversible redox-active groups and/or the aromatic rings, the material might show greater tendency to uptake/release electrons and transport through conductive graphitic structure (Figure 1-i) [36–38]. First, a suitable precursor may introduce a given proportion of O, N, P, S and metals on the final biochar [39,40]. Second, the choice of suitable heating conditions strongly affects the nature and concentration of superficial functional groups: at higher pyrolysis temperatures, both O/C and H/C ratios decrease [36], as well as the proportion of less-stable O-functional groups in favor of more stable ones [41]. When prepared at lower temperatures (<700ºC), the ET in biochar is mainly mediated by surface functional groups (i.e. phenolic/quinoid groups) [26,42]. All the different functional groups are susceptible of exhibiting redox activity. Besides the well-known phenolic/quinone couple, other have been demonstrated as abiotic electroactive functional groups: anhydride [43], N-(pyridine/pyridinic) [39] and P-groups [44].

Table 1 - Studies reporting properties of e-biochars, fabrication techniques, observed effects on microbial communities, observed ET mechanisms.

Precursor Feedstock	Pyrolysis conditions and treatments	Particle size or geometrical shape	BET* Surface Area (m^2 g^{-1})	Porosity range	Electrical conductivity (mS cm^{-1})	Surface heteroatoms / functional groups
a. Studied in abiotic electrodes						
Pomelo peel	1000 °C	n.r.*	622.2	63% micro, 36% meso	n.r.	Fe, N
Dewatered sewage sludge	800 °C	n.r.	265.05	Mesopores	n.r.	N, S, Fe
Cellulose	250-500 °C	0.8-2 mm	199 - 557	Mesopores	n.r.	N, P
Coconut shell	800 °C	Carbon paste electrode (mixed with spectro grade paraffin wax)	2536	Micropores	n.r.	n.r.
Cotton microfiber	700 – 850 °C	n.r.	912.1	Mesopores	n.r.	N
Sawdust and sugarcane straw	800 °C	n.r.	590	Micropores	n.r.	n.r.
b. Studied in MET at laboratory scale						
Pine	700°C for 30 sec & 500°C for 15 min	≤0.4 mm	15	n.a	4.4	n.r.
Wood chip	620°C	0.1-0.3 μm and a significant fraction of 3−30 μm	341	n.a	49.7	N, Fe
Rape-straw	350 °C, 20 °C min^{-1} held constant for 4 h	0.165-mm	2.12	n.r.	n.r.	n.r.
Rice straw	increase at 20°C min^{-1} up to 900°C for 1 h	0.15 mm	10.85	n.r.	2.4	n.r.
Sieving residues	550ºC for 2 h	n.r.	193.9	n.r.	n.r.	n.r.
Mature coconut shell	900 °C for 1.5 h	0.3 mm	n.r.	n.r.	2.6	n.r.
Activated sludge	increase at 10ºC min^{-1} up to 500ºC	0.15 mm	n.r.	n.r.	n.r.	n.r.
Fruitwoods	800-900ºC	2-5 mm, 0.5-1 mm and 75-150 μm	n.r.	n.r.	n.r.	n.r.

Rice-straw treated with 3.2 g $FeCl_3$:100 g	500 °C for 2 h	0.15 mm	5.48	Mesopores	n.r.	n.r.
Pine chips	800-1000 °C for 8 h	0.5-1.0 mm	8.92	n.r.	n.r.	n.r.
Rice straw	5 °C min^{-1} up to maximum T° for 2 h: 300 °C, 800 °C	0.15 mm	2.6 205	n.r.	8.4 20.4	n.r.
Pine wood lumber	1000 °C	Fine frit glass filter funnel	183.0	82% Micropores	n.r.	Traces of metals
Bananas	550-900 °C	Ground to powder	105.2 - 172.3	n.r.	n.r.	N
Chestnut shell	900 °C	Natural chestnut shell shape and powder	468	71% Microopores	n.r.	N
Corncob	250, 350, 450, 550, 650, 750 °C for 2 h	Ground to powder	n.r.	n.r.	n.r.	n.r.

c. Self-standing 3D shaped e-biochar bioelectrodes

Pinewood sawdust pellets and chips	1000 °C	26-700 mm^3	0.04	Small mesopores	16 - 35	n.r.
Giant cane (*Arundo donax L.*) stalks	900 °C	Natural cylindrical shape (10 mm diameter, 10-20 cm length)	114	Micropores	11	N, P
Kenaf (*Hibiscus cannabinus*)	1000 °C	Natural cylindrical shape 4 mm/10 mm inner/outer diameters	n.r.	Macro-channels of 50-60 µm	n.r.	n.r.
Bamboo	1000°C	Tubes with inner diameter: 1 mm, 1.5 mm, 2 mm and 3 mm	n.r.	n.r.	n.r.	n.r.
Pomelo peel	900°C	Sponge-like architecture	n.r.	Macroporous architecture	n.r.	n.r.
King mushroom, wild mushroom and corn stem	1000°C	Sponge-like architecture	n.r.	Macroporous architecture	n.r.	n.r.
Natural Loofah Sponge	900°C	Sponge-like architecture	445-504	Macroporous architecture	n.r.	N

d. Potentially-scalable bioelectrodes configurations (some studies were based on non-biogenic carbons)

Graphite granules fixed bed	-	2-3.5 mm	n.r.	n.r.	n.r.	n.r.
Graphite particles/glassy carbon particles	-	0.42 to 0.69 mm/0.63 to 1 mm	n.r.	n.r.	n.r.	n.r.

unspecified	n.r.	Granules of 1–3 mm diameter	764	n.r.	n.r.	n.r.
Coke granules fixed bed	-	5-20 mm	n.r.	n.r.	n.r.	n.r.
Quercus wood biochar fixed bed		6-12 mm	250 (N_2 isoterm) 550 (CO_2 isoterm)	Hierarchical structure	0.37	O, Phenols, Quinones, Fe,

Under abiotic conditions, an amount of 1.57 mmol quinone g^{-1} was found among the highest pseudocapacitive (electroactive) contributions ever reported in carbon materials [45]. Above 1200 °C, most superficial functional groups are typically decomposed [46]. Another factor greatly affecting the redox- and electroactivity may be the presence of certain minerals (mineral oxides, silicates and salt phases) [47]. Special attention must be paid to the effects of some metallic species, particularly alkaline metals and other nutrients commonly present in biomass, which are well-known catalysts of the chemical activation of chars [36].

The porous texture (see Nomenclature) is the last piece of this complex puzzle. Several literature reports revealed pore size distribution of extraordinary hierarchical architectures (Figure 2). Roughness and macroporosity mainly depend on the precursor (Figure 1a-b). Except for some thermoplastic biopolymers (which fluidize at certain temperature), the carbon-enriched material retains the initial characteristic shape (Table 1-c). Thus, some biochars can exhibit the vascular structure of preceding plant trunks/stems (Figure 2A-C). The meso-/microporosity inherently develops with increasing temperature by the loss of volatile matter, up to a maximum (800-1000°C) [36,48] and then decreases due to solid reorganization. These features usually lead to surface areas in the 10-600 $m^2 g^{-1}$ (Table 1).

Remarkably, a larger volume of micro-/mesopores reduces conductivity, but simultaneously provides a larger number of sites with distinct electroactive functional groups [49]. Meso- and micropores also determine the double-layer capacitance (electrostatic storage of charge by reversible adsorption of ions onto the surface, Figure 1-m). Since e-biochar particles must be globally neutral, the number of electrons exchanged by electroactive microorganisms are likely to be limited by the capability of the surface to compensate this negative charge. The effective adsorption of positive charges on a larger (microporous) surface area might therefore be a determining factor towards ET from biofilms. This hypothesis is in line with the geobattery mechanism [22] and should be better investigated. An equilibrium between conductivity and superficial electroactive properties should be found, according to the target application, and deserve dedicated studies.

Finally, precursors (which can be both biomass or conventional agriculture-derived biochars, Figure 1-a) can be conformed into suitable conformations (pellets, monoliths, granules etc.) for specific applications (Figure 1-b). Several pre-, in-situ, and/or post-modification treatments (Figure 1-c) might tailor bulk e-biochars with optimized structural, textural and chemical features, similarly to activated carbons (Table 1). Surfaces can be chemically-/physically activated [40,50]. P-functional groups can be introduced by H3PO4-activation [37,44,46] and various oxidative treatments may induce O-, N- and S- superficial functional groups [41,51,52]. Electrochemical post-treatments may be a green choice to incorporate electroactive phenolic/quinoid groups [33]. However, any additional treatment may increase the production costs and impacts of bulk e-biochar.

4. Properties and characterization techniques to define e-biochar

Structural, chemical, and textural properties should be thoroughly studied using a range of analytical techniques (Table 2).

Table 2 - Properties and characterization techniques used to define e-biochar.

Property	**Technique**	**Parameters**
Electrical Conductivity	Four-Point Probe Resistivity	Resistivity (Ω cm) or conductivity (S cm^{-1})
	AC impedance	
Structural order	XRD *	Features of (002) and (100) peaks
	Raman	Features of D, G and 2D bands
Surface chemistry	XPS	Surface % C, N, S, O, P and metals (and qualitative)
	TPD-MS *	mmol (CO_2/CO-evolving O-functionality)/g e-biochar (and qualitative)
Chemical composition	Elemental analysis ICP-MS	Bulk % C, H, N, S, O, ash
Porous texture	N_2 adsorption-desorption isotherms	S_{BET} (m^2 g^{-1}), Vmicro and Vmeso (cm^3 g^{-1})

	CO_2 adsorption	ACO_2 (m^2 g^{-1}), VCO_2 (cm^3 g^{-1})
	Hg porosimetry	VHg (cm^3 g^{-1}) macroporosity, porosity (%), density
Morphology	SEM *	Rugosity, pore size and shape
Redox properties	Potentiostatic electrochemical analysis	Electron-exchange Capacity (EEC)
	Hydrodynamic electrochemical techniques	Electron-Accepting Capacity (EAC) Electron-Donating Capacity (EDC)
Electrochemical properties	CV *	Electrochemically-active surface area (EAS), electro-active species, ion-diffusion, charge-transfer under abiotic conditions
	EIS *	
Microbial electrochemical properties	Chronoamperometry, linear voltammetry, CV, EIS	Electrogenic current density, bacteria-biochar charge transfer (potential, current, resistance)
Biofilm morphology, identification of microorganisms	SEM, Confocal microscopy, FISH, DAPI *	
Specific enzymatic activity	assessment of dehydrogenase activity (DH), fluorescein diacetate hydrolysis activity (FDA), others	
Microbial communities composition and functional analysis	16S rDNA Illumina sequencing and/or rRNA intergenic spacer analysis (RISA)	

* **CV:** cyclic voltammetry; **EIS:** electrochemical impedance spectroscopy; **SEM:** scanning electron microscopy; **TPD-MS:** temperature-programmed desorption coupled to a mass spectrometer; **XRD:** X-ray diffraction; **XPS:** X-ray photoelectron spectroscopy; **FISH:** fluorescence in situ hybridization; **DAPI**: 4',6-diamidino-2-phenylindole dye coupled to fluorescence microscope used for cells counting.

These properties strongly affect the abiotic redox-activity and electroactivity, features that have been often confused in the literature. Biochar's electroactivity is estimated as electron exchange capacity (EEC), i.e. the sum of the electron donating and accepting capacities (EDC, EAC) [53]. These properties are associated exclusively to reversible electroactive functional groups and often measured by mediated (indirect) electrochemical analysis [28,42,54]. However, these methods detect also redox-active species that are irreversibly oxidized/reduced at biochar's surface [42,54]. The characterization should be complemented by electrochemical techniques like CV and EIS [35]: the electrochemically-active surface area (EAS) and the ion diffusion capability determine the reversible (abiotic) charge transfer with biochar surface. These properties are strongly influenced by the available micro- and meso-porous surface area. Remarkably, the electroactivity of quinoid-like groups, proposed to mediate in ET with bacteria, can be characterized by CV [26], and the involved charge may be related to their number and accessibility of these groups, the conductivity, etc.

The actual capability of the material to promote ET in microbial reactions completes the definition of e-biochar. The e-accepting/donating capacity of e-biochar in MET is proportional to the abundance and diversity of electroactive biofilm communities grown on the solid surface. As the ultimate charge transfer depends on microbial EET kinetics, which are typically much slower than in abiotic ET, electrochemical techniques are often adapted to such conditions [55]. The morphology of biofilms can be revealed by several microscope techniques, coupled to selective probes. Microbial electroactive communities can also be investigated by molecular, culture-dependent analyses and microscopic techniques (Table 2).

5. State of the art of biochar in MET

Little is rigorously proven about the possible electrochemical interactions between microorganisms and biochar. In the agricultural and soil science framework, positive effects of biochar on soil microbial pool have been largely reported [17]. However, electrochemical aspects were rarely taken into account. Only more recently, the emerging scientific community of microbial electrochemistry published a relatively small number of studies on the behavior of biochar as electrode interface in specific MET (Table 1). Some authors used biochar on MET electrodes, but limited the focus to particular electrocatalytic properties of the material on abiotic electrodes (Table 1-a). Several other authors reported that the presence of biochar on bioelectrodes enhanced redox reactions towards metals or organic compounds, by enriching the biofilm community with electroactive microbial species [20,21,23,24,56,57]. Remarkably, biochar was demonstrated to act as promoter of direct interspecies ET for different syntrophic

associations of microorganisms, thanks to its electrical conductivity and stimulating capacity of EET by pili or other direct membrane mediators [14]. In this study, microbial co-cultures did not need to form aggregates, suggesting that the cells were electrically connected through the biochar, which permitted EET. Besides, the addition of biochar particles in anaerobic fermenters was found to increase overall electrical conductivity in the bulk liquid and facilitate EET, between both fermentative and methanogenic communities [58-62]. Interestingly, SEM images of the biofilm showed that both microbial cells and high-density structure of extracellular polymeric substances (EPS) were increasingly denser in the vicinity of biochar particles [58].

In these studies, however, several reasons have often led to uncertain conclusions. Biochars are complex materials showing inter-related properties, affecting extracellular ET in different ways. There is a lack of systematic studies analyzing the influence of only one property, disregarding others. Tailoring specific properties, without affecting the others, is difficult; in most works the characterization of biochar was incomplete; both surface chemistry and porous texture of biochar were insufficiently considered for their influence in extracellular ET (Table 1).

The accessibility to the electrochemically-active surface area (EAS) includes more aspects than in abiotic systems, implying the capability to host microbes (Figure 1-h) and/or promote diffusion of many different primary agents, i.e. ions, electrons, redox mediators, electron shuttles (see Nomenclature) and increase hydrophilic properties of the material. In e-biochar-based bioelectrodes, surface area and pore volume distribution (Figure 2) likely play a relevant role for reasons other than affecting conductivity and superficial redox reactions. Suitable pore textures are essential to host microbial communities and promote biofilm growth [63]. Also, EET reactions depend on the accessibility of surface area to the primary agents of redox reactions, including microbial cells, molecular electron shuttles, soluble carbon sources and dissolved ions.

In particular, surface roughness and macroporous surface area (Figure 1-j) strongly influence the access of microbes to surface [64] and biofilm anchorage [65,66]. This aspect is well known and carbon powders are widely used to increase the surface of plain carbon-cloth bioelectrodes and improve their bioelectrochemical performances [67]. Although, most studies on carbon-based bioelectrodes lack of data regarding architectural and dimensional features at macroporous scales, focusing only on meso- and micro-pores [2].

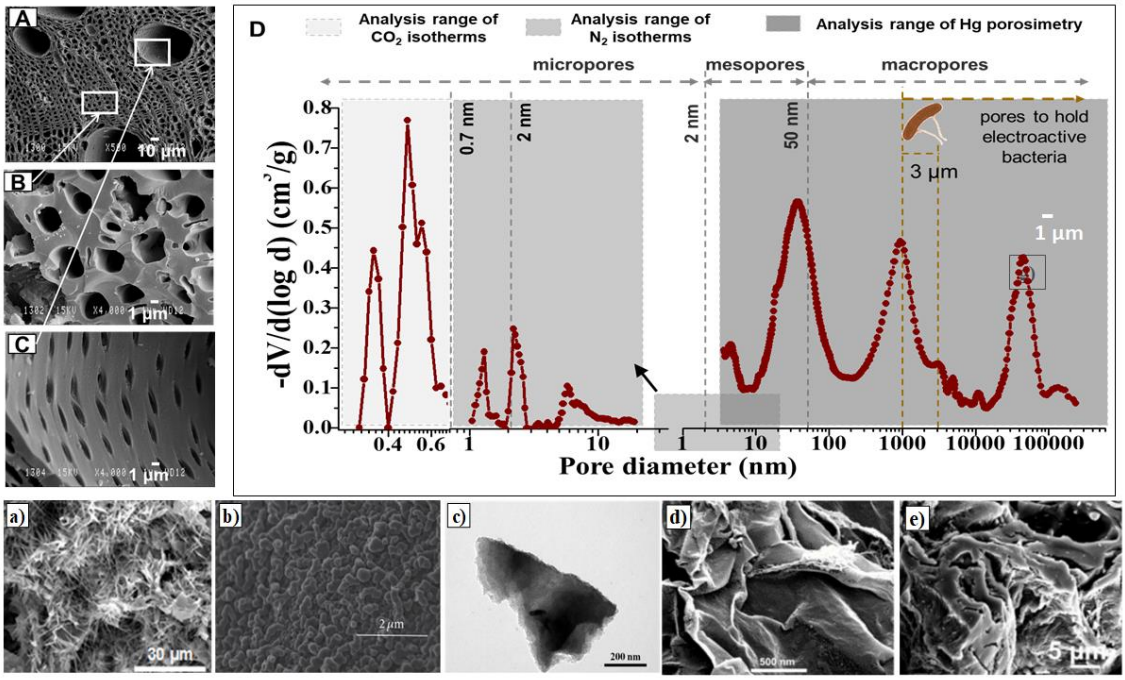

Figure 2 - Scanning electron microscopy (SEM) images of biochars synthesized by different groups in the literature: A-C) Prado et al., 2018 ; D) Pore size distributions from different techniques (considering DFT model and Washburn's equation for isotherms and porosimetry, respectively) of a quercus-derived biochar shown in A-C. Other SEM reports at different scales: a) Q. Chen et al., 2018; b) Lin et al., 2017; c) Ma et al., 2016; d) Yuan et al., 2014; e) Zha et al., 2016 (Chen et al. 2018; Lin et al. 2017; Ma et al. 2016; Yuan et al. 2014; Zha et al. 2016). SEM images demonstrating biochar-mediated interspecies electron transfer in f) G. metallireducens and G. sulfurreducens and g) G. metallireducens (rods) and M. barkeri (spheres) co-cultures (Chen et al. 2014). Reprinted (adapted) with permission from (Chen et al. 2018; Lin et al. 2017; Ma et al. 2016; Yuan et al. 2014; Zha et al. 2016). Copyright © 2017, American Chemical Society and Elsevier.

The surface area of meso-pores (Figure 1-l) is inaccessible to microbial cells (< 50 nm, Figure 2) and eventually available only to molecular electron shuttles (Figure 1-h). In fact, EET processes performed by electroactive microorganisms are based either on direct contact with the cell, or through redox-active molecules, that interact with the components of the respiratory redox-chain and diffuse in the outer medium [27] (Figure 1-h). Up to date, four types of cell-surface redox proteins (see Nomenclature) were identified to be responsible for ET across the cell-surface of electroactive organisms. Among these, cell-surface exposed

cytochromes were found as principal cellular components in interacting with solid conductors and with different electron shuttles 68. Redox proteins (particularly multiheme cytochromes) form conductive ET chains that allows the exchange of electrons with solid electron donor or acceptors outside of the cell [30]. Furthermore, numerous electroactive microorganisms may employ cellular structures, such as nanowires or pili to improve EET [69]. Recently, it has also been demonstrated that EPS also facilitate EET [70].

The accessibility of such molecules to all potential meso-, micro- and ultramicro-porous surface area might greatly affect the overall ET. Smaller pores are likely to act as cut-off barriers for such biomolecules, according to their molecular dimension and architecture. These aspects should particularly be focus of deeper insights.

6. Large scale bioelectrodes based on e-biochar?

Bioelectrodes architectures generally include different features, such as defined structural shapes (e.g. plain, granular, cylindrical, sponge-like), porous separation layers (e.g. air-water interface for air-exposed cathodes [71,72]), and current collection frameworks [2]. Many carbon-based 'technological' materials (e.g. carbon fibers, cloths and rods, graphite) have excellent structural and conductive properties, but generally very low EAS [73]. Therefore, many of them can barely act as current collectors, rather than efficient bioelectrodes [72]. On the other side, activated carbon powders, carbon nanotubes and other nanomaterials with high surface areas were largely employed to increase biofilm adhesion, improve EAS and/or abiotic electrocatalytic properties [2]. To this end, polymeric binders, resins and other adhesives have been extensively employed to create layers of these powders on current collectors in lab-scale MET applications [2,72].

Lab-scale studies have seldom taken into account the real applicability at large scales of intensively-manufactured materials (carbon fibers, cloths, meshes, felts), non-renewable or engineered carbons (graphites, charcoal, cokes, activated carbon powders, nanotubes) and non-biocompatible additives (PTFE, Nafion®, polyvinyl alcohol and other binders) [72]. Very few authors have been mentioning the economic costs of such materials [74,75] and even less have assessed their life cycle and environmental compatibility [76], envisioning large scales manufacturing [10].

Optimized e-biochar have potential of being more efficient and versatile (with customized fabrication design and properties), including the characteristics of both structural features of a current collector (defined conformation, mechanical rigidity, conductivity) and high EAS. This

idea is supported by a reasonable number of reports, where electrodes designs are based on biochar monoliths with self-supported 3-Dimensional structures (Table 1-c). Good examples are binder-free air-cathodes made of sintered activated carbon powders, which were found to be inexpensive and easily mass manufactured [72]. Other authors fabricated bioelectrodes via ligno-cellulosic biomass carbonization, while preserving the original 3-D shape. Bioanodes were obtained from carbonized plant stems (kenaf and bamboo), corn cobs, marine loofah sponges, king/wild mushrooms [64,77-79]. Rigid air-breathing biocathodes were obtained from Giant cane stems, which maintained their original cylindrical shape and simultaneously acted as microporous air-water separators [71,80].

Bioelectrodes configurations even closer to scaled-up MET applications were also proposed, even if in some cases the employed carbon materials (e.g. activated carbon granules) were from origins other than biomass (Table 1-d). Fluid-like bioelectrodes made of floating carbon particles are very promising configurations [81]. Electroconductive granules are fluidized in a bioreactor acting as "planktonic" electrodes supporting microbial electroactivity [82]. Electrons accumulate on the material and are discharged to a collector by periodic contact. The potentials of this concept is currently under investigation at Bioe group (University of Alcalá, Spain).

Until today, most of the experiments on biochar have been run using regular electrochemical cells configurations, i.e. with well-defined anodic and cathodic electrode surfaces, with uniform electrochemical potential. However, we envisage the most interesting applications of e-biochar with not well-defined anodic or cathodic electrode surfaces. Every single niche created by electroactive communities at the surface of biochar might behave like an anode or a cathode, depending on the redox conditions in the electrolyte as well as on the surface of conductive portion of biochar.

Granular carbons of macroscopic size and sufficient mechanical rigidity (diameters in the range of 5 – 20 mm) were also the base of fixed- or packed-bed bioelectrodes (either anodes or cathodes), for different purposes [83-85]. This design has been applied to probably the largest-scale application of MET, which merges the use of electroactive material with the concept of constructed wetland. The result is the so-called 'METland' concept where the classical bed biofilter made of inert material can be substituted by electroconductive material [86]. Based on this concept, a 20 m^2 METland made of e-biochar was constructed for treating around 7 m^3 day^{-1} of urban wastewater. The e-biochar acts as electroconductive bed for electroactive biofilm and helps in avoiding electron acceptor limitations for bacteria. The final outcome is a

stimulation of the ET mechanism that resulted in a large enhancement of the biodegradation rates for organic pollutants in the wastewater with no energy cost and under extremely low growth yield [86].

METland biofilters made of e-biochar have been also used at large scale for enhancing anaerobic treatment in a real-scale wastewater treatment plant (serving a community of around 200 people) recently constructed by the startup company METfilter at Otos (Murcia, Spain). Interestingly, in METlands e-biochar was considerably more efficient for wastewater treatment than more conductive materials (coke and graphite) [87]. Higher performances were observed under a wide range of operational conditions, including polarization at 0.4 and 0.6 V (vs. Ag/AgCl/Cl ref.) [87]. Higher working potentials showed higher currents for graphite, but overall lower COD removal efficiency, as compared to e-biochar. Hence, larger EAS, hierarchical pore architecture and richer surface chemistry (including phenol and quinones) might dominate over conductivity in some systems. Such aspects deserve deeper investigation.

7. Outlook and future challenges

e-biochar is an intriguing candidate to realize the ambitious promises of large-scale MET applications. However, many aspects remain definitely open, due a substantial lack of comprehensive and multidisciplinary approaches in the existing literature reports. Both fundamental studies and applied research are still needed, involving a wide variety of cross-disciplines. A lot of work has still to be done to identify and obtain the best characteristics of the material according to different targets. To achieve this goal, all available knowledge on biochar involving surface material chemistry, thermochemical processing, nanotechnology and abiotic electrochemistry, should be strictly complemented with approaches coming from bioelectrochemistry, molecular studies on ET, microbial metabolism and microbial biofilm ecology. In parallel, environmental and bioprocess engineering should accompany basic studies to foresee the viability of potential applications at certain scales. Up to date, the large majority of studies lacks a vision for scalable bioelectrodes configurations.

In spite of the attractive “circular economy” concept (Figure 1), both economic and environmental sustainability of e-biochar production at target scales should be analyzed by proper tools, such as exhaustive Life Cycle Assessment. For example, hydrothermal carbonization (HTC) might bring some advantages on conventional pyrolysis, excluding energy-intensive drying before or during the process. This opens up the field to several alternative

sources: wet animal manures, human waste, sewage sludges, municipal solid waste (MSW), as well as aquaculture and algal residues [88].

Finally, soil science and agronomy should also be involved both at the beginning and end of the chain. Sustainable biomass supply, including agricultural and agro-industry residues and green waste, is the first key element towards the sustainability of the whole concept. Simultaneously, studies should assess the possibility of fully recycle e-biochar after bielectrodes working life, as amendment for agricultural soil application in view of long-term carbon storage as strategy to mitigate climate change [12].

Acknowledgements

This work has been financed by the Italian Ministry of University and Research (MIUR), within the SIR2014 Grant, project RBSI14JKU3. Dr. R. Berenguer also thanks the Spanish Ministerio de Economía y Competitividad and FEDER funds (RYC-2017-23618) for financial support.

Nomenclature

Biochar: a chemically-stable form of carbon (charcoal) derived from thermochemical conversions of biomass.

Bioelectrode: electrodes where the electrocatalysis is driven by living microbes.

Cell-surface redox proteins: Proteins present at the cell-surface of organisms, containing one or several redox groups, responsible to transfer electrons with electrodes, soluble electron shuttles, or insoluble metals. Examples of these proteins are the outer-membrane cytochromes, including MtrC and OmcA from Shewanella oneidensis MR-1, OmcS, OmcB, OmcF and OmcZ from Geobacter sulfurreduces, PioA from Rhodopseudomonas palustris, among others [68].

Electron shuttles: Mobile compounds produced by microorganisms that can assist EET, including quinones, flavins, humic substrances and phenazines.

e-pili and nanowires: Electrically-conductive appendages and outer-membrane extensions described in Gram-negative bacteria that assist in the process of EET.

Electron transfer (ET): chemical/biochemical processes driving the exchange of electrons by redox and electroconductive mechanisms.

Extracellular electron transfer: The process by which microorganisms exchange electrons across the cell surface for the reduction/oxidation of extracellular compounds. Metal-reducing organisms use EET to respire metal oxides/hydroxides, while others to exchange electrons with solid electrodes.

Electroactive microorganisms: Microorganisms that are able to exchange electrons with an electrochemically-active surface such as an electrode.

Electroactive: a material/surface with chemical and textural properties allowing efficient ET from/to external sources/sinks of electrons.

Microbial electrochemical technologies (METs). Electrochemical devices where ET from/to electrodes is mediated by living microbial cells. Several applications (e.g. microbial fuel, electrolysis, electrofermentation and electrosynthesis cells) are used to enhance a range of bioprocesses of environmental interest (e.g. wastewater treatment, water desalination, nutrients recovery, soil bioremediation, environmental sensing, biomass processing, CO_2 fixation towards bio-molecules and biofuels production).

Porous texture: Macropores: pores with diameter (d) more than 50 nm; Mesopores: pores with $2 < d < 50$ nm; Micropores: pores with $d < 2$ nm; Ultra-micropores: pores with $d < 0.7$ nm.

Thermochemical conversions: Biochars are produced either by pyrolysis or hydrothermal carbonization (HTC). Both processes involve thermochemical decomposition of biomass in absence of stoichiometric oxygen, leading to a progressive increase in C-content (carbonization) [34]. Both processes are esoergonic, with the production of heat and reduced volatile molecules (H2, CO, etc.). Pyrolysis is carried out under reducing atmosphere (at >200ºC), while HTC (also called wet pyrolysis) under autogenous pressure (< 20 bar) and temperature (<350°C) in subcritical water. The product is known as hydrochar [34,88]. Typical solid yields of (slow or intermediate) pyrolysis are 20-40%, whereas 50-80 % for HTC in relatively short times (1-24 h) [88].

References

(1) Kracke, F.; Vassilev, I.; Krömer, J. O. Microbial Electron Transport and Energy Conservation - the Foundation for Optimizing Bioelectrochemical Systems. Front. Microbiol. 2015, 6 (Jun), 575. https://doi.org/10.3389/fmicb.2015.00575.

(2) Xie, X.; Criddle, C.; Cui, Y. Design and Fabrication of Bioelectrodes for Microbial Bioelectrochemical Systems. Energy Environ. Sci. 2015, 8 (12), 3418–3441. https://doi.org/10.1039/c5ee01862e.

(3) Wei, J.; Liang, P.; Huang, X. Recent Progress in Electrodes for Microbial Fuel Cells. Bioresour. Technol. 2011, 102 (20), 9335–9344. https://doi.org/10.1016/j.biortech.2011.07.019.

(4) Goglio, A.; Tucci, M.; Rizzi, B.; Colombo, A.; Cristiani, P.; Schievano, A. Microbial Recycling Cells (MRCs): A New Platform of Microbial Electrochemical Technologies Based on Biocompatible Materials, Aimed at Cycling Carbon and Nutrients in Agro-Food Systems. Sci. Total Environ. 2019, 649, 1349–1361. https://doi.org/10.1016/J.SCITOTENV.2018.08.324.

(5) Daud, S. M.; Kim, B. H.; Ghasemi, M.; Daud, W. R. W. Separators Used in Microbial Electrochemical Technologies: Current Status and Future Prospects. Bioresour. Technol. 2015, 195, 170–179. https://doi.org/10.1016/j.biortech.2015.06.105.

(6) Logan, B. E.; Hamelers, B.; Rozendal, R.; Schröder, U.; Keller, J.; Freguia, S.; Aelterman, P.; Verstraete, W.; Rabaey, K. Microbial Fuel Cells: Methodology and Technology. Environ. Sci. Technol. 2006, 40 (17), 5181–5192. https://doi.org/10.1021/es0605016.

(7) Wang, H.; Ren, Z. J. A Comprehensive Review of Microbial Electrochemical Systems as a Platform Technology. Biotechnol. Adv. 2013, 31 (8), 1796–1807. https://doi.org/10.1016/j.biotechadv.2013.10.001.

(8) Krieg, T.; Sydow, A.; Schröder, U.; Schrader, J.; Holtmann, D. Reactor Concepts for Bioelectrochemical Syntheses and Energy Conversion. Trends Biotechnol. 2014, 32 (12), 645–655. https://doi.org/10.1016/j.tibtech.2014.10.004.

(9) Rossi, R.; Jones, D.; Myung, J.; Zikmund, E.; Yang, W.; Gallego, Y. A.; Pant, D.; Evans, P. J.; Page, M. A.; Cropek, D. M.; et al. Evaluating a Multi-Panel Air Cathode through Electrochemical and Biotic Tests. Water Res. 2019, 148, 51–59. https://doi.org/10.1016/j.watres.2018.10.022.

(10) Zhang, J.; Yuan, H.; Deng, Y.; Zha, Y.; Abu-Reesh, I. M.; He, Z.; Yuan, C. Life Cycle Assessment of a Microbial Desalination Cell for Sustainable Wastewater Treatment and Saline Water Desalination. J. Clean. Prod. 2018, 200, 900–910. https://doi.org/10.1016/J.JCLEPRO.2018.07.197.

(11) Santoro, C.; Artyushkova, K.; Babanova, S.; Atanassov, P.; Ieropoulos, I.; Grattieri, M.; Cristiani, P.; Trasatti, S.; Li, B.; Schuler, A. J. Parameters Characterization and Optimization of Activated Carbon (AC) Cathodes for Microbial Fuel Cell Application. Bioresour. Technol. 2014, 163, 54–63. https://doi.org/10.1016/j.biortech.2014.03.091.

(12) Qian, K.; Kumar, A.; Zhang, H.; Bellmer, D.; Huhnke, R. Recent Advances in Utilization of Biochar. Renewable and Sustainable Energy Reviews. Pergamon 2015, pp 1055–1064. https://doi.org/10.1016/j.rser.2014.10.074.

(13) Bachmann, H. J.; Bucheli, T. D.; Dieguez-Alonso, A.; Fabbri, D.; Knicker, H.; Schmidt, H.-P.; Ulbricht, A.; Becker, R.; Buscaroli, A.; Buerge, D.; et al. Toward the Standardization of Biochar Analysis: The COST Action TD1107 Interlaboratory Comparison. J. Agric. Food Chem. 2016, 64 (2), 513–527. https://doi.org/10.1021/acs.jafc.5b05055.

(14) Chen, S.; Rotaru, A.-E.; Shrestha, P. M.; Malvankar, N. S.; Liu, F.; Fan, W.; Nevin, K. P.; Lovley, D. R. Promoting Interspecies Electron Transfer with Biochar. Sci. Rep. 2014, 4, 5019. https://doi.org/10.1038/srep05019.

(15) Prado, A.; Berenguer, R.; Esteve-Núñez, A. Electroactive Biochar Outperforms Highly Conductive Carbon Materials for Biodegrading Pollutants by Enhancing Microbial Extracellular Electron Transfer. Carbon N. Y. 2019, 146, 597–609. https://doi.org/10.1016/J.CARBON.2019.02.038.

(16) Atkinson, C. J.; Fitzgerald, J. D.; Hipps, N. A. Potential Mechanisms for Achieving Agricultural Benefits from Biochar Application to Temperate Soils: A Review. Plant Soil 2010, 337 (1–2), 1–18. https://doi.org/10.1007/s11104-010-0464-5.

(17) Lehmann, J.; Rillig, M. C.; Thies, J.; Masiello, C. A.; Hockaday, W. C.; Crowley, D. Biochar Effects on Soil Biota – A Review. Soil Biol. Biochem. 2011, 43 (9), 1812–1836. https://doi.org/10.1016/j.soilbio.2011.04.022.

(18) Komang T., R.-S.; Caroline, H. O. Biochar Application Essential Soil Microbial Ecology; Elsevier Science, 2016. https://doi.org/http://dx.doi.org/10.1016/B978-0-12-803433-0.00001-1.

(19) Tong, H.; Hu, M.; Li, F. B.; Liu, C. S.; Chen, M. J. Biochar Enhances the Microbial and Chemical Transformation of Pentachlorophenol in Paddy Soil. Soil Biol. Biochem. 2014, 70, 142–150. https://doi.org/10.1016/j.soilbio.2013.12.012.

(20) Kappler, A.; Wuestner, M. L.; Ruecker, A.; Harter, J.; Halama, M.; Behrens, S. Biochar as an Electron Shuttle between Bacteria and Fe(III) Minerals. Environ. Sci. Technol. Lett. 2014, 1 (8), 339–344. https://doi.org/10.1021/ez5002209.

(21) Yu, L.; Yuan, Y.; Tang, J.; Wang, Y.; Zhou, S. Biochar as an Electron Shuttle for Reductive Dechlorination of Pentachlorophenol by Geobacter Sulfurreducens. Sci. Rep. 2015, 5 (1), 16221. https://doi.org/10.1038/srep16221.

(22) Saquing, J. M.; Yu, Y. H.; Chiu, P. C. Wood-Derived Black Carbon (Biochar) as a Microbial Electron Donor and Acceptor. Environ. Sci. Technol. Lett. 2016. https://doi.org/10.1021/acs.estlett.5b00354.

(23) Yu, L.; Wang, Y.; Yuan, Y.; Tang, J.; Zhou, S. Biochar as Electron Acceptor for Microbial Extracellular Respiration. Geomicrobiol. J. 2016, 33 (6), 530–536. https://doi.org/10.1080/01490451.2015.1062060.

(24) Chen, Z.; Wang, Y.; Xia, D.; Jiang, X.; Fu, D.; Shen, L.; Wang, H.; Li, Q. B. Enhanced Bioreduction of Iron and Arsenic in Sediment by Biochar Amendment Influencing Microbial Community Composition and Dissolved Organic Matter Content and Composition. J. Hazard. Mater. 2016, 311 (422), 20–29. https://doi.org/10.1016/j.jhazmat.2016.02.069.

(25) Yuan, Y.; Bolan, N.; Prévoteau, A.; Vithanage, M.; Biswas, J. K.; Ok, Y. S.; Wang, H. Applications of Biochar in Redox-Mediated Reactions. Bioresour. Technol. 2017, 246, 271–281. https://doi.org/10.1016/j.biortech.2017.06.154.

(26) Sun, T.; Levin, B. D. A.; Guzman, J. J. L.; Enders, A.; Muller, D. A.; Angenent, L. T.; Lehmann, J. Rapid Electron Transfer by the Carbon Matrix in Natural Pyrogenic Carbon. Nat. Commun. 2017, 8, 14873. https://doi.org/10.1038/ncomms14873.

(27) Gralnick, J. A.; Newman, D. K. Extracellular Respiration. Mol. Microbiol. 2007, 65 (1), 1–11. https://doi.org/10.1111/j.1365-2958.2007.05778.x.

(28) Chacón, F. J.; Cayuela, M. L.; Roig, A.; Sánchez-Monedero, M. A. Understanding, Measuring and Tuning the Electrochemical Properties of Biochar for Environmental Applications. Rev. Environ. Sci. Bio/Technology 2017, 16 (4), 695–715. https://doi.org/10.1007/s11157-017-9450-1.

(29) Schievano, A.; Goglio, A.; Erckert, C.; Marzorati, S.; Rago, L.; Cristiani, P. Organic Waste and Bioelectrochemical Systems: A Future Interface between Electricity and Methane Distribution Grids. Detritus 2018, 01, 57–63.

(30) Costa, N. L.; Clarke, T. A.; Philipp, L.-A.; Gescher, J.; Louro, R. O.; Paquete, C. M. Electron Transfer Process in Microbial Electrochemical Technologies: The Role of Cell-Surface Exposed Conductive Proteins. Bioresour. Technol. 2018, 255, 308–317. https://doi.org/10.1016/J.BIORTECH.2018.01.133.

(31) Schroeder, U.; Harnisch, F. Life Electric — Nature as a Blueprint for the Development of Microbial Electrochemical Technologies. Joule 2017, 244–252. https://doi.org/10.1016/j.joule.2017.07.010.

(32) Huggins, T.; Wang, H.; Kearns, J.; Jenkins, P.; Ren, Z. J. Biochar as a Sustainable Electrode Material for Electricity Production in Microbial Fuel Cells. Bioresour. Technol. 2014, 157, 114–119. https://doi.org/10.1016/j.biortech.2014.01.058.

(33) Tabti, Z.; Berenguer, R.; Ruiz-Rosas, R.; Quijada, C.; Morallon, E.; CAZORLA-AMOR^|^Oacute;S, D. Electrooxidation Methods to Produce Pseudocapacitance-Containing Porous Carbons. Electrochemistry 2013, 81 (10), 833–839. https://doi.org/10.5796/electrochemistry.81.833.

(34) Fitzer, E.; Kochling, K.-H.; Boehm, H. P.; Marsh, H. Recommended Terminology for the Description of Carbon as a Solid (IUPAC Recommendations 1995). Pure Appl. Chem. 1995, 67 (3), 473–506. https://doi.org/10.1351/pac199567030473.

(35) Berenguer, R.; García-Mateos, F. J.; Ruiz-Rosas, R.; Cazorla-Amorós, D.; Morallón, E.; Rodríguez-Mirasol, J.; Cordero, T. Biomass-Derived Binderless Fibrous Carbon Electrodes for Ultrafast Energy Storage. Green Chem. 2016, 18 (6), 1506–1515. https://doi.org/10.1039/c5gc02409a.

(36) Menendez, J. A.; Xia, B.; Phillips, J.; Radovic, L. R. On the Modification and Characterization of Chemical Surface Properties of Activated Carbon : Microcalorimetric , Electrochemical , and Thermal Desorption Probes. Langmuir 1997, 13 (19), 3414–3421. https://doi.org/10.1021/la970200x.

(37) Bandosz, T. J.; Ania, C. O. Activated Carbon Surfaces in Environmental Remediation. Interface Sci. Technol. 2006, 7, 159–229. https://doi.org/10.1016/S1573-4285(06)80013-X.

(38) Montes-Morán, M. A.; Suárez, D.; Menéndez, J. A.; Fuente, E. On the Nature of Basic Sites on Carbon Surfaces: An Overview. Carbon N. Y. 2004, 42 (7), 1219–1224. https://doi.org/10.1016/j.carbon.2004.01.023.

(39) Ruiz-Rosas, R.; Valero-Romero, M. J.; Salinas-Torres, D.; Rodríguez-Mirasol, J.; Cordero, T.; Morallón, E.; Cazorla-Amorós, D. Electrochemical Performance of Hierarchical Porous Carbon Materials Obtained from the Infiltration of Lignin into Zeolite Templates. ChemSusChem 2014, 7 (5), 1458–1467. https://doi.org/10.1002/cssc.201301408.

(40) Rosas, J. M.; Berenguer, R.; Valero-Romero, M. J.; RodrÃ-guez-Mirasol, J.; Cordero, T. Preparation of Different Carbon Materials by Thermochemical Conversion of Lignin. Front. Mater. 2014, 1, 29. https://doi.org/10.3389/fmats.2014.00029.

(41) Figueiredo, J. .; Pereira, M. F. .; Freitas, M. M. .; Órfão, J. J. . Modification of the Surface Chemistry of Activated Carbons. Carbon N. Y. 1999, 37 (9), 1379–1389. https://doi.org/10.1016/S0008-6223(98)00333-9.

(42) Klüpfel, L.; Keiluweit, M.; Kleber, M.; Sander, M. Redox Properties of Plant Biomass-Derived Carbon Black (Biochar). Env. Sci Technol 2014, 48, 5601–5611. https://doi.org/10.1021/es500906d.

(43) Bleda-Martínez, M. J.; Lozano-Castelló, D.; Morallón, E.; Cazorla-Amorós, D.; Linares-Solano, A. Chemical and Electrochemical Characterization of Porous Carbon Materials. Carbon N. Y. 2006, 44 (13), 2642–2651. https://doi.org/10.1016/j.carbon.2006.04.017.

(44) Berenguer, R.; Ruiz-Rosas, R.; Gallardo, A.; Cazorla-Amorós, D.; Morallón, E.; Nishihara, H.; Kyotani, T.; Rodríguez-Mirasol, J.; Cordero, T. Enhanced Electro-Oxidation Resistance of Carbon Electrodes Induced by Phosphorus Surface Groups. Carbon N. Y. 2015, 95, 681–689. https://doi.org/10.1016/j.carbon.2015.08.101.

(45) Itoi, H.; Nishihara, H.; Ishii, T.; Nueangnoraj, K.; Berenguer-Betrián, R.; Kyotani, T. Large Pseudocapacitance in Quinone-Functionalized Zeolite-Templated Carbon. Bull. Chem. Soc. Jpn. 2014, 87 (2), 250–257. https://doi.org/10.1246/bcsj.20130292.

(46) Valero-Romero, M. J.; García-Mateos, F. J.; Rodríguez-Mirasol, J.; Cordero, T. Role of Surface Phosphorus Complexes on the Oxidation of Porous Carbons. Fuel Process. Technol. 2017, 157 (January 2018), 116–126. https://doi.org/10.1016/j.fuproc.2016.11.014.

(47) Joseph, S.; Graber, E.; Chia, C.; Munroe, P.; Donne, S.; Thomas, T.; Nielsen, S.; Marjo, C.; Rutlidge, H.; Pan, G.; et al. Shifting Paradigms: Development of High-Efficiency Biochar Fertilizers Based on Nano-Structures and Soluble Components. Carbon Manag. 2013, 4 (3), 323–343. https://doi.org/10.4155/cmt.13.23.

(48) Ruiz-Rosas, R.; Bedia, J.; Lallave, M.; Loscertales, I. G.; Barrero, A.; Rodríguez-Mirasol, J.; Cordero, T. The Production of Submicron Diameter Carbon Fibers by the Electrospinning of Lignin. Carbon N. Y. 2010, 48 (3), 696–705. https://doi.org/10.1016/j.carbon.2009.10.014.

(49) Radovic, L. R.; Bockrath, B. On the Chemical Nature of Graphene Edges: Origin of Stability and Potential for Magnetism in Carbon Materials. J. Am. Chem. Soc. 2005, 127 (16), 5917–5927. https://doi.org/10.1021/ja050124h.

(50) Rodríguez-Reinoso, F.; Molina-Sabio, M. Activated Carbons from Lignocellulosic Materials by Chemical and/or Physical Activation: An Overview. Carbon N. Y. 1992, 30 (7), 1111–1118. https://doi.org/10.1016/0008-6223(92)90143-K.

(51) Ternero-Hidalgo, J. J.; Rosas, J. M.; Palomo, J.; Valero-Romero, M. J.; Rodríguez-Mirasol, J.; Cordero, T. Functionalization of Activated Carbons by HNO3treatment: Influence of Phosphorus Surface Groups. Carbon N. Y. 2016, 101, 409–419. https://doi.org/10.1016/j.carbon.2016.02.015.

(52) Mostazo-López, M. J.; Ruiz-Rosas, R.; Morallón, E.; Cazorla-Amorós, D. Generation of Nitrogen Functionalities on Activated Carbons by Amidation Reactions and Hofmann Rearrangement: Chemical and Electrochemical Characterization. Carbon N. Y. 2015, 91, 252–265. https://doi.org/10.1016/j.carbon.2015.04.089.

(53) Sharma, M.; Alvarez-Gallego, Y.; Achouak, W.; Pant, D.; Sharma, P.; Dominguez-Benetton, X. Electrode Material Properties for Designing Effective Microbial Electrosynthesis Systems. J. Mater. Chem. A 2019. https://doi.org/10.1039/C9TA04886C.

(54) Prévoteau, A.; Ronsse, F.; Cid, I.; Boeckx, P.; Rabaey, K. The Electron Donating Capacity of Biochar Is Dramatically Underestimated. Sci. Rep. 2016, 6 (1), 32870. https://doi.org/10.1038/srep32870.

(55) Sharma, M.; Bajracharya, S.; Gildemyn, S.; Patil, S. a.; Alvarez-Gallego, Y.; Pant, D.; Rabaey, K.; Dominguez-Benetton, X. A Critical Revisit of the Key Parameters Used to Describe

Microbial Electrochemical Systems. Electrochim. Acta 2014, No. September 2015. https://doi.org/10.1016/j.electacta.2014.02.111.

(56) Chen, S.; Tang, J.; Fu, L.; Yuan, Y.; Zhou, S. Biochar Improves Sediment Microbial Fuel Cell Performance in Low Conductivity Freshwater Sediment. J. Soils Sediments 2016, 16 (9), 2326–2334. https://doi.org/10.1007/s11368-016-1452-z.

(57) Chen, Q.; Pu, W.; Hou, H.; Hu, J.; Liu, B.; Li, J.; Cheng, K.; Huang, L.; Yuan, X.; Yang, C.; et al. Activated Microporous-Mesoporous Carbon Derived from Chestnut Shell as a Sustainable Anode Material for High Performance Microbial Fuel Cells. Bioresour. Technol. 2018, 249, 567–573. https://doi.org/10.1016/j.biortech.2017.09.086.

(58) Liu, Y.; He, P.; Shao, L.; Zhang, H.; Lü, F. Significant Enhancement by Biochar of Caproate Production via Chain Elongation. Water Res. 2017, 119, 150–159. https://doi.org/10.1016/j.watres.2017.04.050.

(59) Qin, Y.; Wang, H.; Li, X.; Cheng, J. J.; Wu, W. Improving Methane Yield from Organic Fraction of Municipal Solid Waste (OFMSW) with Magnetic Rice-Straw Biochar. Bioresour. Technol. 2017, 245 (September), 1058–1066. https://doi.org/10.1016/j.biortech.2017.09.047.

(60) Lü, F.; Luo, C.; Shao, L.; He, P. Biochar Alleviates Combined Stress of Ammonium and Acids by Firstly Enriching Methanosaeta and Then Methanosarcina. Water Res. 2016, 90, 34–43. https://doi.org/10.1016/j.watres.2015.12.029.

(61) Cruz Viggi, C.; Simonetti, S.; Palma, E.; Pagliaccia, P.; Braguglia, C.; Fazi, S.; Baronti, S.; Navarra, M. A.; Pettiti, I.; Koch, C.; et al. Enhancing Methane Production from Food Waste Fermentate Using Biochar: The Added Value of Electrochemical Testing in Pre-Selecting the Most Effective Type of Biochar. Biotechnol. Biofuels 2017, 10 (1), 303. https://doi.org/10.1186/s13068-017-0994-7.

(62) Mumme, J.; Srocke, F.; Heeg, K.; Werner, M. Use of Biochars in Anaerobic Digestion. Bioresour. Technol. 2014, 164, 189–197. https://doi.org/10.1016/J.BIORTECH.2014.05.008.

(63) Tan, Z.; Lin, C. S. K.; Ji, X.; Rainey, T. J. Returning Biochar to Fields: A Review. Applied Soil Ecology. 2017, pp 1–11. https://doi.org/10.1016/j.apsoil.2017.03.017.

(64) Chen, S.; He, G.; Hu, X.; Xie, M.; Wang, S.; Zeng, D.; Hou, H.; Schröder, U. A Three-Dimensionally Ordered Macroporous Carbon Derived from a Natural Resource as Anode for

Microbial Bioelectrochemical Systems. ChemSusChem 2012, 5 (6), 1059–1063. https://doi.org/10.1002/cssc.201100783.

(65) Vijayaraj, M.; Gadiou, R.; Anselme, K.; Ghimbeu, C.; Vix-Guterl, C.; Orikasa, H.; Kyotani, T.; Ittisanronnachai, S. The Influence of Surface Chemistry and Pore Size on the Adsorption of Proteins on Nanostructured Carbon Materials. Adv. Funct. Mater. 2010, 20 (15), 2489–2499. https://doi.org/10.1002/adfm.201000288.

(66) Champigneux, P.; Delia, M.-L.; Bergel, A. Impact of Electrode Micro- and Nano-Scale Topography on the Formation and Performance of Microbial Electrodes. Biosens. Bioelectron. 2018, 118 (June), 231–246. https://doi.org/10.1016/j.bios.2018.06.059.

(67) Santoro, C.; Artyushkova, K.; Babanova, S.; Atanassov, P.; Ieropoulos, I.; Grattieri, M.; Cristiani, P.; Trasatti, S.; Li, B.; Schuler, A. J. Parameters Characterization and Optimization of Activated Carbon (AC) Cathodes for Microbial Fuel Cell Application. Bioresour. Technol. 2014, 163, 54–63. https://doi.org/10.1016/j.biortech.2014.03.091.

(68) Paquete, C. M.; Fonseca, B. M.; Cruz, D. R.; Pereira, T. M.; Pacheco, I.; Soares, C. M.; Louro, R. O. Exploring the Molecular Mechanisms of Electron Shuttling across the Microbe/Metal Space. Front. Microbiol. 2014, 5, 318. https://doi.org/10.3389/fmicb.2014.00318.

(69) Gorby, Y. A.; Yanina, S.; McLean, J. S.; Rosso, K. M.; Moyles, D.; Dohnalkova, A.; Beveridge, T. J.; Chang, I. S.; Kim, B. H.; Kim, K. S.; et al. Electrically Conductive Bacterial Nanowires Produced by Shewanella Oneidensis Strain MR-1 and Other Microorganisms. Proc. Natl. Acad. Sci. U. S. A. 2006, 103 (30), 11358–11363. https://doi.org/10.1073/pnas.0604517103.

(70) Xiao, Y.; Zhang, E.; Zhang, J.; Dai, Y.; Yang, Z.; Christensen, H. E. M.; Ulstrup, J.; Zhao, F. Extracellular Polymeric Substances Are Transient Media for Microbial Extracellular Electron Transfer. Sci. Adv. 2017, 3 (7), e1700623. https://doi.org/10.1126/sciadv.1700623.

(71) Marzorati, S.; Goglio, A.; Fest-Santini, S.; Mombelli, D.; Villa, F.; Cristiani, P.; Schievano, A. Air-Breathing Bio-Cathodes Based on Electro-Active Biochar from Pyrolysis of Giant Cane Stalks. Int. J. Hydrogen Energy 2018. https://doi.org/10.1016/J.IJHYDENE.2018.07.167.

(72) Walter, X. A.; Greenman, J.; Ieropoulos, I. Binder Materials for the Cathodes Applied to Self-Stratifying Membraneless Microbial Fuel Cell. Bioelectrochemistry 2018, 123, 119–124. https://doi.org/10.1016/J.BIOELECHEM.2018.04.011.

(73) Guo, K.; Pré, A.; Patil, S. A.; Rabaey, K. Engineering Electrodes for Microbial Electrocatalysis. Curr. Opin. Biotechnol. 2015, 33, 149–156. https://doi.org/10.1016/j.copbio.2015.02.014.

(74) Logan, B. E. Scaling up Microbial Fuel Cells and Other Bioelectrochemical Systems. Appl. Microbiol. Biotechnol. 2010, 85 (6), 1665–1671. https://doi.org/10.1007/s00253-009-2378-9.

(75) Pant, D.; Singh, A.; Van Bogaert, G.; Gallego, Y. A.; Diels, L.; Vanbroekhoven, K. An Introduction to the Life Cycle Assessment (LCA) of Bioelectrochemical Systems (BES) for Sustainable Energy and Product Generation: Relevance and Key Aspects. Renew. Sustain. Energy Rev. 2011, 15 (2), 1305–1313. https://doi.org/10.1016/J.RSER.2010.10.005.

(76) Foley, J. M.; Rozendal, R. A.; Hertle, C. K.; Lant, P. A.; Rabaey, K. Life Cycle Assessment of High-Rate Anaerobic Treatment, Microbial Fuel Cells, and Microbial Electrolysis Cells. Environ. Sci. Technol. 2010, 44 (9), 3629–3637. https://doi.org/10.1021/es100125h.

(77) Yuan, Y.; Zhou, S.; Liu, Y.; Tang, J. Nanostructured Macroporous Bioanode Based on Polyaniline-Modified Natural Loofah Sponge for High-Performance Microbial Fuel Cells. Environ. Sci. Technol. 2013, 47 (24), 14525–14532. https://doi.org/10.1021/es404163g.

(78) Chen, S.; Liu, Q.; He, G.; Zhou, Y.; Hanif, M.; Peng, X.; Wang, S.; Hou, H. Reticulated Carbon Foam Derived from a Sponge-like Natural Product as a High-Performance Anode in Microbial Fuel Cells. J. Mater. Chem. 2012, 22 (35), 18609. https://doi.org/10.1039/c2jm33733a.

(79) Li, J.; Zhang, J.; Ye, D.; Zhu, X.; Liao, Q.; Zheng, J. Optimization of Inner Diameter of Tubular Bamboo Charcoal Anode for a Microbial Fuel Cell. Int. J. Hydrogen Energy 2014, 39 (33), 19242–19248. https://doi.org/10.1016/j.ijhydene.2014.04.124.

(80) Marzorati, S.; Goglio, A.; Mombelli, D.; Mapelli, C.; Trasatti, S. P.; Cristiani, P.; Schievano, A. Giant Cane as Low-Cost Material for Microbial Fuel Cells Architectures. In Proceedings of EFC2017 European Fuel Cell Technology & Applications Conference - Piero Lunghi Conference December 12-15, 2017, Naples, Italy; 2017; p 114.

(81) Tejedor-Sanz, S.; Ortiz, J. M.; Esteve-Núñez, A. Merging Microbial Electrochemical Systems with Electrocoagulation Pretreatment for Achieving a Complete Treatment of Brewery Wastewater. Chem. Eng. J. 2017, 330, 1068–1074. https://doi.org/10.1016/j.cej.2017.08.049.

(82) Tejedor-Sanz, S.; Quejigo, J. R.; Berná, A.; Esteve-Núñez, A. The Planktonic Relationship Between Fluid-Like Electrodes and Bacteria: Wiring in Motion. ChemSusChem 2017, 10 (4), 693–700. https://doi.org/10.1002/cssc.201601329.

(83) Liu, D.; Roca-puigros, M.; Geppert, F.; Caizán-juanarena, L. Granular Carbon-Based Electrodes as Cathodes in Methane-Producing Bioelectrochemical Systems. 2018, 6 (June), 1–10. https://doi.org/10.3389/fbioe.2018.00078.

(84) Ghafari, S.; Hasan, M.; Aroua, M. K. Nitrate Remediation in a Novel Upflow Bio-Electrochemical Reactor (UBER) Using Palm Shell Activated Carbon as Cathode Material. Electrochim. Acta 2009, 54 (17), 4164–4171. https://doi.org/10.1016/j.electacta.2009.02.062.

(85) Rodrigo Quejigo, J.; Rosa, L. F. M.; Harnisch, F. Electrochemical Characterization of Bed Electrodes Using Voltammetry of Single Granules. Electrochem. commun. 2018, 90, 78–82. https://doi.org/10.1016/J.ELECOM.2018.04.009.

(86) Aguirre-Sierra, A.; Bacchetti-De Gregoris, T.; Berná, A.; Salas, J. J.; Aragón, C.; Esteve-Núñez, A. Microbial Electrochemical Systems Outperform Fixed-Bed Biofilters in Cleaning up Urban Wastewater. Environ. Sci. Water Res. Technol. 2016, 2 (6), 984–993. https://doi.org/10.1039/C6EW00172F.

(87) Prado, A.; Berenguer, R.; Esteve-Núñez, A. Electroconductive Carbon Biofilters for Efficient and Sustainable Treatment of Urban Wastewater. In CARBON 2018. The World Conference on Carbon; 2018; p 2.

(88) Jain, A.; Balasubramanian, R.; Srinivasan, M. P. Hydrothermal Conversion of Biomass Waste to Activated Carbon with High Porosity: A Review. Chem. Eng. J. 2016, 283, 789–805. https://doi.org/10.1016/J.CEJ.2015.08.014.

(89) Ma, M.; You, S.; Wang, W.; Liu, G.; Qi, D.; Chen, X.; Qu, J.; Ren, N. Biomass-Derived Porous Fe3C/Tungsten Carbide/Graphitic Carbon Nanocomposite for Efficient Electrocatalysis of Oxygen Reduction. ACS Appl. Mater. Interfaces 2016, 8 (47), 32307–32316. https://doi.org/10.1021/acsami.6b10804.

(90) Yuan, S.-J.; Dai, X.-H.; Jaroniec, M.; Qiao, S. Z.; Zhang, D. Y. H.; Che, R. C.; Tang, Y.; Su, D. S.; Asiri, A. M.; Zhao, D. Y.; et al. An Efficient Sewage Sludge-Derived Bi-Functional Electrocatalyst for Oxygen Reduction and Evolution Reaction. Green Chem. 2016, 18 (14), 4004–4011. https://doi.org/10.1039/C5GC02729B.

(91) Nieva Lobos, M. L.; Sieben, J. M.; Comignani, V.; Duarte, M.; Volpe, M. A.; Moyano, E. L. Biochar from Pyrolysis of Cellulose: An Alternative Catalyst Support for the Electro-Oxidation of Methanol. Int. J. Hydrogen Energy 2016, 41 (25), 10695–10706. https://doi.org/10.1016/j.ijhydene.2016.04.041.

(92) Zha, D. W.; Li, L. F.; Pan, Y. X.; He, J. B. Coconut Shell Carbon Nanosheets Facilitating Electron Transfer for Highly Efficient Visible-Light-Driven Photocatalytic Hydrogen Production from Water. Int. J. Hydrogen Energy 2016, 41 (39), 17370–17379. https://doi.org/10.1016/j.ijhydene.2016.07.227.

(93) Lin, X.; Wang, X.; Li, L.; Yan, M.; Tian, Y. Rupturing Cotton Microfibers into Mesoporous Nitrogen-Doped Carbon Nanosheets as Metal-Free Catalysts for Efficient Oxygen Electroreduction. ACS Sustain. Chem. Eng. 2017, 5 (11), 9709–9717. https://doi.org/10.1021/acssuschemeng.7b01398.

(94) Mendonça, F. G. de; Cunha, I. T. da; Soares, R. R.; Tristão, J. C.; Lago, R. M. Tuning the Surface Properties of Biochar by Thermal Treatment. Bioresour. Technol. 2017, 246 (May), 28–33. https://doi.org/10.1016/j.biortech.2017.07.099.

(95) Tong, H.; Hu, M.; Li, F. B.; Liu, C. S.; Chen, M. J. Biochar Enhances the Microbial and Chemical Transformation of Pentachlorophenol in Paddy Soil. Soil Biol. Biochem. 2014, 70, 142–150. https://doi.org/10.1016/j.soilbio.2013.12.012.

(96) Wang, S.; Zheng, Y.; Yan, W.; Chen, L.; Dummi Mahadevan, G.; Zhao, F. Enhanced Bioleaching Efficiency of Metals from E-Wastes Driven by Biochar. J. Hazard. Mater. 2016, 320, 393–400. https://doi.org/10.1016/j.jhazmat.2016.08.054.

(97) Chen, G.; Zhang, Z.; Zhang, Z.; Zhang, R. Redox-Active Reactions in Denitrification Provided by Biochars Pyrolyzed at Different Temperatures. Sci. Total Environ. 2017, 615, 1547–1556. https://doi.org/10.1016/j.scitotenv.2017.09.125.

(98) Huggins, T. M.; Pietron, J. J.; Wang, H.; Ren, Z. J.; Biffinger, J. C. Graphitic Biochar as a Cathode Electrocatalyst Support for Microbial Fuel Cells. Bioresour. Technol. 2015, 195, 147–153. https://doi.org/10.1016/J.BIORTECH.2015.06.012.

(99) Yuan, H.; Deng, L.; Qi, Y.; Kobayashi, N.; Tang, J. Nonactivated and Activated Biochar Derived from Bananas as Alternative Cathode Catalyst in Microbial Fuel Cells. Sci. World J. 2014, 2014, 832–850. https://doi.org/10.1155/2014/832850.

(100) Li, M.; Zhang, H.; Xiao, T.; Wang, S.; Zhang, B.; Chen, D.; Su, M.; Tang, J. Low-Cost Biochar Derived from Corncob as Oxygen Reduction Catalyst in Air Cathode Microbial Fuel Cells. Electrochim. Acta 2018, 283, 780–788. https://doi.org/10.1016/J.ELECTACTA.2018.07.010.

(101) Karthikeyan, R.; Wang, B.; Xuan, J.; Wong, J. W. C.; Lee, P. K. H.; Leung, M. K. H. Interfacial Electron Transfer and Bioelectrocatalysis of Carbonized Plant Material as Effective Anode of Microbial Fuel Cell. Electrochim. Acta 2015, 157, 314–323. https://doi.org/10.1016/j.electacta.2015.01.029.

Chapter 5 - Air-breathing Bio-cathodes Based on Electro-active Biochar from Pyrolysis of Giant Cane Stalks

S. Marzorati[a], A. Goglio[a], S. Fest-Santini[b], D. Mombelli[c], F. Villa[d], P. Cristiani[e], A. Schievano[a]*

a e-Bio Center, Department of Environmental Science and Policy, Università degli Studi di Milano, via Celoria 2, 20133, Milano, Italy

b Department of Management, Information and Production Engineering, University of Bergamo, viale Marconi 5, 24044, Dalmine (BG), Italy

c Sezione Materiali per Applicazioni Meccaniche, Dipartimento di Meccanica - Politecnico di Milano, via La Masa 1, 20156, Milano, Italy

d Department of Food Environmental and Nutritional Sciences, Università degli Studi di Milano, Via Mangiagalli 25, 20133, Milano , Italy

e RSE - Ricerca sul Sistema Energetico S.p.A., via Rubattino 54, 20100, Milano, Italy

* corresponding author. Email: andrea.schievano@unimi.it

Published in:

Marzorati S., Goglio A., Fest-Santini S., Mombelli D., Villa F., Cristiani P., Schievano A., 2018. Air-breathing bio-cathodes based on electro-active biochar from pyrolysis of Giant Cane stalks. International Journal of Hydrogen Energy. doi:10.1016/j.ijhydene.2018.07.167

Abstract

An innovative low-tech solution to fabricate electro-active biochar (e-biochar) electrodes for bio-electrochemical systems (BES) is proposed. Ligno-cellulosic stalks of Giant Cane (Arundo Donax L.) were subjected to pyrolysis treatment at 900 °C for 1 h. The material kept its original hollow cylindrical shape, rigid morphology and porous texture, as confirmed by 3DX-ray micro-computed tomography. These characteristics are suitable for its use at the air-water interface in BES, as air-breathing bio-cathodes. BET (Brunauer-Emmett-Teller) specific surface area was equal to 114 ± 4 $m^2 g^{-1}$, with more than 95% of pores in the microporosity range (pore diameter < 1 nm). Surface electrocatalytic activity was sufficient to sustain oxygen reduction reaction at pH 7, in terms of both onset potential (-0.02 V vs Ag/AgCl) and reduction limiting current density (1 A m^{-2}). Electrical resistivity measurements confirmed sufficient conductivity (8.9×10^{-3} ± 1×10^{-4} Ωm) of the material and Raman spectroscopy allowed to estimate a graphitization degree in relation to the ID/IG, equal to 2.26. In parallel, the e-biochar were tested as air-exposed bio-cathodes in BES, coupled to carbon cloth bio-anodes. After inoculation with wastewater from swine-farming, current densities were generated in the range of 100-150 mA m^{-2}, along more than 2 months of operation, under sodium acetate feeding. Confocal laser scanning imaging revealed consistent biofilm formation on the water-side surface of the cathodes, while a nearly-complete absence of it at the air-side. These e-biochar electrodes might open innovative perspectives to scale-up BES for different applications. Here, consistent salts depositions on the material after 70 days of exposure to the wastewater, suggest that e-biochar biocathodes might serve to recycle nutrients to agricultural soils, through minerals-enriched biochar.

Keywords: Electroactive Biochar, e-biochar, Bio-electrochemical Systems, Air-cathode, Wastewater treatment, Pyrolysis

1. Introduction

Real scale application of bio-electrochemical systems (BES) has been facing the need to find an optimal balance between processes efficiencies and costs. Many researches are addressing to develop low-cost and environmentally-compatible materials to fabricate electrodes for large scale applications, such as wastewater treatment, soil bioremediation, etc. [1–3]. To date, the most competitive materials are based on carbon and include graphite-based rods, fiber brushes and granules, carbon-fiber cloths, carbon paper sheets, carbon felt and reticulated vitreous carbon [1,2,4]. They are selected due to their strong biocompatibility and inert properties at

room temperature. The use of such materials as air-breathing cathodes has been coupled to the fabrication of microporous layers, made of activated carbon, pressed on carbon cloths (or other current collector) in the presence of polymeric binders (Nafion, PTFE, etc.) [5,6]. High surface area favors the cathodic oxygen reduction reaction (ORR) that needs the simultaneous presence of solid, liquid and gaseous phases. Microporous layers also act as gas diffusion layer at air-water interface, because the porous structure allows the diffusion of air in contact with the wet surface, impeding water to leak to the air-side [7–9]. Finally, high surface areas promote the formation of electroactive biofilms, able to highly boost a series of cascade reactions towards oxygen reduction which characterize the behavior of aerobic and anaerobic bio-cathode [10,11]. These 'structural' functions is really important for the application of such materials as air-exposed bio-cathodes [11].

However, these composites have some intrinsic limitations for large-scale applications of BES. A major challenge of commercial application of BES is often the high capital cost, especially material cost of anodes, cathodes, and separators. In a literature work [12], the capital cost of the BES was estimated to be around 100 \$ m^{-2} for carbon cloth anode and 5000 \$ m^{-3} for reactor. Some novel solutions with macroporous hollow fibers were recently proposed [13], still in the field of high-tech materials.

After relatively short time of operation (typically after 1-3 months [14], or 1 year in some optimized case [15]), biofouling and salts deposition phenomena, tend to hinder cathode's performances. Unless restored by specific treatments [16,17], such electrodes should be substituted by new ones. However, these materials are not fully recyclable. Carbon-cloths are based on mixtures of carbon fibers with non-biogenic materials, such as polymeric binders (PTFE, Nafion, etc.). The compactness of the activated carbon mixtures on carbon-cloth electrodes is also guaranteed by the massive presence of water-resistant binders [18,19].

In view of environmental large-scale applications of these electrodes, such as wastewater treatment or soil bioremediation, where harvesting electrical power is not the main goal [20,21], avoiding "high-tech", expensive and non-recyclable materials might result in a substantial advantage. An alternative approach should be based on a circular economy concept, where bio-electrodes are fabricated with bio-based and fully-recyclable materials. In this view, biomass-derived charcoal (biochar) represents a class of target materials that would satisfy this purpose. Biochar, the product of biomass thermochemical conversions, has been receiving increasing attention, for several applications. The versatility of biochar depends on its chemical and structural properties. Biochar is often porous and possesses high surface area [22]. Few

groups recently started using biochar in BES [23–27], demonstrating its ability of promoting interspecies electron transfer [28]. For example, a variety of biomass-derived biochar (i.e. from pomelo peel and wood chips) was recently used in biofilm-driven water treatment processes possessing characteristics of low cost, high specific area, good biocompatibility and moderate electrical conductivity, which basically meet the requirements of biocathode materials [29,30]. In Table 1 some examples of biochar-based electrodes and their main properties is displayed.

Table 1 - Examples of biochars and their characteristics for microbial electrochemical application.

Biomass source	**Pyrolysis temperature / °C**	**S_{BET} / m^2 g^{-1}**	**Application**	**Achieved power density / mW m^{-2}**	**Reference**
Pine wood lumber	1000	183.0	Electrocatalytic support in MFCs	146.7	[30]
Pomelo peel	1000	622.2	ORR electrocatalysis	799	[29]
Pine sawdust pellets	1000	0.04	MFCs electrodes	457	[25]
Bananas	550-900	105.2 - 172.3	MFCs cathode	500	[31]
Chestnut shell	900	468	MFCs anodes	N/A	[32]

The fabrication of biochar as base for bio-electrodes, should aim at simultaneously enhancing electrical conductivity, abiotic electrocatalytic properties (e.g. ORR), biocompatibility and the capacity to host microbial biofilm communities. These properties would characterize a particular class of biochars. Here, we propose to call it ‘electro-active biochar’ or ‘e-biochar’. The possibility to obtain e-biochar materials with intrinsic structural rigidity, would open the possibility to use them as air-breathing bio-cathodes at the air-water interface, in lieu of

microporous layer/gas diffusion layer-based electrodes. Also, the availability of the original biomass in large amounts, at relatively low costs and environmental impacts, would also be a key-factor for success of e-biochar in large-scale BES.

In a recent experiment, Giant Cane (Arundo donax L.) stalks were tested as air-water cylindrical separators, in air-cathode BES [33]. Giant Cane is a wild, perennial plant of emerging interest for sustainable biomass production [34]. In terms of cultivation inputs it is characterized by very low requirements; it easily adapts to a variety of soil and climatic conditions and has been recently considered one of the most promising biomass crops [35]. The plant's stalks, characterized by porous and rigid cylindrical structure, avoided water leaks to the air-side and allowed spontaneous electricity production using an organic-rich wastewater, with carbon-cloth electrodes [33].

Here, we fabricate air-breathing bio-cathodes with a rigid cylindrical shape, based on e-biochar obtained from controlled pyrolysis of Giant cane stalks. The physico-chemical and electrocatalytic properties were investigated, as well as their performance as air-breathing bio-cathodes in BES aimed at recovering nutrients from wastewater.

2. Materials and Methods

2.1 Fabrication of e-biochar air-cathodes

Giant Canes were collected in Cascina Marianna (Landriano, PV) from the experimental fields of the Università degli Studi di Milano. Canes with an external homogeneous diameter of 2.5 cm and thickness of about 0.4 cm were selected, cleaned from leaves and cut into cylinders of 15 cm length.

The canes were positioned in a quartz tube inside a horizontal furnace (Carbolite) and pyrolized according to the following protocol: 25 min at 25 °C, slow heating (10 °C min^{-1}) up to 900 °C, 1 h held at 900 °C and, finally, cooling down to 25 °C. Some literature methods were taken into account when choosing the optimized temperature and temperature ramp in order to obtain a sufficiently graphitized sample [36–38]. During all the pyrolysis treatment, nitrogen was flowing constantly at 14 NL h^{-1}.

Hereafter, 900 °C-pyrolized giant cane stalks will be named simply as 'e-biochar air-cathodes': e-BAC.

2.2 Physical-chemical characterization

The Brunauer-Emmett-Teller (BET) specific surface area (SSA) was obtained from N_2 physisorption isotherms at 77 K by an ASAP 2020 (Micrometitics) instrument. Before measurements, sample powders were outgassed at 110 °C for 3 h to remove adsorbed species. SSA value and porosity distribution were determined employing a multipoint BET interpolation of adsorption isotherms and BJH method, respectively.

Raman spectra were obtained on a Raman microscope (Micro-Raman Horiba Jobin Yvon HR800 UV) equipped with a CCD camera using 532 nm excitation laser. The acquired spectra were normalized to carry out the curve fitting of the G, D1, D2, D3 and D4 bands. The different bands were adjusted to Voigt type curves, finding the best fit to the experimental data without including the D2 band, as is usual with carbon black samples. The degree of graphitization has been expressed as the ratio of integral intensities of bands G and D1.

2.3 Morphological characterization

Scanning Electron Microscopy (SEM) was performed using a Zeiss SEM EVO 50 microscope.

Morphology description and porosity quantification were obtained from X-ray microcomputed tomography. The used microCT unit is based on an open type X-ray source 160 kVp @ 200 µA, a high-precision air-bearing rotating stage and Amorphous Silicon (a-Si) sensor array detector acquiring 16-bit grey level with a pixel matrix of 4096 x 4096 at 100 micrometers. Concerning further technical details of the microCT setup, refer to [39].

Fundamentals of tomography are based on the irradiation of a rotating specimen by an X-ray beam and recording the transmitted radiation for different angle steps allowing the 3D reconstruction. 2D grey-scale virtual slices are obtained through retro-projection. Different levels of grey correspond to certain attenuation coefficients, while every voxel represents an exact element of the digitalized object. Through segmentation and further image processing, information related to void space and solid can be extracted. The applicability of this characterization technique depends on the X-ray attenuation (absorption) of the material, which in turn depends on the atomic number of the chemical element, material density and object dimensions. e-BAC, like most of biological samples, is expected to be low density material making their 3D morphological inspection in the micrometer scale challenging. Here, this limitation are overcome working with low photon energy and a high dynamic range of the

detector: 4000 projections with a resolution of 3.425 μm (calibrated resolution, refer to [39]) acquired at 45 kV, 30 μA and 5300 ms integration time.

The global volumetric intensity histogram was expected to be bimodal with peaks referring to the void space and the material matrix. Instead, a further peak was observed having high intensity values whose indicate a high atomic number element. Thereby, a multi-level thresholding method, multi Otsu method, was utilized for the segmentation of the digitalized e-BAC volume differencing in voids, e-BAC matrix and high X-ray attenuation matter. The latter is a residue of pyrolysis and probably of mineral nature.

2.4 Electrochemical characterizations

Electrical resistivity measurements were performed setting the electrical contacts on opposite ends of the e-BACs. A potential scan was performed in the potential window E= + 0.1 / + 0.5 V at a scan rate of 0.010 V s-1. The electrical resistivity ▫ was calculated by the equation:

$$\rho = R\,A/l$$

Where R is the resistance calculated by the slope of the E vs I plot, A is the area of the section of the e-BAC and l is the length of the analyzed cylinder. Five different measurements of different sample lengths were performed to ensure the technique reproducibility.

Electrochemical active surface area (ECSA) determinations were performed by voltammetric curves recorded in N_2-saturated 100 mM PBS (Phosphate-buffered saline) solution in the double layer region at various scan rates as in previous work by Łukaszewski et al. [40]. A three-electrode configuration was used. A weighted piece of e-BAC was set as the working electrode, a Pt-wire was the counter electrode and an Ag/AgCl (Amel) in KCl (sat.) was the reference electrode.

The specific mass capacitance (Cg) of the electrode was calculated from cyclic voltammograms according to the following equation:

$$C_g = \frac{1}{mv(V_c - V_a)} \int_{Va}^{Vc} i(V)dV \quad (1)$$

where C is the specific capacitance (F g-1), m is the mass (g) of electroactive materials in the electrode, v is the potential scan rate (V s-1), Vc and Va (V) are the integration limits of the voltammetric curve, and i(V) denotes the current density (A) [41].

ECSA (m^2 g^{-1}) was then calculated by:

$$ECSA = \frac{C_g}{C_{ref}} \qquad (2)$$

and compared to the SSA as determined by BET measurements. The chosen reference value of capacity per the unit area [42] used in calculation was C_{ref} = 9.57 μF cm^{-2}.

2.5 Oxygen reduction reaction (ORR) electrocatalytic activity

Preliminary electrochemical characterization of the cathode was performed in 100 mM PBS solution (pH 7.8) by cyclic voltammetry (CV), using a potentiostat (Materials M 510). e-BACs were reduced into powders and dispersed in water (10 mg mL^{-1}), sonicated for 5 min and 7 μL were pipetted onto the glassy carbon tip (working electrode, geometric surface area: A = 0.07 cm^2) and dried in a bottom-up position. An electrochemical cell with a graphite counter electrode (Amel 201/S-016) and an Ag/AgCl reference electrode (Amel) in KCl (sat.) was used. Before CV recording, the working electrode was conditioned by cycling in N2 saturated solution within the E = −1.000 / +0.250 V potential range. When using carbonate buffer solution, the potential range was E = −1.2 / +0.1 V. This step was followed by cycling in O2 saturated solution (v = 0.005 V s^{-1}).

2.6 BES assembly and operation

Fig. 1 shows a schematic of the BES experimental setup. The e-BACs (rigid carbonaceous cylinders) were sealed on the bottom side, by attaching a polymethyl methacrylate disk with an inert glue (Gomma Liquida, Bostik®) and were ready to be used as hollow-cylindrical cathodes. The e-BACs were wrapped by synthetic felt (polyester fibers) as to avoid the short circuit with the anode. The anode was fixed around the external face of the cylinder, by a nylon wire, to completely wrap the cane outside the felt. This system was positioned in a plastic jar, immersed in the electrolyte. To prevent evaporation and oxygen diffusion in the wastewater, the jar was covered by a polystyrene disk, preserving anaerobic conditions, while letting air reach the internal cylindrical e-BACs. A plastic net guaranteed the anode's immersion in the electrolyte solution.

BES were run in triplicate in batch mode at (25±1) °C. The cell potential difference was recorded every 20 min across a proper external load using a multichannel Data Logger (Graphtec midi LOGGER GL820). The generated current (I) was calculated by the Ohm's law (I

= V R-1, where R is the external resistive load and V is the cell potential difference) and normalized by the cathode's area to obtain the current density (j).

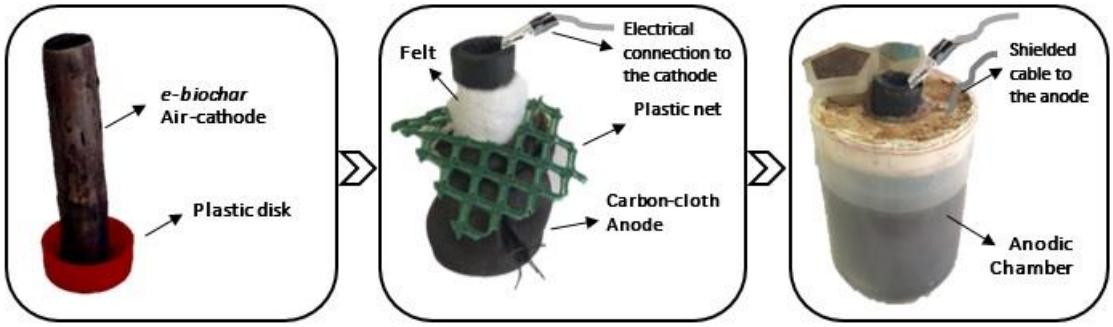

Figure 1 - Schematic of the BES experimental setup.

Anodes were made of plain carbon-cloth (SAATI C1), without any surface treatment. 28 x 9 cm carbon-cloth rectangles were cut and electrically connected to a plastic-insulated copper wire. The electrical connection was then protected by two layers of a bi-component epoxy resin (PROCHIMA COLLA EPOXY).

The inoculum was a swine manure collected in a pig-farm near Milan (Italy). Concentrated swine manure (120 mL, COD = 6 g L^{-1}) were added to the anodic chamber at the beginning of the experiment (t=0). Distilled water (0.5 mL) was dropped into the cathodic chamber ensure the cathode's complete wetness and electrolytic contact.

After the first decline of the current generated by the system, the anolyte was removed and then refilled by the same amount (120 mL), this time composed half by the same swine manure and half by a synthetic medium. The synthetic medium was chosen according to literature [43,44]. Briefly, it was a 100 mM phosphate buffer solution (PBS; 70 g Na_2HPO_4 and 12 g KH_2PO_4 per liter) with the following components in 1 L of deionized water: NH_4Cl (0.41 g); 1 mL of 4 g L^{-1} $FeCl_2$ solution; 10 mL of mineral medium. The mineral media had the composition described by Parameswaran et al. [44]: EDTA (0.5 g L^{-1}); $CoCl_2 \cdot 6H_2O$ (0.082 g L^{-1}); $CaCl_2 \cdot 2H_2O$ (0.114 g L^{-1}); H_3BO_3 (0.01 g L^{-1}); $Na_2MoO_4 \cdot 2H_2O$ (0.02 g L^{-1}); Na_2SeO_3 (0.001 g L^{-1}); $Na_2WO_4 \cdot 2H_2O$ (0.01 g L^{-1}); $NiCl_2 \cdot 6H_2O$ (0.02 g L^{-1}); $MgCl_2$ (1.16 g L^{-1}); $MnCl_2 \cdot 4H_2O$ (0.59 g L^{-1}); $ZnCl_2$ (0.05 g L^{-1}); $CuSO_4 \cdot 5H_2O$ (0.01 g L^{-1}); $AlK(SO_4)_2$ (0.01 g L^{-1}).

After the subsequent current decline, the anolyte was removed and refilled by the same amount of electrolyte (120 mL), this time composed entirely by the synthetic medium added with 7.7 g L^{-1} of sodium acetate. This refill established the end of the acclimation phase and

the starting point of the operational period of each system. A schematic overview of the acclimation and operational phases electrolytes is given in Table 2.

Table 2 - Timeline and details of each experimental phase

ACCLIMATION		**OPERATIONAL PERIOD**			
A1: Day 0 – Day 17	**A2:** Day 17 – Day 25	**P1:** Day 25 – Day 40	**P2:** Day 40 – Day 58	**P3:** Day 58 – Day 72	**P4:** Day 72 – Day 90
120 mL swine manure	60 mL swine manure + 60 mL synthetic medium	7.7 g L^{-1} CH_3COONa in 120 mL synthethic medium	7.7 g L^{-1} CH_3COONa in 120 mL synthethic medium	7.7 g L^{-1} CH_3COONa in 120 mL synthethic medium	7.7 g L^{-1} CH_3COONa in 120 mL synthethic medium

Along the experiment, power curves were periodically recorded with a two-electrode configuration. Before each electrochemical measurement, 1 h equilibration time was found necessary to allow the BES system, disconnected from the data logger, to reach its open circuit potential (OCP). The anode was set as working electrode and the cathode as reference electrode. A linear sweep polarization (v = 0.010 V min^{-1}) was recorded from the cell OCP to 10 mV. Power (P) was calculated by P = I V and plotted vs current density (j).

2.7 Biofilms visualization by fluorescence microscopy

Biofilms growing on both external and internal sides of e-BAC bio-cathodes were visualized by fluorescence microscopy. The samples were collected using adhesive tape strips that reproduce the mirror image of the biofilm present in the selected area. The lectin Concanavalin A-Texas Red conjugate (ConA, Invitrogen, Italy) was used to visualize the polysaccharide component of biofilm matrix (extracellular polymeric substances, EPS), whereas the fluorescent nucleic acid stain 4', 6-diamidino-2-phenylindole (DAPI, Sigma-Aldrich srl, Milan, Italy) was used to display biofilm cells. Samples were incubated with 200 µg $µL^{-1}$ ConA and 10 µg mL^{-1} DAPI solution in

ddH_2O at room temperature in the dark for 30 min, and then rinsed. Images were collected using a Leica DM 4000 B microscope equipped with specific filter sets, and a 63X 0.7NA water immersion objective. Digital images acquired using the CoolSNAP CF digital camera (Photometrics Roper Scientific) and elaborated using the ImageJ 1.34s software.

2.8 ICP-MS

Inductively coupled plasma mass spectrometry (ICP-MS) was used to measure total contents of single elements in the e-BAC at t=0 and t=70 days. Weighted amounts of materials were mineralized by a microwave digestor system (Anton Paar MULTIWAVE-ECO) in Teflon tubes filled with 10 mL of 65% HNO_3 by applying a one-step temperature ramp (210 °C reached in 10 min and maintained for further 10 min). After 20 min of cooling time, the mineralized samples were transferred in polypropylene test tubes. Solutions of mineralized samples were diluted 1:100 with 0.3 M HNO_3 in MILLI-Q water and the concentration of elements was measured by ICP-MS (BRUKER Aurora-M90 ICP-MS). An aliquot of a 2 mg L^{-1} of an internal standard solution (72Ge, 89Y, 159Tb) was added both to samples and calibration curve to give a final concentration of 20 µg L^{-1}. Typical polyatomical analysis interferences were removed by using CRI (Collision-Reaction-Interface) with an H_2 flow of 75 mL min^{-1} flown through skimmer cone.

3. Results and discussion

3.1 Rigid and porous cylindrical structure

After the 900 °C-pyrolysis treatment, the materials maintained its structural rigidity and cylindrical shape (Fig. 1). This was the first fundamental requirement fulfilled by this experiment. By sealing its bottom and immersing its external surface in water, the internal surface got wet because of water penetration but without filling the internal part of the cylinder over time. This means that the porous structure of the material was enough to let water pass through it. At the same time, pores volume and diameters were impeding fast flow of the liquid towards the air-exposed side. At the air-water interface, evaporation has time to take place, being evaporation and water flow well balanced. Similar approaches in BES field were developed by other research groups, introducing air-water separators (such as terracotta ref [45]) which had the function of hindering water to flow out rapidly and without introducing too high resistance. The 'terracotta' (typical porosity 60-500 nm [3,46]) gets imbibed and acts as porous medium that allows electrolytes mobility. In a previous experiment from our group [33], we employed a ligno-cellulosic biomass (Giant Cane), as separator between electrodes. However, since plant materials underwent partial biodegradation over time, they released

elements inside the anolytes. In each of these examples however, the separator was acting as the structural element of the BES. In this experiment we verified that, by direct pyrolysis of the biomass, the cathodic electrode itself is able to give the structure to the BES, without any further separator (and hence resistance) addition.

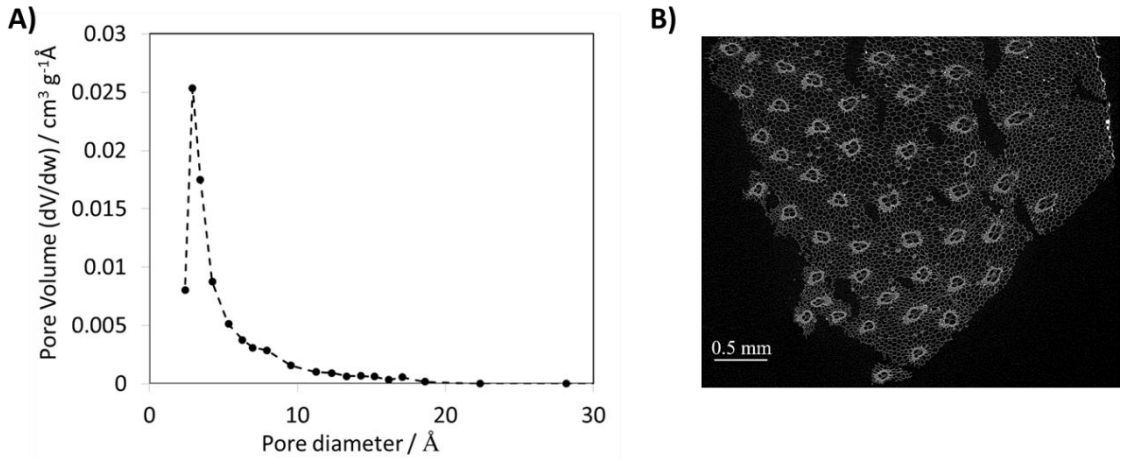

Figure 2 - A) Pore size distribution by BJH analysis. B) MicroCT cross-sections of e-biochar air-cathode.

e-BACs underwent N_2 adsorption/desorption, to measure the BET specific surface area (SSA) which was found equal to 114 ± 4 $m^2 g^{-1}$. Higher specific surface area was hence obtained, with respect to the dry and non-pyrolysed Giant Cane, as reported in the literature by Basso et al. (0.7 $m^2 g^{-1}$) [36]. The same authors also reported the specific surface area value obtained treating Giant Cane stems at 800 °C, a temperature similar to what was used in the present work and they obtained 101 $m^2 g^{-1}$ [36]. This is in line with the specific surface area measured for e-BACs. From the analysis of the porosity, the great part (> 95%) of e-BAC surface area is comprised in pores with a diameter smaller than 1 nm. Basso et al. [36] found similar results for the 800 °C treated sample, with a mean pore radius of about 1.1 nm. Microporosity is therefore the predominant range of pores in the analysed sample, as displayed in Fig. 2A, showing the pore size distribution.

The largest pores, in the macroporosity range, are not quantifiable by BJH analysis and a 3D micro-computed tomography was performed in order to evaluate the morphology of the pyrolized sample in the □m range. A sub-volume of 51.44 mm^3 were analyzed containing 74.77 % voids, 25.17 % e-BAC matrix and 0.06 % residue of pyrolysis (volume %). In Fig. 2B, a microCT

cross section of e-BAC is shown. The structure of the vascular bundles is still present after the pyrolysis. From the inner to the outer surface, a continuous accumulation of vascular bundles can be observed resisting greater static stresses in this zone. The bundle fiber thickness is in the range of 15 and 25 μm. These points were confirmed by Rüggeberg et al. [47], describing the morphological and anatomical features at different structural levels of Giant Cane. The culms are subdivided into nodes and internodes with numerous isolated vascular bundles with enclosing fibre rings embedded in lignified parenchyma further stiffen the culm, as shown in Fig. 2B after the pyrolysis process. The same features were found in the cross section images in the paper by Rüggeberg et al. [47].

Analyzing the inner surface and volume of the void space, the specific surface area was determined equal to 29 mm^2/mm^3. From the arithmetic mean value of the volume-related surface area of single pores approximated as long cylinders, the equivalent diameter is estimated to be about 38.9 μm. Further, the average particle diameter of pyrolysis residue is to be about 21.9 μm.

3.2 Graphitization degree and electrical conductivity

Another important parameter to be determined for e-BACs is its electrical conductivity. Raman spectroscopy is one of the most useful tools to establish the graphitization degree, which correlates with the electrical resistance (and hence the electrical conductivity) [48]. Fig. 3A shows Raman spectra of e-BACs which displays the two typical carbon bands: the D band between 1300 and 1400 cm−1, related to vibrations that are forbidden in perfect graphite and become active in the presence of disorder and defects, and the G band between 1500 and 1600 cm−1 attributable to in-plane bond-stretching vibrations of trigonally bonded carbon atoms (sp2 centers)[49]. From the ratio between the D and G peaks intensity, it is possible to discern the presence of disordered/ordered graphene structures affecting the sample conductivity. Usually, upon annealing, the D peak becomes more intense respect to the G one [48]. An increase in the number and size of graphitic clusters is known to translate into an increase in ID/IG in amorphous carbons, according to the three-stage model of Ferrari et al. [48]. A ID/IG, equal to 2.26 was indeed found for the e-BAC. This is also coherent with other measurements found in the literature [50].

Starting from the acquired spectrum and using the equation provided by Cancado et al. [51], 8.46 nm was determined as the crystallite size.

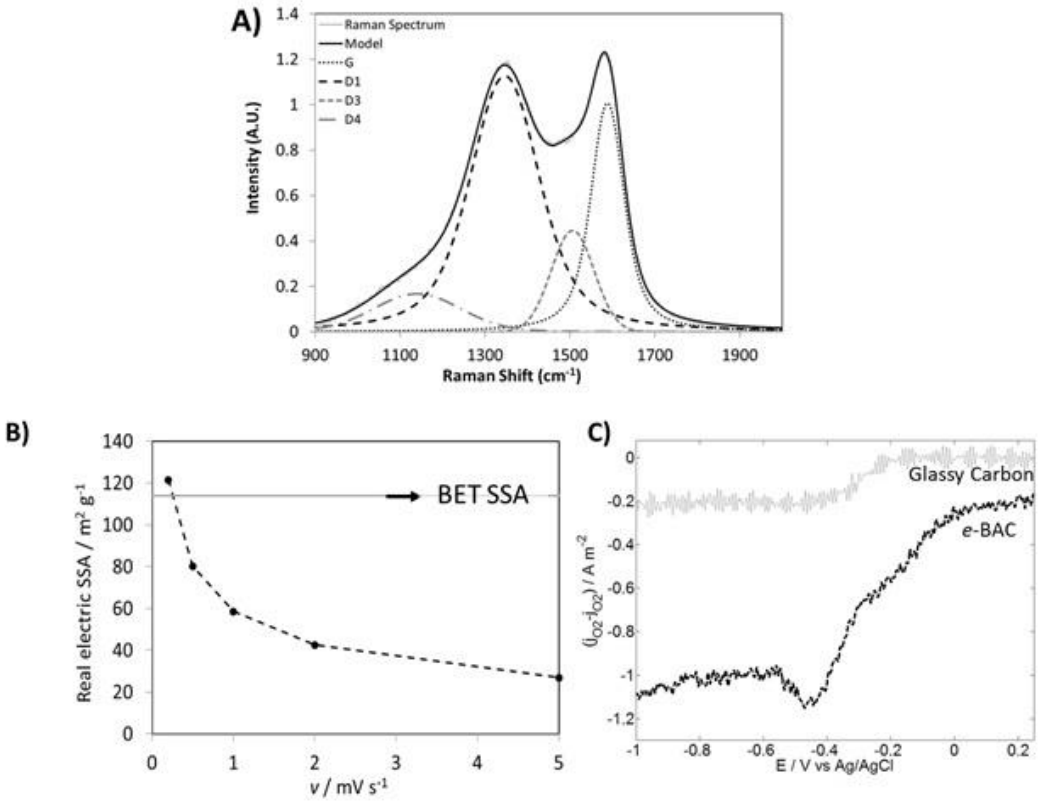

Figure 3 - A) Raman spectrum of e-biochar air-cathodes. B) specific ECSA determinations. C) ORR cathodic polarization curves.

The electrical c of e-BACs was measured and compared to other carbon materials in the literature. The method applied in this work on e-BACs, resulted in an electrical resistivity value of 8.9×10−3 ± 1x10−4 Ω m. As expected, this value indicates a higher resistivity with respect to graphite. Graphite is well-known to possess electrical resistivity varying depending on the measurement axes [52,53] and equal to 2.50×10−6 - 5.00×10−6 Ω m if measured parallel to the basal plane and about 3.00×10−3 Ω m if measured perpendicularly to the basal plane [53]. However, the e-BACs matrix displays a comparable or lower resistivity, and hence a higher conductivity, as compared to other biochar-based materials, reported in the literature. For instance, resistivity was around 5.15×10−3 Ω m for activated carbon [54], 0.98 Ω m for rice straw treated at 800 °C [55].

Double layer charging currents were then recorded within the scan rates range between 0.2 mV s^{-1} and 5 mV s^{-1}. Higher scan rates avoided the system to reach an electrical charging equilibrium due to the large presence of micropores, hindering ions diffusion inside pores. Fig. 3B shows the values of specific ECSA, calculated at different scan rates. As expected, the real available surface area decreased with increasing scan rates. This is due to the presence of micropores, hindering ions diffusion inside the material, hence unable to reach an electrical charging equilibrium if the potential variation over time is too fast.

The highest value of specific ECSA was obtained by the lowest scan rate (0.2 mV s^{-1}) and this value is in fact very similar to the BET specific surface area (114 ± 4 m^2 g^{-1}). This means that the electric surface area corresponds to the BET surface area only with scan rates equal or lower than 0.2 mV s^{-1}.

In general, characterization of carbon/solution interfaces is more complex than that of metals [56]. As explained by equation (2), the weak point of the calculation is relative to the choice of the appropriate Cref value. An improper choice of Cref might drive to unreliable calculations of real electrical SSA. Pore accessibility is the most critical point dealing with capacitance of carbon materials [56]. Other problems arise due to the fact that carbons are not ideally polarizable, as noble metals (e.g. Hg) are. This is attributable to surface oxidation or intercalation processes [56].

Here, the chosen reference value of specific capacity was Cref = 9.57 µF cm^{-2}, for similarity to materials with similar characteristics [42]. This value refers to Vulcan XC72, a material with similar BET surface area (131.6 m^2 g^{-1}), as compared to e-BACs (114 ± 4 m^2 g^{-1}). Also, the specific mass capacitance of this reference material (12.6 µF g^{-1}) is very close to that one calculated for e-BACs sample at the lowest scan rate (11.6 µF g^{-1}).

3.3 ORR electrocatalytic activity

The electrocatalytic properties of e-BAC towards the ORR were investigated. Fig. 3C shows the ORR polarization curves for a glassy carbon electrode (GC) covered by the e-BAC powder. For comparison, the figure also reports a second polarization curve for the bare GC electrode, recorded in the same conditions. Cathodic limiting current densities (normalized by the geometric area of the GC electrode) were equal to -1 A m^{-2} and -0.2 A m^{-2} for e-BAC and GC, respectively. The presence of the e-BAC catalyst not only enhanced the limiting currents, but also shifted the onset potential from -0.200 V vs Ag/AgCl (E1/2=-0.3 V vs Ag/AgCl) to cathodic value of -0.020 V vs Ag/AgCl (E1/2=-0.2 V vs Ag/AgCl).

As compared to other catalysts used in the literature to maximize current generation in fuel cells or microbial fuel cells, e-BAC produced relatively low ORR currents displaying higher overpotentials. For example, Liu et al. doped graphene-based cathodes with nitrogen heteroatoms [57]: the onset potential was found to be 200 mV less cathodic, compared to e-BAC, at the same pH conditions. Also, reduction currents were higher by one order of magnitude. Many other examples in the literature were presented in the direction of electrocatalytic activity enhancement without any precious metal content [58]. The kinetics characteristics of these kind of carbon towards ORR are better [58] compared to what obtained in this work, nevertheless, the production of these carbon-based catalysts is usually time-consuming. Moreover, synthetic or costly reactants are employed. Instead, in this work, despite lower electrocatalytic performance were achieved, e-BACs were fabricated with facile pyrolysis of Giant Cane stalks, without any kind of pre- or post-treatment. This aspect is advantageous in terms of simplicity in electrodes preparation and a potential greater suitability for applications in natural environments, for processes such as biodegradation of pollutants, where even a slow electrocatalysis could be enough.

3.4 e-biochar air-exposed bio-cathodes performances in BES

e-BACs were tested as potential hosts of electroactive biofilm communities, as air-exposed bio-cathodes. After assembling e-BACs in simple BES architectures as shown in Fig. 1, currents were monitored over time. The current density trends, reported in Fig. 4A, showed a standard deviation between the triplicates of about 5%. During a first acclimation period (A1), the anolyte was totally composed by swine manure as inoculum. After an initial and expected delay, around day 12 the systems started producing current, up to a maximum of about 100 mA m^{-2}. In a second acclimation period (A2), during which half of the anolyte was substituted by the synthetic medium, the systems produced less current compared to the previous cycle (with a maximum of about 70 mA m^{-2}), and this might be due to the sudden replacement of the medium of the bacteria colonizing the electrodes which still needed to adapt to the new environment. After the A2 phase, the real operational period (P1) began, characterized by the whole presence of the synthetic medium as the anolyte and sodium acetate (7.7 g L^{-1}) as the standard feed for bacteria. During cycle P1 the current production was comparable to the last cycle of acclimation. This, once again, could be related to the last sudden replacement of the bacteria environment. In a second acetate batch cycle (P2) in fact the recorded current densities are higher and equal to about 130 mA m^{-2}. However, during the next cycles P3 and P4, the systems were not further able to produce current higher as before, showing a maximum

current densities of 25 mA m^{-2} and 15 mA m^{-2} in cycles P3 and P4, respectively. Also power densities were much lower (less than 5 mW m^{-2}) as compared to the starting operational period of the system, as reported in Fig. 4B.

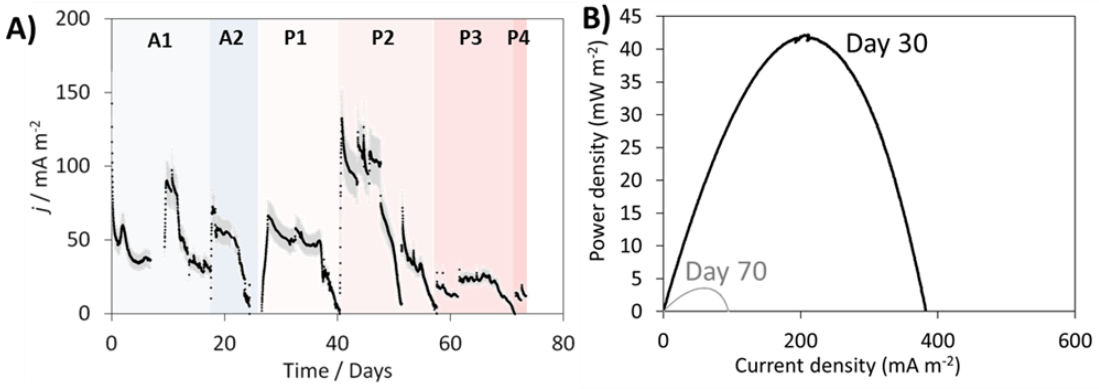

Figure 4 - A) Trends of current density obtained by BES, equipped with e-biochar air-cathode. Black line shows the average trend, the grey region shows the standard deviation of triplicate experiments. In acclimation batch-cycles (A1, A2) swine manure was fed to the anodic chamber; in successive batch cycles (P1-P4) sodium acetate (7.7 g L^{-1}) was used as carbon source. B) Power density curves at day 30 and at day 70.

Representative biofilm structures observed for the e-BAC bio-cathode are presented in Fig. 5. The images display microbial colonization of the water-side of the cathode (Fig. 5 A-B), exposed to bacteria. The biofilm is characterized by a marked structural heterogeneity, showing several morphotypes of microorganisms assembled in dense clusters. The lectin-binding analysis combined with fluorescence microscopy revealed the presence of extracellular polymeric substances glycol-conjugates (i.e. polysaccharides, including those ones covalently linked to proteins and/or lipids) in all the samples colonizing the external side of an e-BAC.

By contrast, the inner surface of an e-BAC, exposed to air was poorly colonized, showing few coccoid morphotypes organized in small assemblages. No signal derived from the lectin-binding analysis was detected, indicating the absence of an extracellular matrix typical of mature and well structured biofilms (Fig. 5C).

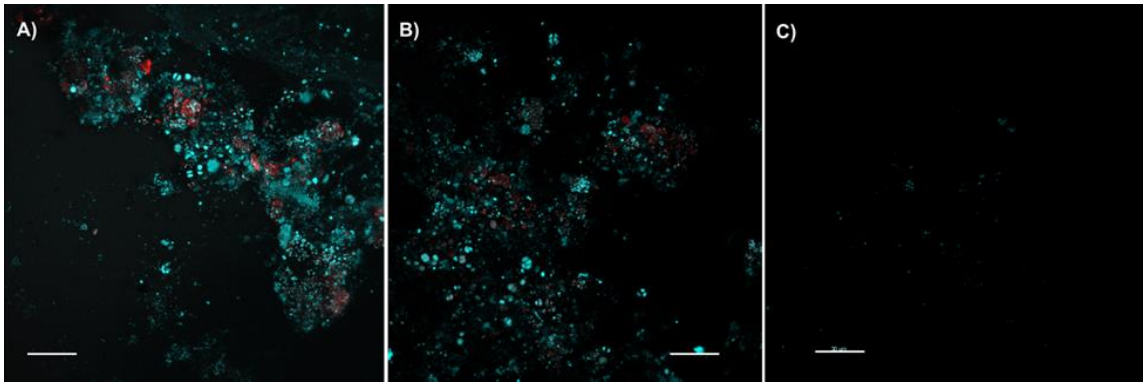

Figure 5 - Fluorescent images of the biofilms colonizing the water-side (panel A-B) and air-side (panel C) of a e-biochar air-exposed bio-cathode. Color key: Biofilm cells, blue (DAPI); EPS matrix, red (ConA). Scale bars 30 μm.

These results indicate that the dimension of pores of the e-biochar impeded the passage of microorganisms from the anolyte towards the air-side. In this region, the electroactive sites of e-BAC exposed to air catalyse the ORR with an electroactivity that was previously investigated by electrochemical reduction polarization curves measured on e-BAC powder (Fig. 3B). However, it cannot be excluded that bacteria, colonizing the water-side of the cathode facing the anolyte, take part in the cathodic oxygen reduction reaction, being in contact with a region where oxygen is likely present, even if at low concentration. e-BAC cylinder could be in fact able to diffuse O2 throughout its thickness, until it reaches the microorganisms. Furthermore, the reduced products from the metabolism of bacteria, such as sulphides, could be able to sustain a chain of cathodic reactions diffusing through the cathode porosity. These aspects that characterized the electrochemical behavior of air-breathing carbon bio-cathode, as discussed in previous works [10,46,59], deserve further investigations and detailed studies.

3.5 Possible applications of e-biochar air-exposed bio-cathodes

Power density curves (Fig. 4B) report maximum of about 40 mW m^{-2}, recorded at day 30, during the plateau reached under feeding condition. Similar values were obtained in low-tech BES, e.g. with Giant Cane stalk or terracotta are employed as air-water separators, using carbon cloth-based electrodes [33,46]. In general, higher-tech microbial fuel cells aimed at energy harvesting in the literature achieve higher current and power densities, as compared to the e-BAC [60,61]. Further work would be needed to optimize abiotic ORR reactions, in the direction of introducing more active electrocatalytic centers and increase the ECSA and [62], in parallel, promote microbial colonization of e-BAC [63].

However, energy harvesting and maximizing power densities might not be the main goal in many applications of e-BACs. For example, terracotta-based microbial fuel cells systems were utilized by Gajda et al. as self- powered wastewater electrolyser for electrocoagulation of heavy metals, caustic production at cathode (pH > 10) and CO_2 sequestration [64]. They also observed how current generation in cylindrical terracotta microbial fuel cells contributed to generate an electro-osmotic drag and reported catholyte formation (attributed to water transport) in proportion to power performance [65]. pH increase was demonstrated to be responsible of inorganic salts deposition (e.g carbonates precipitation) [66] and accumulation as a layer between the cathode and the biofilm, thus preventing charge transfer processes.

Here, the relatively low power density (Fig. 4B) was sufficient to generate an electrical field, driving ions migration at cathode and inducing salts deposition phenomena (likely thanks also to locally increased pH conditions [67]). The observed decrease in currents and maximum power density (Fig. 4) fit with the hypothesis of salts deposition phenomena. After 70 operational days, e-BAC appeared covered by salts deposits (Fig. 6). The materials were analyzed by SEM microscopy, ICP-MS and BET, to detect the presence and the amount of elements that underwent deposition over time. In SEM images (Fig. 6A), the structure of the pristine, pyrolysed Giant Cane is clearly visible. In Fig 6B, the presence of crystals of different shapes, deposited on the external side of the e-BAC cylinder, facing the wastewater is massive.

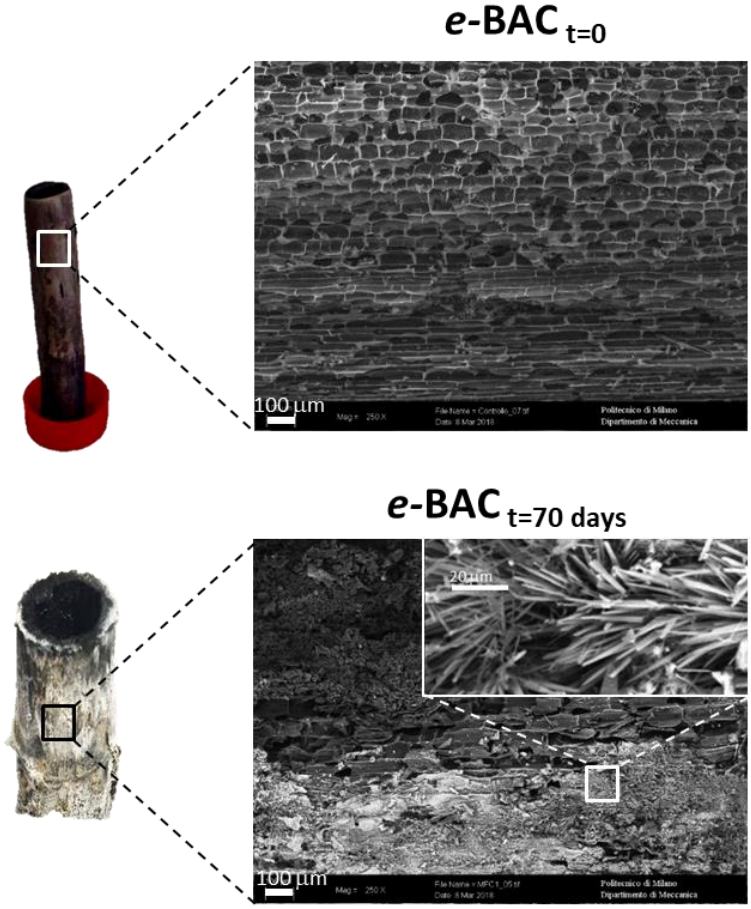

Figure 6 - Pictures and SEM images of the e-BAC at t=0 and after 70 days operation in BES.

From ICP-MS, several elements originally contained in the synthetic wastewater were retrieved on the e-BAC. Na content in the solid material increased by 79 folds, as compared its initial value. Ca and P increased by 1.3 and 5 folds, respectively. Nitrogen was not measured in this work and would deserve particular attentions in future experiments.

Salts deposition likely caused a decrease in the availability of the electroactive sites on the cathode and clogged its porous texture. Accordingly, BET surface area measured at day 70 was under the instrumental detection limit. Even if the precise value could not be measured, the e-BAC material underwent a decrease of at least two-orders of magnitude in available surface area, along the 70-days test.

The phenomenon of salts deposition in air-exposed biocathodes was recently documented in the literature by Santini et al. [14]. Together with carbonates, other salts are likely to deposit (such as struvite and other salts containing macro- e micro-nutrients previously dissolved or suspended in the wastewater). This aspect could be of great interest for environmental application such as nutrients recovery in agro-food systems. When salts deposition clogs the cathode, impeding charge transfer processes, the e-biochar cathode could be substituted with a new one. The e-biochar enriched of plant nutrients might be recycled directly as agricultural soil conditioner. Biochar is widely considered as a soil-fertility promoter and a way to achieve long-term carbon storage [68]. Thereby, salts deposition phenomena on e-BACs can be considered as an advantage, to maximize nutrients recovery from wastewater in agro-food systems. On the other hand, future studies in this field should consider to detect possible contaminants (e.g. heavy metals, antibiotics, etc.) that might be contained in the treated wastewater.

4. Conclusions

e-biochar was prepared by controlled pyrolysis of Giant Cane stalks and characterized for physico-chemical and electrochemical features. The structure and shape of Giant Cane were maintained after the pyrolysis process and it was advantageous in building cylindrical and self-structured air-exposed biocathode. This new material might reduce the need of technological materials in BES, and the cost of bioelectrodes, especially for some applications. The fragility of the e-BAC structure represents an actual drawback which needs an improvement, this might be overcome by addition of compounds that anyway must not decrease the conductivity and properties of the overall matrix. The step forward would be to work on the structure and prepare composite materials through which the thickness would result increased, together with an enhanced rigidity. Despite improvements would be needed to achieve current/power densities of more technological and optimized materials, the e-biochar could open new frontiers in BES' architectures, where energy harvesting is not the main goal. The produced currents induced ions migration and salts deposition, clogging porous texture and enriching e-biochar of minerals. This approach goes into the direction of achieving fully-recyclable BES architectures, directly reusable to produce soil fertilizers. In parallel, further developments are needed to design bigger scale biocathodes/anodes and to optimize their properties and performances, according to the desired application.

Acknowledgements

This work was financed by the SIR 2014 Grant (PROJECT RBSI14JKU3, BiofuelcellAPP), Italian Ministry of University and Research (MIUR) and by the Research Fund for the Italian Electrical System in compliance with the Decree of March 19th, 2009. Authors thank Prof. S. R. Pilu from the University of Milan who furnished the Giant Cane stalks.

References

[1] Wei J, Liang P, Huang X. Recent progress in electrodes for microbial fuel cells. Bioresour Technol 2011;102:9335–44. doi:10.1016/j.biortech.2011.07.019.

[2] Zhou M, Chi M, Luo J, He H, Jin T. An overview of electrode materials in microbial fuel cells. J Power Sources 2011;196:4427–35. doi:10.1016/j.jpowsour.2011.01.012.

[3] Santoro C, Artyushkova K, Gajda I, Babanova S, Serov A, Atanassov P, et al. Cathode materials for ceramic based microbial fuel cells (MFCs). Int J Hydrogen Energy 2015;40:14706–15. doi:10.1016/j.ijhydene.2015.07.054.

[4] Kumar GG, Sarathi VGS, Nahm KS. Recent advances and challenges in the anode architecture and their modifications for the applications of microbial fuel cells. Biosens Bioelectron 2013;43:461–75. doi:10.1016/j.bios.2012.12.048.

[5] You J, Santoro C, Greenman J, Melhuish C, Cristiani P, Li B, et al. Micro-porous layer (MPL)-based anode for microbial fuel cells. Int J Hydrogen Energy 2014;39:21811–8. doi:10.1016/j.ijhydene.2014.07.136.

[6] Santoro C, Lei Y, Li B, Cristiani P. Power generation from wastewater using single chamber microbial fuel cells (MFCs) with platinum-free cathodes and pre-colonized anodes. Biochem Eng J 2012;62:8–16. doi:10.1016/j.bej.2011.12.006.

[7] Santoro C, Agrios A, Pasaogullari U, Li B. Effects of gas diffusion layer (GDL) and micro porous layer (MPL) on cathode performance in microbial fuel cells (MFCs). Int J Hydrogen Energy 2011;36:13096–104. doi:10.1016/j.ijhydene.2011.07.030.

[8] Srikanth S, Pant D, Dominguez-Benetton X, Genné I, Vanbroekhoven K, Vermeiren P, et al. Gas Diffusion Electrodes Manufactured by Casting Evaluation as Air Cathodes for Microbial Fuel Cells (MFC). Materials (Basel) 2016;9:601. doi:10.3390/ma9070601.

[9] Terayama Y, Haji T, Furukawa S, Nomura M, Nishihara M, Lyth SM, et al. Carbon black / PTFE composite hydrophobic gas diffusion layers for a water-absorbing porous electrolyte electrolysis cell. Int J Hydrogen Energy 2018;43:2018–25. doi:10.1016/J.IJHYDENE.2017.12.045.

[10] Rago L, Cristiani P, Villa F, Zecchin S, Colombo A, Cavalca L, et al. Influences of dissolved oxygen concentration on biocathodic microbial communities in microbial fuel cells. Bioelectrochemistry 2017;116:39–51. doi:10.1016/j.bioelechem.2017.04.001.

[11] Guerrini E, Grattieri M, Faggianelli A, Cristiani P, Trasatti S. PTFE effect on the electrocatalysis of the oxygen reduction reaction in membraneless microbial fuel cells. Bioelectrochemistry 2015;106:240–7. doi:10.1016/j.bioelechem.2015.05.008.

[12] Fan Y, Han S-K, Liu H, Keller J, Buisman CJ, Rittmann BE, et al. Improved performance of CEA microbial fuel cells with increased reactor size. Energy Environ Sci 2012;5:8273. doi:10.1039/c2ee21964f.

[13] Katuri KP, Kalathil S, Ragab A, Bian B, Alqahtani MF, Pant D, et al. Dual-Function Electrocatalytic and Macroporous Hollow-Fiber Cathode for Converting Waste Streams to Valuable Resources Using Microbial Electrochemical Systems. Adv Mater 2018:1707072. doi:10.1002/adma.201707072.

[14] Santini M, Marzorati S, Fest-Santini S, Trasatti S, Cristiani P. Carbonate scale deactivating the biocathode in a microbial fuel cell. J Power Sources 2017;356. doi:10.1016/j.jpowsour.2017.02.088.

[15] Zhang F, Pant D, Logan BE. Long-term performance of activated carbon air cathodes with different diffusion layer porosities in microbial fuel cells. Biosens Bioelectron 2011;30:49–55. doi:10.1016/J.BIOS.2011.08.025.

[16] Pant D, Van Bogaert G, Porto-Carrero C, Diels L, Vanbroekhoven K. Anode and cathode materials characterization for a microbial fuel cell in half cell configuration. Water Sci Technol 2011;63:2457. doi:10.2166/wst.2011.217.

[17] Rossi R, Yang W, Zikmund E, Pant D, Logan BE. In situ biofilm removal from air cathodes in microbial fuel cells treating domestic wastewater. Bioresour Technol 2018;265:200–6. doi:10.1016/J.BIORTECH.2018.06.008.

[18] Cheng S, Liu H, Logan BE. Increased performance of single-chamber microbial fuel cells using an improved cathode structure. Electrochem Commun 2006;8:489–94. doi:10.1016/j.elecom.2006.01.010.

[19] Kim JR, Cheng S, Oh S-E, Logan BE. Power Generation Using Different Cation, Anion, and Ultrafiltration Membranes in Microbial Fuel Cells. Environ Sci Technol 2007;41:1004–9. doi:10.1021/es062202m.

[20] Franks AE, Nevin KP. Microbial fuel cells, a current review. Energies 2010;3:899–919. doi:10.3390/en3050899.

[21] Rismani-Yazdi H, Carver SM, Christy AD, Tuovinen OH. Cathodic limitations in microbial fuel cells: An overview. J Power Sources 2008;180:683–94. doi:10.1016/j.jpowsour.2008.02.074.

[22] Ioannidou O, Zabaniotou A. Agricultural residues as precursors for activated carbon production-A review. Renew Sustain Energy Rev 2007;11:1966–2005. doi:10.1016/j.rser.2006.03.013.

[23] Yuan Y, Liu T, Fu P, Tang J, Zhou S. Conversion of sewage sludge into high-performance bifunctional electrode materials for microbial energy harvesting. J Mater Chem A 2015;3:8475–82. doi:10.1039/C5TA00458F.

[24] Qian K, Kumar A, Zhang H, Bellmer D, Huhnke R. Recent advances in utilization of biochar. Renew Sustain Energy Rev 2015;42:1055–64. doi:10.1016/j.rser.2014.10.074.

[25] Huggins T, Wang H, Kearns J, Jenkins P, Ren ZJ. Biochar as a sustainable electrode material for electricity production in microbial fuel cells. Bioresour Technol 2014;157:114–9. doi:10.1016/j.biortech.2014.01.058.

[26] Chen S, Tang J, Fu L, Yuan Y, Zhou S. Biochar improves sediment microbial fuel cell performance in low conductivity freshwater sediment n.d. doi:10.1007/s11368-016-1452-z.

[27] Cruz Viggi C, Simonetti S, Palma E, Pagliaccia P, Braguglia C, Fazi S, et al. Enhancing methane production from food waste fermentate using biochar: the added value of electrochemical testing in pre-selecting the most effective type of biochar. Biotechnol Biofuels 2017;10:303. doi:10.1186/s13068-017-0994-7.

[28] Chen S, Rotaru A-E, Shrestha PM, Malvankar NS, Liu F, Fan W, et al. Promoting interspecies electron transfer with biochar. Sci Rep 2014;4:5019. doi:10.1038/srep05019.

[29] Ma M, You S, Wang W, Liu G, Qi D, Chen X, et al. Biomass-Derived Porous Fe 3 C/Tungsten Carbide/Graphitic Carbon Nanocomposite for Efficient Electrocatalysis of Oxygen Reduction. ACS Appl Mater Interfaces 2016;8:32307–16. doi:10.1021/acsami.6b10804.

[30] Huggins TM, Pietron JJ, Wang H, Ren ZJ, Biffinger JC. Graphitic biochar as a cathode electrocatalyst support for microbial fuel cells. Bioresour Technol 2015;195:147–53. doi:10.1016/j.biortech.2015.06.012.

[31] Yuan H, Deng L, Qi Y, Kobayashi N, Tang J. Nonactivated and activated biochar derived from bananas as alternative cathode catalyst in microbial fuel cells. ScientificWorldJournal 2014;2014:832850. doi:10.1155/2014/832850.

[32] Chen Q, Pu W, Hou H, Hu J, Liu B, Li J, et al. Activated Microporous-Mesoporous Carbon Derived from Chestnut Shell as a Sustainable Anode Material for High Performance Microbial Fuel Cells. Elsevier Ltd; 2017. doi:10.1016/j.biortech.2017.09.086.

[33] Marzorati S, Schievano A, Colombo A, Lucchini G, Cristiani P. Ligno-cellulosic materials as air-water separators in low-tech microbial fuel cells for nutrients recovery. J Clean Prod 2018;170:1167–76. doi:10.1016/J.JCLEPRO.2017.09.142.

[34] Corno L, Pilu R, Adani F. Arundo donax L.: A non-food crop for bioenergy and bio-compound production. Biotechnol Adv 2014;32:1535–49. doi:10.1016/j.biotechadv.2014.10.006.

[35] Valli F, Trebbi D, Zegada-Lizarazu W, Monti A, Tuberosa R, Salvi S. In vitro physical mutagenesis of giant reed (Arundo donax L.). GCB Bioenergy 2017;9:1380–9. doi:10.1111/gcbb.12458.

[36] Basso MC, Cerrella EG, Buonomo EL, Bonelli PR, Cukierman AL. Thermochemical Conversion of Arundo Donax into Useful Solid Products. Energy Sources 2005;27:1429–38. doi:10.1080/009083190523280.

[37] Jeguirim M, Trouvé G. Pyrolysis characteristics and kinetics of Arundo donax using thermogravimetric analysis. Bioresour Technol 2009;100:4026–31. doi:10.1016/j.biortech.2009.03.033.

[38] Longhi M, Marzorati S, Checchia S, Sacchi B, Santo N, Zaffino C, et al. Sugar-based catalysts for oxygen reduction reaction. Effects of the functionalization of the nitrogen precursors on the electrocatalytic activity. Electrochim Acta 2016. doi:10.1016/j.electacta.2016.11.036.

[39] Santini M, Guilizzoni M, Fest-Santini S. X-ray computed microtomography for drop shape analysis and contact angle measurement. J Colloid Interface Sci 2013;409:204–10. doi:10.1016/J.JCIS.2013.06.036.

[40] Lukaszewski M, Soszko M, Czerwiński A. Electrochemical methods of real surface area determination of noble metal electrodes - an overview. Int J Electrochem Sci 2016;11:4442–69. doi:10.20964/2016.06.71.

[41] Du F, Yu D, Dai L, Ganguli S, Varshney V, Roy AK. Preparation of Tunable 3D Pillared Carbon Nanotube Graphene Networks for High Performance Capacitance. Chem Mater 2011:4810–6. doi:10.1021/cm2021214.

[42] Capacitance limits of high surface area activated carbons for double layer capacitors. Carbon N Y 2005;43:1303–10. doi:10.1016/J.CARBON.2005.01.001.

[43] Rago L, Guerrero J, Baeza JA, Guisasola A. 2-Bromoethanesulfonate degradation in bioelectrochemical systems. Bioelectrochemistry 2015;105:44–9. doi:10.1016/j.bioelechem.2015.05.001.

[44] Parameswaran P, Torres CI, Lee HS, Krajmalnik-Brown R, Rittmann BE. Syntrophic interactions among anode respiring bacteria (ARB) and non-ARB in a biofilm anode: Electron balances. Biotechnol Bioeng 2009;103:513–23. doi:10.1002/bit.22267.

[45] Pasternak G, Greenman J, Ieropoulos I. Comprehensive Study on Ceramic Membranes for Low-Cost Microbial Fuel Cells. ChemSusChem 2015:88–96. doi:10.1002/cssc.201501320.

[46] Rago L, Zecchin S, Marzorati S, Goglio A, Cavalca L, Cristiani P, et al. A study of microbial communities on terracotta separator and on biocathode of air breathing microbial fuel cells. Bioelectrochemistry 2018;120:18–26. doi:10.1016/J.BIOELECHEM.2017.11.005.

[47] Ruggeberg M, Burgert I, Speck T. Structural and mechanical design of tissue interfaces in the giant reed Arundo donax. J R Soc Interface 2010;7:499–506. doi:10.1098/rsif.2009.0273.

[48] Ferrari AC, Robertson J. Interpretation of Raman spectra of disordered and amorphous carbon. Phys Rev B 2000;61:14095–107. doi:10.1103/PhysRevB.61.14095.

[49] Marzorati S, Vasconcelos JM, Ding J, Longhi M, Colavita PE, Carrette L, et al. Template-free ultraspray pyrolysis synthesis of N/Fe-doped carbon microspheres for oxygen reduction electrocatalysis. J Mater Chem A 2015;3:18920–7. doi:10.1039/C5TA02570B.

[50] Bernard S, Beyssac O, Benzerara K, Findling N, Tzvetkov G, Brown GE. XANES, Raman and XRD study of anthracene-based cokes and saccharose-based chars submitted to high-temperature pyrolysis. Carbon N Y 2010;48:2506–16. doi:10.1016/j.carbon.2010.03.024.

[51] Caņado LG, Takai K, Enoki T, Endo M, Kim YA, Mizusaki H, et al. General equation for the determination of the crystallite size la of nanographite by Raman spectroscopy. Appl Phys Lett 2006;88:1998–2001. doi:10.1063/1.2196057.

[52] Deprez N, McLachlan DS. The analysis of the electrical conductivity of graphite conductivity of graphite powders during compaction. J Phys D Appl Phys 1988;21:101–7. doi:10.1088/0022-3727/21/1/015.

[53] Pierson HO. Handbook of Carbon, Graphite, Diamond and Fullerenes. Handb Carbon, Graph Diam Fullerenes 1993:25–69. doi:http://dx.doi.org/10.1016/B978-0-8155-1339-1.50008-6.

[54] Barroso-Bogeat A, Alexandre-Franco M, Fernández-González C, Macías-García A, Gómez-Serrano V. Electrical conductivity of activated carbon–metal oxide nanocomposites under compression: a comparison study. Phys Chem Chem Phys 2014;16:25161–75. doi:10.1039/C4CP03952A.

[55] Adinaveen T, Vijaya JJ, Kennedy LJ. Comparative Study of Electrical Conductivity on Activated Carbons Prepared from Various Cellulose Materials. Arab J Sci Eng 2016;41:55–65. doi:10.1007/s13369-014-1516-6.

[56] 9.3.Double layer capacitance of carbon.pdf n.d.

[57] Liu Y, Liu H, Wang C, Hou S-X, Yang N. Sustainable Energy Recovery in Wastewater Treatment by Microbial Fuel Cells: Stable Power Generation with Nitrogen-doped Graphene Cathode. Environ Sci Technol 2013;47:13889–95. doi:10.1021/es4032216.

[58] Kodali M, Santoro C, Herrera S, Serov A, Atanassov P. Bimetallic platinum group metal-free catalysts for high power generating microbial fuel cells. J Power Sources 2017;366:18–26. doi:10.1016/j.jpowsour.2017.08.110.

[59] Cristiani P, Carvalho ML, Guerrini E, Daghio M, Santoro C, Li B. Cathodic and anodic biofilms in Single Chamber Microbial Fuel Cells. Bioelectrochemistry 2013;92:6–13. doi:10.1016/j.bioelechem.2013.01.005.

[60] Nguyen MT, Mecheri B, Iannaci A, D'Epifanio A, Licoccia S. Iron/Polyindole-based Electrocatalysts to Enhance Oxygen Reduction in Microbial Fuel Cells. Electrochim Acta 2016;190:388–95. doi:10.1016/j.electacta.2015.12.105.

[61] Cristiani P, Carvalho ML, Guerrini E, Daghio M, Santoro C, Li B. Cathodic and anodic biofilms in Single Chamber Microbial Fuel Cells. Bioelectrochemistry 2013;92:6–13. doi:10.1016/j.bioelechem.2013.01.005.

[62] Ruiz-Rosas R, Valero-Romero MJ, Salinas-Torres D, Rodríguez-Mirasol J, Cordero T, Morallón E, et al. Electrochemical Performance of Hierarchical Porous Carbon Materials Obtained from the Infiltration of Lignin into Zeolite Templates. ChemSusChem 2014;7:1458–67. doi:10.1002/cssc.201301408.

[63] Strelko V., Kuts V., Thrower P. On the mechanism of possible influence of heteroatoms of nitrogen, boron and phosphorus in a carbon matrix on the catalytic activity of carbons in electron transfer reactions. Carbon N Y 2000;38:1499–503. doi:10.1016/S0008-6223(00)00121-4.

[64] Gajda I, Stinchcombe A, Greenman J, Melhuish C, Ieropoulos I. Microbial fuel cell e A novel self-powered wastewater electrolyser for electrocoagulation of heavy metals 2016. doi:10.1016/j.ijhydene.2016.06.161.

[65] Gajda I, Greenman J, Melhuish C, Santoro C, Li B, Cristiani P, et al. Water formation at the cathode and sodium recovery using Microbial Fuel Cells (MFCs). Sustain Energy Technol Assessments 2014;7:187–94. doi:10.1016/j.seta.2014.05.001.

[66] Santini M, Marzorati S, Fest-Santini S, Trasatti S, Cristiani P. Carbonate scale deactivating the biocathode in a microbial fuel cell. J Power Sources 2017;356:400–7. doi:10.1016/j.jpowsour.2017.02.088.

[67] Gajda I, Greenman J, Melhuish C, Santoro C, Li B, Cristiani P, et al. Electro-osmotic-based catholyte production by Microbial Fuel Cells for carbon capture. Water Res 2015. doi:10.1016/j.watres.2015.08.014.

[68] Woolf D, Amonette JE, Street-Perrott FA, Lehmann J, Joseph S. Sustainable biochar to mitigate global climate change. Nat Commun 2010;1:1–9. doi:10.1038/ncomms1053.

Chapter 6 - Capturing carbon and nutrients from organic-rich wastewater by bioelectrochemically-enhanced deposition on electro-active biochar

Andrea Goglio[a], Stefania Marzorati[a], Sarah Zecchin[b], Lucia Cavalca[b], Stefano Bocchi[a], Andrea Schievano[a]*

a e-BioCenter, Department of Environmental Science and Policy, University of Milan, Via Celoria 2, 20133 Milan, Italy

b e-BioCenter, Department of Food Environmental and Nutritional Science, University of Milan, Via Mangiagalli 25, 20133 Milan, Italy

* Corresponding author: andrea.schievano@unimi.it

Abstract

An emerging class of biogenic materials for potential applications in bioelectrochemical systems has been recently proposed, based on biochar with tailored electroactive properties. Here, we carbonized Giant Cane stems to produce cylindrical electro-active biochar elements. We tested such elements in the treatment of organich-rich wastewater. The hollow structure of stems helps maximizing the available surface area at the air-water interface. This configuration is thought to promote bioelectrochemical oxidation of organics, by enhancing electron flows towards terminal acceptors (e.g. NO_3-, SO_4^{2-}, O_2). Soluble fractions of organic carbon were removed over 95%, with all types of configuration (double electrodes, short-circuit, open circuit). The electrical field should favour ions transport towards the surface, promoting salts deposition on the material, where in the double electrodes configuration the nutrients recovery was 3 times higher that the other two configurations.

Keywords

Bioelectrochemical systems, microbial recycling cells, electroactive biochar, nutrients recovery, wastewater treatment.

1. Introduction

Real scale application of bio-electrochemical systems (BES) has been facing the need to find an optimal balance between processes efficiencies and costs. Many researches are addressing to develop low-cost and environmentally compatible materials to fabricate electrodes for large scale applications, such as wastewater treatment, soil bioremediation, etc. (Wei et al., 2011). To date, the most competitive materials are based on carbon and include graphite-based rods, fiber brushes and granules, carbon-fiber cloths, carbon paper sheets, carbon felt and reticulated vitreous carbon (kumar et al., 2013; Zhou et al., 2011). They are selected due to their strong biocompatibility and inert properties at room temperature. The use of such materials as air-breathing cathodes has been coupled to the fabrication of microporous layers, made of activated carbon, pressed on carbon cloths (or other current collector) in the presence of polymeric binders (Nafion, PTFE, etc.) (Santoro et al., 2012; You et al., 2014). High surface area favors the cathodic oxygen reduction reaction (ORR) that needs the simultaneous presence of solid, liquid and gaseous phases. Microporous layers also act as gas diffusion layer at air-water interface, because the porous structure allows the diffusion of air in contact with the wet surface, impeding water to leak to the air-side (Santoro et al., 2011; Terayama et al., 2018). Finally, high surface areas promote the formation of electroactive biofilms, able to

highly boost a series of cascade reactions towards oxygen reduction which characterize the behavior of aerobic and anaerobic bio-cathode (Guerrini et al., 2015; Rago et al., 2017). These 'structural' functions is really important for the application of such materials as air-exposed bio-cathodes (Guerrini et al., 2015). However, these composites have some intrinsic limitations for large-scale applications of BES. Some novel solutions with macroporous hollow fibers were recently proposed, still in the field of high-tech materials (Katuri et al., 2018). After relatively short time of operation, biofouling and salts deposition phenomena, tend to hinder cathode's performances. Unless restored by specific treatments (Rossi et al., 2018), such electrodes should be substituted by new ones. However, these materials are not fully recyclable. Carbon-cloths are based on mixtures of carbon fibers with non-biogenic materials, such as polymeric binders (PTFE, Nafion, etc.). The compactness of the activated carbon mixtures on carbon cloth electrodes is also guaranteed by the massive presence of water-resistant binders (Cheng et al., 2006; Jung et al., 2007). In view of environmental large-scale applications of these electrodes, such as wastewater treatment or soil bioremediation, where harvesting electrical power is not the main goal (Franks and Nevin, 2010; Rismani-Yazdi et al., 2008), avoiding "high-tech", expensive and non-recyclable materials might result in a substantial advantage. An alternative approach should be based on a circular economy concept, where bio-electrodes are fabricated with bio-based and fully recyclable materials. In this view, biomass-derived charcoal (biochar) represents a class of target materials that would satisfy this purpose. Biochar, the product of biomass thermochemical conversions, has been receiving increasing attention, for several applications (Schievano et al., 2019). The versatility of biochar depends on its chemical and structural properties. Biochar is often porous and possesses high surface area (Ioannidou and Zabaniotou, 2007). Few groups recently started using biochar in BES (Cruz Viggi et al., 2017; Yuan et al., 2015), demonstrating its ability of promoting interspecies electron transfer (Chen et al., 2014). For example, a variety of biomass-derived biochar (i.e. from pomelo peel and wood chips) was recently used in biofilm-driven water treatment processes possessing characteristics of low cost, high specific area, good biocompatibility and moderate electrical conductivity, which basically meet the requirements of biocathode materials (Huggins et al., 2015; Ma et al., 2016). The fabrication of biochar as base for bio-electrodes, should aim at simultaneously enhancing electrical conductivity, abiotic electrocatalytic properties (e.g. ORR), biocompatibility and the capacity to host microbial biofilm communities. These properties would characterize a particular class of biochars. Here, the possibility to obtain e-biochar materials with intrinsic structural rigidity, would open the possibility to use them as air-breathing bio-cathodes at the air-water interface, in lieu of microporous layer/gas diffusion

layer-based electrodes. Also, the availability of the original biomass in large amounts, at relatively low costs and environmental impacts, would also be a key-factor for success of e-biochar in large-scale BES. In a recent experiment, Giant Cane (Arundo donax L.) stalks were tested as air-water cylindrical separators, in air-cathode BES (Marzorati et al., 2018). The plant's stalks, characterized by porous and rigid cylindrical structure, avoided water leaks to the air-side and allowed spontaneous electricity production using an organic-rich wastewater, with carbon cloth electrodes (Marzorati et al., 2018). Here, we fabricate air-breathing bio-cathodes with a rigid cylindrical shape, based on e-biochar obtained from controlled pyrolysis of Giant Cane stalks. The physico-chemical and electrocatalytic properties were investigated, as well as their performance as air-breathing bio-cathodes in BES aimed at recovering nutrients from wastewater.

Lately, in BES area, also low-tech microbial electrochemical systems are involved in the process of scaling-up. In this scenario the snorkel systems are taking an important place, because it is a very simple, example of microbial electrochemical technology. It consists of the direct coupling of a microbial anode with a cathode, which may or may not be biotic (Erable et al., 2011a). In other words, it can be considered as a short-circuited microbial fuel cell (MFC) (Santoro et al., 2017). Basically, a microbial electrochemical snorkel (MES) is a short-circuited microbial fuel cell (MFC). MFCs are characterized by a bell-shaped power current curve. When short-circuited, an MFC no longer produces any power, because the voltage between anode and cathode is zero, but it works at the maximum possible current. The main advantage of an MES is thus to sustain the maximum current between cathode and anode that an MFC can produce. The reaction rates are raised to the maximum that the system can support. This way of operating is ideal when the objective is to raise electrochemical reaction rates rather than to produce electrical power (Hoareau et al., 2019). However, the MES is really performing in the organic compound degradation and soil remediation by antibiotic but its permanence degrease drastically when is mandatory a different working potential between anode and cathode as in soil remediation and nutrients recovery contrary to MFC (Dominguez-Benetton et al., 2018; Wu et al., 2018; Yan et al., 2019).

2. Materials and methods

2.1 Cylindrical MRCs configuration and experimental set-up

In this experiment, electro-active biochar cathodes produced as Marzorati et al. (Marzorati et al., 2018) described, were studied as air-cathode in different set-ups: close circuit, snorkel effect and as a control to study the material adsorption. These arrangements were studied to compare different electrochemical forces, to recover organic matter, inorganic carbon macro, meso- and micro-nutrients. Fig. 1-a shows a schematic configuration of the lab-scale setup.

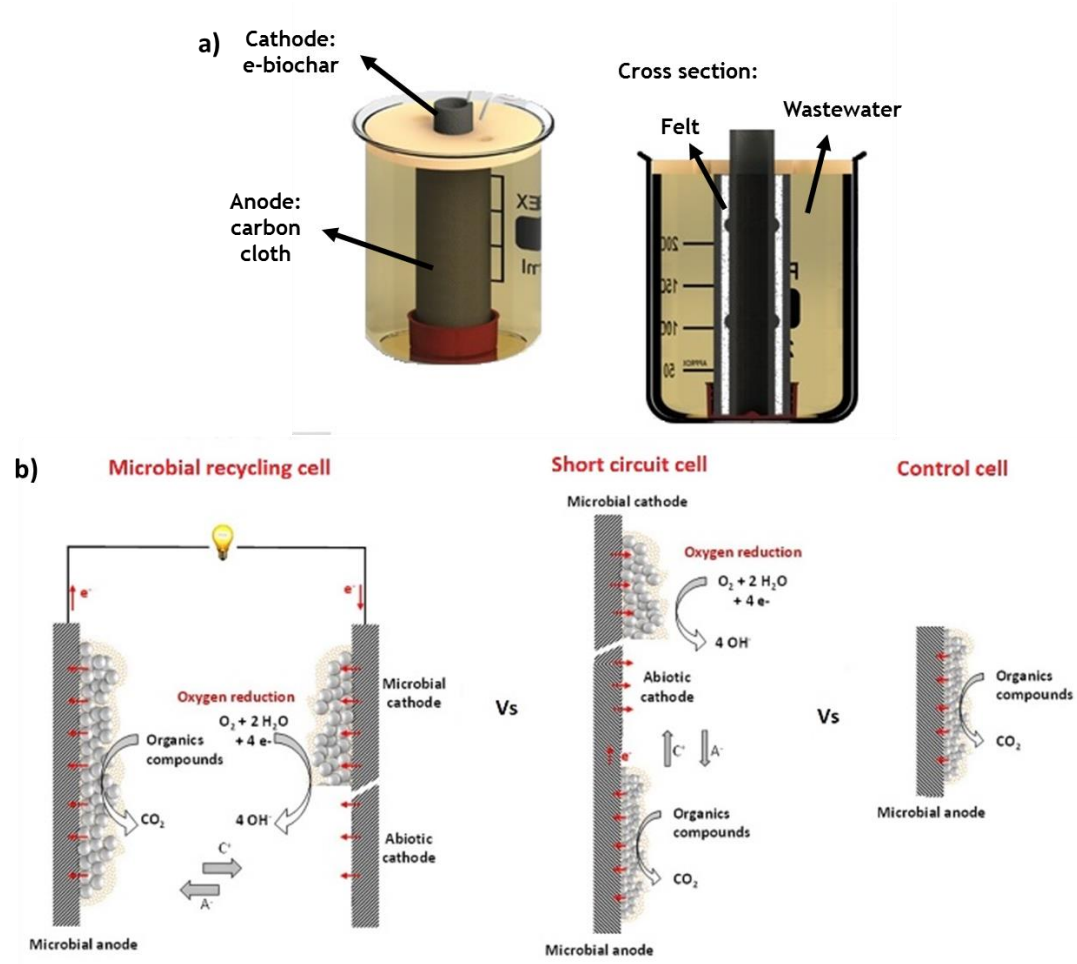

Figure 1 – Configuration of the lab-scale reactors used in this experiment (a) and the different systems involved in the experiment (b).

The e-biochar cathodes were sealed on the bottom side, by attaching a polymethylmethacrylate disk with an inert glue (Gomma Liquida, Bostik®) and were ready to be used as hollow-cylindrical cathodes. The systems were wrapped by synthetic felt (polyester fibers) as to avoid the short circuit with the anode. The anode was fixed around the external face of the cylinder, by a nylon wire, to completely wrap the cane outside the felt. This system was positioned in a plastic jar, immersed in the electrolyte. To prevent evaporation and oxygen diffusion in the wastewater, the jar was covered by a polystyrene disk, preserving anaerobic conditions, while letting air reach the internal cylindrical e-biochar cathodes. A plastic net guaranteed the anode's immersion in the electrolyte solution.

Anodes were made of plain carbon-cloth (SAATI C1, Appiano Gentile, Italy), without any surface treatment. 9 cm carbon-cloth rectangles were cut and electrically connected to a plastic-insulated copper wire. The electrical connection was then protected by two layers of a bi-component epoxy resin (PROCHIMA COLLA EPOXY). For the short circuit reactors we utilised the same design, materials, treatments and size of electrodes without though that anode and cathode were divided by a layer of felt and also for the control that everything was immersed. The inoculum was a swine manure collected in a pig-farm near Milan (Italy). The artificial wastewater was chosen according to literature (Parameswaran et al., 2009; Pasternak et al., 2015). Briefly, it was a 100 mM phosphate buffer solution (PBS; 70 g Na_2HPO_4 and 12 g KH_2PO_4 per litre) with the following components in 1 L of deionized water: NH_4Cl (0.41 g); 1 mL of 4 g L_{-1} $FeCl_2$ solution; 10 mL of mineral medium. The mineral media had the composition described by Parameswaran et al. (Parameswaran et al., 2009): EDTA (0.5 g L^{-1}), $CoCl_2 \cdot 6H_2O$ (0.082 g L^{-1}), $CaCl_2 \cdot 2H_2O$ (0.114 g L^{-1}), H_3BO_3 (0.01 g L^{-1}), $Na_2MoO_4 \cdot 2H_2O$ (0.02 g L^{-1}), Na_2SeO_3 (0.001 g L^{-1}), $Na_2WO_4 \cdot 2H_2O$ (0.01 g L^{-1}), $NiCl_2 \cdot 6H_2O$ (0.02 g L^{-1}), $MgCl_2$ (1.16 g L^{-1}), $MnCl_2 \cdot 4H_2O$ (0.59 g L^{-1}), $ZnCl_2$ (0.05 g L^{-1}), $CuSO_4 \cdot 5H_2O$ (0.01 g L^{-1}), $AlK(SO_4)_2$ (0.01 g L^{-1}). In particular, timeline and details of each experimental phase are describe in Table 1. Three different set ups (close circuit, snorkel and open circuit) were studied over 40 days at 25°C ±1 in experimental double to demonstrate and to compare the importance of the electrochemical forces. The electrochemical performances of the MRCs were measured over time. The fate of soluble fractions of organic matter and nutrients was monitored in the liquid phase along the observed period and at the end of the test were characterized the enrichment in organic matter and macro-, meso- and micro-nutrients of the electro-active biochar.

Table 1 - Timeline and details of each experimental phase

A1	A2	C1	C2
Day 0 - 7	Day 7 - 18	Day 18 - 26	Day 26 - 40
120 mL swine manure	60 mL swine manure + 60 mL synthetic medium	7.7 g L^{-1} CH_3COONa in 120 mL synthetic medium	7.7 g L^{-1} CH_3COONa in 120 mL synthetic medium

2.2 Electrochemical analyses

Throughout the duration of the experiment, several electrochemical measurements were carried out: current density trends, power curves, anodic polarization and working potential. For each MRC anode and cathode were connected across an external load of 100 Ω and their potential was recorded every 20 minutes using a multichannel Data Logger (Graphtech midi Logger GL820). Power curves were measured at the start, middle and at the end of the experiment with a two-electrode configuration. Before each electrochemical measurement, 1 h of equilibration time was found necessary to allow the system, disconnected from the data logger, to reach OCP. The anode was set as working electrode and the cathode as reference electrode. A linear sweep polarization (scan rate v=0.010 V min^{-1}) was recorded from the cell OCP to 10 mV. The power was calculated by $P = I \bullet V$, normalized by the cathodic area and plotted vs current density.

Moreover, there were performed also anodic polarization at the start, middle and at the end of the experiment with a three-electrode configuration. The anode was set as working electrode in the anodic polarization and as counter in the cathodic one and the third electrode was the reference in both situation. The anodic polarization measurements were performed with a scan rate of 0.010 V min^{-1} and they were recorded in a range from the anodic OCP to 0.4 V. In addition, during the experiment it was measured the working potential of all the set ups with a multimeter to understand at which potential there are working and which electrochemical reactions are taking place.

2.3 Physico-chemical characterization

The chemical composition of the wastewaters along the cycles was monitored by several parameters: chemical oxygen demand (COD), total nitrogen (TN) and total content of the main macro- and micro-nutrients (K, P, Mg, Fe, Mn) analysed by inductively coupled plasma mass spectrometry (ICP-MS). In addition, the enrichment in these elements on the terracotta separators was determined at the end of the experiment, adding also nitrate (NO3-), ammonia (NH4+), inorganic carbon (IC) analyses.

The soluble fractions of COD and TN in the anolyte were determined using spectrophotometric method after specific reactions using test kits (Hach Company, Loveland, CO, USA). The samples were filtered (0.45 µm Nylon filters) before the analysis. ICP-MS (BRUKER Aurora-M90 ICP-MS) was used to measure single elements in the soluble fractions and in the extracts of the e-biochar. The extracts were made in milliQ water to simulate the solubility of the nutrients. The mixture of e-biochar and solutions (ratio 1:10) was mixed for 30 minutes and after that it was filtrated with 0.45 µm nylon filters ("Metodi di Analisi dei Fertilizzanti," 2001.).

The inorganic carbon was analysed using a SIEVERS 820 Portable Total Organic Carbon Analyzer (GE Analytical Instruments, UK). This tool provides an extremely sensitive measurement of the TOC, IC and TC concentration in solutions. Moreover, TN, NO_3- and NH_4+ were measured in the extracts of the e-biochar using spectrophotometric method after specific reactions using test kits (Hach Company, Loveland, CO, USA).

2.4 Identification of the microbial populations enriched on the electrodes by 16S rRNA genes Illumina sequencing

The composition of the microbial communities enriched at the anodes and cathodes of MRC, SCC and CC were characterized by 16S rRNA gene Illumina sequencing. For each electrode, an area of about 18 cm3 was washed with sterile milliQ water to collect the microbial biomass. DNA was extracted from approximately 250 mg of material using DNeasy® PowerSoil® (QIAGEN, Germany) according to manufacturer's instructions. Bacterial and archaeal 16S rRNA genes were sequenced using primers 341F/806R (respectively, 5'-CCTACGGGAGGCAGCAG-3' and 5'-GGACTACHVGGGTWTCTAAT-3') and 344F/806R (respectively, 5'- ACGGGGTGCAGGCGCGA-3' and 5'- GGACTACHVGGGTWTCTAAT-3'). Library preparation, pooling and sequencing was performed on a MiSeq platform at the Center for Genomic Research – DNA Service Facility, University of Illinois at Chicago, according to Green et al. (2015) and Bybee et al. (2011). Paired reads were merged with PEAR (Zhang et al., 2014). Trimming was performed on ambiguous

nucleotides and primer sequences. Reads with internal ambiguous nucleotides or lacking primer sequence were discarded. Further trimming was performed at quality threshold of 0.01 and resulting reads shorter than 325 bp were discarded. Chimeric sequences were identified using the UCHIME algorithm as compared with the SILVA SSU Ref dataset (Edgar, 2010; Quast et al., 2013). Further analyses were performed using QIIME (Caporaso et al., 2010). Unique sequences were dereplicated and sequences with similarity of 97% or higher were clustered and taxonomically classified using USEARCH and the SILVA SSU Ref dataset (Edgar, 2010). The communities were clustered with Unweighted Pair Group Method with Arithmetic mean (UPGMA, Hamady et al., 2009; Sneath et al., 1973) and compared with non-metric multidimensional scaling (NMDS, Faith et al., 1987) on Bray-Curtis dissimilarities between the samples, using the R package vegan version 2.5-5 (Oksanen et al., 2018).

3 - Results and Discussion

3.1 - Current generation trends and electrochemical characterization

As show in Figure 1b, in a view of electrochemical reactions the experiment is composed by 3 different kind of set-up: microbial recycling cell (close circuit), short circuit cell (short circuit) and control cell (open circuit). The close circuit system is characterised by two different electrodes, anode and cathode that work separately. In the anodic compound happens the oxidation of the organic matter and it is the anaerobic part of the system, while, the cathodic electrode is the place where happen the reduction of the oxygen and this compound is characterised by a positive or a slightly negative potential. These differences between anode and cathode are fundamental because permit the electron flow from the anode to the cathode across an external load and in the same time triggers the cations migration from the anolyte to the cathode. Instead the short circuit is composed just by a unique electrode who works as an hybrid between anode and cathode, making both the oxidation of the organic matter and the reduction of the oxygen in the same compound. This system is characterised by the same potential in all the system. While, the open circuit is characterized just by the cations exchange capacity of the material that compose the cell. Strictly correlated with the electrochemical reactions showed in Figure 1 there are the results in Table 2 that explain how the electrochemical forces and reactions involved in the system can affect the pH at the cathode and the working potential of the cell. These two data are very important in a view of nutrient recovery and wastewater treatment because the high cathodic pH can increase the salt precipitation and a more positive working potential can help the system in the exchange electrons with the atmosphere.

Table 2 - Measurements of wastewater pH, cathodic pH and working potential

	Wastewater pH	Cathodic pH	Working potential (mV)
Microbial Recycling Cell	8.07 ± 0.2	9.1 ± 0.6	-165 ± 15
Short Circuit Cell	7.83 ± 0.3	6.1 ± 0.4	-444 ± 45
Control Cell	8.05 ± 0.2	7.0 ± 0.3	-534 ± 42

Table 2 shows strongly the differences that we have between the microbial recycling cell vs the short circuit and the open circuit because the close circuit can increase the electrochemical reaction in the system. In particular if we have the two electrodes who work separately the system work properly and well so we can maximise both the oxidation and the reduction and the separation of reactions permit a more positive working potential of the system and a more high pH at the cathode that increase the salt precipitation.

The current density trends, reported in Figure 2, show that during the first acclimation period (A1), the anolyte was totally composed by swine manure as inoculum.

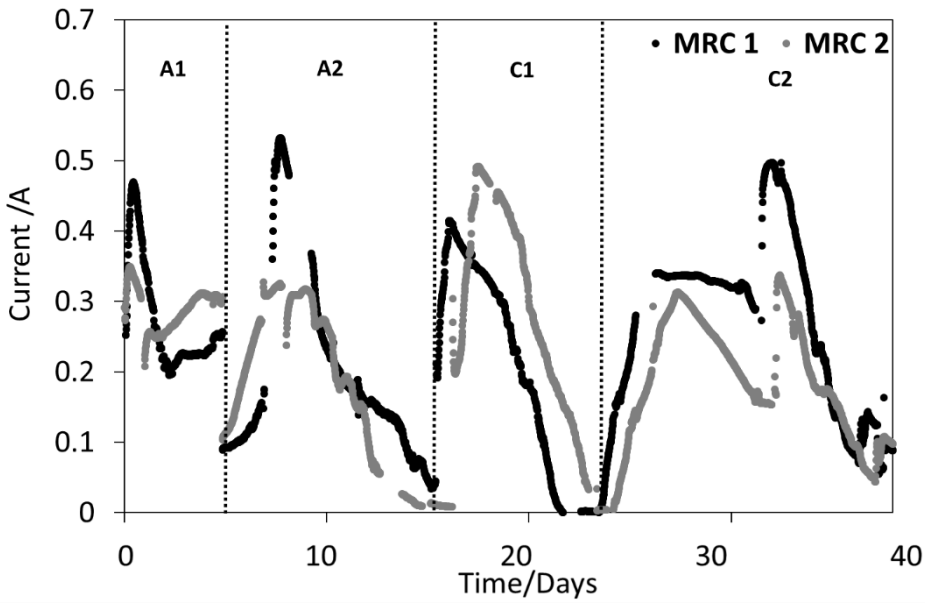

Figure 2 - Current density trends during 40 days observation of the MRCs.

After an initial and expected delay, the systems started producing current, up to a maximum of about 100 mA m-2 in the second acclimation period (A2), during which half of the anolyte was substituted by the synthetic medium. After the acclimation phase, the real operational period (C1-2) began, characterized by the whole presence of the synthetic medium as the anolyte and sodium acetate (7.7 g L^{-1}) as the standard feed for bacteria. The systems produced less current compared to the previous cycle (with a maximum of about 70 mA m^{-2}), and this might be due to the sudden replacement of the medium of the bacteria colonizing the electrodes which still needed to adapt to the new environment. Moreover, during cycle C2 the current production was comparable to the last cycle of acclimation. These results are also confirmed in Figure 3 were power curves (-a) and anodic polarizations (-b) are respectly showed.

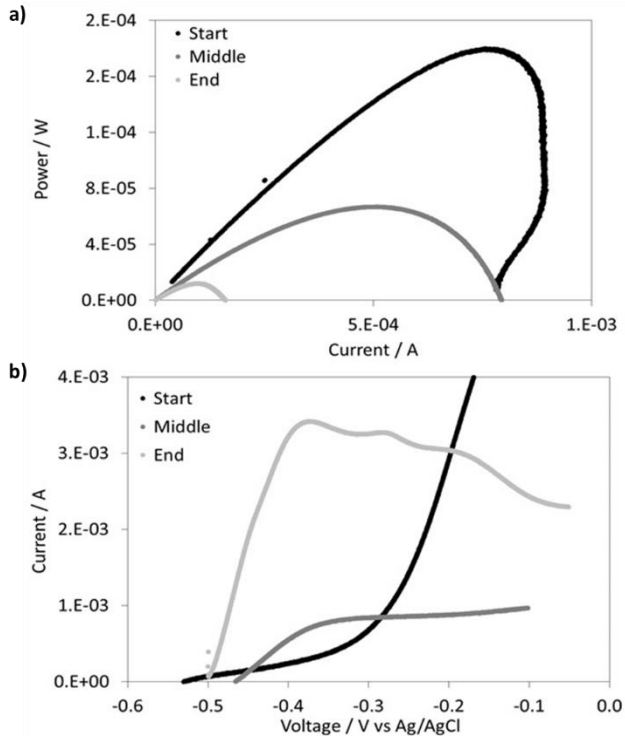

Figure 3 - Electrochemical characterisations during the experiment: power curves (a) and anodic polarizations (b)

The power curves show that the power of the systems decrease during the operation time to due the increasing of the internal resistance of the system by the salt deposition and biofouling phenomena.

Whereas, the Figure 3b indicate an increase of the bacteria activity at the anode that demonstrate a perfect adaptation of the biofilm at the medium changing and confirm the increasing of the performances in the last cycle (C2).

3.2 - Effects of the MRCs on the wastewater treatment and nutrients recovery

Figure 4 shows the removal of macro- and micro-nutrients over 40 days of operation time. In this figure is interesting the comparison between MRC, SCC and CC systems, where is possible to observe that the electrochemical forces involved in the wastewater treatment processes play an important role.

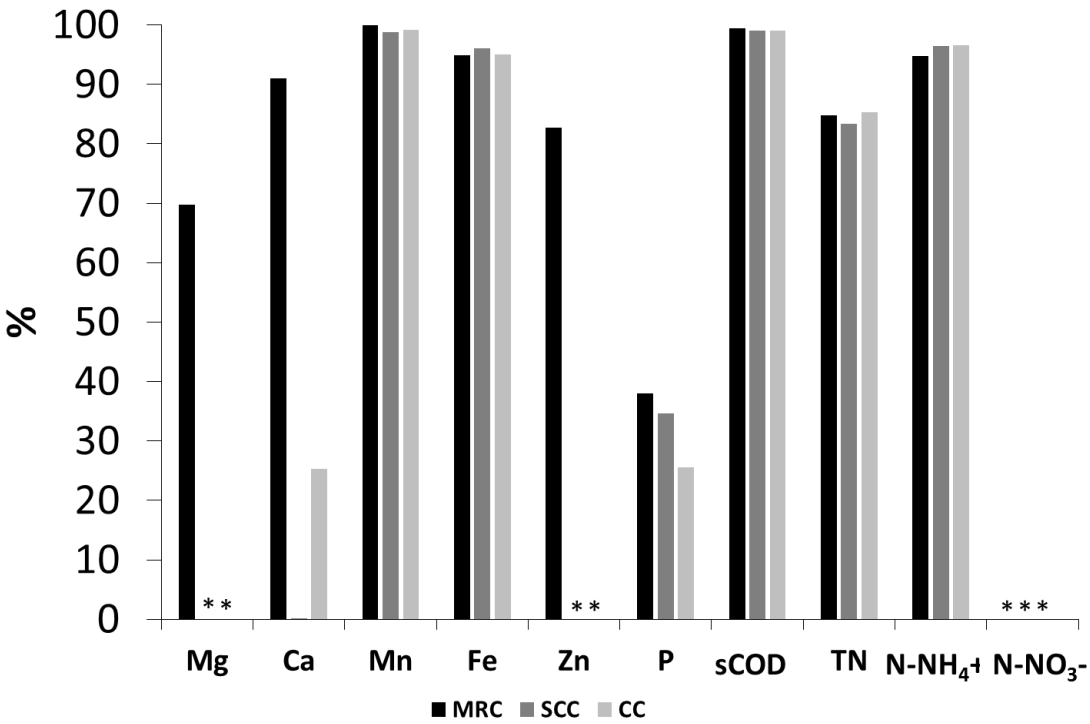

Figure 4 - Percentage removal efficiency of the soluble fraction of the main nutrients from the bulk liquid phase during 40 days (* under detection limits).

Figure 4 proves also an interesting different between the organic and inorganic forms of macro- and micro-nutrients in a view of wastewater treatments, as also Erable et al. explains in his study (Erable et al., 2011). It is possible to observe that the removal of organic carbon (COD), total nitrogen (TN) and NH_4^+ are similar in all the systems but due to different reactions. This happened because in the MRC systems the oxidation of the organic matter happened in the

anodic compound causing the electrons flow from the anode to the cathode and the consequently cations migration, so it is recorded a removal in organic carbon and a decreasing of the level of the total nitrogen by the biological oxidation. Moreover, due to the high cathodic pH there is a loosing of NH_4+ in NH_3 emissions. In the other two systems, the situation is different both for organic carbon and for nitrogen. In the SCC system, the COD decrease with the same reaction of the MRCs without the starting of the cations migration to the cathode because the system is composed just by one electrode. Focusing on the nitrogen form, the situation is quite different because we have just the denitrification of the nitrogen forms. Instead, the situation in the CC system is very different because the anaerobic bacteria decrease both the COD and TN and they produce GHGs emissions because they do not have an easily electron acceptor.

In other hand, we have a strongly differences for the inorganic elements because thanks to the differences of working potential that we have between anode and cathode in the MRC systems and the cations migration triggered by the electrons flow there is an important removal due to the electrochemical forces involved in the scenario compere the other two systems.

The same situation is confirmed in Figure 5 that shows the amounts of nutrients (measured as extracts in milli-Q water) recovered on electro-active biochar used as cathode along 40 days of operation. For all the elements is possible to observe at list an increasing of nutrients recovery in the electro-active biochar of 10% in MRC confirming as said before, accept of the NH4+ due to the reaction explained before.

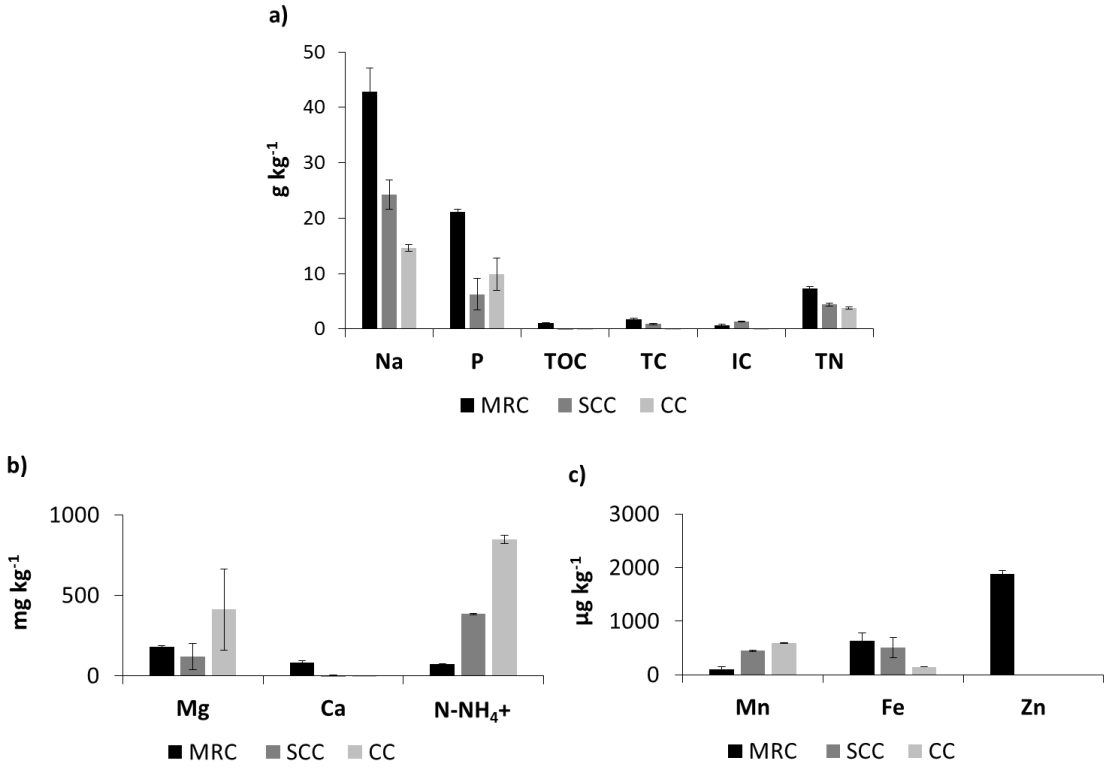

Figure 5 - Amounts of nutrients (measured as extracts in milli-Q water after 30 minutes of mixing) recovered on electro-active biochar used as cathode along 40 days of operation: macronutrients (a), mesonutriens (b) and micronutrients (c).

3.3 – The importance of two electrodes and the connection of different forces

All the result trends converge in one direction, if we want to maximize the wastewater treatment and the nutrients recovery, we need two different electrodes (anode and cathode) with a different potential between them.

The microbial recycling cell is characterised by the structural design of the system and the characteristics of the material as the other two system. The interesting performance in wastewater treatment and nutrients recovery is obtained thanks due to the adsorption materials by the presence of the active sites of the electro-active biochar and its cations exchange capacity, as the CC system. The MRC system is also powered by the chimney effect and evaporation as the SCC system. This expression is referred to the capacity of pyrolyzed Arundo Donax stems to provide an equilibrium between two processes: water evaporation and water infiltration toward their internal cavity. To better understand, we can imagine the

reactor solution being hydrodynamically forced toward the internal cathodic cavity. While water is infiltrating, its contemporary evaporation causes an increasing concentration of solutes and water density. As consequence, the infiltration flow slows down, salts precipitation occurs into the internal structure (Goglio et al., 2019). The capillary action movement of water upwards in vascular tissue that characterizes this type of plants is strictly linked to this mechanism and plays a major role. Moreover, the salts deposition should interest also the air-exposed part of biochar reeds.

Moreover, in the electrochemical view, the MRC system is the most complete system because in one set-up encloses the reactions of all the bioelectrochemical systems. As describe in the paragraph 3.1, the MRC system is more complex, but the presence of the 2 electrodes maximize the electrons flow and the cations migration. This two electrodes set-up increase also the cathodic pH that helps in the salt deposition phenomena. These electrochemical reactions joined with the structural design of the system and the characteristics of the material definitely performed the nutrients removal/recovery.

3.4 Microbial communities inhabiting the electrodes

Sequencing of 16S rRNA genes performed of the biofilm grown on the electrodes in the different systems showed a clear differentiation of the microbial communities in relation to the experimental setup as well as to the type of electrode (Figure 6).

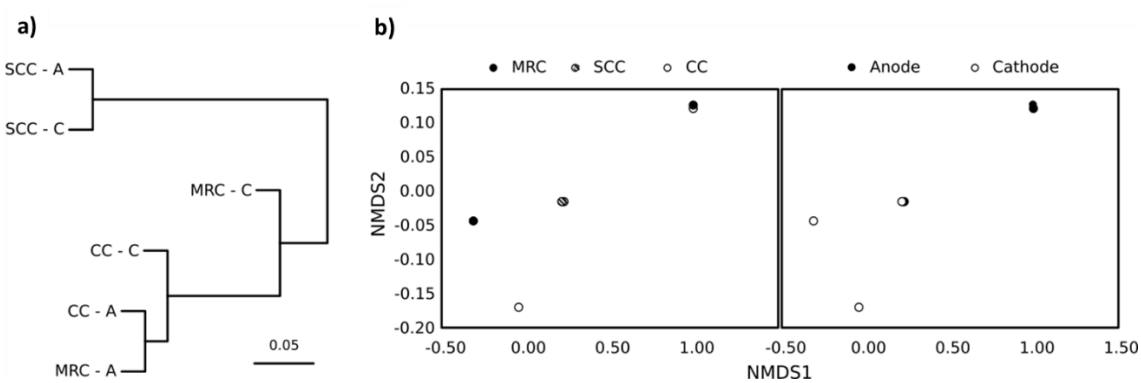

Figure 6 - Comparison between the microbial communities developed in cathodes and anodes of microbial recycling cells (MRC-C and MRC-A), short circuit cells (SCC-C and SCC-A) and control cell (CC-C and CC-A) by means of Unweighted Pair Group Method with Arithmetic mean (UPGMA, a) and non-metric multidimensional scaling (NMDS, b).

UPGMA showed that the anodic compartment was a main driver in the development of specific populations likely selected by the physico-chemical composition of the anodic matrix (Figure 6a). NMDS confirmed that the type of electrode was the main driver in the enrichment of specific populations (Figure 6b). The communities in SCC were very similar, probably due to the fact that the electrode was essentially the same and the working potential was identical in the whole system.

The MRC system enriched a higher number of species (864) with respect to SCC (643) and CC (730) (Figure 7a, 7b and 7c).

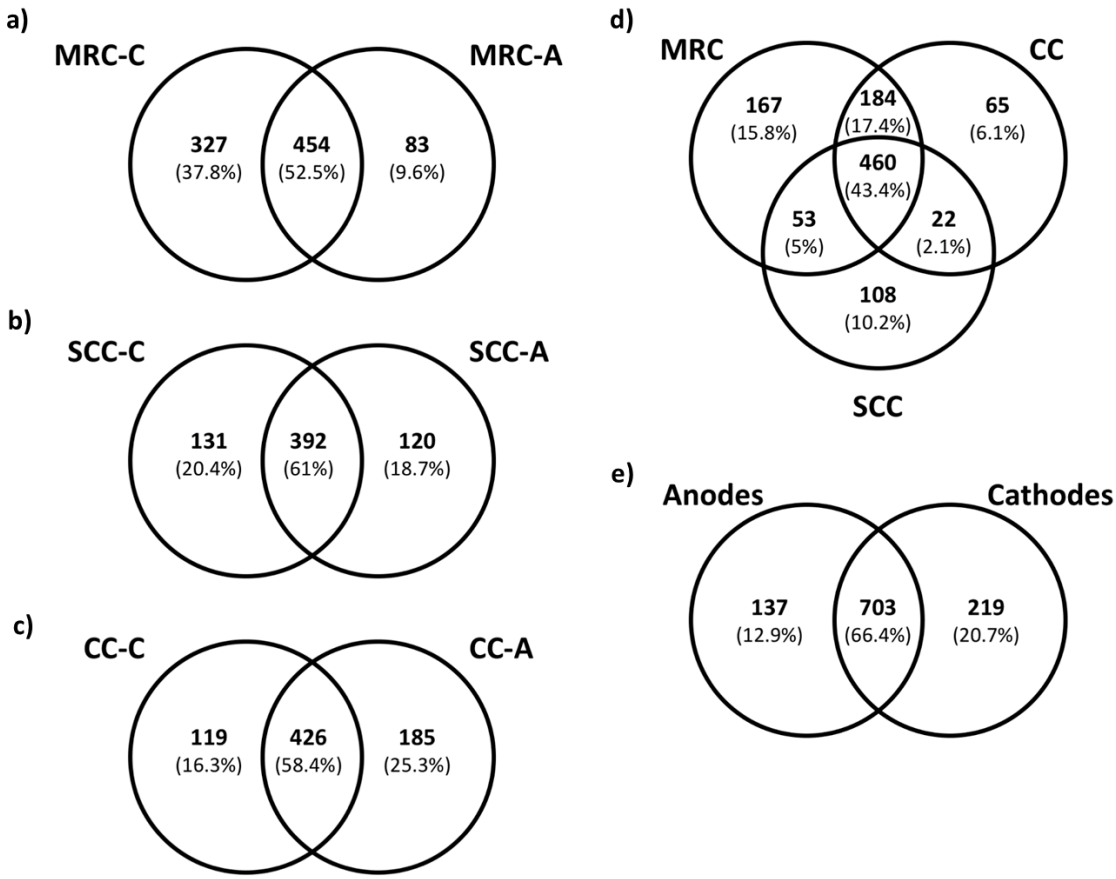

Figure 7 - Shared microbiome performed between each compartment of the different systems (a, b, c), between different systems (d) and between different electrode types (e).

The majority of MRC species, accounting for 52.5% of the total, was shared between cathode and anode. 37.8% of the species were exclusively enriched on the cathode, while 9.6% was uniquely found on the anode. In SCC and CC, this sharp difference between anodes and

cathodes was not present, indicating a major role of fully flowing electricity in the system. Overall, the majority of species was shared between systems (Figure 7d) and between electrode type (Figure 7e). However, a higher number of exclusive species was retrieved in MRC and in cathodes. These outcomes show that e-biochar represents a favourable environment for the development of an electoactive biofilm resistant to extreme alkaline conditions.

In all systems, three dominant phyla could be identified: Proteobacteria, Firmicutes and Bacteroidetes (Figure 8a).

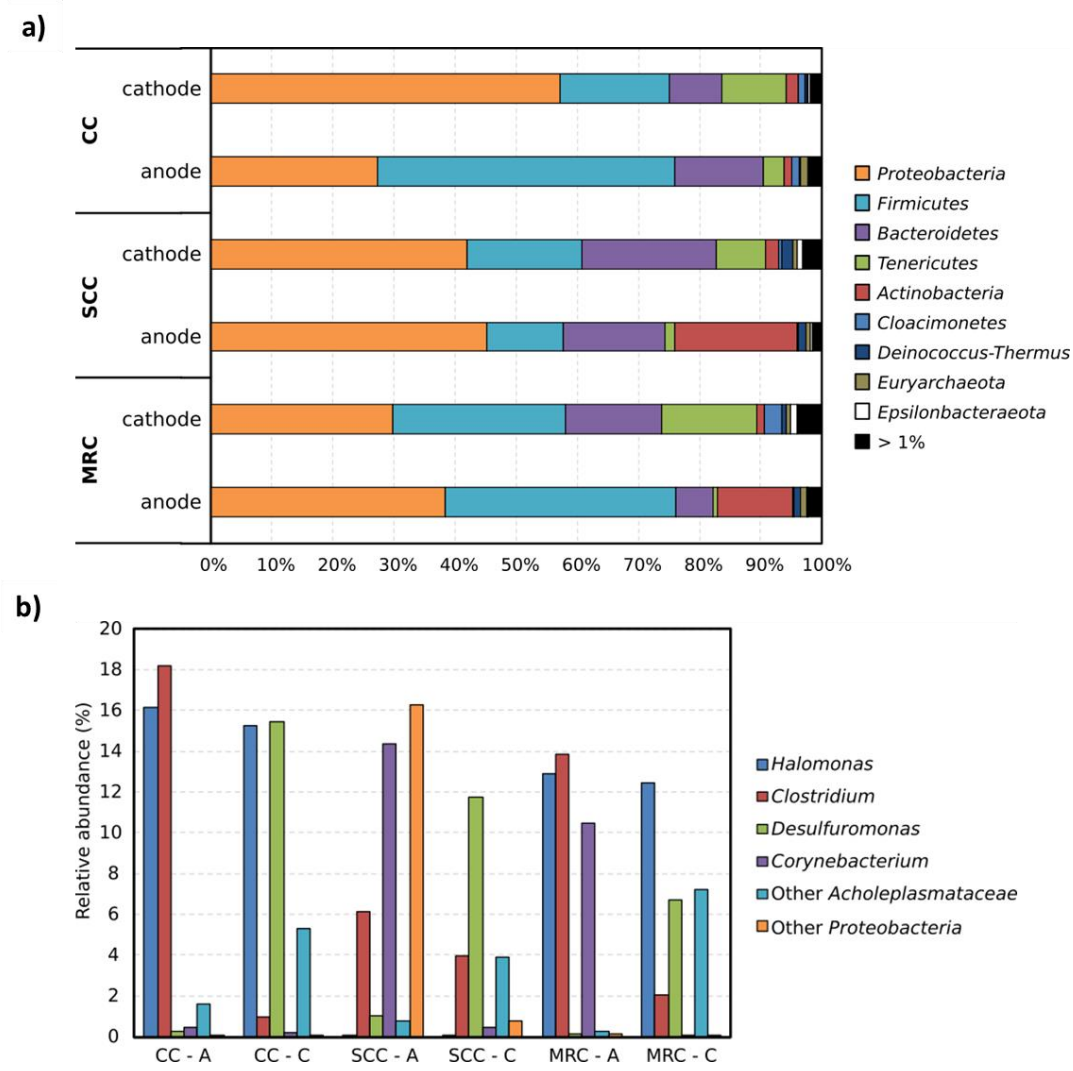

Figure 8 – Microbial composition in cathodes and anodes of the different systems analysed at phylum (a) and genus (b) level.

These phyla have been reported to include several exoelectrogenic species, playing a role in different BES (Almatouq et al., 2020; Rago et al., 2018). In anodes with flowing current (MRC and SCC), the proportion of Actinobacteria increased, due to the enrichment of members of the genus Corynebacterium . In bioelectochemical denitrification systems, Actinobacteria have been reported to be one of the main taxa responsible for denitrification (Liu et al., 2015; Chen et al., 2016). Specifically, Corynebacterium glutammicum is used for the industrial production of aminoacids, organic acids, diamines and biofuels (Vassilev et al., 2017). In a BES, this species was shown to couple anodic respiration to the oxidation of NADH, stabilyzing its redox state and promoting anaerobic production of lysin (Xafenias et al., 2017).

Tenericutes were enriched at the cathodic compartment in all systems, given by uncultered members of the family Acholeplasmataceae (Fiure 8a and 8b). Members of this family have been previously found on the cathodic compartment in different BES (Rago et al., 2018). Several members of the family Acholeplasmataceae are not cultivable in axenic cultures and are usually associated to animal fluids, which is compatible with the inoculum used in this study (Rosenberg et al., 2014). Their association with cathodes has never been elucidated, but previous experiments indicated a possible external electron transfer activity (Xiao et al., 2020).

In both cathodes and anodes of MRC and CC, members of the genus Halmonas accounted for more of 12% of the total community (Figure 8b).This genus include halophilic species (Mata et al., 2001), and in MRC-C were likely promoted by salt deposition and high pH values. On the other hand, members of the genus Halomonas have been reported to metabolise acetate with anode as electron acceptor has been (Erable et al., 2009).

In all anodes independently form the presence of an electric current, the genus Clostridium was enriched, probably due to affinity to the anodic composition, as previously showed by several authors (reviewed by Lovley et al., 2017). In all cathodes, the genus Desulfuromonas was co-dominant with Halomonas and uncultured members of the family Acholeplasmataceae. In MRC-C, the relative abundance of Halomonas and Desulfuromonas decreased, due to the increase of the total number of species, as seen in Figure 7a. Sulfur-reducing Desulfuromonas are typically found in bioanodes, where they couple anodic respiration to the oxidation of sulfur to sulfate (Zhang et al., 2014). In this study, however its high abundance at the cathodic compartment in all systems might suggest a more general affinity for e-biochar.

4. Conclusions

This study can help to maximize the wastewater treatments and nutrients recovery with the idea of using of two electrodes systems. The increase of the electrochemical forces generated by anodic oxidations, the local increase of cathodic pH driven by incomplete oxygen reduction reaction and local water evaporation were the main drivers towards cations migration to the cathode and to inorganic salts or organic matter deposition join to the chimney effect and cations exchange capacity of the e-biochar. Moreover, the use of low-cost and biocompatible material, as e-biochar, which could be directly recycled as base for organic-mineral fertilizers and soil conditioners, increase the possibility of the scaling-up of this technology; starting from organic scraps obtaining resource, preserving the soil and increase the possibility of interactions with soil microbiome, rhizosphere and plants' roots.

Acknowledgements

This work was financed by the SIR 2014 Grant (PROJECT RBSI14JKU3), Italian Ministry of University and Research (MIUR) by the Research Fund for the Italian Electrical System in compliance with the Decree of March, 19th 2009.

References

Almatouq, A., Babatunde, A.O., Khajah, M., Webster, G., Alfodari, M., 2020. Microbial community structure of anode electrodes in microbial fuel cells and microbial electrolysis cells. J. Water Process Eng. 34, 101140. doi:10.1016/j.jwpe.2020.101140

Bybee, S.M., Bracken-Grissom, H., Haynes, B.D., Hermansen, R.A., Byers, R.L., Clement, M.J., Udall, J.A., Wilcox, E.R., Crandall, K.A., 2011. Targeted Amplicon Sequencing (TAS): A scalable Next-Gen Approach to multilocus, multitaxa phylogenetics. Genome Biol. Evol. 3, 1312–1323. doi:10.1093/gbe/evr106

Caporaso, J.G., Kuczynski, J., Stombaugh, J., Bittinger, K., Bushman, F.D., Costello, E.K., Fierer, N., Peña, A.G., Goodrich, J.K., Gordon, J.I., Huttley, G.A., Kelley, S.T., Knights, D., Koenig, J.E., Ley, R.E., Lozupone, C.A., McDonald, D., Muegge, B.D., Pirrung, M., Reeder, J., Sevinsky, J.R., Turnbaugh, P.J., Walters, W.A., Widmann, J., Yatsunenko, T., Zaneveld, J., Knight, R., 2010. QIIME allows analysis of high-throughput community sequencing data, Nat. Methods 7, 335–336. doi:10.1038/nmeth.f.303

Chen, X., Cui, Z., Fan, M., Vitousek, P., Zhao, M., Ma, W., Wang, Zhenlin, Zhang, Weijian, Yan, X., Yang, J., Deng, X., Gao, Q., Zhang, Q., Guo, S., Ren, J., Li, S., Ye, Y., Wang, Zhaohui, Huang, J., Tang, Q., Sun, Y., Peng, X., Zhang, J., He, M., Zhu, Y., Xue, J., Wang, G., Wu, Liang, An, N., Wu, Liangquan, Ma, L., Zhang, Weifeng, Zhang, F., 2014. Producing more grain with lower environmental costs. Nature 514, 486–489. doi:10.1038/nature13609

Chen, D., Wei, L., Zou, Z., Yang, K., & Wang, H., 2016. Bacterial communities in a novel three-dimensional bioelectrochemical denitrification system: the effects of pH. Appl. Microbiol. Biotechnol. 100(15), 6805-6813. doi:10.1007/s00253-016-7499-3

Cheng, S., Liu, H., Logan, B.E., 2006. Increased power generation in a continuous flow MFC with advective flow through the porous anode and reduced electrode spacing. Environ. Sci. Technol. 40, 2426–2432. doi:10.1021/es051652w

Cruz Viggi, C., Simonetti, S., Palma, E., Pagliaccia, P., Braguglia, C., Fazi, S., Baronti, S., Navarra, M.A., Pettiti, I., Koch, C., Harnisch, F., Aulenta, F., 2017. Enhancing methane production from food waste fermentate using biochar: the added value of electrochemical testing in pre-selecting the most effective type of biochar. Biotechnol. Biofuels 10, 303. doi:10.1186/s13068-017-0994-7

Dominguez-Benetton, X., Varia, J.C., Pozo, G., Modin, O., Ter Heijne, A., Fransaer, J., Rabaey, K., 2018. Metal recovery by microbial electro-metallurgy. Prog. Mater. Sci. 94, 435–461. doi:10.1016/J.PMATSCI.2018.01.007

Edgar, R.C., 2010. Search and clustering orders of magnitude faster than blast. Bioinformatics 26(19), 2460-2461. doi:10.1093/bioinformatics/btq461

Erable, B., Roncato, M. A., Achouak, W., Bergel, A., 2009. Sampling natural biofilms: a new route to build efficient microbial anodes. Environ. Sci. Technol. 43(9), 3194-3199. doi:10.1021/es803549v

Faith, D.P., Minchin, P.R., Belbin, L., 1987. Compositional dissimilarity as a robust measure of ecological distance. Vegetatio 69, 57-68. doi:10.1007/BF00038687

Erable, B., Etcheverry, L., Bergel, A., 2011a. From microbial fuel cell (MFC) to microbial electrochemical snorkel (MES): maximizing chemical oxygen demand (COD) removal from wastewater. Biofouling 27, 319–26. doi:10.1080/08927014.2011.564615

Franks, A.E., Nevin, K.P., 2010. Microbial Fuel Cells, A Current Review. Energies 3, 899–919. doi:10.3390/en3050899

Goglio, A., Marzorati, S., Rago, L., Pant, D., Cristiani, P., Schievano, A., 2019. Microbial recycling cells: First steps into a new type of microbial electrochemical technologies, aimed at recovering nutrients from wastewater. Bioresour. Technol. 277, 117–127. doi:10.1016/J.BIORTECH.2019.01.039

Green, S.J., Venkatramanan, R., Naqib, A., 2015. Deconstructing the polymerase chain reaction: Understanding and correcting bias associated with primer degeneracies and primer-template mismatches. PLoS One. 10, e0128122. doi:10.1371/journal.pone.0128122

Guerrini, E., Grattieri, M., Faggianelli, A., Cristiani, P., Trasatti, S., Guerrini, Edoardo; grattieri, matteo; F., 2015. PTFE effect on the electrocatalysis of the oxygen reduction reaction in membraneless microbial fuel cells. Bioelectrochemistry 106, 240–247. doi:10.1016/j.bioelechem.2015.05.008

Hamady, M., Knight, R., 2009. Microbial community profiling for human microbiome projects: tools, techniques and challenges. Genome Res. 19, 1141–1152. doi:10.1101/gr.085464.108

Hoareau, M., Erable, B., Bergel, A., 2019. Microbial electrochemical snorkels (MESs): A budding technology for multiple applications. A mini review. Electrochem. commun. 104, 106473. doi:10.1016/J.ELECOM.2019.05.022

Huggins, T.M., Pietron, J.J., Wang, H., Ren, Z.J., Biffinger, J.C., 2015. Graphitic biochar as a cathode electrocatalyst support for microbial fuel cells. Bioresour. Technol. 195, 147–153. doi:10.1016/j.biortech.2015.06.012

Ioannidou, O., Zabaniotou, A., 2007. Agricultural residues as precursors for activated carbon production-A review. Renew. Sustain. Energy Rev. doi:10.1016/j.rser.2006.03.013

Jung, R.K., Cheng, S., Oh, S.E., Logan, B.E., 2007. Power generation using different cation, anion, and ultrafiltration membranes in microbial fuel cells. Environ. Sci. Technol. 41, 1004–1009. doi:10.1021/es062202m

Katuri, K.P., Kalathil, S., Ragab, A., Bian, B., Alqahtani, M.F., Pant, D., Saikaly, P.E., 2018. Dual-Function Electrocatalytic and Macroporous Hollow-Fiber Cathode for Converting Waste Streams to Valuable Resources Using Microbial Electrochemical Systems. Adv. Mater. 30, e1707072. doi:10.1002/adma.201707072

Kumar, G.G., Sarathi, V.G.S., Nahm, K.S., 2013. Recent advances and challenges in the anode architecture and their modifications for the applications of microbial fuel cells. Biosens. Bioelectron. 43, 461–475. doi:10.1016/J.BIOS.2012.12.048

Liu, C.S., Zhao, D.F., Yan, L.H., Wang, A.J., Gu, Y.Y., Lee, D.J., 2015. Elemental sulfur formation and nitrogen removal from wastewaters by autotrophic denitrifiers and anammox bacteria. Bioresour. Technol. 191, 332–336. doi:10.1016/j.biortech.2015.05.027

Lovley, D.R., 2017. Syntrophy goes electric: Direct interspecies electron transfer. Annu. Rev. Microbiol. 71, 643-664. doi:10.1146/annurev-micro-030117-020420

Ma, M., You, S., Wang, W., Liu, G., Qi, D., Chen, X., Qu, J., Ren, N., 2016. Biomass-derived porous Fe3C/tungsten carbide/graphitic carbon nanocomposite for efficient electrocatalysis of oxygen reduction. ACS Appl. Mater. Interfaces 8, 32307–32316. doi:10.1021/acsami.6b10804

Marzorati, S., Goglio, A., Fest-Santini, S., Mombelli, D., Villa, F., Cristiani, P., Schievano, A., 2018. Air-breathing bio-cathodes based on electro-active biochar from pyrolysis of Giant Cane stalks. Int. J. Hydrogen Energy 1–12. doi:10.1016/j.ijhydene.2018.07.167

Marzorati, Stefania, Schievano, A., Colombo, A., Lucchini, G., Cristiani, P., 2018a. Ligno-cellulosic materials as air-water separators in low-tech microbial fuel cells for nutrients recovery. doi:10.1016/j.jclepro.2017.09.142

Mata, J.A., Martínez-Cánovas, J., Quesada, E., Béjar, V., 2002. A detailed phenotypic characterisation of the type strains of Halomonas species. Syst. Appl. Microbiol. 25(3), 360-375. doi:10.1078/0723-2020-00122

Metodi di Analisi dei Fertilizzanti, n.d. , in: Gazzetta Ufficiale Del 26/01/01 n.21, DM 21/12/00, Suppl. n.8.

Oksanen, J., Blanchet, F. G., Kindt, R., Legendre, P., Minchin, P. R., O'hara, R. B., et al., 2013. Package 'vegan'. Community ecology package, version, 2(9), 1-295. See https://cran.r-project.org/web/packages/vegan/index.html.

Parameswaran, P., Torres, C.I., Lee, H.-S., Krajmalnik-Brown, R., Rittmann, B.E., 2009. Syntrophic interactions among anode respiring bacteria (ARB) and Non-ARB in a biofilm anode: electron balances. Biotechnol. Bioeng. 103, 513–523. doi:10.1002/bit.22267

Pasternak, G., Greenman, J., Ieropoulos, I., 2015. Comprehensive Study on Ceramic Membranes for Low-Cost Microbial Fuel Cells. ChemSusChem 88–96. doi:10.1002/cssc.201501320

Quast, C., Pruesse, E., Yilmaz, P., Gerken, J., Schweer, T., Yarza, P., Peplies, J., Glockner, F.O., 2013. The SILVA ribosomal RNA gene database project: improved data processing and web-based tools, Nucleic Acids Res. 41, 590–596. doi:10.1093/nar/gks1219

Rago, L., Cristiani, P., Villa, F., Zecchin, S., Colombo, A., Cavalca, L., Schievano, A., 2017. Influences of dissolved oxygen concentration on biocathodic microbial communities in microbial fuel cells. Bioelectrochemistry 116, 39–51. doi:10.1016/j.bioelechem.2017.04.001

Rago, L., Zecchin, S., Marzorati, S., Goglio, A., Cavalca, L., Cristiani, P., Schievano, A., 2018. A study of microbial communities on terracotta separator and on biocathode of air breathing microbial fuel cells. Bioelectrochemistry 120. doi:10.1016/j.bioelechem.2017.11.005

Rismani-Yazdi, H., Carver, S.M., Christy, A.D., Tuovinen, O.H., 2008. Cathodic limitations in microbial fuel cells: An overview. J. Power Sources 180, 683–694. doi:10.1016/j.jpowsour.2008.02.074

Rosenberg, E., DeLong, E. F., Lory, S., Stackebrandt, E., Thompson, F. (Eds.). 2014. The prokaryotes: firmicutes and tenericutes. Berlin Heidelberg: Springer.

Rossi, R., Yang, W., Zikmund, E., Pant, D., Logan, B.E., 2018. In situ biofilm removal from air cathodes in microbial fuel cells treating domestic wastewater. Bioresour. Technol. 265, 200–206. doi:10.1016/J.BIORTECH.2018.06.008

Santoro, C., Agrios, A., Pasaogullari, U., Li, B., 2011. Effects of gas diffusion layer (GDL) and micro porous layer (MPL) on cathode performance in microbial fuel cells (MFCs). Int. J. Hydrogen Energy 36, 13096–13104. doi:10.1016/J.IJHYDENE.2011.07.030

Santoro, C., Arbizzani, C., Erable, B., Ieropoulos, I., 2017. Microbial fuel cells: From fundamentals to applications. A review. J. Power Sources. doi:10.1016/j.jpowsour.2017.03.109

Santoro, C., Lei, Y., Li, B., Cristiani, P., 2012. Power generation from wastewater using single chamber microbial fuel cells (MFCs) with platinum-free cathodes and pre-colonized anodes. Biochem. Eng. J. 62, 8–16. doi:10.1016/J.BEJ.2011.12.006

Schievano, A., Berenguer, R., Goglio, A., Bocchi, S., Marzorati, S., Rago, L., Louro, R.O., Paquete, C.M., Esteve-Núñez, A., 2019. Electroactive Biochar for Large-Scale Environmental

Applications of Microbial Electrochemistry. ACS Sustain. Chem. Eng. doi:10.1021/acssuschemeng.9b04229

Sneath, P.H.A., Sokal, R.R., 1973. Numerical Taxonomy. The Principles and Practice of Numerical Classification, Freeman, W.H., and Company, San Francisco, USA.

Terayama, Y., Haji, T., Furukawa, S., Nomura, M., Nishihara, M., Lyth, S.M., Sone, Y., Matsumoto, H., 2018. Carbon black / PTFE composite hydrophobic gas diffusion layers for a water-absorbing porous electrolyte electrolysis cell. Int. J. Hydrogen Energy 43, 2018–2025. doi:10.1016/J.IJHYDENE.2017.12.045

Vassilev, I., Gießelmann, G., Schwechheimer, S. K., Wittmann, C., Virdis, B., Krömer, J. O., 2018. Anodic electro-fermentation: Anaerobic production of L-Lysine by recombinant Corynebacterium glutamicum. Biotechnol. Bioeng. 115(6), 1499-1508. doi: 10.1002/bit.26562

Wei, J., Liang, P., Huang, X., 2011. Recent progress in electrodes for microbial fuel cells. Bioresour. Technol. 102, 9335–9344. doi:10.1016/J.BIORTECH.2011.07.019

Wu, Y., Jing, X., Gao, C., Huang, Q., Cai, P., 2018. Recent advances in microbial electrochemical system for soil bioremediation. Chemosphere 211, 156–163. doi:10.1016/J.CHEMOSPHERE.2018.07.089

Xafenias, N., Kmezik, C., Mapelli, V., 2017. Enhancement of anaerobic lysine production in Corynebacterium glutamicum electrofermentations. Bioelectrochemistry, 117,40–47. doi: 10.1016/j.bioelechem.2017.06.001

Xiao, E., Zhou, Y., Xu, D., Lu, R., Chen, Y., Zhou, Q., Wu, Z., 2020. The physiological response of Arundo donax and characteristics of anodic bacterial community in BE-CW systems: Effects of the applied voltage. Chem. Eng. J. 380, 122604. doi:10.1016/j.cej.2019.122604

Yan, Weifu, Xiao, Y., Yan, Weida, Ding, R., Wang, S., Zhao, F., 2019. The effect of bioelectrochemical systems on antibiotics removal and antibiotic resistance genes: A review. Chem. Eng. J. 358, 1421–1437. doi:10.1016/J.CEJ.2018.10.128

You, J., Santoro, C., Greenman, J., Melhuish, C., Cristiani, P., Li, B., Ieropoulos, I., 2014. Micro-porous layer (MPL)-based anode for microbial fuel cells. Int. J. Hydrogen Energy 39, 21811–21818. doi:10.1016/j.ijhydene.2014.07.136

Yuan, Y., Liu, T., Fu, P., Tang, J., Zhou, S., 2015. Conversion of sewage sludge into high-performance bifunctional electrode materials for microbial energy harvesting. J. Mater. Chem. A 3, 8475–8482. doi:10.1039/c5ta00458f

Zhang, T., Bain, T. S., Barlett, M. A., Dar, S. A., Snoeyenbos-West, O. L., Nevin, K. P., Lovley, D. R., 2014. Sulfur oxidation to sulfate coupled with electron transfer to electrodes by Desulfuromonas strain TZ1. Microbiology 160(1), 123-129. doi:10.1099/mic.0.069930-0

Zhang, J., Kobert, K., Flouri, T., Stamatakis, A., 2014. PEAR: a fast and accurate Illumina Paired-End reAd merger. Bioinformatics 30, 614–620. doi:10.1093/bioinformatics/btt593

Zhou, M., Chi, M., Luo, J., He, H., Jin, T., 2011. An overview of electrode materials in microbial fuel cells. J. Power Sources 196, 4427–4435. doi:10.1016/J.JPOWSOUR.2011.01.012

Chapter 7 - Improving microbial oxidation and nutrients recovery from agro-industrial wastewater in constructed wetlands based on electro-active biochar

Marco Dal Zoppo[a], Andrea Goglio[a], Amanda Prado de Nicolás[b], Carlos Manchón Vállegas[b], Cristina Ortiz Martín[b], Colin Wardman[c], Abraham Esteve Núñez[b,c], Andrea Schievano[a*]

a e-BioCenter, Department of Environmental Science and Policy, University of Milan, Via Celoria 2, 20133 Milan, Italy

b Department of Chemical Engineering, Universidad de Alcalá, Alcalá de Henares, Madrid, Spain

c IMDEA WATER, Parque Tecnológico de la Universidad de Alcalá, Alcalá de Henares, Madrid, Spain

* Corresponding author: andrea.schievano@unimi.it

Abstract

The concept of bioelectrochemically-active constructed wetlands (CW) (also called electrochemical biofilter) have already shown its potentialities for re-using wastewaters in delocalized and small-scale facilities, while minimizing the use of auxiliary energy. Besides the goal of oxidizing organic loadings, the recovery of nutrients (N, P, K, Ca, Mg, etc.) is an increasingly important aim, especially in the farming and food-industry sectors, to control nutrients cycles disruption in ecosystems and to implement circular economy approaches. In this study, we propose the implementation of an innovative approach to improve the electrochemical biofilter performances in organic loading oxidation and to recover nutrients. We tested these novel air biochar steam cathodes to produce microbial recycling cells (MRCs), i.e. BESs fabricated with low-cost, biocompatible and fully-recyclable materials. Mass transport due to electrochemical potential gradients (generated by microbial electro-activity) and salts deposition on the porous surfaces of the biochar stems should deliver a nutrients-enriched biochar, re-usable in agriculture as a soil conditioner. The results showed a relevant accumulation of nutrients and the presence of the air biochar stems cathode allowed higher performances in COD degradation rates (550 mg COD/L/day) compare to the electrochemical biofilter (450 mg COD/L/day).

Keywords

Bioelectrochemical systems, microbial recycling cells, electrochemical biofilter, nutrients recovery, agro-industrial wastewater treatment

1. Introduction

In the meantime, several regions around the world have seen the development of huge urban areas with high population densities. Consequently, a giant volume of wastewater is daily produced and it will become increasingly difficult to manage [1]. The overall result is a flow of nutrients convoyed to the environment with several negative impacts on soils, water bodies, atmosphere and in some cases, human health [2].

Promoting a sustainable usage of natural resources is now a priority to provide a solid future for our next generations [3]. This purpose should be applied to every single human productive sector, from agriculture to industry. Under this perspective, it is rising a global acknowledgement about a necessary progressive conversion of the current linear economy toward a more circular system [4].

Indeed, traditional wastewater treatment technologies applied to different types of industrial and urban wastewater or sewage effluents are decreasing the impact on the environment [5]. However, a high quantity of external input of energy and high economic costs are the major drawbacks. Several alternatives have been proposed for secondary and tertiary treatment. Constructed wetlands became a worldwide used system, but it is not yet the final solution duo to their area footprint (much larger the traditional systems) [6].

Thus, development of new technologies able to reduce surface-area requirements of constructed wetlands and carbon/energy footprint of traditional sewage treatment plants represent some of the most ambitious challenges pursued by many research programs [7][8][9][10]. Considering the goals achieved by BES during last ten years, the idea of combine microbial electrochemical technologies (METs) with constructed wetland could be a profitable development direction [11][12]. About that, a system of this type has already shown its potentialities as new concept for biofilters operating with a low use of auxiliary energy [13]. Proposed under the name of microbial electrochemical-based CW (METland), it has marked an improvement in terms of biodegradation rates in comparison with similar CWs and also a decreased electron availability for biomass build-up and methane production [14][15][16][17].

This system rely on the activity of electroactive bacteria (AEB) communities that drive the process of biodegradation thanks to the presence of conductive materials [18]. Starting from this mechanism, they realized reactors able to exploit a phenomenon called "snorkel effect" [19]. A unique operational electrode that works thanks to the existing difference of conditions between its extremities. The pole's surfaces exposed to anaerobic conditions provides a physical support for electroactive microorganism's growth while the air-exposed part allows chemical reduction reactions of oxygen. The internal surface of the biochar poles works as cathode, catalysing the oxygen reduction. Because of the alkalinity of the wastewater, the ORR pathway is oriented toward the production of hydroxyl ions [20][21].

The increased pH near to the cathodic surface and the migration of cations towards the cathode duo to charges balancing tendency trigger the "salts precipitation" processes [22]. When cathodic electrodes are made of smooth materials, such as carbon cloth, or metals, like platinum, salts precipitation interests the bottom of the chamber or the cathodic surface [23][24]. Contrary, if the cathode is made of porous material, the deposition will mainly occur inside its structure.

Besides the snorkel effect and salts deposition, the proposed system exploits another physical phenomenon, called "chimney effect or evaporation". This expression is referred to the capacity of pyrolyzed Arundo Donax stems to provide an equilibrium between two processes: water evaporation and water infiltration toward their internal cavity. To better understand, we can imagine the reactor solution being hydrodynamically forced toward the internal cathodic cavity. While water is infiltrating, its contemporary evaporation causes an increasing concentration of solutes and water density. As consequence, the infiltration flow slows down, salts precipitation occurs into the internal structure [25]. The capillary action movement of water upwards in vascular tissue that characterizes this type of plants is strictly linked to this mechanism and plays a major role. Moreover, the salts deposition should interest also the air-exposed part of biochar reeds.

Following the METlands concept, we have a biofiltering media as unique electrode: it composed by conductive carbon coke granules. Thus, the internal conductive resistance of the system is theoretically very low: electrons are free to move directly along the conductive matrix. Since the current is maximal, the system ensures the highest rate for organic matter oxidation. Therefore, the emissions of harmful greenhouse gases, as nitrogen peroxide and methane, by-product of nitrate-nitrite reductions and fermentative processes are mainly inhibited. Organic nitrogen is mainly used by bacterial communities for their own growth while ammonia undergoes salts deposition on the cathode surface due to high pH values [22].

In view of a greater circularity among agricultural and food productive processes, microbial recycling cell is a new BES design based on the use of low-tech, biocompatible and fully recyclable materials in the fabrication of electrodes, separators and structural frames [22]. The main aspect concerns the possibility of reuse these "exhausted" materials after their operational period as enriched fertilizers and soil conditioners. In addition, the replacement of expensive components could favourite the up-scalability of METs toward a wider applicability in environmentally sustainable treatment processes [26].

2. Materials and methods

2.2 Experimental set-up

For this experimentation, we choose 5 types of systems and we set up 10 reactors in order to work on experimental double. Every reactor was filled with carbon coke granules with 5 mm of diameter, except for non-conductive biofilters (“Wetland”) in which we put only river gravel.

As external support, we used plastic containers with dimensions of 10 cm (length) x 30 cm (height) x 6 cm (width).

As control based on a METland design, we prepared two conductive carbon coke granules biofilters ("METLand") in which we put only coke granules. For the remaining three couples of reactors, we inserted biochar steams, terracotta and plastic tubes respectively by ensuring the contact with coke matrix. An explicative graphical representation is proposed in Figure 1a - b.

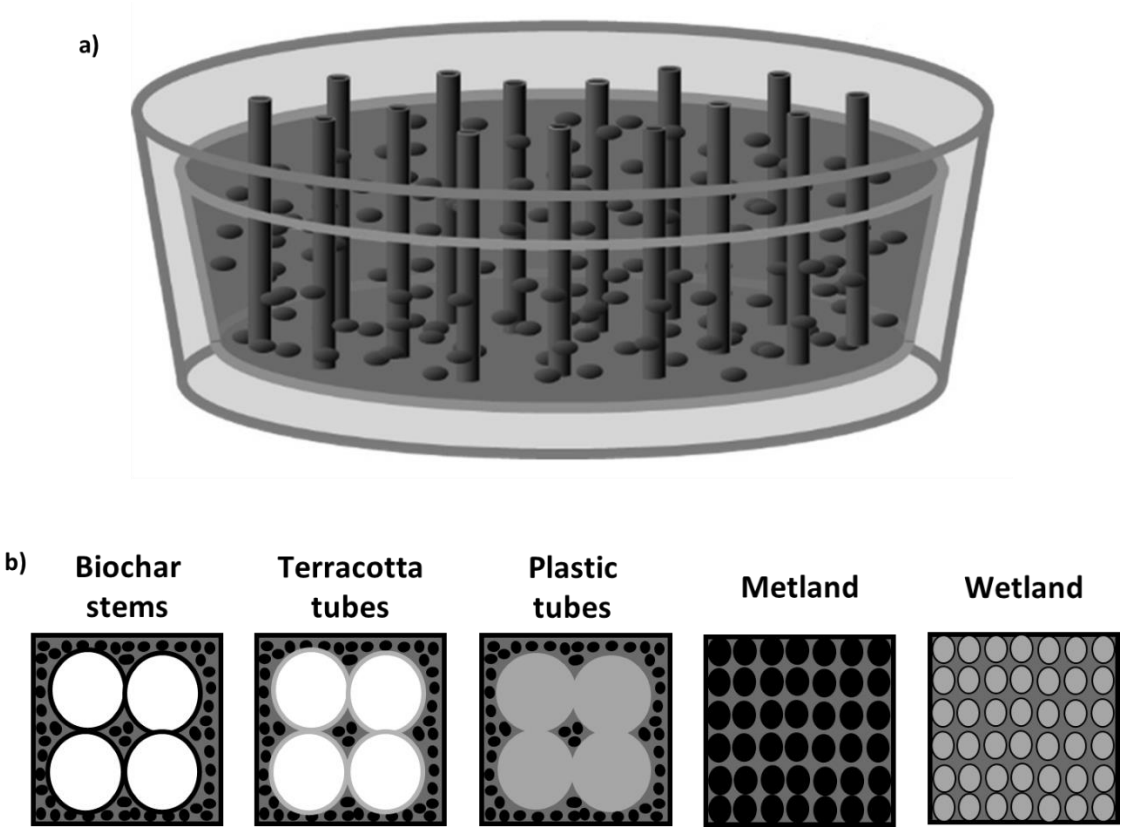

Figure 1 – Representation of the constructed wetlands based on electro-active biochar (a) and the experimental setup (b): electrochemical biofilter + biochar stems (biochar stems), electrochemical biofilter + terracotta tubes (terracotta tubes), electrochemical biofilter + plastic tubes (plastic tubes), electrochemical biofilter (METLand) and non-conductive biofilter (Wetland).

The experiment was realized in "batch mode", starting from low COD concentrations and then increasing it step by step. The reactors volume was 0.6 litres of wastewater. To take advantage from the chimney and snorkel effects, we always worked keeping the water level below the

upper portion of the reactors. We put inside each reactor three plastic loggins to allow and facilitate pH measurements and solution sampling at increasing depth levels: top, middle and bottom.

Following the same scheme, each reactor was outfitted with three knotted carbon clothes tied by titanium wire long enough to reach the reactor's surface and to allow electric potential measurements with a handheld digital voltmeter. A reference Ag/AgCl electrode with KCl saturated solution was placed at the surface of the reactor.

These reactors are designed to work in a short-circuit mode. Thus, during our experimentation, measurements of electric potential have been taken in order to follow the evolution of the process along the vertical gradient. Further investigations and analysis regarding pH and conductibility of reactor solutions has been done throughout around 60 days of operational period. Likewise, COD kinetic and nitrogenous forms removal have been investigated.

As shown in Figure 1a, we can briefly describe our experimental reactor concept based on MRCs as a tank filled with carbon coke granules where the wastewater is periodically extracted and replaced with a new untreated volume. Biochar from Arundo Donax stems are inserted vertically inside the granular matrix. The upper part remains exposed to the air, above the liquid surface.

2.2 Brewery wastewater, inoculum and biochar

For this set-up, we chosen brewery wastewater as feeding substrate. This by-product is produced during one of the first phases of brewery industry. It was collected all on the same day from the brewery plant "Birrificio Italiano - Officina Alchemica" in Limido Comasco, Lombardy (IT), and stored at 4 °C until used.

The inoculum was taken from one of the denitrification tanks operating at Nosedo's wastewater treatment plant. Thus, during the first week every reactor was fed with sewage derived from aeration tanks based on activated sludge for secondary treatment of urban wastewater.

Chemical and physical properties of biochar are direct consequence of feedstock and biomass thermochemical conversion involved during its production [27][28]. Therefore, we paid attention on those aspects: we chosen stems of Arundo Donax as initial biomass, then we pyrolyzed them at 900°C for an hour under nitrogen gas flow. Their behaviour as cathodic electrode is the aspect on which this study is based, the chosen pyrolyzation process was aimed

to preserve the original natural micro and meso porosity structure, as consequence of the vegetal internal tissues.

To imitate the shape and to study the effect delivered by porosity, we used terracotta and plastic tubes with a similar diameter and height. An important aspect concerns the necessity to plug every tube and reed on the bottom with duct tape, waterproof rubber and epoxy resin in order to maintain water out from internal cavities.

2.3 Electrochemical analyses

Electric potential (EP) was measured three times a day using a handheld digital voltmeter. Plastic falcons were inserted into the carbon coke matrix of each reactor by leaving 2 cm of top part exposed to the air. To allow the inlet of the reaction's solution, every falcon was previously performed to the matrix diameter to avoid clogging problems. Therefore, a reference Ag/AgCl electrode with KCl saturated solution was inserted into the plastic falcon. The reference electrode was coupled with a knotted carbon cloth tied by titanium wire. The knotted carbon clothes were placed at different depth levels (top, middle and bottom) during the assembly phase.

2.4 Physico-chemical characterization

Samples from feeding substrate and from the outlet of each reactor were taken at the end of every feeding cycle. Every samples were filtered with at 45 µm. We used LCK cuvette tests to determine COD, total nitrogen (TN), ammonia (NH_4+) and nitrate (NO_3-) concentrations. Every measurement performed by using LCK cuvette tests was made and performed through a Hach's DR3900 spectrophotometer. In addition, COD determination method were used. This method works within a COD range between 0-900 mg L^{-1}. The measures reading is made through Hach's DR3900 spectrophotometer (600 nm wavelength). Same type of cuvette from LCK tests are usable, and the obtained absorbance values are converted to mg L^{-1} by using a regression function. Every test is prepared by adding two reactants into a cleaned cuvette: (1) 0,75 ml digestion solution prepared with $K_2Cr_2O_7$ and $HgSO_4$ and (2) 1,25 ml of Ag_2SO_4 solution. For every measure is required exactly 1 ml of sample. Once this quantity is added to the previously prepared cuvette, this one is shaked and then heated using a furnace at 174°C for 15 minutes. After cooling, it is possible to take the absorbance measure at 600 nm with deionized water as blank.

Sievers Portable Total Organic Carbon Analyzer TOC-820 was used to obtain total organic carbon (TOC) measurements. Electrical conductivity (EC) (Amel model 2131) and pH (Amel model 2335) were measured daily by extracting a part of volume from each reactor.

Moreover, samples of air-exposed, top and bottom parts of exhausted biochar steams and terracotta tubes were collected and crushed at the end of the experiment. These solids samples were extracted by milliQ water, 2% v v-1 $C_6H_8O_7$ and 1% v v-1 HCl to simulate the solubility of the nutrients in short, medium and long time. The mixture of exhausted solids and solutions (ratio 1:10) was mixed for 30 minutes and after that it was filtrated with 0.45 µm nylon filters [29].

3. Results and Discussion

3.1 COD degradation kinects

As shown in the charts in Figure 2, we defined the organic matter removal rates of the systems, in terms of COD kinetic, during the following 24 hours after the initial load of brewery wastewater.

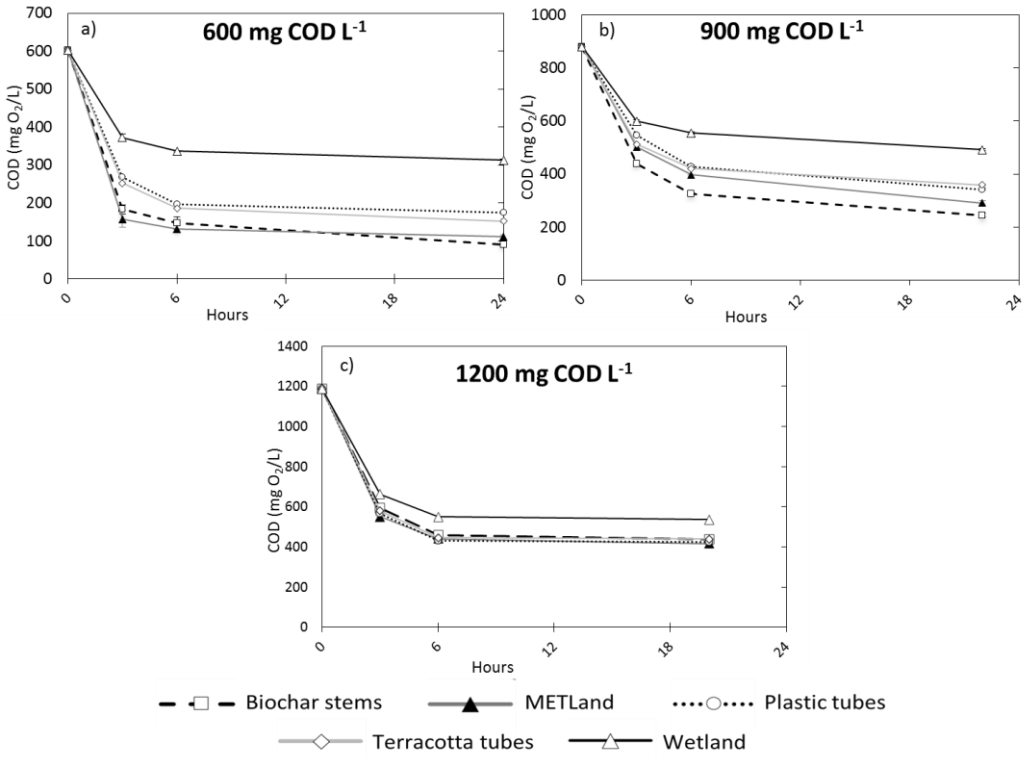

Figure 2 - COD degradation kinects: 600 mg L^{-1} (a), 900 mg L^{-1} (b), 1200 mg L^{-1} (c)

The systems were studied starting from a low COD concentration inlet, about 300 mg COD L^{-1}, for the first 3 weeks. Then we raised the WW inlet concentration every 2 weeks until reaching the 1200 mg COD L^{-1}, along the remaining 6 weeks of experimentation. The COD kinetic measurements were taken during the last day of each different charge circle, except from the first charge period (300 mg COD L^{-1} ww inlet conc.).

Looking at figure 2, three charts show COD degradation kinetics during 600 (a), 900 (b) and 1200 (c) mg COD L^{-1} cycles. The comparison between them all allow us to understand how reactors work in different ways. Indeed, we can say that coke biofilters showed a quicker removal kinetics if compared to wetland biofilters ones. Instead, among coke biofilters during the 600 mg COD L^{-1} cycle, the biochar stems reactors didn't deliver higher performances than METLand ones. This happens because inlet WW concentration was low: biochar and METLand reactors can both work under not saturated conditions with similar degradation rates.

The same thing didn't happen during the 900 mg COD L^{-1} cycle: METLand reactors reached their breaking point duo to the higher WW COD concentration while the biochar stems reactors marked a solid degradation kinetic. Biochar stem reactors obtained a higher percentual degradation than METLand one: at the 3rd, 11th and 22nd hour from the feeding moment, we found respectively an advantage of 9%, 11% and 7% on the amount of consumed COD. Indeed, the faster degradation rate is one of the most relevant aspects brought by this experiment.

The experimentation has continued with an increased WW concentration until 1200 mg COD L^{-1} per day. The lower chart in figure 2 show how lastly biochar reactors exceeded the breaking point: we cannot spot any considerable difference among the reactors, besides the wetlands. However, after 8 weeks, also processes of salts deposition and biofilm formation all over the biochar surfaces may played a role in undermine the benefits from their cathodic activity.

Moreover, no difference can be detected in the results obtained from terracotta and plastic tubes biofilters: all along the experimentation, they always showed a similar behaviour. So, we can say that no benefit is delivered by terracotta tubes to METLand-based reactors.

3.2 Working potential trends

The charts in figures 3 and 4 describe EP profiles of tested systems during the 600 and 900 mg COD L^{-1} cycles. Biochar stems system showed a slightly higher working potential evolution along vertical gradient compared to METland while Wetland always recorded the lowest values. This difference is less evident looking at the bottom EP profiles (600 mg COD L^{-1} cycles). Indeed,

the augmented air-water interface of biochar steam rectors delivered higher potential values at the superficial zones in comparison with METland and wetland.

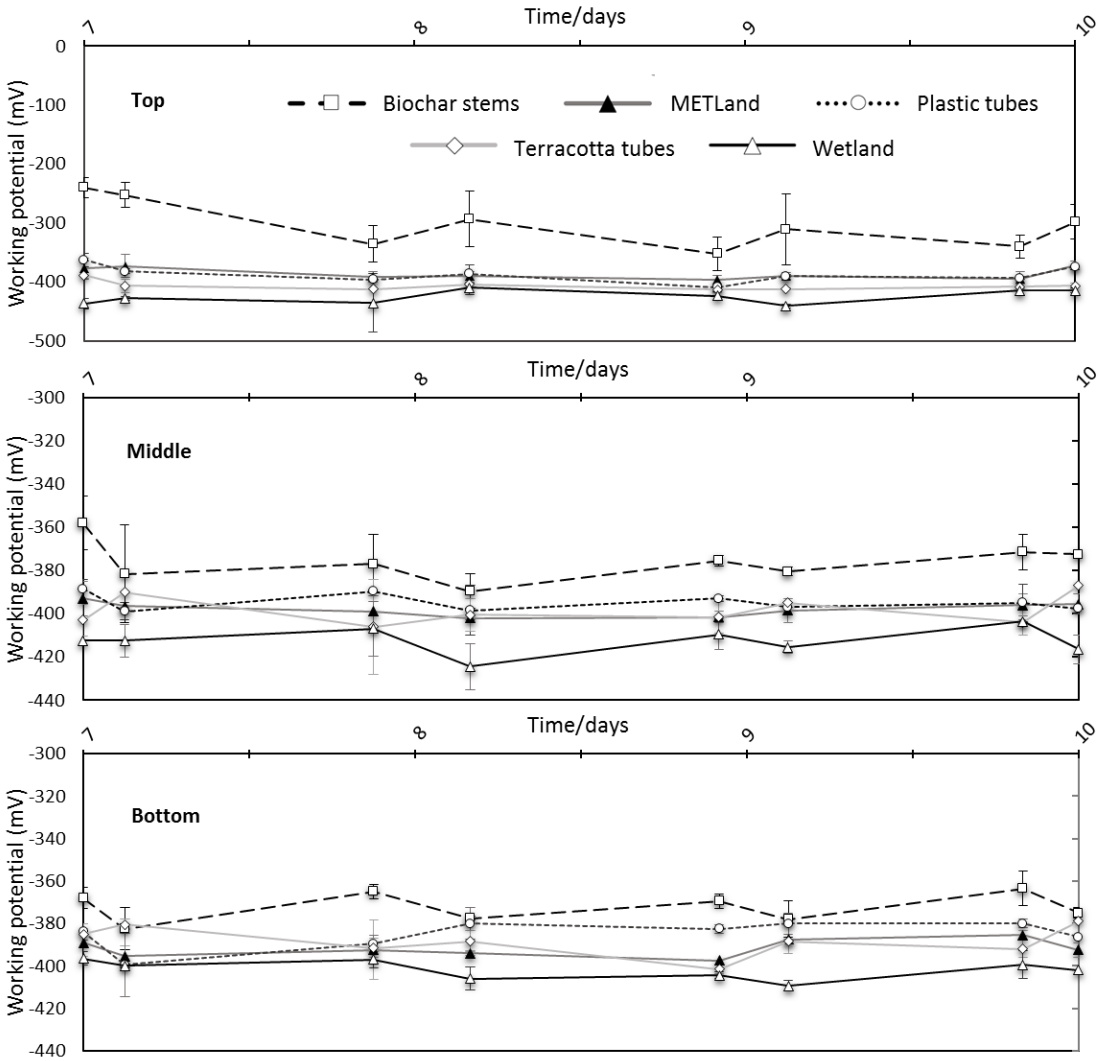

Figure 3 - Electric potential profiles (averages and SD) along the vertical gradient (top, middle and bottom) during the 600 mg COD L^{-1} cycle. A reference Ag/AgCl electrode with KCl saturated solution was used.

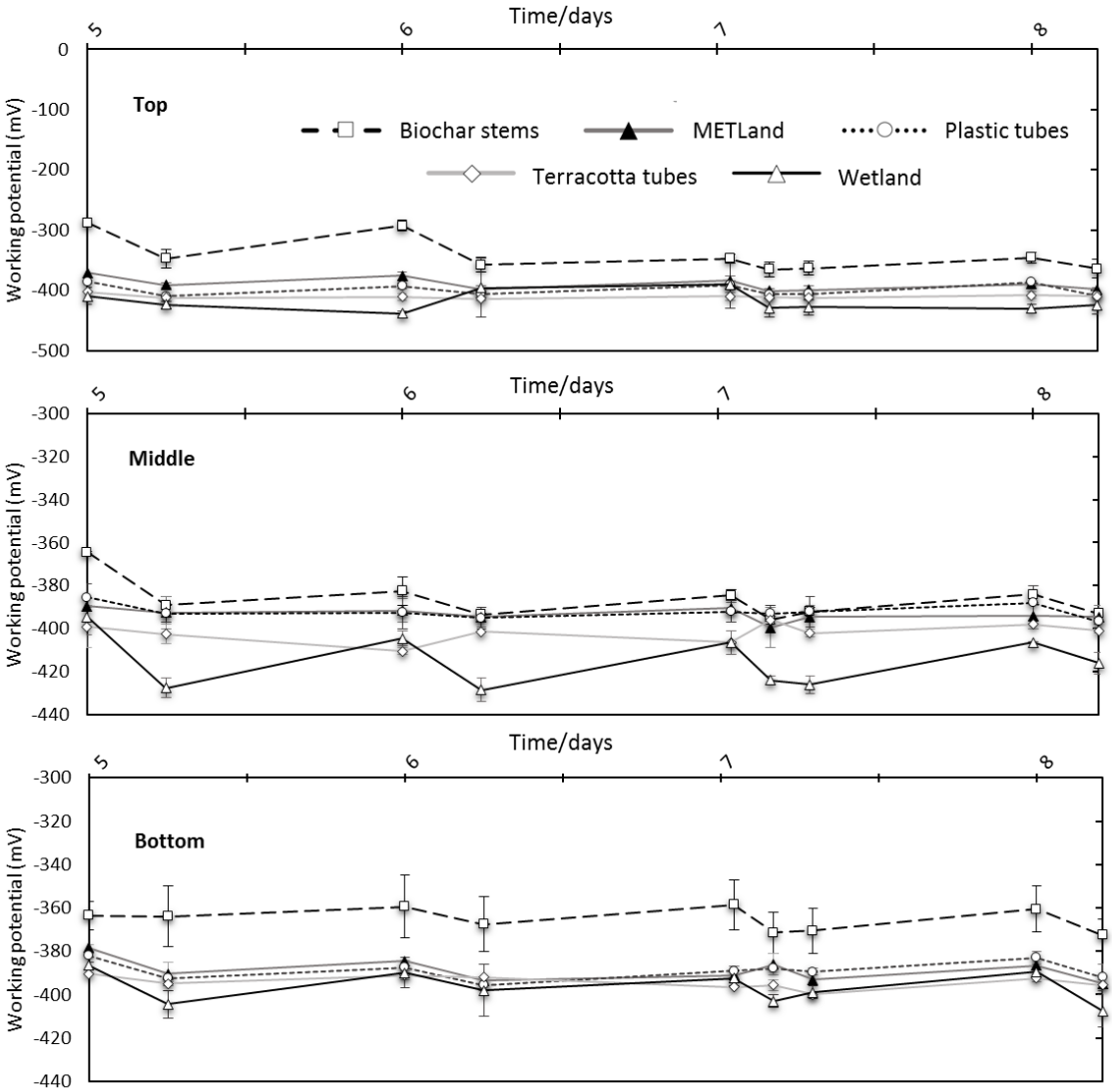

Figure 4 - Electric potential profiles (averages and SD) along the vertical gradient (top, middle and bottom) during the 900 mg COD L^{-1} cycle. A reference Ag/AgCl electrode with KCl saturated solution was used.

3.3 Macro- and micro-nutrients removal

Tables 1 and 2 sum up all the macro- and micro-nutrients removal concentrations during the 600 mg COD L^{-1} and 900 mg COD L^{-1}. As previously describe in paragraph 3.1, the percentages removal of the COD show an increasing of the removal property of the systems composed by an electroactive materials (biochar steams and METland).

Table 1 - Macro- and micro-nutrients average removal during the 600 mg COD L^{-1} cycle.

	Biochar stems	METLand	Terracotta tubes	Plastic tubes	Wetland
	%	%	%	%	%
COD	85	81	71	75	48
TN	65	70	68	70	71
K	-75	91	90	89	88
P	64	83	83	82	91
Na	90	89	90	88	88
Ca	90	90	85	90	86
Mg	90	89	87	89	88
Fe	-135	-244	-24	-146	-143
Mn	37	-31	-5	7	-649
Zn	89	94	83	91	95
NO_3-	56	64	44	44	28
NH_4+	79	73	73	66	52

Table 2 - Macro- and micro-nutrients average removal during the 900 mg COD L^{-1} cycle.

	Biochar stems	METLand	Terracotta tubes	Plastic tubes	Wetland
	%	%	%	%	%
COD	69	66	56	61	40
TN	60	67	68	62	38
K	48	89	91	91	90
P	88	91	93	90	94
Na	91	88	90	89	89
Ca	91	91	84	90	84
Mg	91	90	90	90	90
Fe	-87	-198	57	-103	-242
Mn	86	55	65	72	-284
Zn	99	99	99	99	99
NO_3-	54	53	54	57	57
NH_4+	76	74	76	77	70

In addition, the COD removal increase of 3 - 4 % when we combine the electroactive material with the air-water interface (cylindrical form of the biochar steams). Interesting is the K removal because in the biochar steams reactors is less compare the other reactors. This happened because potassium is very soluble and with a low concentration of organic carbon the cations migration loss intensity and the soluble form of elements start to dissolve in the wastewater.

The percentage removal of the other elements are quite similar for all the systems except for the iron. Both tables 1 and 2 show an impressive improvement in Fe removal with the terracotta tubes both with low and high COD rate. This fact is confirmed also in Figure 5 with the Fe

recovery in the terracotta tubes and it is correlated to the cations exchange capacity of the materials that trap iron.

3.4 Macro- and micro-nutrients recovery

One of the most important objectives was to verify the possibility of recovering macro and micronutrients on the cathodic biochar stems for brewery wastewater. During the 9 weeks of operation time, we followed the evolution of salts accumulation on the top of the biochar stems. From the beginning, salts accumulation became visible immediately after the acclimation week and even more evident during the following 2 weeks. The process reached its maximum on the 4th week, and after that only a small further evolution can be spotted. The accumulation interested both internal and external sides of the cathodic stems, starting from the emerging visible parts up to the top of the steams.

Figure 5 show these phenomena, making distinction between top aired and lower submerged parts of the exhausted biochar steams, in order to study the porosity and material influence.

Considering the comparison with terracotta tubes, Figure 5 shows that an interesting amount of nutrients are accumulated on biochar steams except Calcium and Iron that are trap in the terracotta tubes by the cations exchange capacity of the terracotta. These results are confirmed from all the extractions that we did to study the solubility of the elements. As discussed above, the snorkel effect certainly played a major role in boosting the salt accumulation. Indeed, also the chimney effect confirmed its effectiveness and potentialities. The air-exposed part of biochar steams shown a ready and quick response at the beginning of the experiment. However, the internal vascular tissues undergo clogging processes over the time.

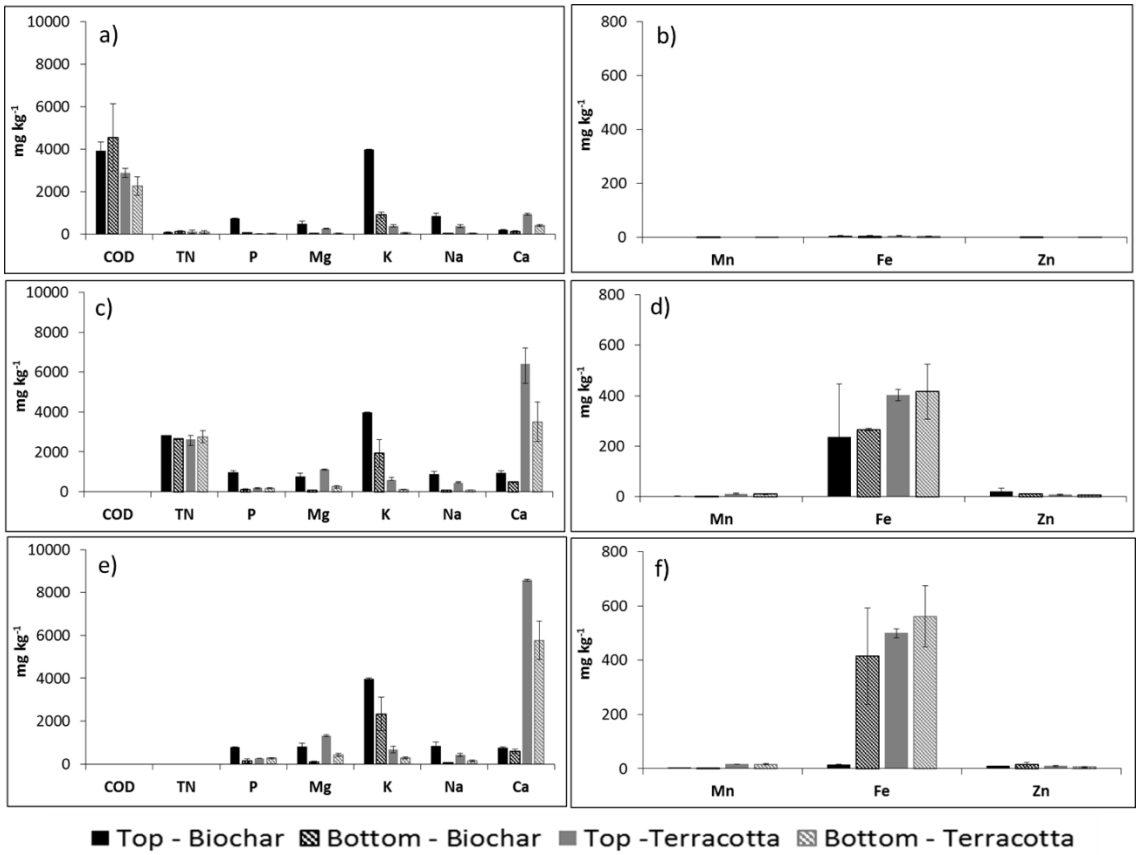

Figure **5** - Amounts of macro- and micro-nutrients recovered on biochar steams and terracotta tubes over the working operation days measured under different extractions: (a-b) milli-q water, (c-d) $C_6H_8O_7$ 2% v v^{-1} and (e-f) HCl 1% v v^{-1}. Error bars stand for standard deviations of duplicate experiments, under identical conditions.

4. Conclusions

Microbial electrochemical technologies have already shown some effective and promising applications for wastewater treatment in delocalized and small-scale facilities (avoiding long-distance wastewater transport), while minimizing the use of auxiliary energy.

The results showed a relevant accumulation of nutrients in the biochar steam and furthermore, the presence of biochar stems allowed higher performances in COD degradation rates (550 mg COD L^{-1} day^{-1}), as compared to control METlands (500 mg COD L^{-1} day^{-1}). This was strictly linked to both the electro-activity and the porosity of material, as shown also by the results obtained by terracotta control reactors (450 mg COD L^{-1} day^{-1}).

However, this new approach could strongly increase the possibility of the scaling-up of this technology; starting from organic scraps obtaining resource and preserving the soil in a view of circular economy.

Acknowledgements

This work was financed by the SIR 2014 Grant (PROJECT RBSI14JKU3), Italian Ministry of University and Research (MIUR) by the Research Fund for the Italian Electrical System in compliance with the Decree of March, 19th 2009.

References

[1] "Wastewater Report 2018 - The reuse opportunity," 2018.

[2] "(PDF) Management of sludge from municipal wastewater treatment plants in the regions of Thessaly and West Macedonia, Greece." .

[3] "Europe's state of the environment 2020: change of direction urgently needed to face climate change challenges, reverse degradation and ensure future prosperity — European Environment Agency." .

[4] European Commission, "Closing the loop - An EU action plan for the Circular Economy," Brussels, 2015.

[5] J. Cantwell, B. Erickson, L. Fillmore, J. Kottwitz, M. Levy, and M. Rickert, "Energy Data Management Manual for the Wastewater Treatment Sector," 2017.

[6] "Guiding Principles For Constructed Treatment Wetlands: Providing for Water Quality and Wildlife Habitat," 2000.

[7] S. Cabred, V. Giunta Ramos, J. E. Busalmen, J. P. Busalmen, and S. Bonanni, "Reduced depth stacked constructed wetlands for enhanced urban wastewater treatment," Chem. Eng. J., pp. 708–714, Sep. 2019.

[8] M. Garfí, L. Flores, and I. Ferrer, "Life Cycle Assessment of wastewater treatment systems for small communities: Activated sludge, constructed wetlands and high rate algal ponds," J. Clean. Prod., vol. 161, pp. 211–219, Sep. 2017.

[9] U. Epa and M. Support Division, "Emerging Technologies for Wastewater Treatment and In-Plant Wet Weather Management," 2013.

[10] AOS Treatment Solutions, “4 Examples of New Wastewater Treatment Technology,” 2016. .

[11] P. T. Kelly and Z. He, “Nutrients removal and recovery in bioelectrochemical systems: A review,” Bioresour. Technol., vol. 153, pp. 351–360, 2014.

[12] S. Bajracharya et al., “An overview on emerging bioelectrochemical systems (BESs): Technology for sustainable electricity, waste remediation, resource recovery, chemical production and beyond,” Renew. Energy, 2016.

[13] A. Aguirre-Sierra, T. Bacchetti-De Gregoris, A. Berná, J. J. Salas, C. Aragón, and A. Esteve-Núñez, “Microbial electrochemical systems outperform fixed-bed biofilters in cleaning up urban wastewater,” Environ. Sci. Water Res. Technol., vol. 2, no. 6, pp. 984–993, Nov. 2016.

[14] C. A. Ramírez-Vargas, C. A. Arias, P. Carvalho, L. Zhang, A. Esteve-Núñez, and H. Brix, “Electroactive biofilm-based constructed wetland (EABB-CW): A mesocosm-scale test of an innovative setup for wastewater treatment,” Sci. Total Environ., vol. 659, pp. 796–806, Apr. 2019.

[15] “A HANDBOOK OF CONSTRUCTED WETLANDS: a guide to creating wetlands.”

[16] A. Esteve-Núñez, B. Barroeta, and J. J. Salas, “iMETland, una nueva generación de humedales electroactivos para el tratamiento de aguas residuales en pequeñas poblaciones,” Feb. 2019.

[17] A. Esteve-Núñez, A. Aguirre-Sierra, J. Salas, C. Aragón, and A. Esteve-Núñez, “Integrating Microbial Electrochemical Technologies (MET) To Constructed Wetlands To Treat Wetland Systems for Water Pollution Control,” 2018.

[18] C. Santoro, C. Arbizzani, B. Erable, and I. Ieropoulos, “Microbial fuel cells: From fundamentals to applications. A review,” J. Power Sources, no. March, 2017.

[19] B. Erable, L. Etcheverry, and A. Bergel, “From microbial fuel cell (MFC) to microbial electrochemical snorkel (MES): maximizing chemical oxygen demand (COD) removal from wastewater.,” Biofouling, vol. 27, no. 3, pp. 319–26, Mar. 2011.

[20] E. Guerrini, P. Cristiani, and S. P. M. Trasatti, “Relation of anodic and cathodic performance to pH variations in membraneless microbial fuel cells,” Int. J. Hydrogen Energy, vol. 38, no. 1, pp. 345–353, 2013.

[21] B. Erable, D. Féron, and A. Bergel, “Microbial catalysis of the oxygen reduction reaction for microbial fuel cells: A review,” ChemSusChem, vol. 5, no. 6, pp. 975–987, 2012.

[22] A. Goglio, M. Tucci, B. Rizzi, A. Colombo, P. Cristiani, and A. Schievano, “Microbial recycling cells (MRCs): A new platform of microbial electrochemical technologies based on biocompatible materials, aimed at cycling carbon and nutrients in agro-food systems,” Sci. Total Environ., vol. 649, pp. 1349–1361, 2019.

[23] H. Carlsson, H. Aspegren, N. Lee, and A. Hilmer, “Calcium phosphate precipitation in biological phosphorus removal systems,” Water Res., vol. 31, no. 5, pp. 1047–1055, 1997.

[24] I. Gajda et al., “Water formation at the cathode and sodium recovery using Microbial Fuel Cells (MFCs),” Sustain. Energy Technol. Assessments, vol. 7, pp. 187–194, 2014.

[25] A. Goglio, S. Marzorati, L. Rago, D. Pant, P. Cristiani, and A. Schievano, “Microbial recycling cells: first steps into a new type of microbial electrochemical technologies, aimed at recovering nutrients from wastewater,” Bioresour. Technol., 2019.

[26] J. Winfield, I. Gajda, J. Greenman, and I. Ieropoulos, “A review into the use of ceramics in microbial fuel cells,” Bioresour. Technol., vol. 215, pp. 296–303, 2016.

[27] J. M. N. Yong Sik Ok, Daniel C.W. Tsang, Nanthi Bolan, Biochar from Biomass and Waste: Fundamentals and Applications. .

[28] S. Marzorati et al., “Air-breathing bio-cathodes based on electro-active biochar from pyrolysis of Giant Cane stalks,” Int. J. Hydrogen Energy, 2018.

[29] “Metodi di Analisi dei Fertilizzanti,” in Gazzetta Ufficiale del 26/01/01 n.21, DM 21/12/00, Suppl. n.8, .

Chapter 8 - Biochar-terracotta conductive composites: new design for bioelectrochemical systems

Pierangela Cristiani[1*], Andrea Goglio[2], Stefania Marzorati[2], Stephanie Fest-Santini[3], Andrea Schievano[2]

1 Ricerca sul Sistema Energetico – RSE S.p.A., via Rubattino, 54, 20134 Milano, Italy

2 e-Bio Center, Università degli Studi di Milano, Department of Environmental Science and Policy, via Celoria 2 – 20133, Milano, Italy

3 Department of Management, Information and Production Engineering, University of Bergamo, Dalmine, Italy

Published in:

Cristiani P., Goglio A., Marzorati S., Fest-Santini S., Schievano A., 2020. Biochar-terracotta conductive composites: new design for bioelectrochemical systems. Frontiers in energy research journal. doi: 10.3389/fenrg.2020.581106

Abstract

Research in the field of bioelectrochemical systems is addressing the need of improving components and reducing their costs in the perspective of their large-scale application. In this view, innovative solid separators of electrodes, made of biochar and terracotta, are investigated. Biochar-based composites are produced from giant cane (*Arundo Donax L.*). Two different types of composite are experimented: i) composite A, produced by pyrolysis of crushed chipping of A.donax L. mixed clay; ii) composite B, produced by pyrolysis of already pyrolyzed giant cane (biochar) mixed with clay. Electrical resistivity, electrical capacity, porosity, water retention, and water leaching of the two composites types (A and B) with 1, 5, 10, 15, 20 and 30 mass percentages of carbon (w/w) are characterized and compared. Less than 1 kΩ cm of electrical resistance is obtained for composite A with a carbon content greater than 10 %, while physical and electrical performances of composite B does not significantly change. SEM micrographs and 3D microcomputed tomography of different composite materials are provided, demonstrating a different matrix structure of carbon in the terracotta matrix. The possibility of suitably decrease electric resistance and increase water retention/leaching of composite A opens the way to a new class of resistive materials that can be simultaneously used as an electrolytic separator and an external electric circuit, allowing a compact microbial fuel cell design. The proposed solution is particularly suitable for nutrient recovery and environment pollution bioremediation, where energy harvesting is not requested.

Keywords

Biochar; Terracotta; Electrical Resistivity; Composite Materials; 3D tomography; Microbial Fuel cells (MFCs); Bioelectrochemical systems (BESs), Microbial Electrochemical Systems (MESs)

1. Introduction

Microbial electrochemical systems (MESs) are new biotechnologies exploring bioelectrochemical phenomena from the perspective of their possible application for generating energy [Santoro et al., 2017], fuels, or value-added chemicals [Tiquia-Arashiro and Pant, 2020; Cruz Viggi et al., 2017]. MESs are particularly promising for the remediation of environmental pollution [Ng et al., 2016], offering also a flexible platform for desalination processes [Elmekawy et al., 2014]. Many other possible engineering functions are currently under investigation, based on the general principle that natural microorganisms catalyze one, or both, anodic and cathodic reactions, on carbon electrodes [Tiquia-Arashiro and Pant, 2020]. Biodegradable substrates can be oxidized by microorganisms at the anode, generating an

electrical current. Bacteria growing on a porous cathode can substitute expensive catalysts (such as platinum or carbon-based catalysts) to increase the oxygen reduction reaction in fuel cells [Zhang et al., 2012; Cristiani et al., 2013; Milner et al., 2016]. The electrons exchanged during the redox reactions, thanks to the created or imposed potential difference between electrodes, flow in an external electric circuit. The latter is usually composed of metal collectors, plastic insulators, and resistors. However, the relatively high economic and environmental costs of such components hinder the large-scale applications of MESs. The same problems affect polymeric electrolytic separators used as ion-exchange membranes, whose costs and environmental concerns can be higher than those of electrodes. Regarding the membrane, various materials have been offered as alternative separators, such as salt bridges, glass fibers, earthenware [Ajayi ans Weigele, 2012; Winfield et al., 2013; Santoro et al., 2015], and composite plastic membranes [Mathuriya et al., 2018]. All those materials can equally contrast oxygen and substrate crossovers than a polymeric membrane, also controlling fouling. Among the others, separators made of terracotta (earthenware) can offer several advantages [Pasternak et al., 2015].

Tubular Microbial Fuel cells (MFCs), with the carbon anode placed on the outer surface and a carbon cathode inside a cylinder made of terracotta, immersed into wastewater, is a configuration that allows perfect separation between the waterside (external) and the airside (inner volume of the cylinder). Several applications were approached with such systems, where the terracotta (ceramic fired clay, which has typical pore sizes of 60-500 nm) acts as a porous medium that allows electrolytes mobility. Using small scale terracotta-MFC modules of roughly 10 cm height and 1 cm diameter in stacked systems, electricity was harvested from urine and other wastewaters to power DC motors and other devices [Walter et al., 2016]. The same MFC design was utilized as a self-powered wastewater electrolyzer for electrocoagulation of heavy metals, caustic production at the cathode (pH>10), and the CO_2 sequestration [Ramírez-Moreno et al., 2014]. Deposited salts as well as stripped ammonia can be thus recovered and utilized as fertilizers for agriculture in a circular-economy approach [Sengupta et al., 2015; Behera et al., 2010].

The earthen pot was effective for proton transfer in such low-cost MFC, giving a comparable performance with respect to much more sophisticated MFCs, even if it was found that the major limitation comes from the low carbon cathode potential [Santoro et al., 2017]. Nevertheless, several studies and experiments have been addressed to demonstrate the effectiveness of such low performing MES systems for water and soil remediation with promising performances [Prado

et al., 2019; Kappler et al., 2014, Schievano et al., 2019, Goglio et al., 2019]. Furthermore, a recent work [Neethu et al.2019] underlined that a novel membrane developed from clay and activated carbon derived from coconut shells better performed than the Nafion 117 membrane, doubling the power density of a MFC. This new type of membrane showed an increased proton diffusion coefficient.

Electroactive biogenic charcoal (biochar), produced from residual biomasses, is the environmentally friendly and efficient solution proposed for electrodes also [Prado et al., 2019]. The biochar achieved from giant cane (Arundo donax L.) is particularly attractive as a suitable and largely available source, at relatively low costs, therefore, a great candidate for MES systems [Schievano et al., 2019, Goglio et al., 2019]. The feedstock sources and heat treatment parameters (temperature, residence time, atmosphere of pyrolysis reactor) are major parameters determining the electrochemical and structural properties of biochar [Goglio et al., 2019; Longhi et al., 2016]. A suitable combination of these parameters allows the achievement of biochar characterized by high conductivity, porosity, and ions conductivity [Giudicianni et al., 2014]. Nitrogen and other macro-micro-nutrients were already recovered from wastewater in single-chamber air-breathing microbial fuel cell systems, entrapped in the porosity of biochar-based cathodes produced by the pyrolysis of giant cane [Marzorati et al., 2018]. The mechanical fragility of biochar based MFC was an underlined issue, in that case, precluding its possible scaling-up.

Aiming at strengthening and improving the design of biochar based MFC for recovering nutrients and environment pollution at large scale, robust biochar-terracotta composites were studied in this work. These composites were produced by a single and double step pyrolysis of Arundo donax L., mixed with clay in varying ratios, and subsequently thermally treated.

Porosity, electrical resistance/ionic conductivity, water permeability of differently pyrolyzed, and differently mixed with terracotta composites were characterized.

The target is to create, for the first time, a new class of composite materials having the double function of ions and electrons conductor, making MFCs suitable for large scale environmental applications.

Suitable balancing of the water retention, electric conductivity, and porosity of components permits to design compact biochar-based MFC for applications in different soil and water environments. These parameters are crucial to guarantee the settlement and life of the microbiological pool operating in the system. In the case of soil remediation, for instance, the

harvesting power is not requested, and the remediation process enhanced by microorganisms is relatively slow. In this case, a low water retention capability of the MFC system could be a concern, as the soil humidity can strongly vary in time, debarring MFC's performance against pollutants. In water environments, on the other hand, an excessive flow through the MFC could contrast the anaerobic condition of the anode and, consequently, the water purification process. Lastly, pores of micrometric dimension allow microorganisms to reach and colonize anodic and cathodic electrodes.

2. Materials and methods

Giant canes (Arundo donax L.), collected in Cascina Marianna (Landriano, PV) from the experimental fields of the Università degli Studi di Milano, were used to produce biochar. The clay used to produce terracotta was a commercial powder (BDIH, Italy) with a slightly alkaline pH and good ionic conductivity. Its elemental composition is illustrated in Table 1.

Table 1 - Clay composition

Element	**Percentage (% $_{w/w}$)**
Si	35.2
Al	9.80
Ti	0.20
Fe	4.40
Mg	22.9
Ca	26.7
Na	0.40
K	0.40

Two types of composite (A and B) and different percentages of carbon mixed with clay (1, 5, 10, 15, 20, and 30 % mass percentages of carbon (w/w), clay balance) have been tested. Biochar-terracotta composites of type A and B differ in the preparation procedure.

Cylindrical samples of each composite type (A and B) with a diameter of 4 cm were molded. In a first test, samples of different thicknesses (4, 8 and 12 mm) have experimented with a relatively low carbon content (1, 5, and 10 %). In a second test, samples with higher carbon content (15, 20, and 30 %) with the selected thickness of 8 mm have experimented. Each sample was built and tested at least in duplicate.

2.1 Composite A preparation (one step of pyrolysis)

Composite A was prepared by mixing raw plant chipping of giant cane with clay and pyrolyzing the molded samples. Chipping was pulverized at a size of 0.5 – 1 mm and uniformly molded with clay in the samples. The pyrolysis was performed with the following protocol: slow heating of the oven hosting the samples (5 °C min^{-1}) up to 900 °C, 1 h held at 900 °C and, finally, cooling down to 25 °C. Nitrogen was flowing constantly at 14 NL h^{-1} during the pyrolysis treatment.

2.2 Composite type B (two steps of pyrolysis)

Composite type B was prepared from already pyrolyzed giant cane (biochar) mixed with clay and pyrolyzed again (two steps of pyrolysis). Raw, dried giant cane chipping was first pyrolyzed as it is, at low temperature (350 °C) and under nitrogen atmosphere (14 NL h^{-1}). The obtained biochar was crushed at a size of 0.5 - 1 mm, and the powder was then mixed with clay and molded as cylindrical samples. Subsequently, samples were pyrolyzed again. This second step of pyrolysis follows the same procedure as for Composite A.

2.3 Electrical resistivity

An estimation of the electrical resistivity ρ of each composite sample after the pyrolysis in dry and wet conditions was measured, in different ways. Dry samples were analyzed carrying out potentiodynamic polarization curves in the range of 0 - 0.5 V, with a scan rate of 0.01 Vs^{-1}. The distance between the counter electrode and working electrodes connected to the sample was 1cm, approximating in this way an electrochemical cell with electrodes area of ~ 1 cm^2 (sample section) at a distance of 1 cm. A linear interpolation (Rint) of voltammetry data (equation 1), normalized for the sample thickness, was used to estimate ρ.

$$R_{int} = \frac{\Delta V}{\Delta I} \qquad (1)$$

Measurements on dry and wet samples of 8 mm thick were also performed using the multimeter Fluke 8808A, pushing 1 cm squared, plate contacts connected to the multimeter, orthogonal to the testing sample. The measured resistance R was normalized to the section of 1 cm, to calculate ρ, by equation (2), where A is the area of the electrode contact (1 cm^2) and l is the distance between the electrodes (8 mm).

$$\rho = 1.2\frac{RA}{l} \quad (2)$$

2.4 Electrical capacitance

Measures of the electrical capacitance of dry and wet samples of 8mm thick were performed using the capacimeter device LC100-A. The measurements were performed at a frequency of 820 kHz.

2.5 Water retention

The water retention capacity (WC) is correlated to macroporosity of the composites. It was evaluated weighting the dried samples (at the start of analysis) and after leaving samples in water for 24 h. The water retention is expressed as the mass of water absorbed per mass of dried sample.

$$W_C = 1000\frac{W_{wet}-W_{dry}}{W_{dry}} \quad (3)$$

Wwet and Wdry are the mass of the dried and wetted samples, respectively.

2.6 Water leaching test

Water leaching in 24 h of wet samples was tested with a set-up of 3 different water column pressure (0.5, 1, and 1.5m height) (Figure S1 of Supplementary Materials). This test was performed posing samples on the bottom of tubes filled with a water column of 0.5, 1, and 1.5m, simulating possible conditions of the environments where MFCs could be used (soils,

water conducts etc.). Water leaching was estimated as grams of water leached from each sample after 24 h.

2.7 Surface analysis

Optical observations of the composite sample surfaces were performed using Olympus Stereo Microscope SZ. Scanning Electron Microscopy (SEM) Zeiss SEM EVO 50 microscope was used to analyze the morphology of the pyrolyzed samples.

3D microCT (microtomography) technique was applied, and digitalized 3D objects of samples were generated. The used microCT is based on an open type X-ray source 160 kVp @ 200 μA, a flat panel detector, and a high-precision air-bearing rotating stage. For detailed information regarding components of the microtomography unit, it is referred to as Santini [Santini et al., 2013]. The objects to be investigated were placed on the stage and rotated by small angular steps. 2D radiographs were acquired at each rotation step. Herefore, X-ray tube voltage and amperage, step angle, and acquisition time were adapted to the measurement task and amounts 120 kV, 14 μA target, 0.075°, and 1.5 s, respectively. During acquisition, the projections were corrected for charge accumulation of the detector, the so-called “dark-field”, and were normalized by “bright-field” correction. The latter characterizes the nonuniform system response due to variation in detector sensitivity and X-ray source flux density. The normalized projections are, then, reconstructed using standard filtered back-projection algorithms. Here, the volume reconstruction is computed by the commercial software VGStudio MAX®. The resolution of the obtained 3D microCT objects was determined with a special calibration and amounts 15.856 μm [Santini et al., 2016].

For the binarization of volumes in solid and void spaces, a watershed algorithm on the high gradient magnitude was applied using the commercial software Avizo®. The subdivision in single pores was obtained by a combination of watershed, distance transform, and numerical reconstruction algorithm. Hereby, the marker extent factor was set to 4 and the connectivity to 26. This operation was conducted in 3D.

3. Results

The optical micrographs images of the two types of composites (A and B) are reported in Figure S2 of Supplementary Materials. The granular structure of the biochar achieved from the pyrolysis of the sole giant cane chipping, before (a) and after (b) crushing, is illustrated in the

SEM micrographs of Figure 1. Traces of the cellular structure is clearly visible in the pyrolyzed chipping of giant cane, while it is completely missed in the biochar after crushing.

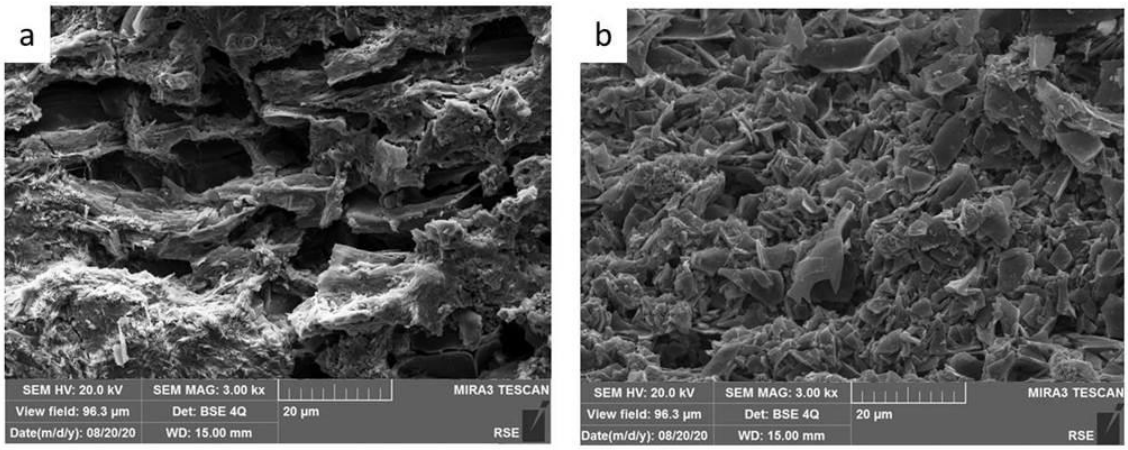

Figure 1 - SEM micrographs (800x) of pyrolized chipping of A.Donax L. before crushing (a) and after crushing (b).

3.1 Microstructure of composites

The different microstructure of the composites A and B are well evidenced by the documentation of the microCT volumes reported in Figures 2 and 3.

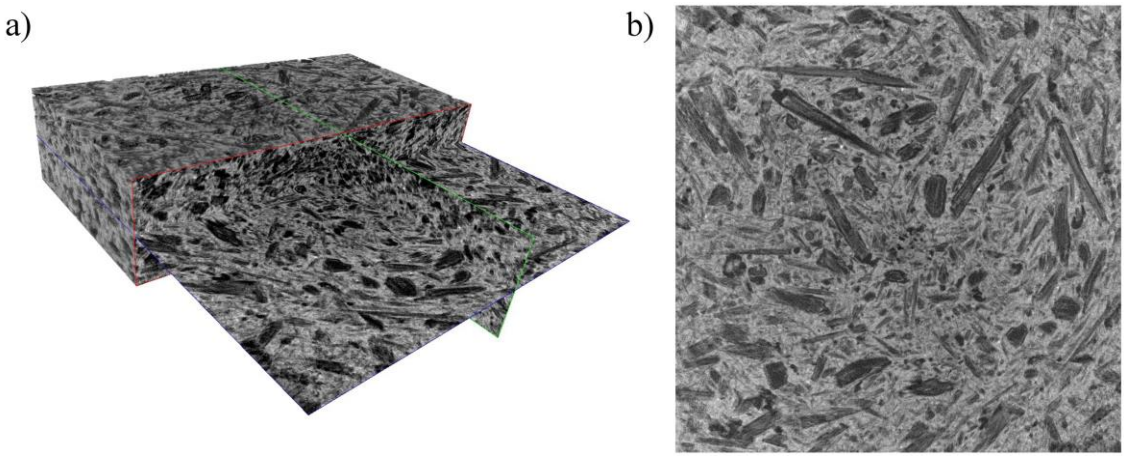

Figure 2 - 3D microCT render (a) and representative slice (b) of the composite A30%. The volume has a dimension of 20.6 x 20.6 x 4.8 mm3.

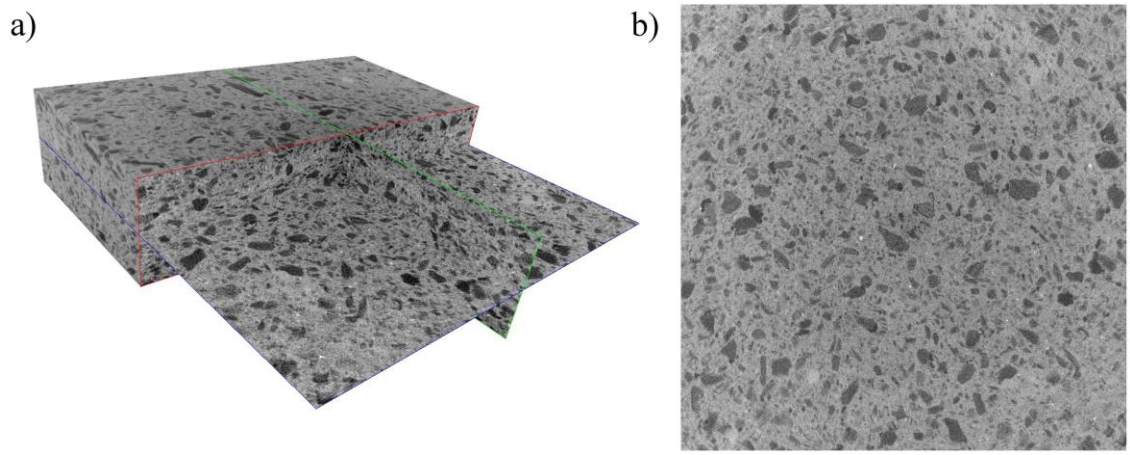

Figure 3 - 3D microCT render (a) and representative slice (b) of the Composite B30%. The volume has a dimension of 20.6 x 20.6 x 4.8 mm3.

Figures 2 and 3 depict 3D render of the structures of composites A30% and B30%, respectively. The pore size distribution and porosity of representative rectangular cuboid sub-volumes (having dimensions of 20.6 x 20.6 x 4.8 mm3) were determined. Figure 4 shows the pore size's probability density functions of composites A30% and B30%.

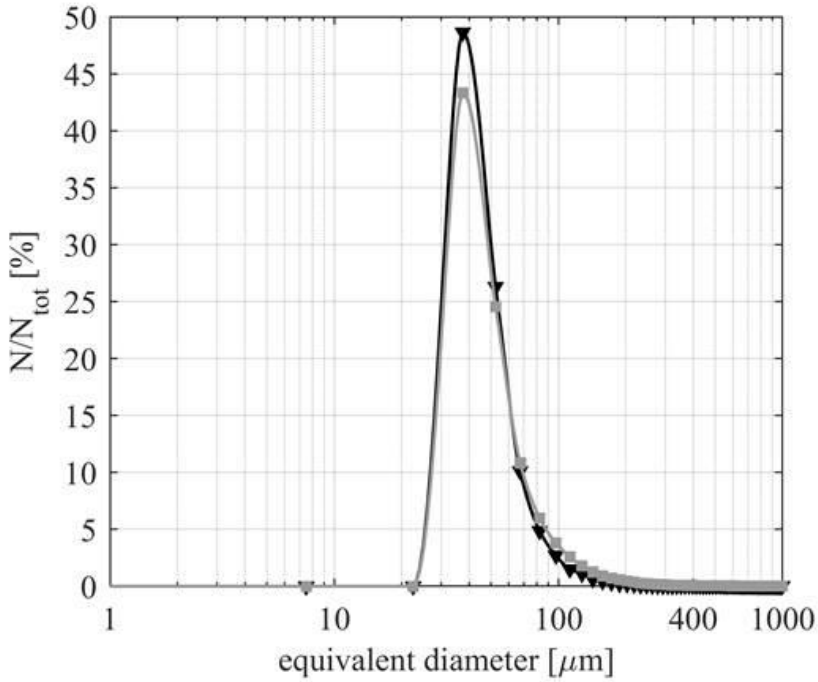

Figure 4 - Probability density functions of the pore space of composites A30% (black) and B30% (gray).

The given pore sizes correspond to the diameter of volume-equivalent spheres. Both composites have similar-sized pores. For the determination of the porosity, voxels assigned to each class were counted. The porosity is obtained by Φ= Vpores/V. The values of four different composites are summarized in Table 2.

Table 2. Porosities Φ and pores' volume to surface ratio V/S of different composites

	A05%	A10%	A30%	B30%
Φ[%]	15.4	16.9	31.5	16.4
V/S [μm]	31.3	31.3	34.2	24.2

It is worth stressing that a filamentous-globular structure of the vegetal giant cane is partially preserved in the sample of Composite A (dark areas), while carbon results more smoothed and uniformly mixed with terracotta in Composite B. The increased content of filamentous carbon in the terracotta andmatrix is evidenced for Composite A05%, A10%, and A30% and for Composite B30% is evidenced by the microCT slices. Such structures, rather absent in the more compact and uniform composite B, formed a sort of connected porous network through the terracotta matrix in composite A (Figure 2).

3.2 Electrical resistivity and capacity

Dry samples

More than nine orders of magnitude space the values of electrical resistivity ρ of the pure biochar (few Ωcm) from the value of the (insulating) clay (>109 Ωcm, the limit of instrumentation) of dry samples. The electrical resistance of the composite B was always greater than 1000 kΩcm for all samples, sticking by terracotta ones. On the contrary, several orders of magnitudes separate the resistivity value of composite A vs the pure clay, in all conditions. The ▫ value was reduced to less than 1 kΩcm increasing the carbon content, but it was highly variable depending on the point of the measurement. The averages of ▫ values for composite A of different carbon percentage were reported in Table 3.

Table 3 - Electric resistivity (ρ) and capacitance (C) estimated on dry and wet samples of composite A with a thickness of 8mm.

Biogenic Carbon (%)	ρ average (dry samples) kΩcm	ρ average (wet samples) kΩcm	C average (wet samples) pF
0	1144130 ± 17978	160±10	1±0.3
1	2750±1909	40±10	3±1
5	1000±424	20±2	50±3
10	45±49.5	1.05±0.1	160±40
15	25±21.2	0.2±0.0	340±40
20	6.75±4.6	0.38±0.0	630±100
30	1.75±1.8	0.3±0.0	1900±1000

The variation of ▫ values, induced by changing the carbon percentage in the range 1 – 30 %, and the sample thickness (4 mm, 8 mm, 12 mm) is shown at logarithmic scale in the histograms of Figure S4 of Supplementary Materials, for both composites A and B. The decrease was drastic and proportional to the carbon percentage for composite A samples. Data were more dispersed for composite B, and the tendency to reduce the resistivity value increasing the carbon percentage was not as evident as for the composite A, where the dispersion of data was evident for samples of different thickness, particularly high only for samples with a minimal percentage of carbon, up to 10 %.

Wet samples

Electrochemical systems typically work with conductive water solutions and preserve wet conditions when microbial biofilm develops. Therefore, the resistivity was also measured on wet samples for both composite A and B. Tests were carried out after the water capacity test with 8 mm thick samples. The water conductivity was 0.5 mS cm^{-1}. This condition simulates a freshwater environment penetrating the porous composites. Filling the pores, the conductive

solution connects tightly the single carbon particle of the composites influencing, in this way, the electric resistivity and capacity of the materials. The average data of capacitance C and resistivity ρ of composite A from the measurement performed in wet conditions are reported in Table 3. The logarithm of ρ averages, plotted in function of carbon percentage, is also shown in the graphic of Figure 5. Two relevant linear tendencies were evidenced for this graphic. The first underlines a linear changing of ρ of several order of magnitudes when low percentages of carbon were added to terracotta. The second underlines a linear tendency of ρ to quickly decrease close to the value of the pure biochar for carbon contents higher than 10%.

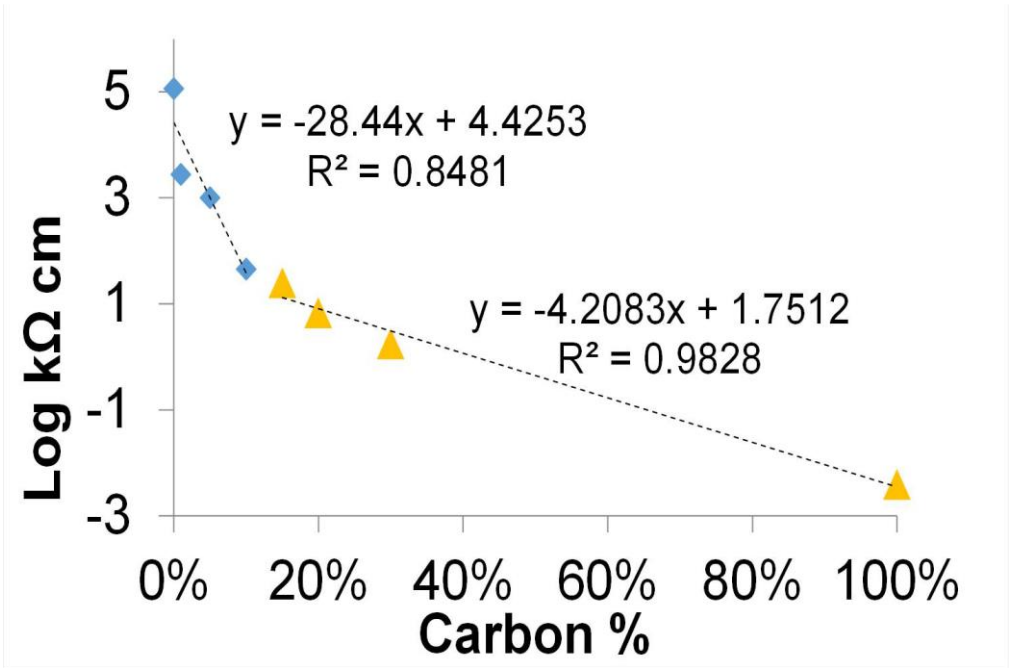

Figure 5 - Graphic of the average of the electrical resistivity of Composite A measured at different carbon %. The linear equation and regression coefficient (R2) for values in the range 0 – 10 % (blue rhomboid points) and 15 – 100 % (orange triangles) are reported.

The resistivity decreases more than one order of magnitude for wet samples and stabilizes at similar values, inferior to 1kΩ, for samples having a carbon content higher than 10%. These data confirm the increase of electric contacts, due to the presence of a (slightly) conductive solution filling the void space of materials.

The strong decrease of the electrical resistance of composite A is obviously due to the presence of a connected filamentous structure of biogenic carbon particles in composite A, documented

in Figure 2. Stable and numerous electrical contacts between the single carbon particles were formed during the pyrolysis process, pressed in the porous terracotta matrix, which still is the main component of the composite. For composite B (Figure 3), the clay isolated the carbon particle before the pyrolysis, hindering the stabilization of tight electrical contacts during the pyrolysis process. Indeed, the values of material resistivity of composite B did not express a net correlation with the carbon percentage, remaining in the range of MΩ and sticking close the values of the pure clay.

3.3 Electrical capacitance

The average electrical capacitance measured for all wet samples with 8 mm of thickness is shown in Table 3. Values were negligible, or very low, for all dry samples of both composite A and B, but they significantly increase with the increase of carbon content for composite A, confirming the presence of an increasing hygroscopic conductive carbon surface in this compound.

3.4 Water retention capacity and leaching

The porosity of the different mixes is in direct correlation with the water retention capacity of the samples. Indeed, water fills the micro and macropores of the material, penetrating in the composite. This parameter directly correlates with the increase of carbon percentage for all samples, as shown in the graphic of Figure 6. Due to the higher intrinsic porosity of biochar than terracotta, it is expected behavior. But, the water adsorption raised of almost one order of magnitude for composite A while it almost doubled for composite B.

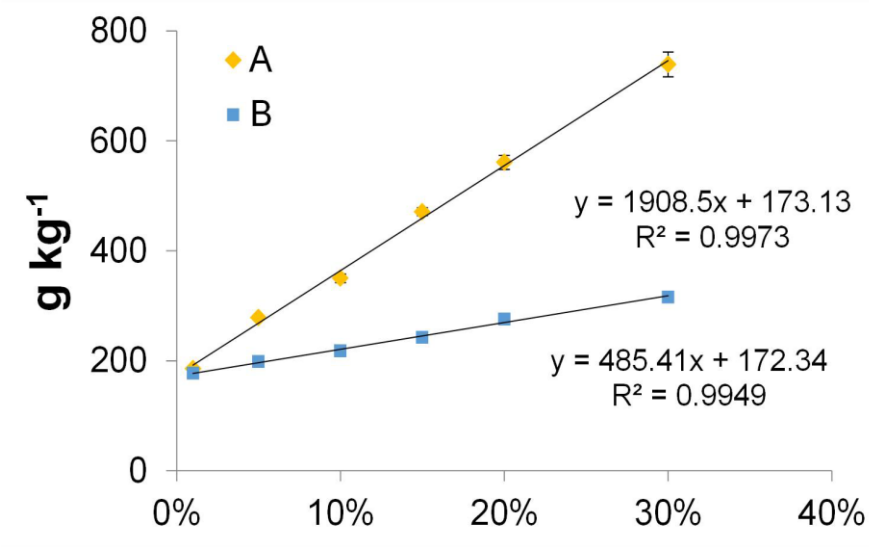

Figure 6 - Graphics of water retention for samples of composite A and B.

The higher capacity of water retention of composite A than B, at the same carbon/clay percentage, indicates that the pyrolysis of a mix of giant cane chipping and clay induces the formation of larger pores inside the composite than the pyrolysis of biochar and clay. This agrees with porosities calculated from microCT data.

The role of the difference in the porosity of biochar formed in a single step of pyrolysis (composite A) and in two steps pyrolysis (composite B) is also underlined by the water leaching, measured at 0.5, 1, and 1.5 m of a water column. The water leaching was always lower than 0.01 ml/h for the sole biochar samples and similar values were found for all tested samples of composite B. On the contrary, water leaching increases of more than one order of magnitude for composite A under a water pressure of 1.5m, when the carbon percentage increases in the samples from 1 % to 10 %. Data of an enhanced water leaching related to the pressure increase for composite A. The kinetic of water leaching through different sample sections (4, 8, and 12 mm) of composite A is shown in Figure 7. Graphics evidence that the linear increase of water leaching stabilizes among sample thicknesses increasing the carbon percentage to 10 %.

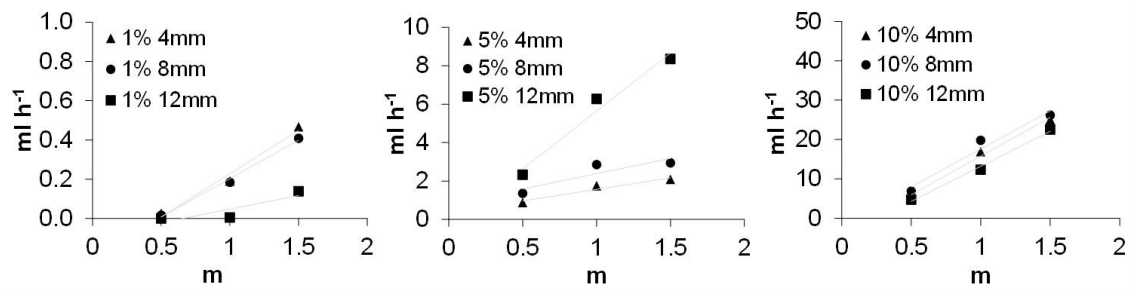

Figure 7 - Leaching kinetic for different water head, in composite A.

4. Discussion

The achieved data are congruent and suggest that the pyrolysis of raw residual biomass, if mixed with clay, produces a solid material (composite A) that is differently performing than one (composite B) produced by pyrolysis of pre-pyrolyzed biomass and clay, in terms of porosity, electrical conductivity, water retention, and leaching.

The structured and connected carbon network of composite A (Figure 2) can justify its lower resistivity in comparison with composite B. Numerous electrical contacts among filamentous carbon particles are built in the matrix of composite A under the pressure of gas bubbles forming and entrapped in the terracotta during the pyrolysis process of biomass. An even more decrease of the electrical resistivity of Composite A is, therefore, expected with an increase

of the biomass percentage over 30%, and with further optimization of the pyrolysis parameters. Such a phenomenon cannot occur for composite B, where the clay envelops already structured biochar particles, working as a perfect insulator among them. Biochar, indeed, does not change the structure during the second step of pyrolysis and does not produce additional gas. In agreement with this explanation, the electrical resistivity and capacity of composite B do not show any correlation with their carbon percentage content, remaining in the range of MΩ and sticking close the values of the pure clay in all cases, also when carbon represents the main component of the composite.

On the other hand, it can be remarked that the biochar from giant cane has a relatively low resistivity value (4 Ωcm), which slightly differs from the value (2.8 Ωcm) of resistivity of carbon cloth commonly used in microbial fuel cells. This conductive biochar was recently tested as an air-cathode electrode of microbial fuel cells targeted to nutrients recovery from wastewaters [Marzorati et al., 2018]. In those experiments, the charge transfer between the electrodes was catalyzed by bacteria settled in the biochar. The current generated, even if low, was sufficient to sustain the bioelectrochemical process.

Two orders of magnitude separate the values of electrical resistivity characterizing the composite A30% (2.4 kΩcm) vs the pure biochar (3.6 Ωcm), and several orders of magnitude in the other cases. This relevant difference makes both composites A and B unattractive for their exploitation as MES electrodes.

Analyzing the results from another perspective, composite A turns out more suitable as an advanced electrolytic separator for a MES. It can allow anodic bacteria to colonize the pores of biochar larger than few microns, which are absent in the pure terracotta. A pure terracotta separator, indeed, impedes the microbial transfer from the anodic chamber to the cathode [Goglio et al., 2019]. Suitably selecting the carbon percentage, it could be possible to control, or enhance, the passage of water and the microorganisms inside the MES system. A similar condition as in the membraneless microbial fuel cells could be reproduced, where the growth of bacteria on the aerobic cathode (as well on the anode) impedes the incoming of oxygen in the anolyte [Rago et al., 2017 and 2018]. Another advantage of this new type of separator could be the improved mechanical property of the system, allowing compact designs and miniaturization. Besides, another recent work [Neethu et al., 2019] proved that composite materials of biochar and terracotta can be a cost-effective alternative to nafion 117 for microbial fuel cells, enhancing ionic hopping inside the material.

Most relevantly, the possibility of reducing electrical resistivity of the composite A simply changing its biogenic carbon percentage lends itself best to be used as the electric connection between the anode and cathode of a MES, replacing the standard external circuit made of a resistor and metal wires. Common electrical resistance usually ranges between 0.1 – 1 kΩ: these values are simply achievable mixing a relatively low percentage of carbon with clay (> 30 %).

The current between the two electrodes (anode and cathode) can be thus suitably limited by tuning the thickness of the separator, as well as the composition ratio of carbon and clay, in function of the application and the environment to be applied on. The possibility of using composite A as a performing electrolytic separator between two electrodes in an innovative MFC concept is sketched in Figure 8.

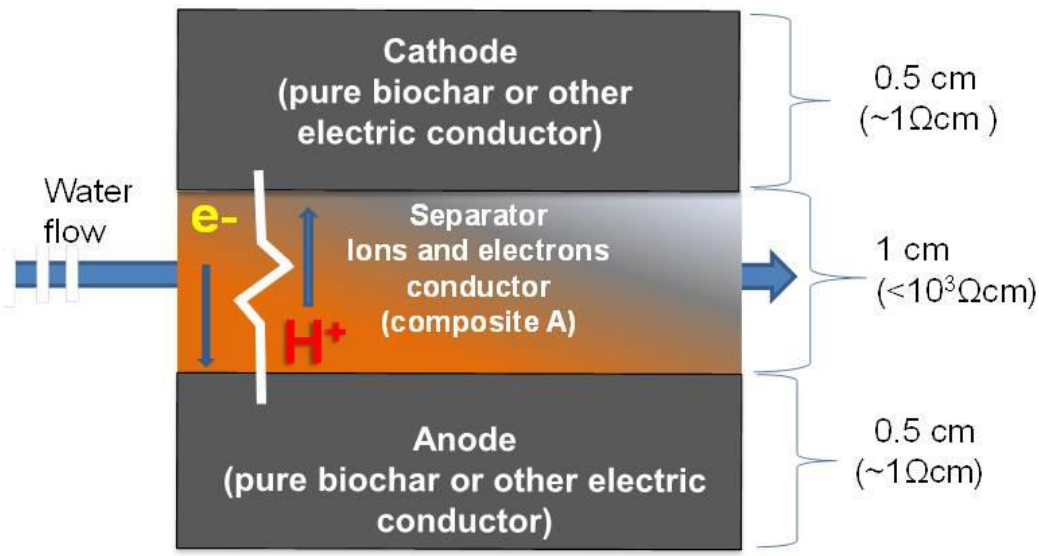

Figure 8 - Schematic of a composite solid MES unit, which electrodes are physically separated by a composite A made of a suitable mix of biochar and terracotta having an electrical resistance of about 1 kΩ.

Based on the achieved results of water leaching, it can be assumed that using a layer of composite A of less than 1 cm and less than 30 % of carbon as separator in a MFC, the water permeability could be high enough to allow the total wetting of the material and continuous water transport across the system, under a relatively low pressure of water. Such a configuration could be suitable also for application in flowing MFC system even for tubular or arbitrary shaped and scaled cells.

4.1 Proof of concept of the new conductive separator

As a simple proof of concept, the performance of different composite separators was tested in single-chamber MFCs. Each selected composite sample (0%, A30%, and B30%) was used to physically connect the anode (carbon cloth) and the air cathode (a titanium grid) of each MFC, avoiding any external electric circuit. For this, the side of the separator facing the anolyte was tightly pressed to a strip of the carbon cloth, while the other face of the separator was pressed to the titanium grid exposed to air.

The test consisted to check the capability of the MFCs to produce power across the separator. If the resistance of the separator is too high, the electrodes operate in an open circuit condition. Consequently, the MFC cannot work. On the contrary, when the ohmic resistance of the composite converges with the internal resistance of the MFC, the circulating current is maximized and the power can peak. Anaerobic conditions at the anode are necessary to create an electromotive force between a more negative anode and a more positive cathode.

Experiments were carried out with a medium of anoxic activated sludge collected from the Milano-Nosedo wastewater plant (Milano, Italy), enriched with 1 g/L of sodium acetate as fuel. Tests lasted 9 days. Conductivity and pH of the solution (anolyte) were measured at the beginning and at the end of the test, in each MFC. No significant differences were detected for these parameters among the MFCs.

The potential of the anode and the cathode were measured vs an Ag/AgCl electrode (3M, Amel, Italy) immersed in the anolyte just for the time of the measurements, on a daily base. Results show that anodes, similarly in all MFCs, become anaerobic in a few days. Cathode potentials were almost constantly positive in the case of MFCs with composite A30% and in one case of composite B30% (which probably suffered because of significant cracks inside the terracotta matrix), while it became negative in the other cases. Possibly, a scarce wetted condition of terracotta and composite B30% separators impeded a good contact with the cathode (airside), so that the measure was most significantly influenced by the negative redox potential of the anolyte, where the reference electrode was immersed.

On the last day of the test, a polarization curve from the MFC voltage to 10 mV between anode and cathode was acquired for each MFC.

Only the MFCs with the composite A30% were able to produce a power, although very low (about 0.04 μW), reaching a maximum power peak in correspondence of resistance of about 1kΩ, as

shown in the graphics of Figure 9. For the other cases, as expected, data suggest that an open circuit condition between electrodes prevailed.

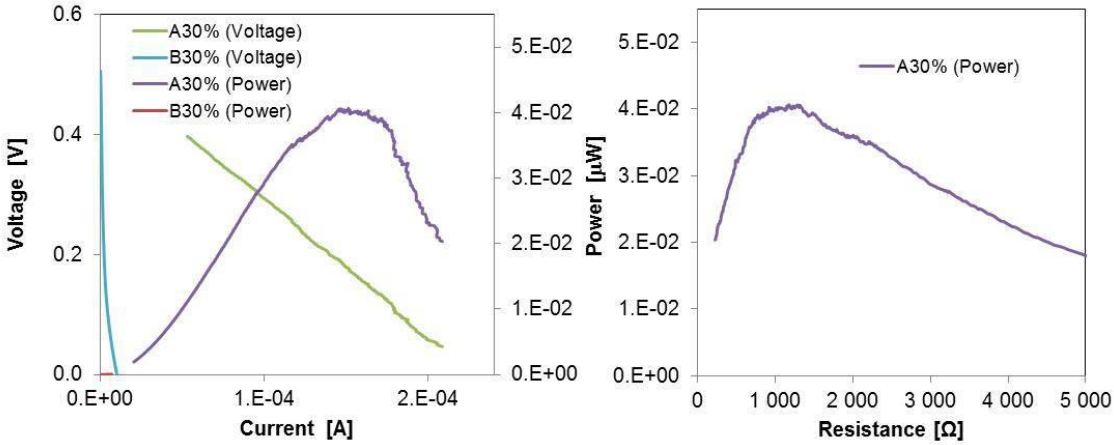

Figure 9 - Power curves of single-chamber MFCs equipped with a composite 30%A and 30%B, respectively, connecting the anode to the cathode instead the external circuit. The power curve plotted vs the corresponding resistance is also plotted.Based on this test, although power produced was almost negligible, it can be confirmed that the composite A30%, among the tested ones, act as an external circuit of about 1000Ω, as explained in the schematic of Fig 8.

At the end of the experiment, composite samples were collected from the MFCs for observations. The side exposed to the anolyte of each separator showed a visible rich biofilm grew on.

Each operated composite sample was, then, dried in a oven for 30 min and fixed by gold before observed by Scanning Electron Microscopy. SEM micrographs of the transversal section of each tested composite separator (0% A30% and B30%) are reported in Figure 10.

Biofilm was not found inside the terracotta sample, as expected. More biofilm was detected on one of the composite 30%B, which presented cracks inside and more positive cathode potential. Traces of biofilm were also detected in the carbon component of the other sample of B30% composite. A consistent layer of biofilm and abundant bacteria on the surface were documented through the entire section of the composites A30%, which cathode sides were also the most wetted ones. Besides for the electrical conductivity, this last result is relevant, because wet conditions across the MFC system can be crucial to maintain microbial fuel cells operating in environmental applications, such as in the soil, where the humidity variation can strongly affect the MFC performance.

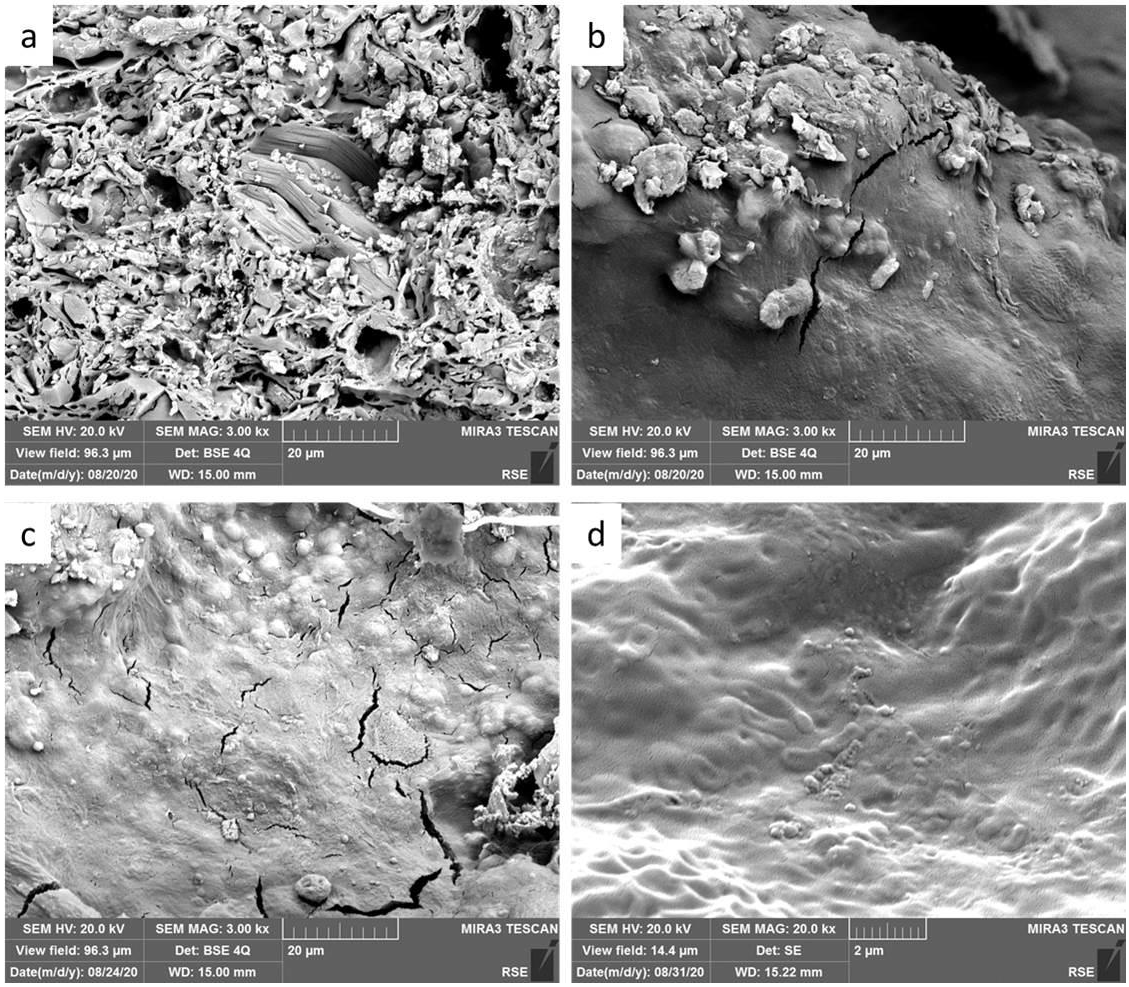

Figure 10 - SEM Micrographs of transversal section of composite after the operation in the MFCs. a) terracotta (0%); b) Composite B30%; c) composite A30%; d) composite A30% at higher magnitude, most evidently showing bacteria shapes.

Although the experiment was short and the used MFC system was low performing, the results clearly underline the suitability of the Composite A as an electrolytic and electric conductor in a MFC, as sketched in Figure 8.

Furthermore, the simple preparation of the composite A through a single step of pyrolysis of raw biomass and clay enhances its attractiveness for cost-effective MESs.

Terracotta and biochar are widely recognized materials for use in agriculture, i.e. as soil fertility promoter or plants containers respectively. Considering hence the possibility of remediating soil and water, as well as recovering nutrients by the microbial fuel cell

technology, the large-scale application of terracotta-biochar composite in MFCs is particularly promising in the perspective of a circular economy concept.

5. Conclusions

A new composite material, produced by the pyrolysis of raw biomass mixed with clay, can cover the double function of ions and electrons conductor. Mixing a relatively low biomass proportion with clay (i.e. 30 % w/w carbon, balance clay), it is possible to produce solid and porous biochar-terracotta composites which electrical resistivity can decrease to less than 1000 Ω and reduces when wetted by water. Such electrical resistance falls in the range usually used for connecting the electrodes of MFC through an external circuit.

This new composite allows, therefore, a new, revolutionary, concept of microbial fuel cell including the electric circuit inside the electrolytic separator.

Eliminating the necessity of external electric circuits, simple and robust devices can be produced, based solely on natural components (residual biomass and clay), that could simplify the large scale application of MFC technology for environmental application such as bioremediation of water and soils and to recovery nutrients for agriculture in a circular economy concept.

The low cost of the components (biochar and terracotta) and the low technological level required for their preparation (clay and residual biomass to be pyrolyzed) could allow a large-scale production and re-use of this MES type in low technological contexts as well as in industrialized countries.

Acknowledgments

This work was financed by the SIR 2014 Grant (PROJECT RBSI14JKU3), Italian Ministry of University and Research (MIUR) and the Research Fund for the Italian Electrical System (Decree: MISE, April 16, 2018). The contribution of Andrea Parozzi for the resistance and capacitance tests is gratefully acknowledged.

References

Ajayi, F. F., Weigele, P. R. (2012). A terracotta bio-battery. Bioresour. Technol., 116, 86-91. DOI: 10.1016/j.biortech.2012.04.019

Behera, M., Jana, P.S., Ghangrekar, M.M. (2010). Performance evaluation of low cost microbial fuel cell fabricated using earthen pot with biotic and abiotic cathode. Bioresour. Technol. 101, 1183–1189. doi:10.1016/j.biortech.2009.07.089

Cristiani, P., Carvalho, M.L., Guerrini, E., Daghio, M., Santoro, C., Li, B. (2013). Cathodic and anodic biofilms in Single Chamber Microbial Fuel Cells. Bioelectrochemistry 92, 6–13. doi:10.1016/j.bioelechem.2013.01.005

Cruz Viggi, C., Simonetti, S., Palma, E., Aulenta, F. (2017). Enhancing methane production from food waste fermentate using biochar: The added value of electrochemical testing in pre-selecting the most effective type of biochar. Biotechnology for Biofuels 10, 303-313. DOI:10.1186/s13068-017-0994-7.

Elmekawy, A., Hega C., H.M., Pant, D. (2014). Review on the Near-Future Integration of Microbial Desalination Cell with Reverse Osmosis Technology. Energy & Environmental Science A 12, 3921-3933. doi:10.1039/x0xx00000x

Giudicianni, P., Cardone, G., Sorrentino, G., Ragucci, R. (2014). Hemicellulose, cellulose and lignin interactions on Arundo donax steam assisted pyrolysis. J. Anal. Appl. Pyrolysis 110, 138–146. doi:10.1016/j.jaap.2014.08.014

Goglio, A, Marzorati, S., Rago, L., Pant, D., Cristiani, P., Schievano, A. (2019). Microbial recycling cells: first steps into a new type of microbial electrochemical technologies, aimed at recovering nutrients from wastewater. Bioresour. Technol. 277, 117-127. doi:10.1016/J.BIORTECH.2019.01.039

Goglio, A., Tucci, M., Rizzi, B., Colombo, A., Cristiani, P., Schievano, A. (2019). Microbial recycling cells (MRCs): A new platform of microbial electrochemical technologies based on biocompatible materials, aimed at cycling carbon and nutrients in agro-food systems. Sci. Total Environ. 649, 1349-1361. doi:10.1016/j.scitotenv.2018.08.324

Kappler, A., Wuestner, M.L., Ruecker, A., Harter, J., Halama, M., Behrens, S. (2014). Biochar as an Electron Shuttle between Bacteria and Fe(III) Minerals, Environ. Sci. Technol. Lett. 1, 339–344. doi:10.1021/ez5002209.

Li, W.-W., Sheng, G.-P., Liu, X.-W., Yu, H.-Q. (2011). Recent advances in the separators for microbial fuel cells. Bioresour. Technol. 102, 244–252. doi:10.1016/j.biortech.2010.03.090

Longhi, M., Marzorati, S., Checchia, S., Sacchi, B., Santo, N., Zaffino, C., Scavini, M. (2016). Sugar-based catalysts for oxygen reduction reaction. Effects of the functionalization of the nitrogen precursors on the electrocatalytic activity. Electrochimica Acta 222, 781-792. doi.org/10.1016/j.electacta.2016.11.036

Marzorati, S., Goglio, A., Fest-Santini, S., Mombelli, D., Villa, F., Cristiani, P., Schievano, A., 2018. Air-breathing bio-cathodes based on electro-active biochar from pyrolysis of giant Cane stalks. Int. J. Hydrogen Energy, 44(9) 4496-4507.doi:10.1016/j.ijhydene.2018.07.167

Mathuriya, A.S., Pant, D. (2018). Assessment of expanded polystyrene as a separator in microbial fuel cell. Environ. Technol. 40 (16) 2052-2061. doi:10.1080/09593330.2018.1435740

Milner, E.M., Popescu, D., Curtis, T., M., Head, I., Scott, K., Yu, E. H. (2016). Microbial fuel cells with highly active aerobic biocathodes, Journal of Power Sources 324, 8-16. Doi:10.1016/j.jpowsour.2016.05.055

Neethu, B., Bhowmick, G.D., Ghangrekar, M.M. (2019). A novel proton exchange membrane developed from clay and activated carbon derived from coconut shell for application in microbial fuel cell. Biochemical engineering journal 148, 170-177. doi: 10.1016/j.bej.2019.05.011

Ng, K.S., Head, I., Premier, G.C., Scott, K., Yu, E., Lloyd, J., Sadhukhan, J., (2016). A multilevel sustainability analysis of zinc recovery from wastes. Resour. Conserv. Recycl. 113, 88–105. doi:10.1016/j.resconrec.2016.05.013

Pasternak, G., Greenman, J., Ieropoulos, I. (2015). Comprehensive Study on Ceramic Membranes for Low-Cost Microbial Fuel Cells. ChemSusChem 9 (1) 88–96. doi:10.1002/cssc.201501320

Prado, A., Berenguer, R., Esteve-Núñez, A., (2019). Electroactive biochar outperforms highly conductive carbon materials for biodegrading pollutants by enhancing microbial extracellular electron transfer, Carbon 146, 597-609. doi:10.1016/J.CARBON.2019.02.038.

Rago, L., Cristiani, P., Villa, F., Zecchin, S., Colombo, A., Cavalca, L., Schievano, A. (2017). Influences of dissolved oxygen concentration on biocathodic microbial communities in microbial fuel cells. Bioelectrochemistry 116, 39–51. doi:10.1016/J.BIOELECHEM.2017.04.001

Rago, L., Zecchin, S., Marzorati, S., Goglio, A., Cavalca, L., Cristiani, P., Schievano, A. (2018). A study of microbial communities on terracotta separator and on biocathode of air breathing microbial fuel cells. Bioelectrochemistry 120, 18-26. doi:10.1016/j.bioelechem.2017.11.005

Ramírez-Moreno, M.J., Romero-Ibarra, I.C., Ortiz-Landeros, J., Pfeiffer, H. (2014). Alkaline and Alkaline-Earth Ceramic Oxides for CO 2 Capture, Separation and Subsequent Catalytic Chemical Conversion, in "CO2 Sequestration and Valorization", chap.14. doi:10.5772/57444

Santini, M., Fest-Santini, S., Foltyn, P. (2016). On the local mass transfer rates around arbitrary shaped particles calculated by X-ray computed microtomography: Prospective for a novel experimental technique. Int. Commun. Heat Mass Transf. 79, 135–139. doi:10.1016/j.icheatmasstransfer.2016.11.001

Santini, M., Guilizzoni, M., Fest-Santini, S. (2013). X-ray computed microtomography for drop shape analysis and contact angle measurement. J. Colloid Interface Sci. 409, 204–210. doi:10.1016/j.jcis.2013.06.036

Santoro, C., Arbizzani, C., Erable, B., Ieropoulos, I. (2017). Microbial fuel cells: From fundamentals to applications. A review. J. Power Sources 356, 225-244. doi:10.1016/j.jpowsour.2017.03.109

Santoro, C., Artyushkova, K., Gajda, I., Babanova, S., Serov, A., Atanassov, P., Greenman, J., Colombo, A., Trasatti, S., Ieropoulos, I., Cristiani, P. (2015). Cathode materials for ceramic based microbial fuel cells (MFCs), in: International Journal of Hydrogen Energy 40 (42) 14706–14715. doi:10.1016/j.ijhydene.2015.07.054

Schievano, A., Berenguer, R., Goglio, A., Bocchi, S., Marzorati, S., Rago, L., Louro, R.O., Paquete, C.M., Esteve-Núñez, A. (2019). Electroactive Biochar for Large-Scale Environmental Applications of Microbial Electrochemistry. ACS Sustain. Chem. Eng. 7, 22, 18198–18212. doi:10.1021/acssuschemeng.9b04229

Sengupta, S., Nawaz, T., Beaudry, J., 2015. Nitrogen and Phosphorus Recovery from Wastewater. Curr. Pollut. Reports. 1, 155–166. doi:10.1007/s40726-015-0013-1

Tiquia-Arashiro, S.M., Pant, D., Microbial Electrochemical Technologies, (2020) CRC Press. 518p.,doi:10.1201/9780429487118.

Walter, X.A., Gajda, I., Forbes, S. Winfield, J., J., Greenman, Ieropoulos, I. (2016). Scaling-up of a novel, simplified MFC stack based on a self-stratifying urine column. Biotechnol Biofuels 9, 93 https://doi.org/10.1186/s13068-016-0504-3

Winfield, J., J., Greenman, Huson, D., J., Ieropoulos, I. (2013). Comparing terracotta and earthenware for multiple functionalities in microbial fuel cells. Bioprocess and Biosystems Engineering 36(12) 1913 – 1921. DOI: 10.1007/s00449-013-0967-6

Zhang, G., Zhao, Q., Jiao, Y., Wang, K., Leec, D.J, Ren, N. (2012). Biocathode microbial fuel cell for efficient electricity recovery from dairy manure. Biosensors and Bioelectronics 31(1), 537-543. doi.org/10.1016/j.bios.2011.11.036.

Chapter 9 - Nutrients-enriched electroactive biochar as soil amendment under anoxic conditions: a circular economy approach

Andrea Goglio[1], Danielle L. Gelardi[2], Devin Rippner[2], Andrea L. Aguilera[2], Sanjai J. Parikh[2], Andrea Schievano[1]

1 e-BioCenter, Department of Environmental Science and Policy (ESP), Università degli Studi di Milano, Via Celoria 2, 20133 Milan, Italy

2 University of California-Davis, Department of Land, Air and Water Resources, One Shields Ave., Davis, CA 95616, United States of America

Abstract

Inorganic salt deposition and biofouling hinder long-term operation of bio-electrochemical systems (BES) used in wastewater treatments. Here, a new version of EC-biofilter, that aims not only at oxidizing organic loading, but also at recovering soluble minerals from the liquid phase as fertilizers. To do this, we propose a new type of cylindric cathodes built by pyrolysis of low-cost lingo-cellulosic materials such as Giant Canes (Arundo Donax L.) connected with an anode (conductive granules). The tests were repeated in subsequent batch tests using swine manure with 6 g COD L^{-1}. Along 60 days, consistent amounts of the main macronutrients (N, P, K, Fe, Mn, Ca, Mg) were removed from the wastewaters and deposited on the biochar cathodic surface. After their life-course, these cathodes were replaced and entirely re-utilized as soil amendment in rice pots and compared with a traditional NPK fertilization in rice cultivation. The results in leaves and roots biomass production confirm the aim of the experiment with a productivity of 15 g of leaves and 70 g of roots for rice plant.

Keywords

Bioelectrochemical systems, electrochemical biofilter, nutrients recovery, soil amendment, e-biochar, rice plant

1. Introduction

As shown by recent studies, the demand for food will continue to increase, mainly as a result of population growth both in high-income countries and even more in low-income countries (sub-Saharan Africa and South Asia) (FAO, 2017). All around the world, agricultural production is showing no significant improvement in output yields since the 1990s. Thus, to satisfy food demand, during the last decades there was an exponential conversion of natural lands toward intensive agriculture usage. However, this tendency brought also negative externalities such as soil degradation (erosion, salinization), depletion and pollution of natural water resources, build-up of pest resistance, biodiversity and environmental quality losses (Jeworski, 2002).

Nonetheless, chemicals and mineral fertilizers played a key role in this increase of the agricultural production. Nitrogen is a major soil-limiting element in the majority of soils (Nhamo et al., 2014). Currently, ammonia, ammonium nitrate, and urea are synthetized following the Haber-Bosh process: high temperature and pressure fixation of atmospheric N_2 in which methane from natural gas is the major source of hydrogen (Haustein, 2019). On the other hand, raw minerals rich in P, K and Mg are extracted from rock mines, with high environmental

footprints (Cordell et al., 2009; Kratz et al., 2016). Nowadays, mineral fertilization is still a supporting column for global agricultural production and frequent over-fertilization and intensive agriculture practises are causing the release of nitrogen compounds in to the environment (FAO, 2017). Serious consequences are eutrophication, contamination of groundwater and drinking water, air pollution and emission of important greenhouse gasses (Pielke, 2013; Weinbaum et al., 2018). The massive fertilization with mineral macronutrients is also strongly contributing to the impoverishment of micronutrients in agricultural soils. In addition, another related problem is the soil organic pool oxidation and following emission as CO_2, CH_4 and N_2O (Mohamed et al., 2015). In fact, soil fertility over long-terms strictly depends on the soil organic matter content, and so on the maintenance of the organic carbon (Fenton et al., 2008; Lobb, 2008).

It is widely recognized that wastewater derived from food production chains should be treated in a sustainable way, to minimize environmental contamination, while maximizing the recovery of valuable resources (carbon and nutrients) (Verstraete et al., 2009). Nutrients removal from water solution and recovery as renewed fertilizers is of particular interest, because of the potential threat of natural water bodies over-fertilization, the limited mining resource and high cost associated with nutrient production (Rittmann et al., 2011). Research in the field of microbial electrochemical systems (MES) has been tremendously expanding over the last decades. Microbial fuel cells (MFCs) and microbial electrolysis cells (MECs) were deeply studied due to their promising ability to treat different kinds of wastewater through bio-electrochemical reactions (Pandey et al., 2016; Puig et al., 2010; Santoro et al., 2013).

This would work only if alternative air-water separators and electrodes were fabricated using low-cost, biogenic and biocompatible materials. Good examples of such materials are terracotta, to be used as porous separator and pyrolysed ligno-cellulosic biomass (bio-charcoal), to be used as conductive electrode material. The catholyte production was generated by the electro-osmotic forces and the high cathodic pH. Also, increased pH and water evaporation from the air-water interface contributed to salts precipitation and heavy metals recovery (Winfield et al., 2016). Moreover, the possibility of recovering macronutrients (e.g. N, P, K, Ca, Mg, etc.) was shown. Ammonium ions are dragged by electro-osmotic forces to the cathodic surface, where pH is typically higher than pH=9; under such conditions ammonia stripping (Santoro et al., 2013) and/or struvite precipitation (Merino-Jimenez et al., 2017) can be favoured to recover nutrients as insoluble salts. Ammonium was also reported to undergo anaerobic or microaerophilic oxidations to nitrites and nitrates, respectively at the anode and

at the air-water interface. Successive denitrification was also reported, in presence of bioavailable organic carbon.

Pyrolysed ligno-cellulosic biomass was introduced in recent studies, for the production of electrode materials (Basso and Cukierman, 2005; Giudicianni et al., 2014; Katuri et al., 2018). Evidences of the positive effects of biochar on soil fertility and to improve carbon sinks are well-known in the literature and the biochar sector is today a reality (Laird et al., 2010; Vaccari et al., 2011). Biochar has been largely studied as agricultural soil amendment, capable of favouring soils properties, acting as carbon sink over long term, stimulating soil microbial communities in several important soil processes (Atkinson et al., 2010; Lehmann et al., 2011). It has been known that the microscopic structure and the textural properties of biochar are primary determinants in its soil conditioning properties; the surface area of the precursor material can be increased several thousand folds. This increased surface area is the result of thermal decomposition of the organic material through which volatiles are driven off and the remaining structure is comprised of highly concentrated carbon chains. In particular, the proportion of micro-, meso- and macro-pores in biochar influence hydrophilic properties and water storage (Brussaard et al., 2007; Lehmann and Joseph, 2015). Biochar can also act on the microflora surrounding the plant root system (Lehmann et al., 2011). The improvement of biological activity, as well as chemical and physical properties of soil is at the basis of conservation agriculture, the green solution to counteract impacts of agronomic practices. Further, redox processes involving the donation and acceptance of electrons play an important part in soils, such as in nutrient cycling, decomposing organic matter, including biochar, can be regarded as an electron-pump supplying electrons to more oxidised species present in the soil system. Additions of high concentrations of biochar into the rhizosphere could introduce an environment that contrasts the one that would naturally develop there from the typical soil clays, silt, sand and organic matter components. The redox potential in the immediate area around the biochar particle could change as solutions rich in organic compounds, cations and anions, diffuse in and out of the macro- and meso-pores of the biochar (Joseph et al., 2015).

2. Materials and methods

2.2 Experimental set-up

The experiment is divided in two different parts, in the first a EC-biofilter coupled with e-biochar air-cathodes is used to treat the swine manure and recovery nutrients at the cathode and in the second one the e-biochar air-cathodes is used as soil amendment in rice pots

cultivation. The first part of the experiment start with a EC-biofilter reactor of 0.50 m tall and a diameter of 0.15 m. Here, a new version of EC-biofilter that aims to oxidize the organic loading to recover the soluble minerals from the liquid phase, as fertilizers. To do this, we propose a new type of cylindric cathodes built by pyrolysis of low-cost lingo-cellulosic materials such as Giant Canes (Arundo Donax L.) immerged in an anode of conductive granules (EC-biofilter). The reactor was feed in batch tests using swine manure.

The second part of the experiment was organised in 25 rice pots. The pots were flooded and composed by 1 kg of Yolo soil. The experiments set-up was organised with 5 trials and everyone had 5 replicates. The 5 trials were: soil without fertilization (control 1), soil + e-biochar without fertilization (control 2), soil with fertilization, soil + e-biochar with fertilization and soil + enriched e-biochar air-cathodes + urea. The rice pots were cultivated in a growing chamber with 16 hours of light and 8 of dark with a changing in temperature from 25°C to 35°C. As fertilization was used a traditional NPK formula for the rice cultivation (165 kg ha^{-1} N, 45 kg ha^{-1} P and 50 kg ha^{-1} K) while, for the pots with the enriched e-biochar air-cathodes was added just 120 kg ha^{-1} of urea.

2.4 Physico-chemical characterization

The chemical composition of the swine manure along the batch cycles was monitored by several parameters: chemical oxygen demand (COD), total nitrogen (TN) and total content of the main macro- and micro-nutrients (K, P, Mg, Fe, Mn) analysed by inductively coupled plasma mass spectrometry (ICP-MS). In addition, the enrichment in these elements on the biochar air-cathodes was determined at the end of the experiment, adding also nitrate (NO_3-) and ammonia (NH_4+).

The samples were filtered (0.45 µm Nylon filters) before the analysis. ICP-MS (BRUKER Aurora-M90 ICP-MS) was used to measure single elements in the soluble fractions and in the extracts of the terracotta separators. Extraction: Soil (1 g) was added to 50 ml volumetric glass digestion vessels and acid digested with 7.0 ml of trace metal grade HCl (12.1 M) and 2.3 mL of HNO_3 and allowed to equilibrate overnight. The following day, soils were digested at 120 °C for 4 hours, vortexed repeatedly to ensure adequate mineralization, and then brought to volume. The resulting digestate was diluted 1:10 with 1% HNO_3 for trace metal analysis by ICP-MS. Calibration curve accuracy was confirmed by certified reference material (1640a), digestion blanks and a loam soil reference material (ERM CC141) were carried through the digestion process for quality control and recovery assurance (Rippner et al., 2018). During the

experiments were monitored also the pH, Eh and chlorophyll trends. The Eh was measured daily with and electrode of carbon cloth fixed at the bottom of the pot vs an Ag/AgCl reference electrode. Instead the chlorophyll trends was measured by the infrared meter ATLEAF.

3. Results and Discussions

3.1 Nutrients enriched e-biochar

Table 1 shows the percentage of elements removed from swine manure in the 4 cycles during the 60 days of operation time.

Table 1 - Percentage of elements removed from swine manure (%)

COD	67.53 ± 4.36
TN	60.21 ± 4.99
NH_4+	59.97 ± 4.73
NO_3-	69.27 ± 14.14
Na	49.60 ± 5.08
Mg	62.68 ± 3.31
K	32.48 ± 1.04
Ca	54.86 ± 6.54
Mn	71.21 ± 2.92
Fe	69.31 ± 15.67
Zn	32.69 ± 26.84
P	71.29 ± 4.63

The results show an interesting removal in the most important nutrient around 60-70% except for the potassium that was 32.48 %. These results are confirmed by the nutrients recovered on the e-biochar air-cathodes. In table 2 are reported the soil and nutrients enriched e-biochar composition.

Table 2 – Soil and nutrients enriched biochar composition (mg kg^{-1})

	Soil	EN-biochar
NH_4+	59.13 ± 3.10	148.52 ± 10.59
NO_3-	32.16 ± 1.50	5.46 ± 1.04
Mg	179.53 ± 43.65	360.82 ± 24.49
K	145.25 ± 53.45	14490.77 ± 2620.67
Ca	124.92 ± 33.60	228.17 ± 28.76
Mn	0.25 ± 0.18	4.02 ± 0.30
Fe	10.17 ± 6.21	1.43 ± 0.27
Zn	0.11 ± 0.08	0.25 ± 0.07
P	29.03 ± 0.84	4565.52 ± 52.29

The results confirmed the high nutrients removal from the wastewater with an increasing of elements in to the e-biochar air-cathode with and high results of recovery for the potassium. This result in potassium recovery explain that the less percentage removal due to the high solubility of this elements that probably was solubilized from the e-biochar. Moreover, the table 2 shows also the characterization of the Yolo soil that appear as a nutrients rich soil. The experiment was performed with the variety of rice M-206 and it was used 1% of e-biochar v v^{-1}. The fertilization that was used as a control was 165 kg ha^{-1} N, 45 kg ha^{-1} P and 50 kg ha^{-1} K, while for the enriched e-biochar air-cathode was added just 120 kg ha^{-1} N (urea).

3.2 e-biochar as soil amendment in anoxic conditions

The aim of this work was to use the nutrients enriched e-biochar air-cathodes as soil amendment and in the same time compare it with the traditional NPK fertilization used in a rice cultivation.

Figure 1 shows the pH and Eh trends of the soil over 60 days where both were drastically different compare the use or not of the e-biochar.

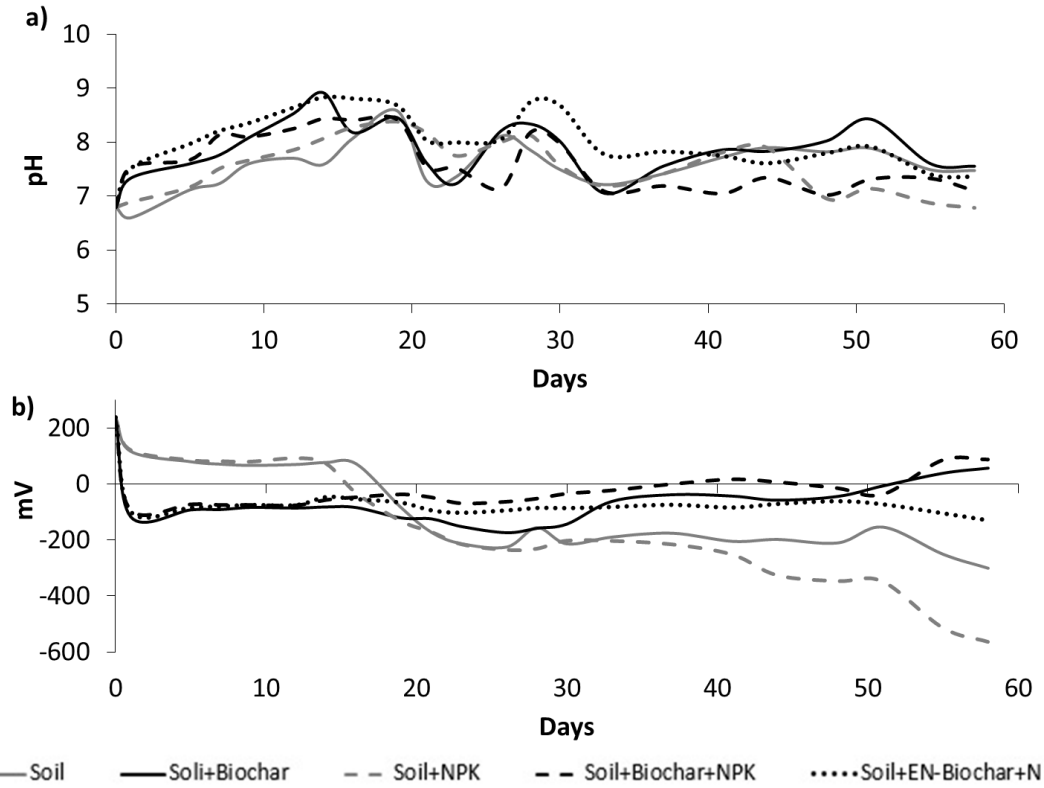

Figure 1 – pH **(a)** and Eh **(b)** of the soil over 60 days.

The pH trend figure evince a different kinetics of pH in the first 2 weeks of experimentation, where the pots with 1% of e-biochar increase their pH of 1 point compare with the pots without e-biochar but after this starting period the pH value return similar for both of them. Different is the situation for the figure 1b where the Eh trends are reported. Here, it is shown a huge different between the pots with or without e-biochar. The pots without e-biochar start with a positive Eh around 200 mV vs SHE and after 14 days start to decrease drastically day by day, while for the e-biochar pots the situation were the opposite, with the pots that after a deep decreasing around -100 mV vs SHE increase their working potential around the neutrality.

Both figures 2 and 3 show a comparable results about the amount of leaves and roots biomass harvested at the end of the experiment. In both of them is possible to observe that the amount of leave biomass in drastically affected by the fertilization, in fact there are significant difference just with or without fertilization. In other hand, the two figures show an interesting different in the roots biomass, they demonstrate that with an adding of electroactive biochar is possible to increase the rhyzosphere and also focusing on the e-biochar air-cathodes is visible

further increase to be attributed to the high presence of micronutrients that stimulated the growth of the root system.

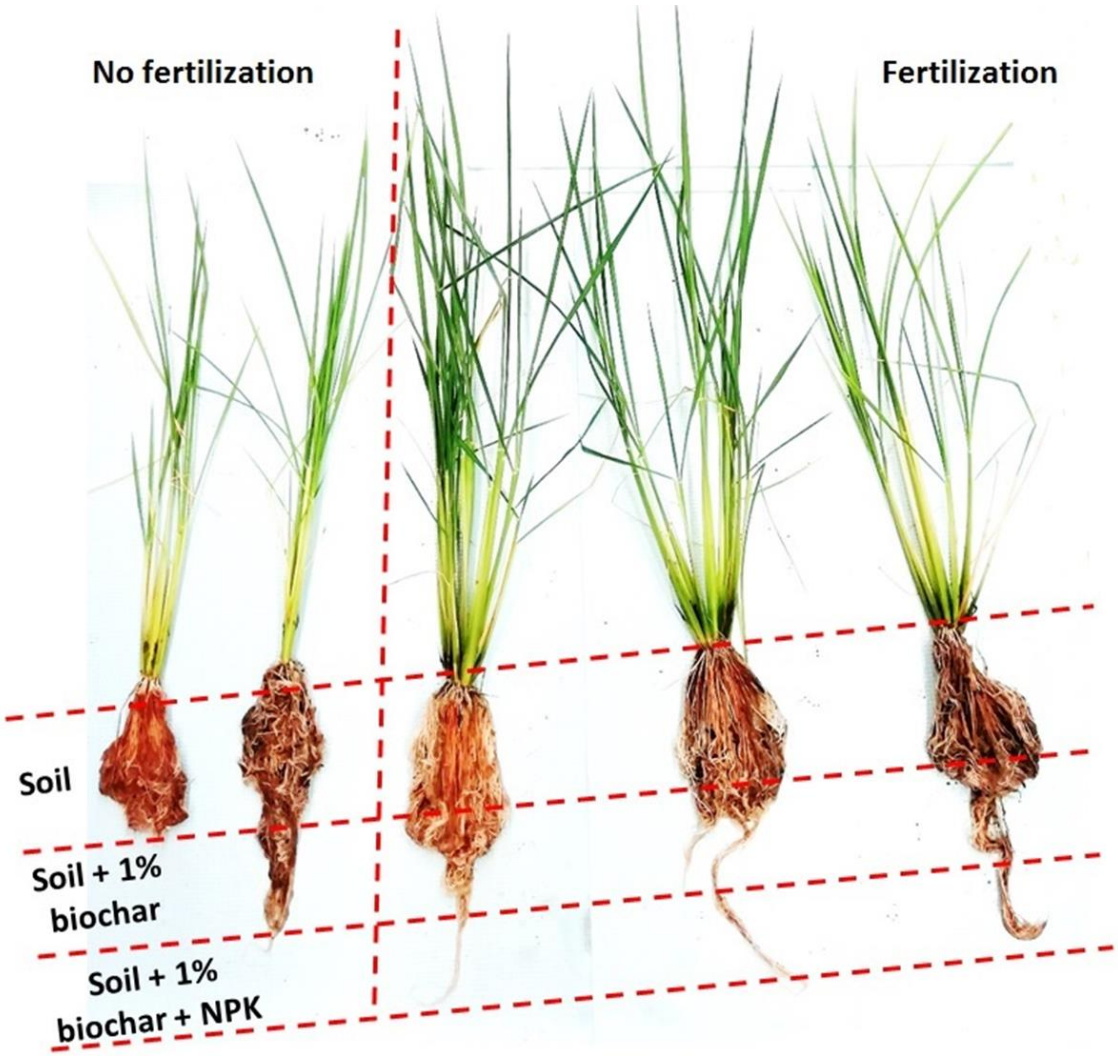

Figure 2 - Photo comparison at the end of the experiment

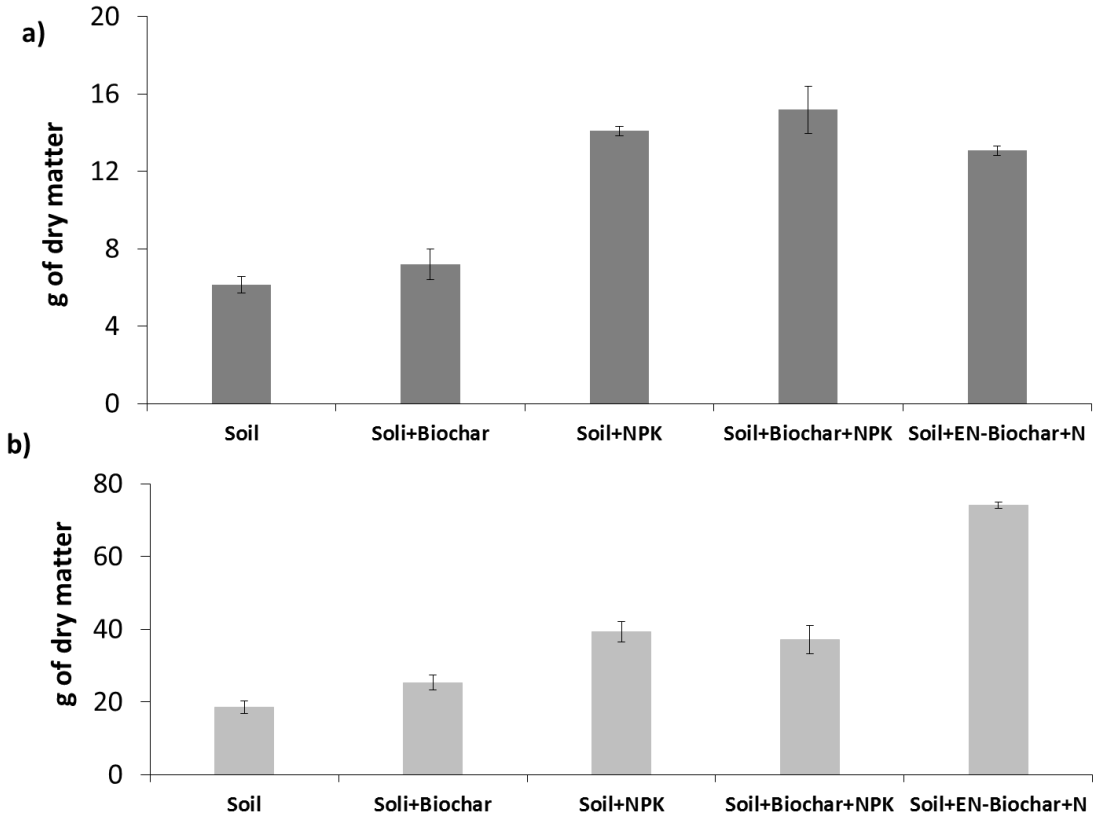

Figure 3 - Leaves (a) and roots (b) biomass at the end of the experiment

Figure 4 shows the trend of chlorophyll in the leaves throughout the experiment. Usually the quantity of chlorophyll in the leaves can also be expressed as the well-being of the plant. In these trends is clearly visible the difference between the pots with or without fertilization and above all the pot fed with enriched e-biochar air-cathodes are perfectly comparable with the other fertilized ones.

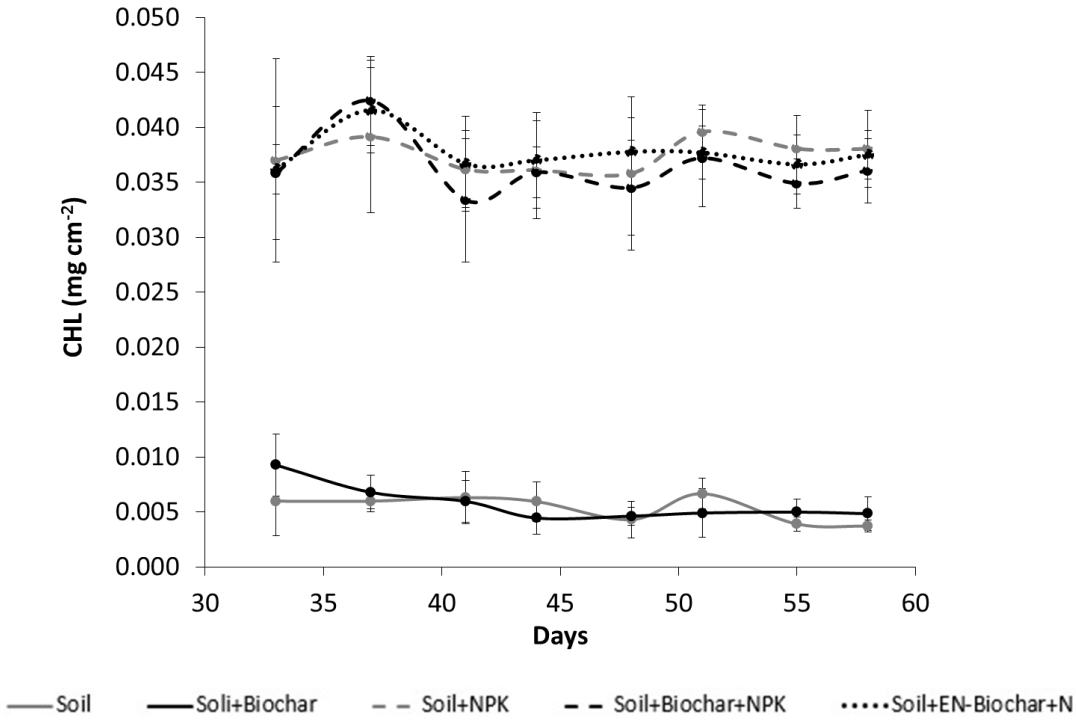

Figure 4 – Chlorophyll trends over 60 days.

Also in figure 5 and 6, where the quantity of elements are present both in the leaves and in the roots, it is observable the same trend of the previous results, in which a big difference can be noted between the pots with and without fertilization. Beyond this difference, the main purpose can be confirmed, that is to demonstrate that the enriched e-biochar is able to obtain the same performance of a traditional NPK fertilization and especially in certain cases by observing an increase in nutrients in the sheets.

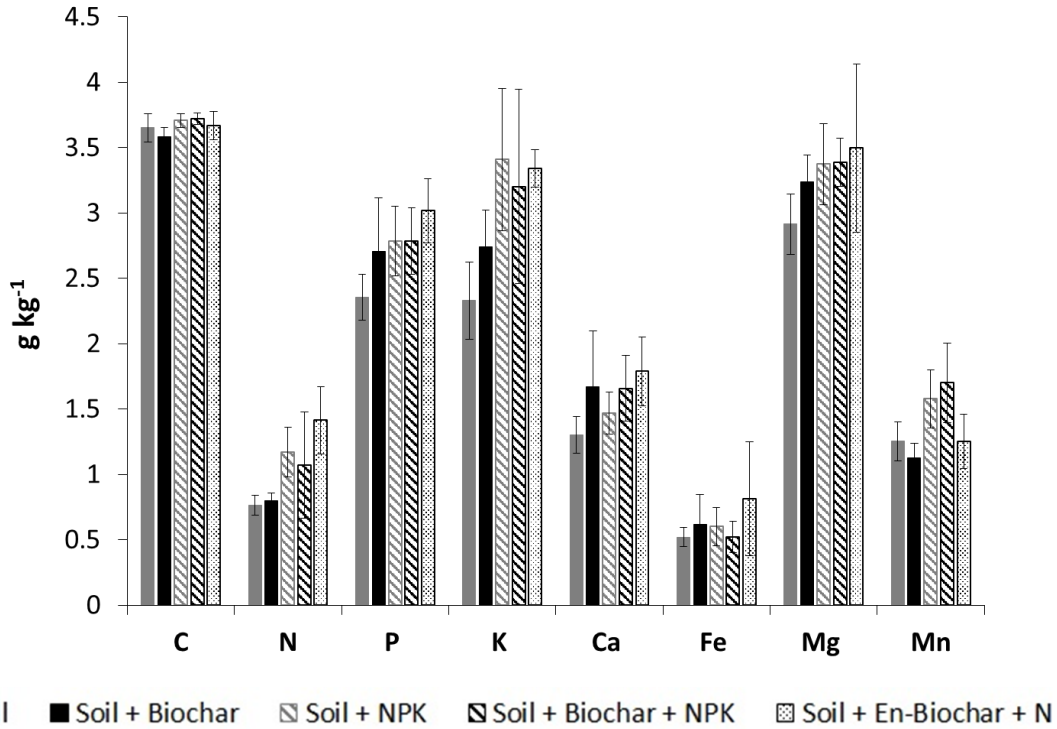

Figure 5 - Elements content in leaves at the end of the experiment

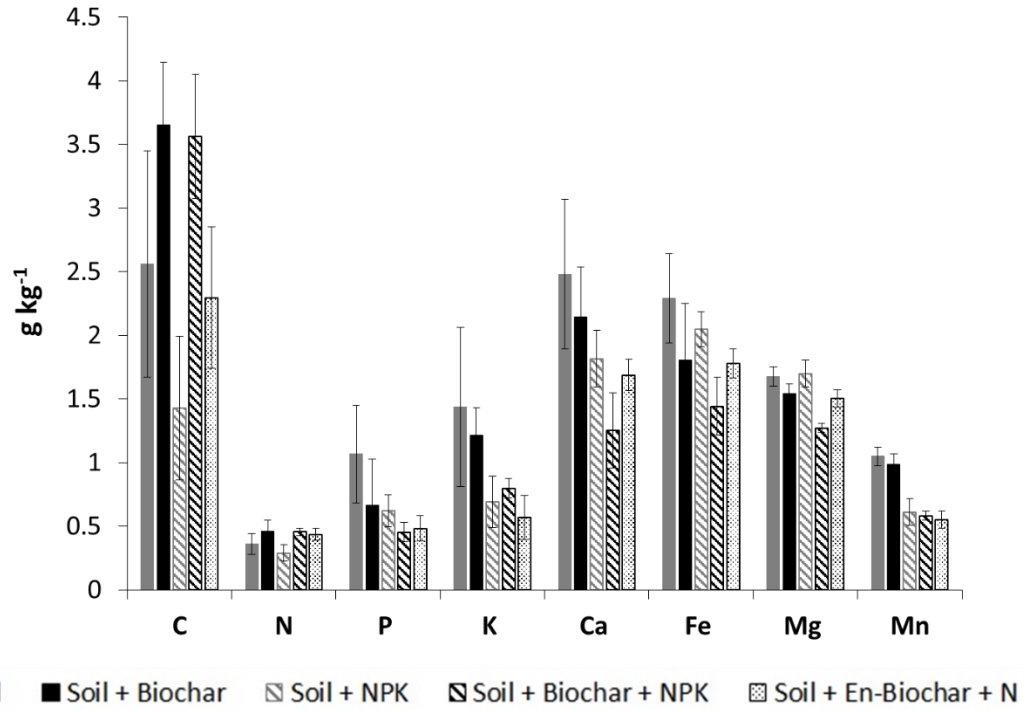

Figure 6 - Elements content in roots at the end of the experiment

4. Conclusions

EC-biofilter coupled with e-biochar air-cathodes built with low-cost, biogenic and biocompatible materials demonstrate the real possibility of recovering nutrients from organic-rich wastewater streams coming from farming and agro-industrial productions. At the end of the operational period of e-biochar air-cathodes, becoming saturated by micro and macronutrients and they are used as soil amendment in rice pots cultivation in a circular economy concept. The experiment shows the real possibility to use the nutrients enriched e-biochar as soil amendment and in the same time compare it with the traditional NPK fertilization used in a rice cultivation, opening a new view in the wastewater treatments.

Acknowledgements

This work was financed by the SIR 2014 Grant (PROJECT RBSI14JKU3), Italian Ministry of University and Research (MIUR) by the Research Fund for the Italian Electrical System in compliance with the Decree of March, 19th 2009 and by the Environmental Soil Chemistry Group of the University of California – Davis.

References

Atkinson, C.J., Fitzgerald, J.D., Hipps, N.A., 2010. Potential mechanisms for achieving agricultural benefits from biochar application to temperate soils: a review. Plant Soil 337, 1–18. doi:10.1007/s11104-010-0464-5

Basso, M.C., Cukierman, A.L., 2005. Arundo d onax -Based Activated Carbons for Aqueous-Phase Adsorption of Volatile Organic Compounds. Ind. Eng. Chem. Res. 44, 2091–2100. doi:10.1021/ie0492294

Brussaard, L., de Ruiter, P.C., Brown, G.G., 2007. Soil biodiversity for agricultural sustainability. Agric. Ecosyst. Environ. 121, 233–244. doi:10.1016/j.agee.2006.12.013

Cordell, D., Drangert, J.O., White, S., 2009. The story of phosphorus: Global food security and food for thought. Glob. Environ. Chang. 19, 292–305. doi:10.1016/j.gloenvcha.2008.10.009

FAO, F.A.O., 2017. The future of food and agriculture–Trends and challenges.

Fenton, M., Albers, C., Ketterings, Q., 2008. Soil Organic Matter Agronomy Fact Sheet Series.

Giudicianni, P., Cardone, G., Sorrentino, G., Ragucci, R., 2014. Hemicellulose, cellulose and lignin interactions on Arundo donax steam assisted pyrolysis. J. Anal. Appl. Pyrolysis 110, 138–146. doi:10.1016/j.jaap.2014.08.014

Haustein, C.H., 2019. NITROGEN (FIXED)-AMMONIA.

Jeworski, I., 2002. Environmental Consequences of Intensive Agricultural Production Practices.

Joseph, S., Husson, O., Graber, E., van Zwieten, L., Taherymoosavi, S., Thomas, T., Nielsen, S., Ye, J., Pan, G., Chia, C., Munroe, P., Allen, J., Lin, Y., Fan, X., Donne, S., 2015. The Electrochemical Properties of Biochars and How They Affect Soil Redox Properties and Processes. Agronomy 5, 322–340. doi:10.3390/agronomy5030322

Katuri, K.P., Kalathil, S., Ragab, A., Bian, B., Alqahtani, M.F., Pant, D., Saikaly, P.E., 2018. Dual-Function Electrocatalytic and Macroporous Hollow-Fiber Cathode for Converting Waste Streams to Valuable Resources Using Microbial Electrochemical Systems. Adv. Mater. 30, e1707072. doi:10.1002/adma.201707072

Kratz, S., Schick, J., Schnug, E., 2016. Trace elements in rock phosphates and P containing mineral and organo-mineral fertilizers sold in Germany. Sci. Total Environ. 542, 1013–1019. doi:10.1016/j.scitotenv.2015.08.046

Laird, D., Fleming, P., Wang, B., Horton, R., Karlen, D., 2010. Biochar impact on nutrient leaching from a Midwestern agricultural soil. Geoderma 158, 436–442. doi:10.1016/J.GEODERMA.2010.05.012

Lehmann, J., Joseph, S., 2015. Biochar for Environmental Management: Science, Technology and Implementation. Taylor & Francis.

Lehmann, J., Rillig, M.C., Thies, J., Masiello, C.A., Hockaday, W.C., Crowley, D., 2011. Biochar effects on soil biota – A review. Soil Biol. Biochem. 43, 1812–1836. doi:10.1016/j.soilbio.2011.04.022

Lobb, D.A., 2008. Soil Movement by Tillage and Other Agricultural Activities, in: Encyclopedia of Ecology, Five-Volume Set. Elsevier Inc., pp. 3295–3303. doi:10.1016/B978-008045405-4.00832-6

Merino-Jimenez, I., Celorrio, V., Fermin, D.J., Greenman, J., Ieropoulos, I., 2017. Enhanced MFC power production and struvite recovery by the addition of sea salts to urine. Water Res. 109, 46–53. doi:10.1016/j.watres.2016.11.017

Mohamed, M.E.F., A, F.A.F., E, A.A.A.E.N., M, S.Z., A, H.F., 2015. Impact of long-term intensive cropping under continuous tillage and unbalanced use of fertilizers on soil nutrient contents in a small holding village. African J. Agric. Res. 10, 4850–4857. doi:10.5897/ajar2015.10499

Nhamo, N., Kyalo, G., Dinheiro, V., 2014. Exploring options for lowland rice intensification under rain-fed and irrigated ecologies in East and Southern Africa: The potential application of integrated soil fertility management principles, in: Advances in Agronomy. Academic Press Inc., pp. 181–219. doi:10.1016/B978-0-12-802139-2.00005-6

Pandey, P., Shinde, V.N., Deopurkar, R.L., Kale, S.P., Patil, S.A., Pant, D., 2016. Recent advances in the use of different substrates in microbial fuel cells toward wastewater treatment and simultaneous energy recovery. Appl. Energy 168, 706–723. doi:10.1016/j.apenergy.2016.01.056

Pielke, R.A., 2013. Climate Vulnerability: Understanding and Addressing Threats to Essential Resources | Request PDF [WWW Document]. Univ. Color. Boulder, Boulder, CO, USA.

Puig, S., Serra, M., Coma, M., Cabré, M., Balaguer, M.D., Colprim, J., 2010. Effect of pH on nutrient dynamics and electricity production using microbial fuel cells. Bioresour. Technol. 101, 9594–9599. doi:10.1016/j.biortech.2010.07.082

Rippner, D.A., Green, P.G., Young, T.M., Parikh, S.J., 2018. Dissolved organic matter reduces CuO nanoparticle toxicity to duckweed in simulated natural systems. Environ. Pollut. 234, 692–698. doi:10.1016/j.envpol.2017.12.014

Rittmann, B.E., Mayer, B., Westerhoff, P., Edwards, M., 2011. Capturing the lost phosphorus. Chemosphere 84, 846–853. doi:10.1016/j.chemosphere.2011.02.001

Santoro, C., Ieropoulos, I., Greenman, J., Cristiani, P., Vadas, T., Mackay, A., Li, B., 2013. Power generation and contaminant removal in single chamber microbial fuel cells (SCMFCs) treating human urine, in: International Journal of Hydrogen Energy. Pergamon, pp. 11543–11551. doi:10.1016/j.ijhydene.2013.02.070

Vaccari, F.P., Baronti, S., Lugato, E., Genesio, L., Castaldi, S., Fornasier, F., Miglietta, F., 2011. Biochar as a strategy to sequester carbon and increase yield in durum wheat. Eur. J. Agron. 34, 231–238. doi:10.1016/J.EJA.2011.01.006

Verstraete, W., Van de Caveye, P., Diamantis, V., 2009. Maximum use of resources present in domestic "used water." Bioresour. Technol. 100, 5537–5545. doi:10.1016/j.biortech.2009.05.047

Weinbaum, S.A., R. Scott Johnson, Dejong, T.M., 2018. Causes and Consequences of Overfertilization in Orchards in: HortTechnology Volume 2 Issue 1 (1992) [WWW Document]. Am. Soc. Hortic. Sci.

Winfield, J., Gajda, I., Greenman, J., Ieropoulos, I., 2016. A review into the use of ceramics in microbial fuel cells. Bioresour. Technol. 215, 296–303. doi:10.1016/j.biortech.2016.03.135

Appendix

1. List of publications

- Marzorati S., Goglio A., Fest-Santini S., Mombelli D., Villa F., Cristiani P., Schievano A., 2018. Air-breathing bio-cathodes based on electro-active biochar from pyrolysis of Giant Cane stalks. International Journal of Hydrogen Energy. doi:10.1016/j.ijhydene.2018.07.167

- Goglio A., Tucci M., Rizzi B., Colombo A., Cristiani P., Schievano A., 2019. Microbial recycling cells (MRCs): A new platform of microbial electrochemical technologies based on biocompatible materials, aimed at cycling carbon and nutrients in agro-food systems. Science of the Total Environment. doi:10.1016/j.scitotenv.2018.08.324

- Goglio A., Marzorati S., Rago L., Pant D., Cristiani P., Schievano A., 2019. Microbial recycling cells: first steps into a new type of microbial electrochemical technologies, aimed at recovering nutrients from wastewater. Bioresource Technology. doi:10.1016/j.biortech.2019.01.039

- Schievano A., Berenguer R., Goglio A., Bocchi S., Marzorati S., Rago L., Louro R.O., Paquete C.M., Esteve-Núñez A., 2019. Electroactive biochar for large-scale environmental applications of microbial electrochemistry. ACS Sustainable Chemistry & Engineering. doi:10.1021/acssuschemeng.9b04229

- Cristiani P., Goglio A., Marzorati S., Fest-Santini S., Schievano A., 2020. Biochar-terracotta conductive composites: new design for bioelectrochemical systems. Frontiers in energy research journal. doi: 10.3389/fenrg.2020.581106

2. List of conference presentations

- European Fuel Cells Conference 2017: The challange of nutrients recovery by terracotta Microbial Fuel Cells (poster presentation). A. Goglio, S. Marzorati, S. Quarto, E. Falletta, P. Cristiani, A. Schievano

- European Fuel Cells Conference 2017: Giant Cane as Low-cost Material for Microbial Fuel Cells Architectures (oral presentation). S. Marzorati, A. Goglio, D. Mombelli, C. Mapelli, S.P. Trasatti, P. Cristiani, A. Schievano

- International Society for Microbial Electrochemistry and Technology Meeting 2017: Ligno-cellulosic Materials in Low-cost Microbial Fuel Cells Architecturesfor Nutrients Recovery (oral presentation). S. Marzorati, A. Goglio, L. Rago, P. Cristiani, A. Schievano

- International Society for Microbial Electrochemistry and Technology Meeting 2017: A new applicative frontier for Microbial Fuel Cells (oral presentation). A. Schievano, A. Goglio, S. Marzorati, A. Colombo, L. Rago

- International Society for Microbial Electrochemistry and Technology Meeting 2017: Treating wastewater while recovering nutrients, electrochemical biofilters coupled to innovative biochar-based cylindrical cathodes (oral presentation). A. Goglio, S. Marzorati, A. Prado de Nicolás, C. Wardman, L. Rago, A. Esteve Núñez, A. Schievano

- International Society for Microbial Electrochemistry and Technology Meeting 2018: e-BioChar, Electroactive Charcoal-based Electrodes for Bioelectrochemical Systems (oral presentation). S. Marzorati, A. Goglio, M. Bahdanchyk, S. Trasatti, P. Cristiani, A. Schievano

- International Society for Microbial Electrochemistry and Technology Meeting 2018: Microbial recycling cells (MRCs), coupling novel air cathodes and electrochemical biofilters for nutrients recovery from food-industry wastewater (oral presentation). A. Goglio, S. Marzorati, A. Prado de Nicolás, C. Manchón Vállegas, C. Ortiz Martín, C. Wardman, A. Esteve Núñez, A. Schievano

- Annual Meeting of the International Society of Electrochemistry 2018: Biochar-based Electrodes for Bioelectrochemical Systems (poster presentation). S. Marzorati, M. Bahdanchyk, A. Goglio, S. Trasatti, A. Schievano, P. Cristiani

- Word Conference on Carbon 2018: Biomass-Derived Electrodes for Bioelectrochemical Systems (oral presentation). S. Marzorati, M. Bahdanchyk, A. Goglio, S. Trasatti, P. Cristiani, A. Schievano

- Agri Biostimulants Conference 2018: e-NEWtrients, microbial electrochemical technologies help in recovering nutrients from wastewater and obtaining renewable soil conditioners and fertilizers (oral presentation). A. Goglio, S. Marzorati, L. Rago, B. Rizzi, A. Schievano

- International Agricultural Symposium 2018: e-NEWtrients, bio-electrochemical systemsat the service of agricultural sciences,nutrients recovery and electro-active soil conditioners (oral presentation). A. Goglio, S. Marzorati, B. Rizzi, A. Schievano

- International Conference on Bioresource Technology for Bioenergy, Bioproducts & Environmental Sustainability 2018: Microbial recycling cells (MRCs), a new platform of microbial electrochemical technologies based on biocompatible materials, aimed at cycling carbon and nutrients in agro-food systems (oral presentation). A. Schievano, A. Goglio, S. Marzorati, M. Tucci, B. Rizzi, P. Cristiani

- European Fuel Cells Conference 2019: Terracotta and Biochar-Derived Electrodes for Bioelectrochemical Systems (oral presentation). P. Cristiani, S. Marzorati, A. Goglio, M. Bahdanchyk, S. Trasatti, A. Schievano

- International Annual Meeting American Society of Agronomy 2019: Electroactive biochar amendment of anoxic soil, enhancing redox reactions and electron transfer to decrease the GHGs emissions (oral presentation). Andrea Goglio, Danielle Gelardi, Devin Rippner, Raul Berenguer, Sanjai J. Parikh, Andrea Schievano

3. PhD Schools

- European Summer School on Electrochemical Engineering, University of Toulouse III, 2018

- The role of Agricultural Chemistry for a sustainable agricultural production and its traceability, Società Italiana di Chimica Agraria, 2018

- Effetti Agronomici del Biochar, Società Italiana Biochar, 2018

4. Patents

Microbial electrochemical technologies based on ligno-cellulosic biomass, biochar and clay - PCT/TB2018/057634 - Andrea Schievano, Stefania Marzorati, Pierangela Cristiani, Andrea Goglio, Alessandra Colombo, Laura Rago.